

Catalytic Chemistry of Heteropoly Compounds

TOSHIO OKUHARA

*Graduate School of Environmental Earth Science
Hokkaido University
Sapporo 060, Japan*

NORITAKA MIZUNO

*Institute of Industrial Science
The University of Tokyo
Roppongi, Minato-ku, Tokyo 106, Japan*

AND

MAKOTO MISONO

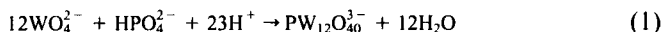
*Department of Applied Chemistry
Graduate School of Engineering
The University of Tokyo
Bunkyo-ku, Tokyo 113, Japan*

I. Introduction

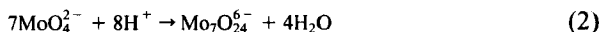
A. HETEROPOLY COMPOUNDS AS CATALYSTS

The catalytic properties of heteropoly compounds have drawn wide attention in the preceding two decades owing to the versatility of these compounds as catalysts, which has been demonstrated both by successful large-scale applications and by promising laboratory results.

Heteropolyanions are polymeric oxoanions formed by condensation of more than two different mononuclear oxoanions, as shown in Eq. (1):



Heteropolyanions formed from one kind of polyanion are called isopolyanions, as shown in Eq. (2):



Acidic elements such as Mo, W, V, Nb and Ta, which are present as oxoanions

in aqueous solution, tend to polymerize by dehydration at low pH, forming polyanions and water (1-3).

The term "heteropoly compound" is used in this review for the acid forms, e.g., $H_3PW_{12}O_{40}$, and their salts, e.g., $Cs_3PW_{12}O_{40}$. Catalysts of which the main components are heteropoly or heteropoly-derived compounds are referred to here as "heteropoly catalysts," and they are the subject of this review. Heteropolyanion-derived compounds are, for example, organic and metallo-organic complexes of polyanions (see Section I.D for the terminology and nomenclature). Although there are many kinds of heteropolyanions (Section II), heteropolyanions having the Keggin structure are the most widely investigated as catalysts because of their stabilities and ease of synthesis. However, other heteropolyanions are also expected to be recognized as good catalysts.

Heteropoly catalysts can be applied in various ways (4-10). They are used as acid as well as oxidation catalysts. They are used in various phases, as homogeneous liquids, in two-phase liquids (in phase-transfer catalysis), and in liquid-solid and in gas-solid combinations, etc. The liquid-solid and gas-solid combinations are represented by the classes of catalysis shown in Fig. 1 and described in the following sections. The advantages of heteropoly catalysts stem from the characteristics summarized in Table I.

As excellent candidates for design at the atomic or molecular level, heteropoly catalysts have proven to be of value in fundamental studies as well as practical applications. But it is also true that much remains to be done. Efforts to establish methodologies for design of practical catalysts are still under way. The acid strength and acid site density can be controlled quite well both in solution and in the solid state, but the redox properties in the solid state are much less well understood because of the lack of sufficient thermal stability of mixed-metal (mixed-addenda) heteropolyanions. The acid strengths of some solid heteropolyacids have been suggested to reach the range of superacids, but they

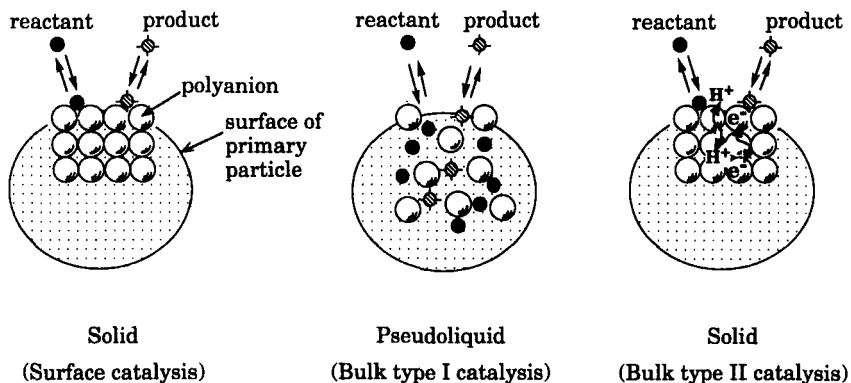


FIG. 1. Three types of catalysis by heteropoly compounds.

TABLE I
Advantages of Heteropoly Catalysts

-
1. *Catalyst design at atomic/molecular levels based on the following:*
 - 1-1. Acidic and redox properties
These two important properties for catalysis can be controlled by choosing appropriate constituent elements (type of polyanion, addenda atom, heteroatom, counteraction, etc.).
 - 1-2. Multifunctionality
Acid-redox, acid-base, multi-electron transfer, photosensitivity, etc.
 - 1-3. Tertiary structure, bulk-type behavior, etc., for solid state
These are well controlled by counteractions.
 2. *Molecularity—metal oxide cluster*
 - 2-1. Molecular design of catalysts
 - 2-2. Cluster models of mixed oxide catalysts and of relationships between solid and solution catalysts
 - 2-3. Description of catalytic processes at atomic/molecular levels
Spectroscopic study and stoichiometry are realistic
Model compounds of reaction intermediates.
 3. *Unique reaction field*
 - 3-1. Bulk-type catalysis
“Pseudoliquid” and bulk type II behavior provide unique three-dimensional reaction environments for catalysis.
 - 3-2. Pseudoliquid behavior
This makes spectroscopic and stoichiometric studies feasible and realistic.
 - 3-3. Phase-transfer catalysis
 - 3-4. Shape selectivity.
 4. *Unique basicity of polyanion*
 - 4-1. Selective coordination and stabilization of reaction intermediates in solution and in pseudoliquid phase, and possibly also on the surface
 - 4-2. Ligands and supports for metals and organometallics.
-

are still weaker acids than sulfated zirconia. Unique complexing or basic properties of polyanions have not been clarified sufficiently, although it appears that they play important roles in industrial liquid-phase processes. The efforts to describe catalytic processes at the molecular level have also made significant progress in the preceding decade, but the number of well-elucidated reactions remains very small.

Early attempts to use heteropoly compounds as catalysts are summarized in reviews published in 1952 (11) and 1978 (1). The first industrial process using a heteropoly catalyst was started up in 1972 for the hydration of propylene in the liquid phase. The essential role of the Keggin structure in a solid heteropoly catalyst was explicitly shown in 1975 in a patent concerning catalytic oxidation of methacrolein. Systematic research in heterogeneous catalysis with these materials started in the mid-1970s and led to the recognition of quantitative relationships between the acid or redox properties and catalytic performance

(4–9). Pseudoliquid-phase catalysis (bulk type I catalysis) was reported in 1979, and bulk type II behavior in 1983. In the 1980s, several new large-scale industrial processes started in Japan based on applications of heteropoly catalysts that had been described before (5, 6, 12): namely, oxidation of methacrolein (1982), hydration of isobutylene (1984), hydration of *n*-butene (1985), and polymerization of tetrahydrofuran (1987). In addition, there are a few small- to medium-scale processes (9, 10). Thus the level of research activity in heteropoly catalysis is very high and growing rapidly.

One of the authors of this chapter has previously reviewed heterogeneous catalysis by heteropoly compounds (4–6). Catalysis in solution has also been described (7–10). In this chapter, we critically survey the literature and attempt to describe the essence of the catalytic chemistry of heteropoly compounds in solution and in the solid state. We have attempted to highlight the advantages of heteropoly catalysts as described in Table I.

B. CLASSES OF CATALYSIS BY HETEROPOLY COMPOUNDS

As will be described in more detail in later sections, in acid and oxidation catalysis by solid heteropoly compounds, that is, gas–solid and liquid–solid systems, there are three different classes of catalysis: (1) surface catalysis, (2) bulk type I (pseudoliquid catalysis), and (3) bulk type II catalysis, as shown in Fig. 1. The latter two have been specifically demonstrated for heteropoly catalysts, and they could be found for other solid catalysts as well.

Surface-type catalysis is ordinary heterogeneous catalysis, whereby the reactions take place on the two-dimensional surface (on the outer surface and pore walls) of solid catalysts. The reaction rate is proportional to the catalyst surface area.

Bulk type I catalysis was found in acid catalysis with the acid forms and some salts at relatively low temperatures. The reactant molecules are absorbed *between* the polyanions (not *in* a polyanion) in the ionic crystal by replacing water of crystallization or expanding the lattice, and reaction occurs there. The polyanion structure itself is usually intact. The solid behaves like a solution and the reaction medium is three-dimensional. This is called “pseudoliquid” catalysis (Sections I.A and VI). The reaction rate is proportional to the volume of the catalyst in the ideal case; the rate of an acid-catalyzed reaction is proportional to the total number of acidic groups in the solid bulk.

Bulk type II catalysis was discovered later for some oxidation reactions at high temperatures. Although the principal reaction may proceed on the surface, the whole solid bulk takes part in redox catalysis owing to the rapid migration into the bulk of redox carriers such as protons and electrons (Sections VII and IX). The rate is proportional to the volume of catalyst in the ideal case.

These three classes of catalysis are distinctly different from each other in the ideal cases. But the extent of the contribution of the inner bulk of the catalyst depends on the rate of the catalytic reaction relative to the rate of diffusion of reactant and product molecules in bulk type I catalysis and on the rate of reaction relative to the rate of diffusion of redox carriers for the bulk type II catalysis.

C. CATALYST DESIGN BASED ON CRYSTALLINE MIXED OXIDES

To develop efficient catalytic technology capable of solving contemporary problems related to energy and resource limitations, synthesis of materials, and environmental protection, novel concepts for catalyst design are needed. Catalyst design at the atomic level utilizing the techniques of advanced surface science is one of the possibilities; but this can be applied only for model catalysts, and the syntheses of industrial catalysts by this method are not yet realistic (6).

Alternatively, we have attempted the molecular design of mixed-oxide catalysts by using crystalline mixed oxides whose bulk structures are known and whose potential for practical use is good. Heteropoly compounds, perovskites, and zeolites are the candidate catalysts.

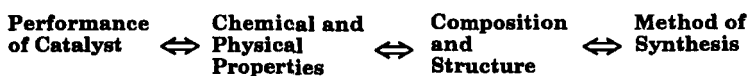
Since we believe that the relationships in Scheme 1 are useful for the design of catalysts (13), we place stress in this chapter on these relationships at atomic/molecular levels of heteropoly compounds. In our opinion, sufficient care must be taken on the structure and stoichiometry in order to design catalysts taking advantage of the molecular nature of heteropoly compounds.

D. TERMINOLOGY AND NOMENCLATURE

1. Generic Terms

Various generic names have been used for oxoacids and oxoanions. Because there are many of them, it is difficult to define the terms unambiguously and consistently. But the following statements may be helpful.

For acid forms, polyacids = polyoxoacids, including heteropolyacids (e.g., $\text{H}_3\text{PW}_{12}\text{O}_{40}$) and isopolyacids (e.g., $\text{H}_2\text{Mo}_6\text{O}_{19}$); and for oxoanions, polyanions = polyoxoanions = polyoxometalates, including heteropolyanions (e.g., $\text{PW}_{12}\text{O}_{40}^{3-}$) and isopolyanions (e.g., $\text{Mo}_6\text{O}_{19}^{2-}$).



SCHEME 1

In addition, such generic terms as metal–oxygen cluster ion, metal-oxide molecule, etc., are used for polyanions (and polyacids). Since the traditional “heteropoly-” and “isopoly-” are unsatisfactory terms to express a variety of polyacids and polyanions, the terms “polyoxometalates” and “polyoxoacids” have been used recently (3). The terminology is still changing, thus reflecting the rapid expansion of the chemistry.

Nonoxygen elements in the inner part of polyanions (usually P, Si, As, etc.) are called *heteroatoms* (in some cases, *central atoms*) and those in the peripheral part (usually Mo, W, V, Nb, etc.) are called *addenda atoms* or *polyatoms* (Section II.A). We use more or less conventional terminology here.

2. Nomenclature

The rigorous and systematic nomenclature addressed by IUPAC (14), in which all atoms and their topological connections are defined unambiguously, is too complicated here. Thus we use traditional names. But the semi-systematic nomenclature accepted by IUPAC (15) is mentioned briefly.

For example, a heteropolyacid, $\text{H}_4\text{SiMo}_{12}\text{O}_{40}$, is called tetrahydrogen hexatriacontaoxo(tetraoxosilicato)dodecamolybdate(4-) [hydrogen nomenclature] or tetrahydrogen silicododecamolybdate [abbreviated semi-trivial name]. Or this is called 12-(or dodeca)molybdosilicic acid for the acid form and 12-(or dodeca)molybdosilicate for the anion [recommendations of IUPAC, 1971 (16)].

II. Structure, Synthesis, Stability, and Characterization

A. PRIMARY, SECONDARY, AND TERTIARY STRUCTURES

Heteropolyanions and isopolyanions are polymeric oxoanions (polyoxometalates) (2, 3, 5, 6). The structure of a heteropolyanion or polyoxoanion molecule itself is called a “primary structure” (5, 6, 17). There are various kinds of polyoxoanion structure (Section II.A.1). In solution, heteropolyanions are present in the unit of the primary structure, being coordinated with solvent molecules and/or protonated. Most heteropolyanions tend to hydrolyze readily at high pH (Section II.C). Protonation and hydrolysis of the primary structure may be major structural concerns in solution catalysis. Heteropoly compounds in the solid state are ionic crystals (sometimes amorphous) consisting of large polyanions, cations, water of crystallization, and other molecules. This three-dimensional arrangement is called the “secondary structure.” For understanding catalysis by solid heteropoly compounds, it is important to distinguish between the primary structure and the secondary structure (5, 6, 17). Recently, it has been realized that, in addition

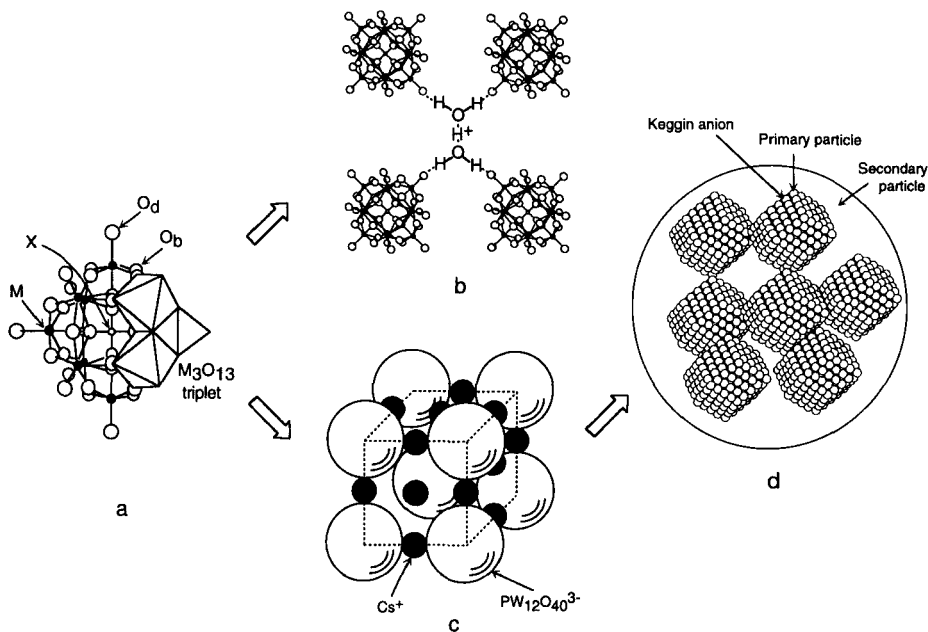


FIG. 2. Primary, secondary, and tertiary structures of heteropoly compounds. (a) Primary structure (Keggin structure, $\text{XM}_{12}\text{O}_{40}$); (b) secondary structure ($\text{H}_3\text{PW}_{12}\text{O}_{40} \cdot 6\text{H}_2\text{O}$); (c) secondary structure ($\text{Cs}_3\text{PW}_{12}\text{O}_{40}$); (d) tertiary structure [$\text{Cs}_{2.5}\text{H}_{0.5}\text{PW}_{12}\text{O}_{40}$, cubic structure as in (c)].

to these structures, tertiary and higher-order structures influence the catalytic function (6). These structures are exemplified in Fig. 2 (3, 18).

1. Primary Structure

a. *Keggin Structure* (1–3, 18, 19). Figures 3a and 3b illustrate the Keggin anions, which are the most popular heteropolyanions in catalysis. The ideal Kegging structure of the α type has T_d symmetry and consists of a central XO_4 tetrahedron (X = heteroatom or central atom) surrounded by twelve MO_6 octahedra (M = addenda atom). The twelve MO_6 octahedra comprise four groups of three edge-shared octahedra, the M_3O_{13} triplet (19), which have a common oxygen vertex connected to the central heteroatom. The oxygen atoms in this structure fall into four classes of symmetry-equivalent oxygens: $\text{X}-\text{O}_a-(\text{M})_3$, $\text{M}-\text{O}_b-\text{M}$, connecting two M_3O_{13} units by corner sharing; $\text{M}-\text{O}_c-\text{M}$, connecting two M_3O_{13} units by edge sharing; and O_d-M , where M is the addenda atom and X the heteroatom. This Keggin structure is called an α isomer (18).

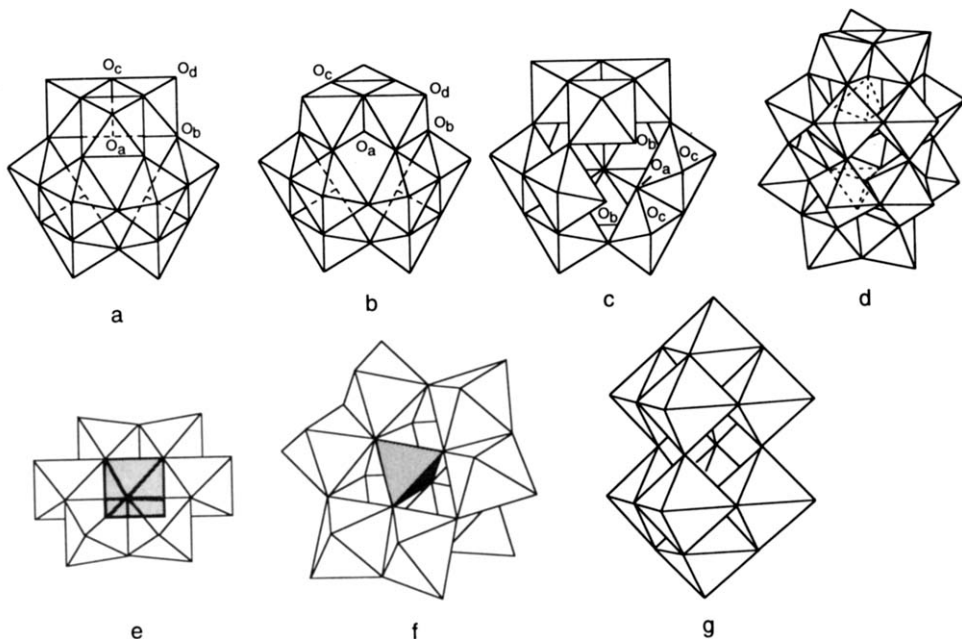


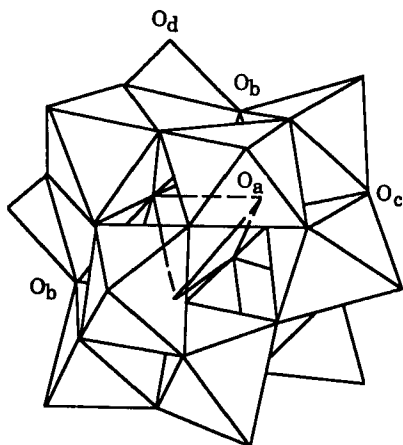
Fig. 3. Primary structures of heteropoly and isopolyanions. (a) Keggin structure, α - $\text{XM}_{12}\text{O}_{40}^{n-}$ (the fourth M_3O_{13} set and the XO_4 tetrahedron are not shown for clarity) (from Refs. 2 and 19); (b) Keggin structure, β - $\text{XM}_{12}\text{O}_{40}^{n-}$ (the fourth M_3O_{13} set and the XO_4 tetrahedron are not shown for clarity) (from Refs. 24 and 25); (c) lacunary Keggin anion (the central XO_4 tetrahedron is not shown) (from Ref. 2); (d) Dawson structure, $\text{X}_2\text{M}_{18}\text{O}_{62}^{n-}$ (from Refs. 29 and 30); (e) Anderson structure, $\text{XM}_6\text{O}_{24}^{n-}$ (shaded tetrahedron indicates the heteroatom site) (from Refs. 18 and 33); (f) $\text{XM}_9\text{O}_{34}^{n-}$ (from Ref. 2); (g) isopolyanions, $\text{W}_{10}\text{O}_{32}^{n-}$ (from Ref. 2).

The known addenda and heteroatoms incorporated in heteropolyanions are summarized in Table II (20). The structures in this table of polyanions with Se(IV), Te(IV), Sb(III), Bi(III), Ti(IV), and Zr(IV) still need to be confirmed, since tetradendral coordination of these ions with oxide ions is seldom observed (2).

In Table III (21, 22), the bond distances in various heteropoly compounds having the Keggin structure are listed. Bond lengths in $\text{PW}_{12}\text{O}_{40}^{3-}$ for $\text{H}_3\text{PW}_{12}\text{O}_{40} \cdot 6\text{H}_2\text{O}$ are 1.71, 1.90, 1.91, and 2.44 Å for O_d -W, O_c -W, O_b -W, and O_a -W bonds, respectively. The existence of isomers has been established for the Keggin anion. Figures 3a and 3b show the α - and β -isomers. They can be separated by fractional crystallization ($\text{X} = \text{B}, \text{Si}$) or prepared separately ($\text{X} = \text{Si}, \text{Ge}$) (23). In β - $\text{SiW}_{12}\text{O}_{40}^{4-}$, one of the three edge-shared W_3O_{13} triplets of the α structure is rotated by 60° , thereby reducing the symmetry of the anion from T_d to C_{3v} (24, 25). The other isomers involving the

TABLE III
Bond Lengths in MO_6 and WO_6 Group in Heteropolyanion (\AA) (21, 22)

Compounds	M-O _d	M-O _c	M-O _b	M ^b O _a	X ^b O _a
H ₃ PW ₁₂ O ₄₀ · 6H ₂ O	1.71	1.90	1.91	2.44	1.53
H ₃ PMo ₁₂ O ₄₀ · 13H ₂ O	1.66	1.96	1.97	2.43	1.53
H ₃ PMo ₁₂ O ₄₀ · 30H ₂ O	1.68	1.91	1.92	2.44	1.54
H ₄ SiMo ₁₂ O ₄₀ · 13H ₂ O	1.67	1.94	1.96	2.35	1.62
K ₄ SiW ₁₂ O ₄₀ · 16H ₂ O	1.68	1.91	1.96	2.38	1.63



M_3O_{13} groups. $H_6As_2Mo_{18}O_{62}$ and $S_2Mo_{18}O_{62}^{4-}$ have also been synthesized (2, 31). A complex containing F ions, $H_2F_6NaW_{18}O_{56}^{7-}$ (32), is isostructural with the Dawson species, $P_2W_{18}O_{62}^{6-}$.

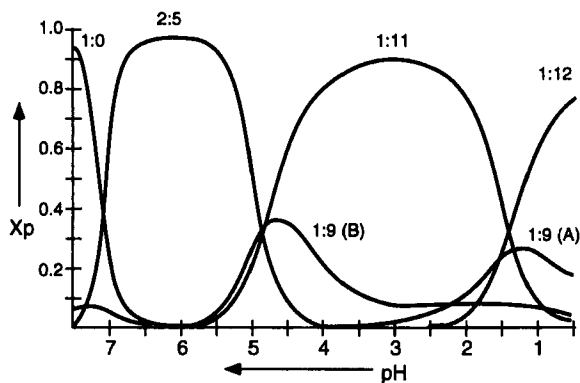


FIG. 4. Distribution diagram for species present in fresh solutions containing MoO_4^{2-} and HPO_4^{2-} in a molar ratio of 12:1 at different pH values. (From Ref. 28.)

d. *Anderson Structure*. The Anderson structure, $\text{XM}_6\text{O}_{24}^{n-}$, comprises seven edge-shared octahedra (Fig. 3e) (18, 33).

2. Secondary Structure of Solid Heteropoly Compounds

In heteropoly acids (acid form) in the solid state, protons play an essential role in the structure of the crystal, by linking the neighboring heteropolyanions. Protons of crystalline $\text{H}_3\text{PW}_{12}\text{O}_{40} \cdot 6\text{H}_2\text{O}$ are present in hydrated species, H_5O_2^+ , each of which links four neighboring heteropolyanions by hydrogen bonding to the terminal $\text{W}-\text{O}_d$ oxygen atoms, and the polyanions are packed in a bcc structure (Fig. 2b) (21). Various heteropolyacid hydrates that differ in the number of waters of crystallization have been reported (34–36); $\text{H}_3\text{PW}_{12}\text{O}_{40} \cdot n\text{H}_2\text{O}$ ($n = 14, 21, 24,$ and 29). The loss of water brings about changes in the anion packing; $n = 29$ [cubic (diamond-like)], $n = 21$ (orthorhombic), $n = 6$ [cubic (bcc)]. $\text{Cs}_3\text{PW}_{12}\text{O}_{40}$, in which the Cs ions are at the sites of H_5O_2^+ ions of hexahydrate (Fig. 2b), has a dense secondary structure and is anhydrous (Fig. 2c) (34). The lattice constants of $\text{Cs}_3\text{PW}_{12}\text{O}_{40}$ and $\text{H}_3\text{PW}_{12}\text{O}_{40} \cdot 6\text{H}_2\text{O}$ are 12.14 and 11.86 Å, respectively (21, 26, 37).

Secondary structures containing organic molecules are known. $\text{H}_4\text{SiW}_{12}\text{O}_{40} \cdot 9\text{DMSO}$ [DMSO = $(\text{CH}_3)_2\text{SO}$] contains nine molecules of DMSO in a unit cell, where there are weak hydrogen bonds between methyl groups and oxygen atoms of the heteropolyanion, polyanion-- $(\text{CH}_3)_2\text{SO}$ -- H^+ -- $\text{OS}(\text{CH}_3)_2$ --polyanion (38). Eight independent DMSO molecules join in four pairs of cations $[\text{H}(\text{O}=\text{S}(\text{CH}_3)_2)_2]^+$ by strong hydrogen bonds, and one DMSO molecule is weakly bonded. Another example is $\text{PW}_{12}\text{O}_{40} \cdot [(\text{C}_5\text{H}_5\text{N})_2\text{H}]_3$, which is obtained by the reaction of anhydrous $\text{H}_3\text{PW}_{12}\text{O}_{40}$ with pyridine (39). As shown in Fig. 5, six pyridine molecules lie almost in a plane, and the pyridine molecules

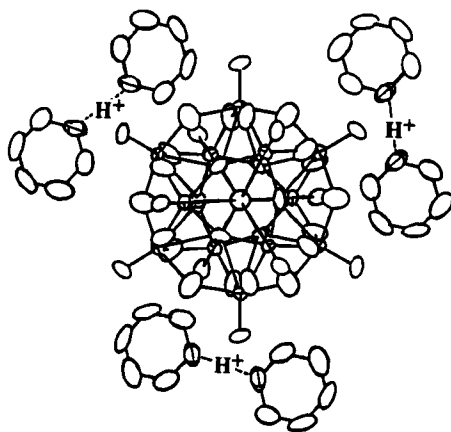


FIG. 5. Structure of $[(\text{C}_5\text{H}_5\text{N})_2\text{H}]_3[\text{PW}_{12}\text{O}_{40}]$. (From Ref. 39.)

are paired, forming N--H--N hydrogen bonding. Similar structures are also formed by the contact of pyridine vapor with heteropolyacids (5). Other examples are $\text{PW}_{12}\text{O}_{40} (\text{H}^+ \text{-quinolin-8-ol})_3 \cdot 4\text{C}_2\text{H}_5\text{OH} \cdot 2\text{H}_2\text{O}$ (40) and $\text{PMo}_{12}\text{O}_{40} [\text{H}^+ \text{-TMU}_2]_3$ (TMU = 1,1,3,3-tetramethyl urea) (41).

3. Tertiary Structure of Solid Heteropoly Compounds

Tertiary structure is the structure of solid heteropoly compounds as assembled (5, 6). The size of the primary and secondary particles, pore structure, distribution of protons and cations, etc. are the elements of the tertiary structure.

a. *Group A and B Salts.* Counteranions greatly influence the tertiary structure of a heteropoly compound. The salts of small ions such as Na^+ [classified into group A salts (42)] behave similarly to the acid form in several respects. The group A salts are highly soluble in water and other polar organic solvents. The surface areas of group A salts are usually low. Polar molecules are readily absorbed in interstitial positions (between polyanions) of the secondary structure (Section VI). On the other hand, the salts of large cations such as NH_4^+ and Cs^+ (classified as group B salts) are insoluble in water and exhibit low absorptivity for polar molecules. Low solubility is due to the low energy of solvation of large cations. The surface areas of group B salts are usually high due to the smaller sizes of the primary particles, giving favorable properties for heterogeneous catalysis (43-46a). The thermal stability of most group B salts is relatively high, which is also important in heterogeneous catalysis.

b. *Surface Area and Pore Structure.* The surface area and pore structure are closely related. Figure 6 shows the surface areas as a function of the extent

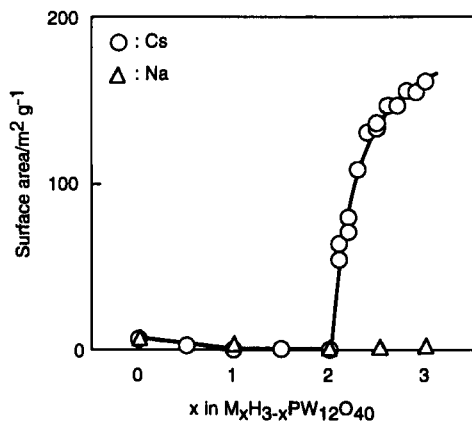


FIG. 6. Surface areas of Na or Cs acidic salt of $\text{H}_3\text{PW}_{12}\text{O}_{40}$ as a function of the extent of Na or Cs substitution. (From Refs. 46 and 47.)

of Na or Cs substitution of $\text{H}_3\text{PW}_{12}\text{O}_{40}$ (46, 47). As the Na content increases, the surface area decreases monotonically (46b). The change of the surface area with increasing Cs content is remarkably different. The surface area increases significantly when the Cs content, x in $\text{Cs}_x\text{H}_{3-x}\text{PW}_{12}\text{O}_{40}$, changes from $x = 2$ ($1 \text{ m}^2 \text{ g}^{-1}$) to $x = 3$ ($156 \text{ m}^2 \text{ g}^{-1}$), although it decreases slightly from $x = 0$ ($6 \text{ m}^2 \text{ g}^{-1}$) to $x = 2$. The surface area increases significantly to more than $130 \text{ m}^2 \text{ g}^{-1}$ when the Cs content exceeds 2.5. $\text{Cs}_{2.5}\text{H}_{0.5}\text{PW}_{12}\text{O}_{40}$ (and also $\text{Cs}_3\text{PW}_{12}\text{O}_{40}$) consists of very fine particles (8–10 nm in diameter) (Fig. 2d).

Pore structure is an important property of solid catalysts. Gregg and Tayyab (43) reported that $(\text{NH}_4)_3\text{PW}_{12}\text{O}_{40}$ has a microporous structure (pore diameter $< 20 \text{ \AA}$) as estimated from the adsorption isotherms of N_2 , n -hexane, and carbon tetrachloride. Moffat *et al.* (44) reported that the salts of NH_4^+ and Cs^+ possess pore structures in the microporous–mesoporous range as revealed by nitrogen adsorption. Figure 7 shows N_2 adsorption isotherms for $(\text{NH}_4)_3\text{PW}_{12}\text{O}_{40}$ and $\text{Cs}_3\text{PW}_{12}\text{O}_{40}$. In the case of $\text{Cs}_3\text{PW}_{12}\text{O}_{40}$, a hysteresis is evident, showing that this salt has mesopores (pore size $> 20 \text{ \AA}$) (44c) as well as micropores. They proposed that these pores exist in the crystal structure. Mizuno and Misono (37) examined the tertiary structure of $\text{Cs}_3\text{PW}_{12}\text{O}_{40}$ by estimating the surface area with three different methods: particle-size distribution measured by TEM (assuming spherical particles), the pore-size distribution measured by N_2 adsorption (assuming cylindrical pores), and the BET equation. The three values are in good agreement with each other, showing that this material is composed of fine primary particles observed by TEM, with the pores being intercrystalline, not

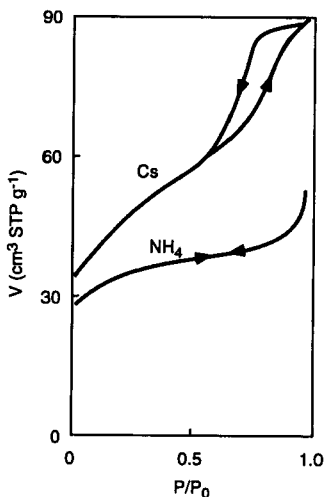


FIG. 7. Nitrogen adsorption-desorption isotherms (77 K) for $\text{Cs}_3\text{PW}_{12}\text{O}_{40}$ and $(\text{NH}_4)_3\text{PW}_{12}\text{O}_{40}$. (From Ref. 44c.)

TABLE IV
 Adsorption Data for $Cs_xH_{3-x}PW_{12}O_{40}$ ($x = 2.1, 2.2, \text{ and } 2.5$) (48)

Molecule C.S. ^a (Å ²)	Kinetic diameter (Å)	Pressure (Torr) (P/P_0) ^b	Temperature (K)	Adsorption amount ($\mu\text{mol g}^{-1}$)			
				Cs2.1	Cs2.2	Cs2.5	Ratio ^c
N ₂ (16.2)	3.6	137 (0.18)	77	487	861	1648	0.52
Benzene (30.5)	5.9	21 (0.20)	300	10	124	232	0.53
Neopentane (37.2)	6.2	99 (0.19)	273	5	179	390	0.46
1,3,5-TMB ^d (41.1)	7.5	0.6 (0.20)	300	—	11	237	0.05
1,3,5-TIPB ^e (59.4)	8.5	9×10^{-3} (0.20)	300	—	15	236	0.06

^a Cross section calculated from the molecular weight and density of liquid. ^b The ratio of the partial pressure introduced (P) to the saturated vapor pressure (P_0). ^c Adsorption amount on Cs2.2 divided by that on Cs2.5. ^d 1,3,5-Trimethylbenzene. ^e 1,3,5-Triisopropylbenzene.

intracrystalline. Considering the size and shape of the Keggin anion and the structure of $Cs_3PW_{12}O_{40}$ (Fig. 2c), there are no open pores in the crystal through which an N₂ molecule (3.6 Å in diameter) can pass.

Recently, it was found that $Cs_{2.2}H_{0.8}PW_{12}O_{40}$ (abbreviated as Cs2.2) is microporous and, according to adsorption experiments, has effective pores of about 7 Å (48). Table IV is a comparison of the adsorption capacities of Cs2.2 and $Cs_{2.5}H_{0.5}PW_{12}O_{40}$ (abbreviated as Cs2.5) for various molecules. Benzene (kinetic diameter = 5.9 Å) and neopentane (kinetic diameter = 6.2 Å) are adsorbed on Cs2.2 and Cs2.5, and the relative adsorption capacity of Cs2.2 and Cs2.5 are similar to the corresponding ratio for N₂ adsorption. On the other hand, both benzene and neopentane are little adsorbed on $Cs_{2.1}H_{0.9}PW_{12}O_{40}$ (Cs2.1), indicating that the effective pore size of Cs2.1 is less than 5.9 Å. Of particular interest are the results observed with 1,3,5-trimethylbenzene (kinetic diameter = 7.5 Å) and 1,3,5-triisopropylbenzene (kinetic diameter = 8.5 Å). These two alkylbenzenes are adsorbed significantly on Cs2.5, but little on Cs2.2, so that the pore size of Cs2.2 is in the range of 6.2–7.5 Å and that of Cs2.5 is larger than 8.5 Å. This result demonstrates that the pore structure can be controlled by the substitution of H⁺ by Cs⁺ (48).

B. SYNTHESIS

Heteropolyacids are prepared in solution by acidifying and heating in the appropriate pH range (1, 49–54). For example, 12-tungstophosphate is formed according to Eq. (1). Free acids are synthesized primarily by the following two methods: (1) by extraction with ether from acidified aqueous solutions and (2) by ion exchange from salts of heteropolyacids. Dawson-type heteropolyanions,

$X_2W_{18}O_{62}^{6-}$, are isolated as soluble ammonium or potassium salts or as free acids by extraction into ether (29, 30).

Mixed addenda heteropolyanions with regiospecific substitution need careful preparation by use of lacunary heteropolyanions. If they are prepared from aqueous solutions of corresponding oxoanions, the products are usually mixtures of heteropolyanions having different compositions of addenda atoms. General procedures for the syntheses of various kinds of heteropolyacids are described in the literature (51–54).

C. STABILITY

Particular attention should be paid to both the stability in solution and the thermal stability. The condensation–hydrolysis equilibria of heteropolyanions in aqueous media are shown in Fig. 8. Each heteropolyanion is stable only at pH values lower than the corresponding solid line (55). Some solid heteropolyacids are thermally stable and applicable in reactions with vapor-phase reactants conducted at high temperatures. The thermal stability is measured mainly by X-ray diffraction (XRD), thermal gravimetric analysis, and different thermal analysis (TG-DTA) experiments. According to Yamazoe *et al.* (56), the decomposition temperatures of $H_3PMo_{12}O_{40}$ and its salts depend on the kinds of cations: Ba^{2+} , Co^{2+} (673 K) < Cu^{2+} , Ni^{2+} (683 K) < H^+ , Cd^{2+} (693 K) < Ca^{2+} , Mn^{2+} (700 K) < Mg^{2+} (710 K) < La^{3+} , Ce^{3+} (730 K), where the

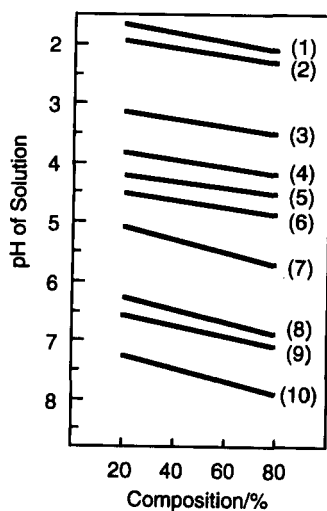
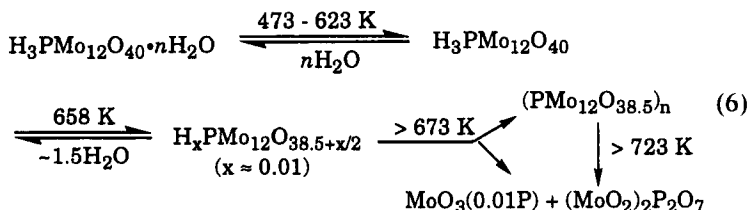


FIG. 8. Stabilities of aqueous heteropolyacids (from Ref. 55): (1) $PMo_{12}O_{40}^{3-}$, (2) $PW_{12}O_{40}^{3-}$, (3) $GeMo_{12}O_{40}^{4-}$, (4) $GeW_{12}O_{40}^{4-}$, (5) $P_2W_{18}O_{62}^{6-}$, (6) $SiW_{12}O_{40}^{4-}$, (7) $PMo_{11}O_{39}^{3-}$, (8) $P_2Mo_5O_{23}^{3-}$, (9) $H_2W_{12}O_{40}^{6-}$, (10) $PW_{11}O_{39}^{3-}$.

decomposition temperature (in parentheses) is estimated by the exothermic peak in DTA.

Herve *et al.* (57) investigated the thermal changes of structures by means of XRD and TG-DTA for Keggin-type heteropolyacids and proposed Scheme 2. Infrared spectroscopy of $H_4PMo_{11}VO_{40}$ showed the release of vanadium atoms to form $H_3PMo_{12}O_{40}$ and vanadium phosphate species (58). Exposure to water vapor induces the decomposition of the latter (indicated by the disappearance of a band at *ca.* $1037\text{--}1030\text{ cm}^{-1}$) (58).

Results from TG and DTA show the presence of two types of water in heteropoly compounds, i.e., water of crystallization and "constitutional water molecules" (59). Loss of the former usually occurs at temperatures below 473 K. At temperatures exceeding 543 K for $H_3PMo_{12}O_{40}$ or 623 K for $H_3PW_{12}O_{40}$, the constitutional water molecules (acidic protons bound to the oxygen of the polyanion) are lost. Data obtained by *in situ* XRD, ^{31}P NMR, and thermoanalysis show that thermolysis of $H_3PMo_{12}O_{40}$ proceeds in two steps, as shown by Eq. (6) (60).



The MoO_3 phase appears at temperatures higher than 573 K.

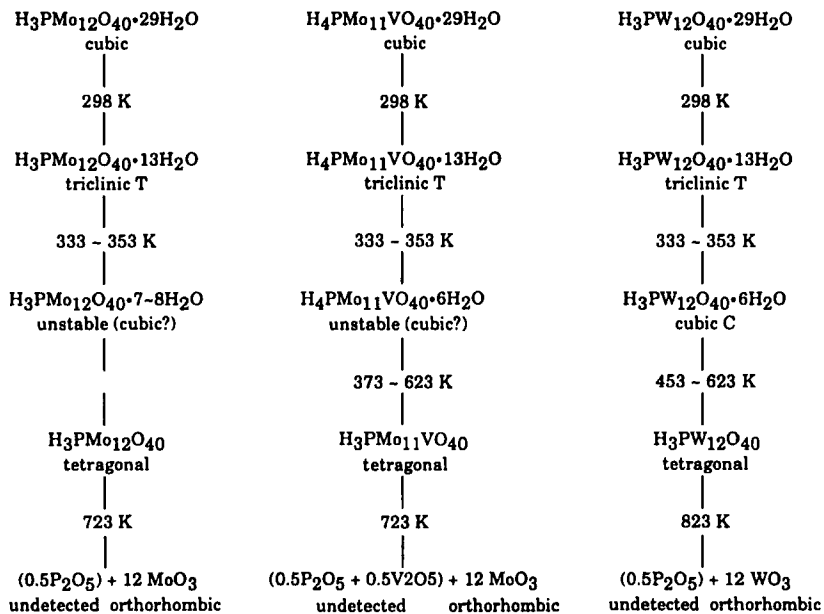
Thermal gravimetric analysis of $H_3PW_{12}O_{40}$ and of $Cs_{2.5}H_{0.5}PW_{12}O_{40}$ showed that entire water molecules of crystallization are lost at temperatures as low as 573 K, and acidic groups are removed as water is formed from protons and lattice oxygens at temperatures exceeding 623 K. The numbers of protons lost, x , in $Cs_{2.5}H_{0.5-x}PW_{12}O_{40-x/2}$ were 0.24, 0.31, and 0.32 after treatment at 623, 673, and 773 K, respectively, whereas infrared spectra of $Cs_{2.5}H_{0.5}PW_{12}O_{40}$ remained unchanged at temperatures up to 773 K (61a). Similar removal of protons of $K_{2.5}H_{0.5}PMo_{12}O_{40}$ begins by 500 K (61b).

D. CHARACTERIZATION OF HETEROPOLY COMPOUNDS

1. Infrared Spectroscopy

Infrared (IR) spectroscopy is a convenient and widely used method for the characterization of heteropolyanions. Keggin, Dawson, and lacunary heteropolyanions can be distinguished by their characteristic bands.

a. *Keggin Structure.* In Table V (62–64), a partial list of the reported IR bands is given with their assignments. IR spectra of $XW_{12}O_{40}^{n-}$, $XMo_{12}O_{40}^{n-}$, and



SCHEME 2.

metatungstate are shown in Fig. 9 (62a). The vibrational mode of XO_4 is almost independent of the others for $\text{X} = \text{P}$, but it is mixed with other vibrational modes for $\text{X} = \text{Si}, \text{Ge}, \text{B}$, etc. (64). The X—O stretching bands (Si , 923 cm^{-1} ; Ge , 830 cm^{-1} ; P , 1080 cm^{-1}) for $\text{XW}_{12}\text{O}_{40}^{n-}$ show higher frequencies than those

TABLE V
Infrared Absorption Bands of Heteropolyacids, cm^{-1} (62-64)

$\text{H}_3\text{PW}_{12}\text{O}_{40}$	$\text{H}_4\text{SiW}_{12}\text{O}_{40}$	$\text{H}_4\text{GeW}_{12}\text{O}_{40}$	$\text{H}_5\text{BW}_{12}\text{O}_{40}$	$\text{H}_6\text{CoW}_{12}\text{O}_{40}$	$\text{H}_6\text{P}_2\text{W}_{18}\text{O}_{62}$	Modes of vibration
1080	926	818	914	445	1091	$\nu_{as}(\text{X}-\text{O})$
982	980	978	960	960	962	$\nu_{as}(\text{W}=\text{O})$
893	878	886	902	895	914	$\nu_{as}(\text{W}-\text{O}-\text{W})$
812	779	765	810	738	780	$\nu_{as}(\text{W}-\text{O}-\text{W})$
$\text{H}_3\text{PMo}_{12}\text{O}_{40}$	$\text{H}_4\text{SiMo}_{12}\text{O}_{40}$	$\text{H}_4\text{GeMo}_{12}\text{O}_{40}$	Modes of vibration			
1070	910	802	$\nu_{as}(\text{X}-\text{O})$			
965	958	955	$\nu_{as}(\text{Mo}=\text{O})$			
870	860	875	$\nu(\text{Mo}-\text{O}-\text{Mo})$			
790	780	765				

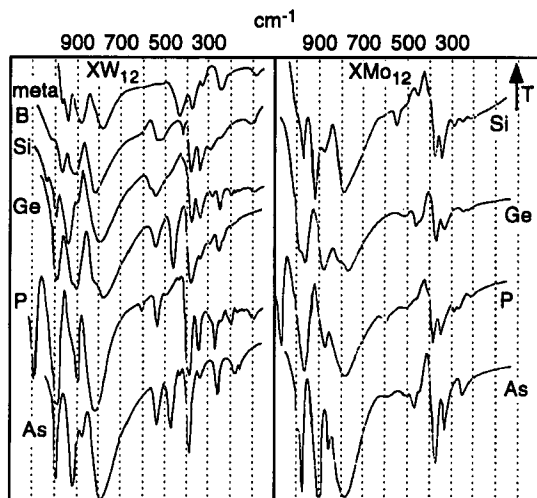


FIG. 9. Infrared spectra of $XW_{12}O_{40}^{n-}$ and $XM_{12}O_{40}^{n-}$. (From Ref. 62a.)

of XO_4^{n-} anions, suggesting higher π -bond character of $X-O$ bonds in the Keggin anion. Cation size influences the $\nu(W-O_d)$ frequencies for β - $SiW_{12}O_{40}^{4-}$; the value of $\nu(W-O_d)$ decreases as the van der Waals radii of tetraalkylammonium cations increase (65). Due to the loss of hydrogen bonding between O_d and water, the $M-O_d$ band ($M = Mo, W$) shifts to a higher frequency and the $P-O$ and $M-O_d$ peak intensities change (5). The $W-O_d$ band for anhydrous $Cu_{1.5}PW_{12}O_{40}$ splits into doublets, suggesting a direct interaction between the polyanion and Cu^{2+} (66).

In Table VI, IR bands of lacunary $XM_{11}O_{39}^{n-}$ are summarized (67). The $P-O$ stretching band for $PW_{11}O_{39}^{7-}$ is split into 1085 and 1040 cm^{-1} . It is believed

TABLE VI
Infrared Absorption Bands of $XM_{11}O_{39}^{n-}$ Compounds (K^+ or NH_4^+ salts), cm^{-1} (67)

$PW_{11}O_{39}^{7-}$	$PMo_{11}O_{39}^{7-}$	$SiW_{11}O_{39}^{8-}$	$SiMo_{11}O_{39}^{8-}$	
{ 1085 1040	1060 1010			$\nu_{as}(P-O)$
950	{ 930 900	952	{ 930 910	$\nu(M-O_d)$
		885	870	$\nu_{as}(Si-O)$
{ 900 860	860	870	830	$\nu(M-O_b-M)$
{ 810 725	{ 790 742	{ 797 725	740	$\nu(M-O_c-M)$

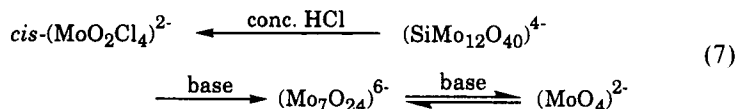
that the change of the symmetry from T_d (XM_{12}) to C_s (XM_{11}) leads to the broadening of the band and sometimes causes bond splitting (67).

The isomers, α - and β - $PMo_{12}O_{40}^{3-}$ or $SiW_{12}O_{40}^{4-}$, can also be distinguished by IR spectroscopy (68). The effects of solvent on the frequency have been reported (69). IR spectra of hydrated $H_3PW_{12}O_{40}$ include a broad OH stretching band and two OH bending bands, at 1610 and 1720 cm^{-1} . The latter two correspond to water and protonated water, respectively (1).

b. *Dawson Structure* (70). The IR spectrum of α - $P_2W_{18}O_{62}^{6-}$ resembles that of $PW_{12}O_{40}^{3-}$. Three IR bands are observed in the PO_4 stretching region, at 1090 (s), 1022 (w), and about 975 cm^{-1} (sh) due to D_{3h} symmetry of two PO_4 groups. IR bands at 960, 912, and 780 cm^{-1} are assigned to $\nu(W-O_b)$, $\nu(W-O_c)$, and $\nu(W-O_b)$, respectively.

2. Raman Spectroscopy

Vibrational frequencies in the Raman spectra of XM_{11} and XM_{12} ($X = Si, P$; $M = Mo, W$) are summarized in Table VII (62, 65, 67, 71). The $X-O$ vibration in T_d symmetry of XO_4 is Raman-inactive. Among $M-O$ bonds, $M-O_d$ is Raman-active. Raman spectra indicate that with an increase in pH, the structure of $PMo_{12}O_{40}^{3-}$ in aqueous solution changes, as shown by Eq. (7).



The states of hydrates of heteropolyacids are best distinguished by Raman spectroscopy, since Raman spectra give better resolved OH stretching bands than IR spectra (62, 72). $H_3PW_{12}O_{40} \cdot 29H_2O$ has bands at 3570, 3525, 3490, 3450, 3205, and 3140 cm^{-1} , which correspond to O-H distances of 2.94, 2.89, 2.86, 2.84, 2.72, and 2.65, respectively. The bands at 3205 and 3140 cm^{-1} are assigned to $\nu(OH)$ of $H(H_2O)_n^+$. The OH frequencies of $H_3PMo_{12}O_{40}$ and $H_4SiW_{12}O_{40}$ appear at 3570 and 3525 cm^{-1} , respectively.

TABLE VII
Raman Vibrational Frequencies of Keggin Anions (Aqueous Solutions), cm^{-1} (62, 65, 67, 71)

$PW_{12}O_{40}^{3-}$	$SiW_{12}O_{40}^{4-}$	$PMo_{12}O_{40}^{3-}$	$SiMo_{12}O_{40}^{4-}$	$PW_{11}O_{39}^{7-}$	$PMo_{11}O_{39}^{7-}$
1011	998	997	982	979	963
996	981	981	962	964	948
					$\nu_\nu(M-O_d)^a$
					$\nu_\alpha(M-O_d)$

^a $\nu_\nu(M-O_d)$ shows polarized vibration.

3. NMR Spectroscopy

a. *Solid-State ^1H NMR Spectroscopy.* The broad-line NMR spectrum of $\text{H}_3\text{PMo}_{12}\text{O}_{40} \cdot 29\text{H}_2\text{O}$ shows that H_3O^+ and H_2O become indistinguishable at temperatures greater than 298 K (73, 74). The NMR spectrum of anhydrous $\text{H}_3\text{PMo}_{12}\text{O}_{40}$ includes a narrow resonance (width <1 G) at 298 K due to equivalent protons (75). The H--H distance in anhydrous $\text{H}_3\text{PW}_{12}\text{O}_{40}$ is estimated to be 4.0–4.5 Å (76).

Three different states of protons are detected by solid-state ^1H MAS NMR spectroscopy for $\text{H}_3\text{PW}_{12}\text{O}_{40} \cdot n\text{H}_2\text{O}$ at room temperature, as shown in Fig. 10 (77). A sharp ^1H resonance observed for $n = 17$ shows that the protons are in a uniform state and highly mobile. Much broader and weaker lines for less hydrated states indicate lower mobility of protons. The chemical shifts for $n = 17$ and $n = 6$ (7.3–7.5 ppm) correspond to clusters of hydrated water, as in Fig. 2a. The resonance at 9.2 ppm, for anhydrous $\text{H}_3\text{PW}_{12}\text{O}_{40}$ was assigned to protons attached to the most basic bridging oxygen atoms, on the basis of IR results (78) and the basicity estimated by ^{17}O NMR spectroscopy (see below).

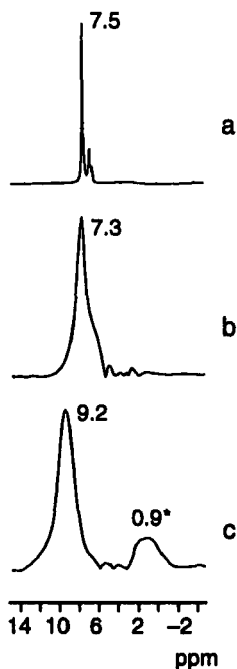


FIG. 10. ^1H MAS NMR spectra of $\text{H}_3\text{PW}_{12}\text{O}_{40} \cdot n\text{H}_2\text{O}$: (a) $n = 17$, (b) $n = 6$, (c) $n = 1.5$. (From Ref. 77.)

TABLE VIII
Chemical Shifts of ^{31}P for Heteropoly Compounds

Solution (ppm)	Reference	Solid (ppm)	Reference		
$\text{PMo}_{12}\text{O}_{40}^{3-}$	-3.9	79	$\text{H}_3\text{PMo}_{12}\text{O}_{40} \cdot 30\text{H}_2\text{O}$	-3.9	61b
$\text{PMo}_9\text{O}_{34}^{9-}$	-1.4	79	$\cdot 0\text{H}_2\text{O}$	-2.9	61b
$\text{P}_2\text{Mo}_{18}\text{O}_{62}^{6-}$	-2.9 to -3.4	79	$\text{Na}_3\text{PMo}_{12}\text{O}_{40}$	-4.0	82
$\text{PMo}_9\text{V}_3\text{O}_{40}^{9-}$	-1.7 to -3.4	^a	$\text{K}_3\text{PMo}_{12}\text{O}_{40}$	-4.4	82
$\text{PW}_{12}\text{O}_{40}^{3-}$	-14.9	79 ^a	$\text{Cs}_3\text{PMo}_{12}\text{O}_{40}$	-4.5	82
$\text{PW}_{11}\text{O}_{39}^{7-}$	-10.4	79 ^a	$(\text{NH}_4)_3\text{PMo}_{12}\text{O}_{40}$	-4.5	82
$\text{P}_2\text{W}_{18}\text{O}_{62}^{6-}$	-12.7	79 ^a	$(\text{NH}_4)_6\text{P}_2\text{Mo}_{18}\text{O}_{62}$	-3.1	82
$\text{PW}_{11}\text{MoO}_{40}^{3-}$	-14.2	79	$\text{Cs}_3\text{PMo}_{11}\text{WO}_{40}$	-5.5	82
$\text{PW}_{11}\text{VO}_{40}^{4-}$	-14.2	85	$\text{H}_3\text{PW}_{12}\text{O}_{40} \cdot 17\text{H}_2\text{O}$	-15.1	77
$\text{PW}_{10}\text{V}_2\text{O}_{40}^{3-}$	-13.6	85	$\cdot 6\text{H}_2\text{O}$	-15.6	77
$\text{PW}_9\text{V}_3\text{O}_{40}^{6-}$	-13.4	85	$\cdot 0.5\text{H}_2\text{O}$	-11.1	77
$\text{PV}_{14}\text{O}_{42}^{9-}$	+1.0	^b	$\text{Cs}_{2.5}\text{H}_{0.5}\text{PW}_{12}\text{O}_{40}$	-10.9 ~ -14.9	47
			$\text{Cs}_3\text{PW}_{12}\text{O}_{40}$	-15.3	47

^aO'Donnell, S. E., and Pope, M. T., *J. Chem. Soc. Dalton*, 2290 (1976). ^bKato, R., Kobayashi, A., and Sasaki, Y., *Inorg. Chem.* **21**, 240 (1982).

b. ^{31}P NMR Spectroscopy. The ^{31}P chemical shift provides important information concerning the structure, composition, and electronic states of these materials. The chemical shifts of typical heteropoly compounds are summarized in Table VIII. The chemical shift in aqueous solutions is correlated with the $\text{P}-\text{O}_a$ bond strength [$\nu(\text{P}-\text{O}_a)$] (70). Little solvent effect on chemical shift indicates that the central atom is effectively shielded. The decrease of the chemical shift in the series $\text{PW}_{12}\text{O}_{40}^{3-} > \text{PMo}_{12}\text{O}_{40}^{3-} > \text{PV}_{12}\text{O}_{40}^{9-}$ parallels the decrease in the IR frequency of PO_4 , with both reflecting $\text{P}-\text{O}$ π -bonding character.

Five resonances observed for $\text{H}_5\text{PV}_2\text{Mo}_{10}\text{O}_{40}$ correspond to the possible five isomers, in which the locations of two vanadium atoms are different (80). $\text{PMo}_6\text{W}_6\text{O}_{40}^{3-}$ in aqueous solution gives 13 peaks expected from the statistical distribution of $\text{PW}_{12-x}\text{Mo}_x\text{O}_{40}$ ($x = 0-12$) (81). Figure 11 shows the solid-state ^{31}P NMR spectrum of $\text{Cs}_3\text{PMo}_{11}\text{WO}_{40}$ (82) prepared from mixed aqueous solutions of $\text{H}_3\text{PMo}_{12}\text{O}_{40}$, $\text{H}_3\text{PW}_{12}\text{O}_{40}$, and CsNO_3 . Five resonances agree well with the spectrum observed from the reaction mixture in solution and are assigned to a statistical mixture of $\text{Cs}_3\text{PMo}_{12-x}\text{W}_x\text{O}_{40}$ ($x = 0-4$). $\text{M}_3\text{PMo}_{12}\text{O}_{40}$ ($\text{M} = \text{H}, \text{Na}, \text{K}, \text{Cs}, \text{and } \text{NH}_4$) give similar chemical shifts.

The ^{31}P NMR chemical shift is greatly dependent on n in $\text{H}_3\text{PW}_{12}\text{O}_{40} \cdot n\text{H}_2\text{O}$ (47, 77), the values being -15.1 to -15.6 ppm for $n = 6$ and -11.1 to -10.5 ppm for $n = 0$. This difference is explained as follows: In the former, protonated water, $\text{H}(\text{H}_2\text{O})_2^+$, is connected with the heteropolyanion by

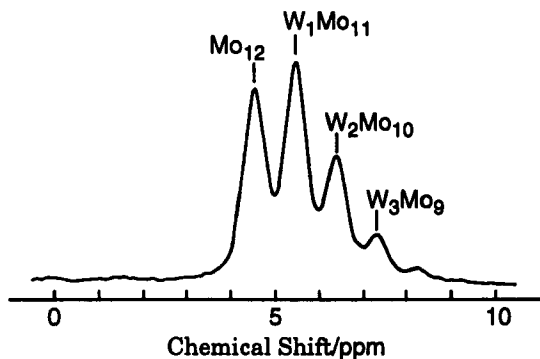


FIG. 11. ^{31}P MAS NMR spectrum of $\text{Cs}_3\text{PMo}_{11}\text{WO}_{40}$. (From Ref. 82.)

hydrogen-bonding at terminal oxygens, and in the latter, protons are directly attached to oxygen atoms of the polyanion.

c. ^{183}W , ^{95}Mo , and ^{29}Si NMR Spectroscopy. ^{183}W Chemical shifts are sensitive to the heteroatom (83), being -130.4 ppm for $\text{BW}_{12}\text{O}_{40}^{5-}$, -111.3 ppm for $\text{H}_2\text{W}_{12}\text{O}_{40}^{6-}$, -103.8 ppm for $\text{SiW}_{12}\text{O}_{40}^{4-}$, and -98.8 ppm for $\text{PW}_{12}\text{O}_{40}^{3-}$. $\text{SiW}_{11}\text{O}_{39}^{8-}$ has five pairs of structurally identical W atoms and one unique W atom. Accordingly, $\text{SiW}_{11}\text{O}_{39}^{8-}$ gives six clearly separated resonances having the intensity ratio of $2:1.6:1:2:2:2$, which is close to the expected ratio of $2:2:1:2:2:2$. Similarly, $\text{P}_2\text{W}_{18}\text{O}_{62}^{6-}$, which has twelve equivalent W atoms around its belt and six equivalent W atoms capping its ends (26), has two resonances; the larger one at -170.14 ppm and the smaller doublet at -124.87 ppm.

The ^{183}W NMR spectrum of 6-electron reduced $\alpha\text{-SiW}_{12}\text{O}_{40}^{4-}$ shows three narrow resonances with the intensity ratio $1:1:2$ (Fig. 12) (84). Two (3W, 6W)

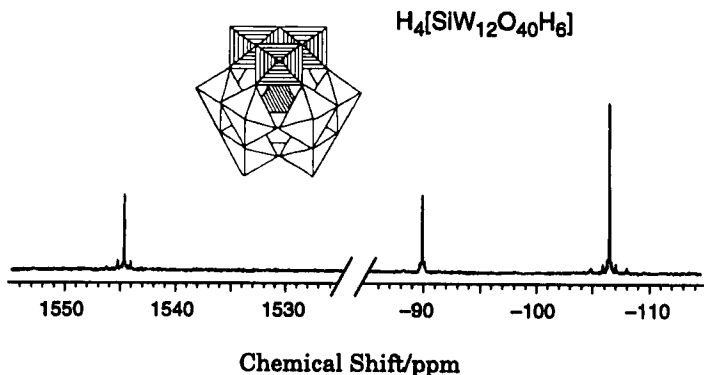


FIG. 12. ^{183}W NMR spectrum of $\text{SiW}_{12}\text{O}_{40}\text{H}_6^{4-}$. The peak at 1545 ppm is due to W(IV) which occupy an edge-shared triad (cross hatched). (From Ref. 84.)

have chemical shifts very close to that in the oxidized state and assigned to W(VI), whereas the third (-1500 ppm) is attributed to a W(IV) anion. This assignment is supported by the chemical shift of the W(IV) cation, $W_3O_4(H_2O)_9^{4+}$. It is suggested that the protonated $W_6(V)W_6(VI)$ polyanion undergoes intramolecular disproportionation to give $W_3(IV)W_9(VI)$ species.

The structures of positional isomers, α -1,2- $XV_2W_{10}O_{40}^{n-}$ and α -1,2,3- $XV_3W_9O_{40}^{(n+1)-}$ ($X = Si, P$), are established from the 2-D connectivity pattern and 1-D spectra of ^{183}W (85). The spectra of $XV_3W_9O_{40}^{n-}$ ($X = Si, P$) are exclusively of the α -1,2,3-isomers. α - And β - $SiW_{12}O_{40}^{4-}$ can be also distinguished by ^{183}W NMR spectroscopy; α - $SiW_{12}O_{40}^{4-}$ gives one singlet (12 equivalent W atoms), and β - $SiW_{12}O_{40}^{4-}$ three resonances in the ratio 1 : 2 : 1 (86).

d. ^{17}O NMR Spectroscopy. ^{17}O NMR spectroscopy gives information about the bonding nature of oxygen atoms. Figure 13 shows the assignments of the chemical shifts (87–89). There is a correlation between the downfield shift and the decreasing number of metal atoms to which the oxygen atom is bonded. The chemical shifts for the $SiMo_{12}O_{40}^{4-}$, $SiW_{12}O_{40}^{4-}$, $PMo_{12}O_{40}^{3-}$, and $PW_{12}O_{40}^{3-}$ are summarized in Table IX.

4. Electronic Spectra

Electronic absorption spectra give information about the electronic states of heteropolyanions (2). $PW_{12}O_{40}^{3-}$ shows absorption at about $38,000\text{ cm}^{-1}$, due to

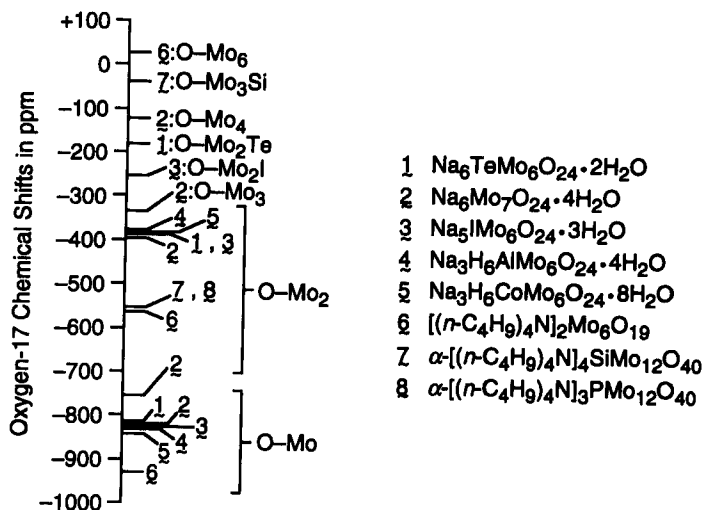


FIG. 13. Assignments of ^{17}O NMR shifts due to various salts of mixed oxides. (From Refs. 87–89.)

TABLE IX
 ^{17}O NMR Spectral Data for Heteropolyanions (87–89)

Anions	Chemical shift (ppm)		
	M–O _d	M–O _b –M, M–O _c –M	M–O _a –(M) ₃
SiMo ₁₂ O ₄₀ ⁴⁻	928	580, 555	41
SiW ₁₂ O ₄₀ ⁴⁻	761	427, 405	21
SiMoW ₁₁ O ₄₀ ⁴⁻	929(Mo–O _d) 726(W–O _d)	504, 469	27
PMo ₁₂ O ₄₀ ³⁻	936	583, 550	78
PW ₁₂ O ₄₀ ³⁻	769	431, 405	—

ligand (oxygen) to metal (W) charge transfer (LMCT) (90). In most cases of $\text{XW}^{5+}\text{W}_{11}\text{O}_{40}^{n-}$ (one-electron reduction heteropoly blues), three absorption bands are observed at 8000–10,000 cm^{-1} (band A), 13,000–16,000 cm^{-1} (band B), and *ca.* 20,000 cm^{-1} (band C) in addition to that at 38,000 cm^{-1} . The bands B and A are the results of intervalence charge-transfer transitions (IVCT) between metal atoms. Two types of transition are possible for reduced Keggin anions, that is, within an edge-shared group of MO₆ octahedra (“intra” transition) and those between metals atoms linked by corner sharing. The band A has tentatively been assigned to an “intra” and the band B to an “extra” transition (2). The UV band positions of various heteropolyacids are summarized in Table X (90–93).

TABLE X
 UV Absorption Bands of Heteropolyanions

Compounds	Absorption ^a (kK)	Half-wave potential ^b (V)
PW ₁₂ O ₄₀ ³⁻	38.0, 50.0	–0.023
SiW ₁₂ O ₄₀ ⁴⁻	38.1	–0.187
FeW ₁₂ O ₄₀ ⁵⁻	37.8	–0.349
BW ₁₂ O ₄₀ ⁵⁻	39.0	–0.520
CoW ₁₂ O ₄₀ ⁶⁻	38.3	–0.510
P ₂ W ₁₈ O ₆₂ ⁶⁻	34.0, 39.0	+0.02 ^a
P ₂ Mo ₁₈ O ₆₂ ⁶⁻	31.0, 47.0	–0.55 ^a
PMo ₁₂ O ₄₀ ³⁻	32.3, 47.2	—
PW ₁₁ V(IV)O ₄₀ ⁵⁻	20.0, 25.0	—
SiVW ₁₁ O ₄₀ ⁶⁻	20.2	—

^a See Refs. 90–93. ^b Pope, M. T., and Varga, G. M., *Inorg. Chem.* **5**, 1249 (1966); Prados, R. A., and Pope, M. T., *Inorg. Chem.* **15**, 2547 (1976).

5. Others

a. *Extended X-Ray Absorption Fine Structure (EXAFS) Spectroscopy.* EXAFS spectra of $\text{PMo}_{12}\text{O}_{40}^{3-}$ and $\text{PW}_{12}\text{O}_{40}^{3-}$ as amine salts have been measured (94, 95). $\text{PW}_{12}\text{O}_{40}^{3-}$ gives distinct peaks due to $\text{W}-\text{O}_d$ (0.16 nm) and $\text{W}-\text{O}-\text{W}$ (0.196 nm), whereas $\text{Mo}-\text{O}$ peaks of $\text{PMo}_{12}\text{O}_{40}^{3-}$ are not discernible. For the latter, a large Debye-Waller factor for $\text{Mo}-\text{O}$ bonds and also multiple scattering effects are presumed.

b. *Scanning Tunneling Microscopy (STM) and Transmission Electron Microscopy (TEM).* $\text{H}_3\text{PW}_{12}\text{O}_{40}$ deposited on freshly cleaved and highly oriented pyrolytic graphite in air has been measured by STM (96). A fairly regular periodic pattern is observed, suggesting that the individual heteropoly species were directly imaged. Individual anions of the Dawson-type cyclopentadienyl titanium (CpTi) heteropoly compound, $\text{K}_7(\text{C}_5\text{H}_5)\text{TiP}_2\text{W}_{17}\text{O}_{61}$, were observed by TEM (97). The size of the anion is estimated to be 1.0–1.5 nm. This is consistent with a size determined from X-ray crystallographic data indicating an ellipsoid of about 1.0×1.5 nm.

c. *Electron Spin Resonance (ESR) Spectroscopy.* ESR spectra give information about mixed-valence structures of reduced heteropoly compounds. ESR data for Keggin-type molybdates reduced by one electron ($1e^-$ reduction) in solution are shown in Table XI (2, 92, 98, 99). A Mo^{5+} signal with hyperfine structure due to Mo^{5+} ($I = 5/2$) is observed for $\text{PMo}^{5+}\text{Mo}_{11}^{6+}\text{O}_{40}^{4-}$ at temperatures less than 40 K (99). At higher temperatures line broadening is observed, and the hyperfine structure disappears. At room temperature, no Mo^{5+} signal is observed. These results indicate the rapid hopping of an electron among

TABLE XI
ESR Parameters of Some Reduced Polymolybdates
(from Ref. 2)

Anion	g_{\parallel}	g_{\perp}
$[\text{Mo}_6\text{O}_{19}]^{3-}$	1.916	1.930
$[\text{MoW}_5\text{O}_{19}]^{3-}$	1.917	1.924
$\alpha\text{-}[\text{PMo}_{12}\text{O}_{40}]^{4-}$	1.938	1.949
$\alpha\text{-}[\text{PMoW}_{11}\text{O}_{40}]^{4-}$	1.913	1.939
$\alpha\text{-}[\text{AsMo}_{12}\text{O}_{40}]^{4-}$	1.935	1.948
$\alpha\text{-}[\text{SiMo}_{12}\text{O}_{40}]^{5-}$	1.931	1.944
$\alpha\text{-}[\text{SiMoW}_{11}\text{O}_{40}]^{5-}$	1.914	1.931
$\alpha\text{-}[\text{GeMo}_{12}\text{O}_{40}]^{5-}$	1.935	1.951

12 equivalent Mo atoms in a Keggin anion at higher temperature, and the mixed valence behavior is classified as class II (99, 100). The extent of electron delocalization increases as the number of molybdenum atoms in a Keggin anion increases. The order of extent of electron hopping is estimated to be $\text{PMo}_{12}\text{O}_{40}^{4-} > \text{GeMo}_{12}\text{O}_{40}^{5-} > \text{Mo}_6\text{O}_{19}^{3-}$ (99). A similar electron hopping is estimated by the very weak signal intensity of Mo^{5+} for solid $\text{H}_{3+x}\text{PMo}_{12}\text{O}_{40}$ reduced by H_2 at 423 K or room temperature (101, 102). Upon $2e^-$ reduction, about 60% and 100% of the electrons are paired for $\text{SiMo}_{12}\text{O}_{40}^{6-}$ and $\text{PW}_{12}\text{O}_{40}^{5-}$, respectively, and the latter shows diamagnetism (2).

Solid $\text{H}_3\text{PMo}_{12}\text{O}_{40}$ reduced by H_2 at a lower temperature shows a very weak ESR signal intensity of Mo^{5+} , probably because most of the Mo^{5+} ions are not detectable due to the rapid hopping of electrons. Heat treatment, which eliminates oxide ions from the heteropoly anion, leads to development of the Mo^{5+} signal, indicating the localization of electrons (101, 102). Early reports of ESR spectra of reduced $\text{H}_3\text{PMo}_{12}\text{O}_{40}$ are likely due to these species. Several different species are observed in highly reduced samples.

The extent of reduction of $\text{H}_3\text{PMo}_{12}\text{O}_{40}$ during the oxidation of methacrolein has also been investigated by application of ESR spectroscopy for detection of Mo^{5+} (103). The states of V in the mixed-valence Keggin anion and Cu countercation were also investigated. The results show that more reducible countercations or addenda atoms such as Cu^{2+} and V^{5+} are reduced first, and an electron is localized on them (104–106).

d. *X-Ray Photoelectron Spectroscopy (XPS)*. XPS gives information about electron density of solid heteropoly compounds (107–115). It was reported that Mo^{5+} was fairly uniformly present throughout the bulk of $\text{H}_3\text{PMo}_{12}\text{O}_{40}$ formed by H_2 reduction, whereas the surface was preferentially reduced by cyclohexane (101). The oxidation states of countercations Pd, Zn, and Cu were investigated by XPS in relation to redox properties and oxidation catalysis. Cu^{2+} and Pd^{2+} , having higher electron affinities than Mo^{6+} , in 12-molybdophosphates are easily reduced by H_2 and act as electron reservoirs (107–109).

The following observations have been made for bulk heteropoly compounds.

1. The binding energy of $\text{O}1s$ electrons decreases with increasing negative charge of the heteropolyanion: $\text{PW}_{12}\text{O}_{40}^{3-} > \text{SiW}_{12}\text{O}_{40}^{4-} \geq \text{BW}_{12}\text{O}_{40}^{5-} > \text{H}_2\text{W}_{12}\text{O}_{40}^{6-} > \text{PW}_{11}\text{O}_{39}^{7-} > \text{SiW}_{11}\text{O}_{39}^{8-} > \text{H}_2\text{W}_{12}\text{O}_{42}^{10-}$ (113).
2. For isostructural heteropolyanions, the $\text{O}1s$ binding energy is higher for tungstates than for molybdates (113).
3. In $\text{PMo}_{12}\text{O}_{40}^{5-}$ and $\text{SiMo}_{12}\text{O}_{40}^{6-}$ ($2e^-$ reduced state), two Mo atoms are in the oxidation state of +5 and ten Mo atoms are in the +6 state (113, 114). A similar result was obtained for $2e^-$ -reduced $\text{PW}_{12}\text{O}_{40}^{3-}$ (113, 114).

4. A good correlation exists between the acid strength and the difference between O1s and W4f binding energies of $H_3PW_{12}O_{40}$ and its salts (115).

III. Acidic Properties

A. ACIDITY IN SOLUTION

Typical heteropolyacids having the Keggin structure, such as $H_3PW_{12}O_{40}$ and $H_4SiW_{12}O_{40}$, are strong acids; protons are dissociated completely from the structures in aqueous solution (8, 116). The dissociation constants, pK_a , of heteropolyacids depend on the solvent. These are summarized in Table XII, together with pK_a values for mineral acids (117–119). Heteropolyacids are much stronger acids than H_2SO_4 , HBr, HCl, HNO_3 , and $HClO_4$. For example, in acetic acid, the acid strength of $H_3PW_{12}O_{40}$ is greater than that of H_2SO_4 by about 2 pK_a units. In acetic acid, which is less polar than water, heteropolyacids behave as relatively weak 1–1 electrolytes.

The effect of solvent is evident for mixed solvents (120); as the concentration of water in aqueous acetic acid changes from 100 vol% to 4 vol%, the Hammett acidity function, H_0 , for $H_3PW_{12}O_{40}$ (0.1 M) decreases from 0.01 to -1.78 ,

TABLE XII
Acid Constants of Heteropolyacids in Nonaqueous Media at 298 K (116–119)

Acid	Acetone			Ethanol			Acetic acid pK_1
	pK_1	pK_2	pK_3	pK_1	pK_2	pK_3	
$H_3PW_{12}O_{40}$	(1.6)	(3.0)	3.98	(1.6)	(3.0)	4.1	4.77
$H_4PW_{11}VO_{40}$	(1.8)	(3.2)	4.37	—	—	—	4.74
$H_5PW_{10}V_2O_{40}$	—	—	—	—	—	—	4.78
$H_4SiW_{12}O_{40}$	(2.0)	3.61	(5.3)	(2.0)	3.96	(6.3)	4.97
$H_3PMo_{12}O_{40}$	(2.0)	3.62	(5.3)	(1.8)	3.41	(5.1)	4.70
$H_4PMo(VI)_{11}Mo(V)O_{40}$	(2.1)	3.69	(5.5)	(1.9)	3.77	(5.9)	—
$H_4PMo_{11}VO_{40}$	(2.1)	3.73	(5.6)	(1.9)	3.74	(5.8)	4.68
$H_4SiMo_{12}O_{40}$	(2.1)	3.90	(5.9)	—	—	—	4.78
$H_4GeW_{12}O_{40}$	—	—	—	—	—	—	4.25
$H_5GeW_{11}VO_{40}$	—	—	—	—	—	—	4.65
$H_6GeW_{10}V_2O_{40}$	—	—	—	—	—	—	4.60
$HClO_4$	—	—	—	—	—	—	4.87
HBr	—	—	—	—	—	—	5.6
H_2SO_4	—	—	—	—	—	—	7.0
HCl	4.0	—	—	—	—	—	8.4
HNO_3	—	—	—	3.57	—	—	10.1

indicating an increase in acid strength. In the case of concentrated aqueous solution of $\text{H}_3\text{PW}_{12}\text{O}_{40}$, the acidity function is less than that of H_2SO_4 by 1–1.5 units (120). Titration curves indicate that the three protons of $\text{H}_3\text{PW}_{12}\text{O}_{40}$ are equivalent in aqueous solution. Three protons of $\text{H}_3\text{PW}_{12}\text{O}_{40}$ dissociate independently in acetic acid, as measured by ^{13}C NMR spectroscopy (121).

The greater acid strength of heteropolyacids than that of mineral acids is explained as follows (122). Since in heteropolyanions the negative charge of similar value is spread over much larger anions than those formed from mineral acids, the electrostatic interaction between proton and anion is much less for heteropolyacids than for mineral acids. An additional important factor is possibly the dynamic delocalizability of the charge or electron. The change in the electronic charge caused by deprotonation may be spread over the entire polyanion unit.

As for the acid strengths of heteropolyacids, the following order has been reported for the compound in acetone (Table XI) (116): $\text{H}_3\text{PW}_{12}\text{O}_{40} > \text{H}_4\text{SiW}_{12}\text{O}_{40} \approx \text{H}_3\text{PMo}_{12}\text{O}_{40} > \text{H}_4\text{PMo}_{11}\text{VO}_{40} > \text{H}_4\text{SiMo}_{12}\text{O}_{40}$. The acid strength decreases when W is replaced by Mo or V and when the central P atom is replaced by Si. The effect of the central atom has been demonstrated for acetonitrile solutions of Keggin-type heteropolytungstates. As shown in Fig. 14, the acidity increases in general with a decrease in the negative charge of the heteropolyanion, or an increase in the valence of the central atom (the valence of the central atom increases in the order $\text{Co} < \text{B} < \text{Si}, \text{Ge} < \text{P}$) (63). This order is reasonable, since the sizes of the polyanions are nearly the same; thus the interaction between the proton and the polyanion would decrease as the negative charge of polyanion decreases.

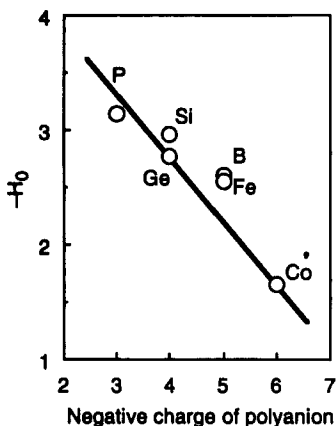
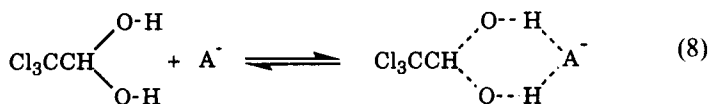


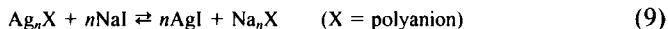
FIG. 14. Values of Hammett acidity function (H_0) of $\text{H}_n\text{XW}_{12}\text{O}_{40}$ as a function of the negative charge of the polyanion. (From Ref. 63.)

Pope *et al.* (123) measured the formation constant of the 1 : 1 complex of 1,1-dihydroxyl-2,2,2-trichloroethane (chloral hydrate) and polyanions in nitrobenzene by using NMR spectrometry [Eq. (8)]:



The formation constants (in parentheses) of the complexes are as follows: $\text{PW}_{12}\text{O}_{40}^{3-}$ (1.30) < $\text{PMo}_{12}\text{O}_{40}^{3-}$ (3.11) < $\text{SiMo}_{12}\text{O}_{40}^{4-}$ (24.7). These values represent the capability of the heteropolyanion to form hydrogen bonds. Thus the acid strength is in the order $\text{H}_3\text{PW}_{12}\text{O}_{40} > \text{H}_3\text{PMo}_{12}\text{O}_{40} > \text{H}_4\text{SiMo}_{12}\text{O}_{40}$. Izumi *et al.* (124) obtained the following order in acid strength by the same technique: $\text{H}_3\text{PW}_{12}\text{O}_{40} > \text{H}_3\text{PMo}_{12}\text{O}_{40} > \text{H}_4\text{SiW}_{12}\text{O}_{40} \approx \text{H}_4\text{GeW}_{12}\text{O}_{40} > \text{H}_4\text{SiMo}_{12}\text{O}_{40} > \text{H}_4\text{GeMo}_{12}\text{O}_{40}$. These orders are in general agreement with those obtained (118, 119) with indicator tests (Table XII).

In addition to the acidity, the softness of the heteropolyanion is an important characteristic relevant in catalysis (124). The softness has been estimated by the equilibrium constant in aqueous solution of the following reaction [Eq. (9)] at 298 K.



The order of softness was found to be the following: $\text{SiW}_{12}\text{O}_{40}^{4-} > \text{GeW}_{12}\text{O}_{40}^{4-} > \text{PW}_{12}\text{O}_{40}^{3-} > \text{PMo}_{12}\text{O}_{40}^{3-} > \text{SiMo}_{12}\text{O}_{40}^{4-} > \text{SO}_4^{2-}$. The softness greatly influences the catalytic behavior in concentrated aqueous solution or in organic solution, as described below.

B. ACIDITY IN THE SOLID STATE

1. Acid Forms

The strength and the number of acid centers as well as related properties of heteropolyacids can be controlled by the structure and composition of heteropolyanions, the extent of hydration, the type of support, the thermal pretreatment, etc.

Solid heteropolyacids such as $\text{H}_3\text{PW}_{12}\text{O}_{40}$ and $\text{H}_3\text{PMo}_{12}\text{O}_{40}$ are pure Brønsted acids and are stronger than conventional solid acids such as $\text{SiO}_2\text{-Al}_2\text{O}_3$ (45, 125). According to an indicator test, $\text{H}_3\text{PW}_{12}\text{O}_{40}$ has a Hammett acidity function less than -8.2 (126), and it has even been suggested to be a superacid (127, 128). A superacid is an acid with a strength greater than that of 100% H_2SO_4 , i.e., a value of $H_0 < -12$ (129). Thermal desorption of basic molecules also reveals the acidic properties. Figure 15 compares the acid strengths of heteropolyacids and $\text{SiO}_2\text{-Al}_2\text{O}_3$ (125). Pyridine adsorbed on $\text{SiO}_2\text{-Al}_2\text{O}_3$ is

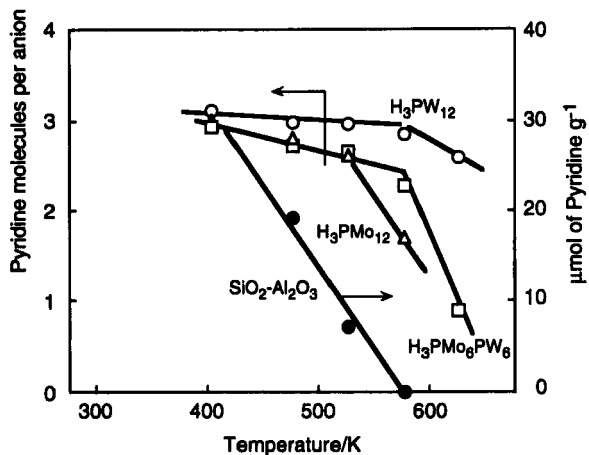


FIG. 15. Thermal desorption of pyridine from heteropolyacids (from Ref. 125). H₃PW₁₂ refers to H₃PW₁₂O₄₀.

completely desorbed at 573 K. On the other hand, sorbed pyridine (see Section VI) in H₃PW₁₂O₄₀ mostly remains at 573 K, indicating that H₃PW₁₂O₄₀ is a very strong acid.

The acid strength can also be demonstrated by temperature-programmed desorption (TPD) of NH₃ (Fig. 16) (127). H₃PW₁₂O₄₀ gives a relatively sharp peak at about 800 K, together with peaks for N₂ and H₂O at the same temperatures (not shown). N₂ is formed by the reaction of NH₃ with oxygen atoms in the heteropolyanions.

NH₃ adsorbed on SiO₂-Al₂O₃ and on HZSM-5 is mostly desorbed at temperatures less than 800 K (127, 130). Thus according to TPD results for NH₃, the order of the acid strength is sulfated zirconia (SO₄²⁻/ZrO₂) > H₃PW₁₂O₄₀ > HZSM-5 > SiO₂-Al₂O₃. The temperature of NH₃ desorption from (or decomposition of) ammonium salts of heteropolyacids is in the following order: (NH₄)₃PW₁₂O₄₀ > (NH₄)₄SiW₁₂O₄₀ > (NH₄)₃PMo₁₂O₄₀ > (NH₄)₄SiMo₁₂O₄₀ (131).

The strengths of heteropolytungstic acids have been determined more quantitatively by calorimetry of NH₃ absorption (132, 133). Figure 17 shows the differential heats of NH₃ absorption after treatment at 423 K. The initial heats of absorption of NH₃ are as follows: 196 kJ mol⁻¹ for H₃PW₁₂O₄₀; 185 kJ mol⁻¹ for H₄SiW₁₂O₄₀; 164 kJ mol⁻¹ for H₆P₂W₂₁O₇₁(H₂O)₃; and 156 kJ mol⁻¹ for H₆P₂W₁₈O₆₂. These values show that the order of acid strength is H₃PW₁₂O₄₀ > H₄SiW₁₂O₄₀ > H₆P₂W₂₁O₇₁(H₂O)₃ > H₆P₂W₁₈O₆₂, in agreement with the statements above. The data also indicate that the Keggin-type heteropolyacids are much stronger acids than Dawson-type heteropolyacids (132).

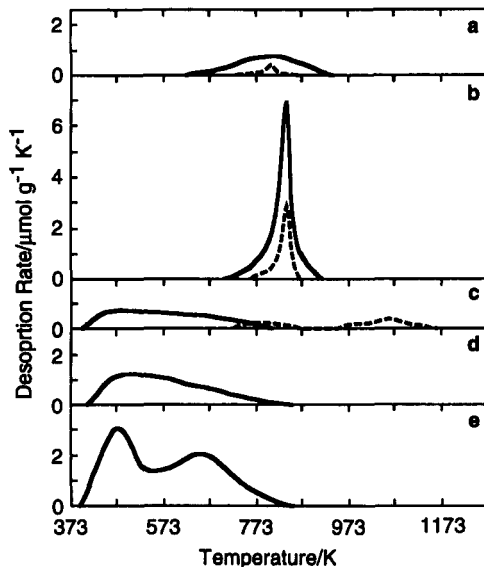


FIG. 16. TPD profiles of NH_3 from various solid acids: (a) $\text{Cs}_{2.5}\text{H}_{0.5}\text{PW}_{12}\text{O}_{40}$, (b) $\text{H}_3\text{PW}_{12}\text{O}_{40}$, (c) $\text{SO}_4^{2-}/\text{ZrO}_2$, (d) $\text{SiO}_2\text{-Al}_2\text{O}_3$, (e) H-ZSM-5. Solid line: NH_3 ($m/e = 17$); dotted line: N_2 ($m/e = 28$). (From Ref. 127.)

Heats of NH_3 absorption further confirm that the heteropolyacids are stronger acids than zeolites or simple metal oxides: 150 kJ mol^{-1} for HZSM-5 and 140 kJ mol^{-1} for $\gamma\text{-Al}_2\text{O}_3$ (133).

Table XIII shows the strengths measured by Hammett indicators with $\text{p}K_a$ values ranging from -5.6 to -14.5 . As described above, dried $\text{H}_3\text{PW}_{12}\text{O}_{40}$ possesses superacidity (127). The order of the acid strengths agrees with that

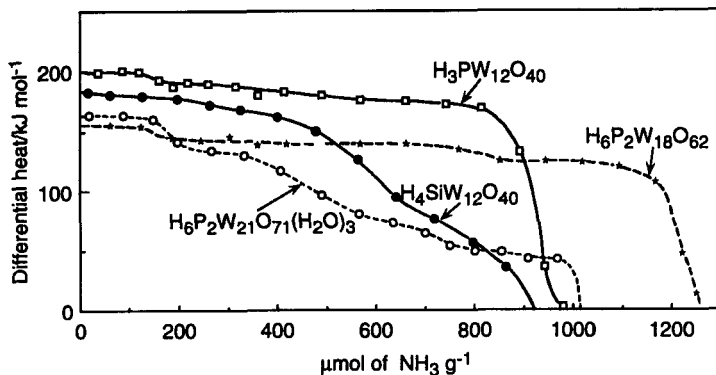


FIG. 17. Differential heat of NH_3 absorption as a function of the ammonia uptake for heteropolyacids. (From Ref. 132.)

TABLE XIII
Acid Strengths Measured by Hammett Indicators (127)

Catalyst ^a	pK _a of indicator ^b						
	-5.6	-8.2	-11.35	-12.70	-13.16	-13.75	-14.52
Cs _{2.5} H _{0.5} PW ₁₂ O ₄₀ (573 K)	+	+	+	+	+	-	-
H ₃ PW ₁₂ O ₄₀ (573 K)	+	+	+	+	+	-	-
HZSM-5 (808 K)	+	+	+	+	-	-	-
SO ₄ ²⁻ /ZrO ₂ (643 K)	+	+	+	+	+	+	+
SiO ₂ -Al ₂ O ₃ (723 K)	+	+	+	+	-	-	-

^a The figures in parentheses are the pretreatment temperatures. ^b Acidic color of the indicator was observed (+), or not (-). Indicators: -5.6, benzalacetophenone; -8.2, anthraquinone; -11.35, *p*-nitrotoluene; -12.70, *p*-nitrochlorobenzene; -13.16, *m*-nitrochlorobenzene; -13.75, 2,4-dinitrotoluene; -14.52, 2,4-dinitrofluorobenzene.

estimated from NH₃ TPD (127). In Fig. 18, various superacids in both solution and solid are summarized with reference to the *H*₀ function (128, 129). H₃PW₁₂O₄₀ is stronger than Nafion (*H*₀ = -12), but weaker than SO₄²⁻/ZrO₂ and AlCl₃-CuSO₄.

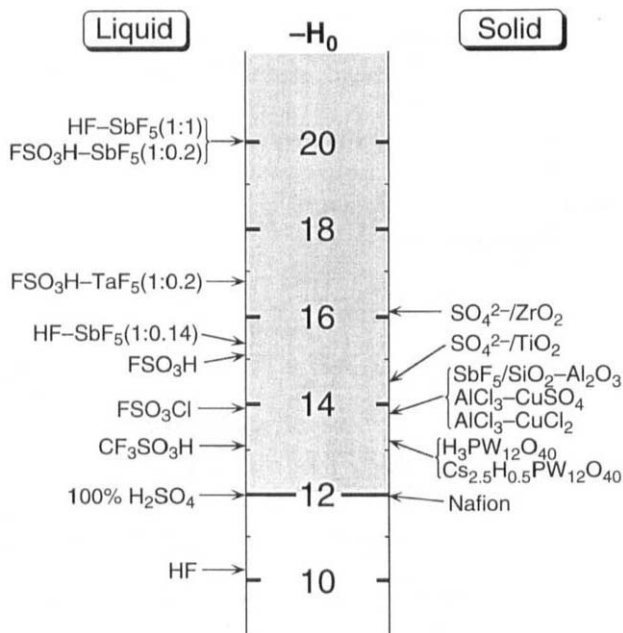


FIG. 18. Acid strengths of liquid and solid superacids. (From Ref. 128.)

Viswanathan *et al.* (115) reported small differences in binding energy between O1s and W4f: $H_3PW_{12}O_{40}$ (495.5 eV) > $Al_{1.5}PW_{12}O_{40}$ (495.4 eV) > $Na_3PW_{12}O_{40}$ (495.1 eV). This is the same order as the order of acid strength: $H_3PW_{12}O_{40} > Al_{1.5}PW_{12}O_{40} > Na_3PW_{12}O_{40}$.

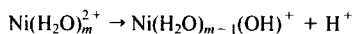
The locations of protons in solid heteropolyacids have been studied by NMR and IR spectroscopies. The protons of $H_3PW_{12}O_{40}$ with a high water content exist in the form of dioxonium ions $H_5O_2^+$ or $H^+(H_2O)_n$ (21). Data obtained by ^{17}O NMR spectroscopy confirm that the bridging oxygen atoms are protonated in CH_3CN solution (88). In the solid state of dehydrated $H_3PW_{12}O_{40}$, there are two possible sites for protonation: the terminal $W=O$ oxygen atoms or the bridging $W-O-W$ oxygen atoms. Kozhevnikov *et al.* (134) assumed on the basis of an ^{17}O NMR study that the terminal $W=O$ oxygen atoms are the predominant protonation sites. The resonance of the terminal $W=O$ oxygen atom shifts upfield 60 ppm, relative to that of the solution spectrum, whereas no such large shift was observed for the bridging $W-O-W$ oxygens.

On the basis of IR band broadening of the $W-O_e-W$ band for anhydrous $H_3PW_{12}O_{40}$ and $D_3PW_{12}O_{40}$, Lee *et al.* (78) concluded that protons are located on the bridging oxygens of $PW_{12}O_{40}^{3-}$. In contrast, there was no difference observed for the $W-O_d$ band. As described above, the most basic oxygen is the bridging oxygen according to ^{17}O NMR spectra of the solution. It was reported in a crystallographic study that reduced $PMo_{12}O_{40}$ is protonated at bridging oxygen (135). Quantum-chemical calculations at the EHMO level (136) and bond-length/bond-strength correlations (137) indicated that the bridging oxygen atoms carry the highest electron density (are the most basic).

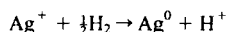
2. Salts

Acidic properties of heteropoly compounds in the solid state are sensitive to counteranions, constituent elements of polyanions, and tertiary structure. Partial hydrolysis and inhomogeneity of composition brought about during preparation are also important in governing the acidic properties. There are several possible types of origins of acidity (5):

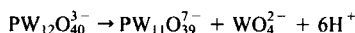
1. Dissociation of coordinated water: for example,



2. Lewis acidity of metal ions.
3. Protons formed by the reduction of metal ions: for example,



4. Protons present in the acidic salts: for example, $Cs_xH_{3-x}PW_{12}O_{40}$.
5. Partial hydrolysis during the preparation process: for example,



As for type (1), Niiyama *et al.* (42) proposed that protons are generated by dissociation of water and that the equilibrium of the dissociation is a function of the electronegativity of the metal cations. Formation of Brønsted acid sites in the aluminum salt of $\text{H}_3\text{PW}_{12}\text{O}_{40}$ as a result of exposure to water vapor at 573 K was confirmed by IR spectra of sorbed pyridine (138).

The presence of Lewis acidity [type (2)] or Brønsted acidity [type (1)] is revealed by the IR spectrum of pyridine sorbed on $\text{Al}_{1.5}\text{PW}_{12}\text{O}_{40}$ (138, 139). IR spectra of sorbed NH_3 show that $\text{Cu}_{1.5}\text{PW}_{12}\text{O}_{40}$ has Lewis acidity as well as Brønsted acidity (140). Ghosh and Moffat (141) measured the acidities of several salts of $\text{H}_3\text{PW}_{12}\text{O}_{40}$ with Hammett indicators. The acid strength increases with an increase in the calculated charge on the peripheral oxygen atom of the polyanion: $\text{Zr} > \text{Al} > \text{Zn} > \text{Mg} > \text{Ca} > \text{Na}$ (141).

Proton formation from H_2 [type (3)] has been demonstrated by IR and NMR spectroscopies for $\text{Ag}_3\text{PW}_{12}\text{O}_{40}$ (142). $\text{Ag}_3\text{PW}_{12}\text{O}_{40}$ treated with hydrogen at 573 K and then pyridine gives IR bands of pyridinium ion. Such bands are not observed for $\text{Ag}_3\text{PW}_{12}\text{O}_{40}$ which had simply been evacuated at 573 K prior to sorption of pyridine. The former sample (in the absence of pyridine) was catalytically much more active than the latter. As shown in Fig. 19, the introduction of H_2 to $\text{Ag}_3\text{PW}_{12}\text{O}_{40}$ at 488 K leads to three resonances at 9.3, 6.4, and 4.1 ppm in the ^1H NMR spectrum (143–145). The resonance at 4.1 ppm is due to H_2O molecules formed by the hydrogen treatment. That at 6.4 ppm increased as the H_2 pressure increased and disappeared as a result of the addition of deuterated pyridine ($\text{C}_5\text{D}_5\text{N}$) at 303 K. The peak at 9.3 ppm was nearly unchanged during the experiments. These results indicate that the acid strength of the proton-containing groups indicated by the resonance at 6.4 ppm is higher than that of the groups indicated by the resonance at 9.3 ppm. This difference in acid strengths is attributed to the differences in the interaction between proton and polyanion.

Group B salts, incorporating acid groups, have high surface areas and high thermal stabilities. In TPD of NH_3 , $\text{Cs}_{2.5}\text{H}_{0.5}\text{PW}_{12}\text{O}_{40}$ gives a desorption peak in the temperature range 633–923 K, and the peak temperature is close to that for $\text{H}_3\text{PW}_{12}\text{O}_{40}$, indicating that the acid strength of $\text{Cs}_{2.5}\text{H}_{0.5}\text{PW}_{12}\text{O}_{40}$ is similar to that of $\text{H}_3\text{PW}_{12}\text{O}_{40}$ (127); $\text{Cs}_{2.5}\text{H}_{0.5}\text{PW}_{12}\text{O}_{40}$ has a slightly broader distribution of acid strengths than $\text{H}_3\text{PW}_{12}\text{O}_{40}$ (Fig. 16).

In group A salts, the acid amount exceeds the number of protons expected from the formula for Na salts of $\text{H}_3\text{PW}_{12}\text{O}_{40}$. Partial hydrolysis has been proposed [type (5)] (46a).

Solid-state ^{31}P NMR spectroscopy was used to demonstrate that all protons of $\text{Cs}_{2.5}\text{H}_{0.5}\text{PW}_{12}\text{O}_{40}$ are distributed randomly through the bulk of the material. Figure 20 is a ^{31}P NMR spectrum for $\text{Cs}_{2.5}\text{H}_{0.5}\text{PW}_{12}\text{O}_{40}$ (47). Special care was necessary in the measurement to protect the sample from moisture. Four resonances (−14.9, −13.5, −12.1, and −10.9 ppm) appeared when

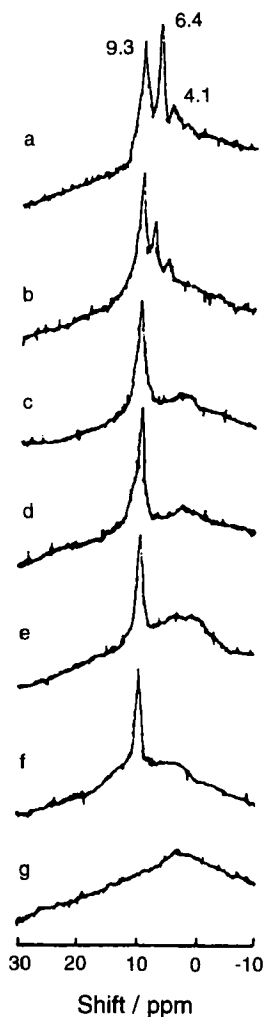


FIG. 19. ^1H NMR spectra (room temperature) in reduced $\text{Ag}_3\text{PW}_{12}\text{O}_{40}$. (a) $\text{Ag}_3\text{PW}_{12}\text{O}_{40}$ reduced with 40 kPa of H_2 at 488 K and recorded in the presence of H_2 ; (b–g) recorded after evacuating H_2 at 77 (b), 303 (c), 333 (d), 488 (e), 523 (f) and 623 K (g). Reprinted with permission from Ref. 143. Copyright 1993 American Chemical Society.

$\text{Cs}_{2.5}\text{H}_{0.5}\text{PW}_{12}\text{O}_{40}$ was evacuated at 573 K. $\text{Cs}_3\text{PW}_{12}\text{O}_{40}$, which has no proton, gives a resonance at -15.3 ppm, which is close to the first resonance (-14.9 ppm). Anhydrous $\text{H}_3\text{PW}_{12}\text{O}_{40}$, which has three protons directly attached to the polyanion, has a resonance at -10.9 ppm. Thus the chemical shift is determined by the number of the protons attached to the polyanion, and the four

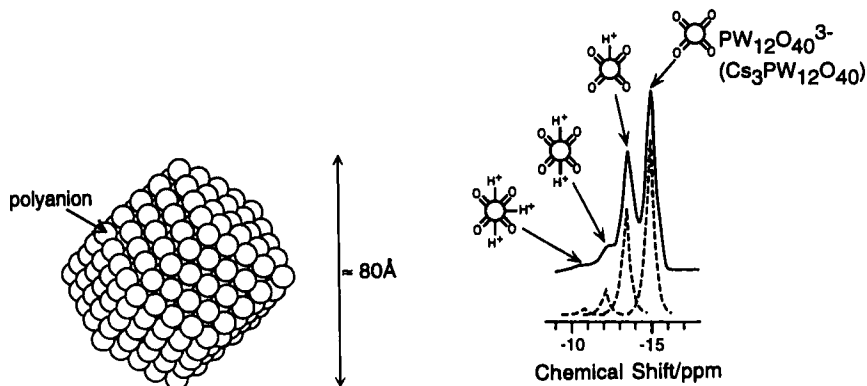


FIG. 20. ^{31}P NMR spectrum (bottom) and one of the primary particles (top) of $\text{Cs}_{2.5}\text{H}_{0.5}\text{PW}_{12}\text{O}_{40}$. The dotted lines in the spectrum show the relative peak intensities expected for the statistical distribution of protons. (From Ref. 47.)

peaks correspond to the Keggin anions having 0, 1, 2, and 3 protons, respectively. The relative intensities of these peaks for $\text{Cs}_{2.5}\text{H}_{0.5}\text{PW}_{12}\text{O}_{40}$ are in good agreement with those expected from a random distribution of protons (broken line, Fig. 20).

The number of protons on the surface (shown in Fig. 21) was estimated by multiplying the formal concentration of protons on the surface by the quantity of polyanions present on the surface calculated from the surface area. As the Cs content increases, the number of surface protons at first decreases, but greatly increases when the Cs content exceeds 2. The increase in the number of surface protons is mainly due to the sharp increase in the surface area (47). When x

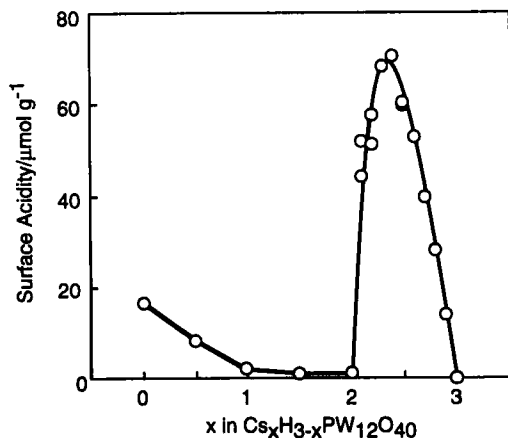


FIG. 21. The amount of surface protons (surface acidity) as a function of Cs content for $\text{Cs}_x\text{H}_{3-x}\text{PW}_{12}\text{O}_{40}$. (From Refs. 47, 48.)

increases from 2.5 to 3.0, since the formal concentrations of protons become low or zero, the number of surface protons decreases greatly. As described in Section V, the catalytic activity is in close correspondence to this surface acidity.

3. Supported Heteropolyacids

Supporting heteropolyacids on solids with high surface areas is a useful method for improving catalytic performance. It is necessary to pay attention to the changes in the acid strength, the structures of the aggregates, and the possibility of decomposition. In general, strong interactions of heteropolyacids with supports are observed at low loadings and the intrinsic properties of heteropolyacids prevail at high loadings. Basic solids such as Al_2O_3 and MgO tend to decompose heteropolyacids (146–149).

Microcalorimetry of NH_3 absorption (adsorption) reveals that when $\text{H}_3\text{PW}_{12}\text{O}_{40}$ is supported on SiO_2 , the acid strength decreases, as shown in Fig. 22 (150). The acid strength of $\text{H}_3\text{PW}_{12}\text{O}_{40}$ diminishes in the sequence of supports $\text{SiO}_2 > \text{Al}_2\text{O}_3 > \text{activated charcoal}$. The acid strengths of heteropolyacids supported on SiO_2 (151) measured by NH_3 TPD is in the following order: $\text{H}_3\text{PW}_{12}\text{O}_{40}$ (865 K) $>$ $\text{H}_4\text{SiW}_{12}\text{O}_{40}$ (805 K) $>$ $\text{H}_3\text{PMo}_{12}\text{O}_{40}$ (736 K) $>$ $\text{H}_4\text{SiMo}_{12}\text{O}_{40}$ (696 K), where the figures in parentheses are the temperatures of desorption.

The interaction between $\text{H}_3\text{PW}_{12}\text{O}_{40}$ and the surface OH groups of SiO_2 has been detected by ^1H and ^{31}P MAS NMR spectroscopies (152). The OH resonance of SiO_2 at 1.8 ppm (relative to tetramethylsilane) becomes smaller as the amount of $\text{H}_3\text{PW}_{12}\text{O}_{40}$ on SiO_2 increases. At 20–50 wt% $\text{H}_3\text{PW}_{12}\text{O}_{40}$, a new type of proton appears at 5 ppm. At loadings > 50 wt%, a resonance at 9.3 ppm

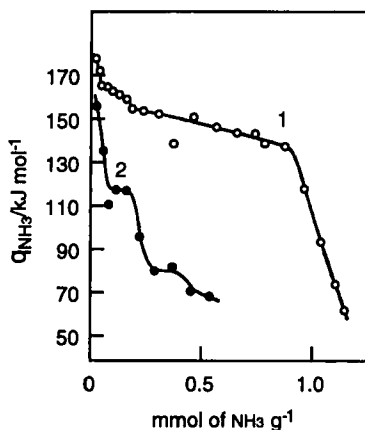
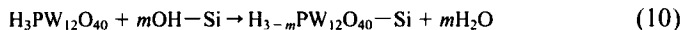


FIG. 22. Differential heats of absorption of NH_3 on (1) $\text{H}_3\text{PW}_{12}\text{O}_{40}$ and (2) 20 wt% $\text{H}_3\text{PW}_{12}\text{O}_{40}/\text{SiO}_2$. (From Ref. 150.)

due to crystalline $\text{H}_3\text{PW}_{12}\text{O}_{40}$ appears. At 20 wt%, ^{31}P NMR also gives a broad resonance at -15.8 ppm, which is different from the -12.4 ppm resonance of crystalline $\text{H}_3\text{PW}_{12}\text{O}_{40}$. The interaction between $\text{H}_3\text{PW}_{12}\text{O}_{40}$ and OH groups on SiO_2 is assumed to be as shown in Eq. (10).



Lefebvre (153) reported for 13–87% $\text{H}_3\text{PW}_{12}\text{O}_{40}$ supported on SiO_2 that two ^{31}P resonances are due to the bulk $\text{H}_3\text{PW}_{12}\text{O}_{40}$ (15.1 ppm) and to $\text{SiOH}_2^+ - \text{H}_2\text{PW}_{12}\text{O}_{40}^-$ (-14.5 ppm). ^{31}P Spin-lattice relaxation of $\text{H}_3\text{PMo}_{12}\text{O}_{40}/\text{SiO}_2$ gives an estimated coverage of $\text{H}_3\text{PMo}_{12}\text{O}_{40}$ on SiO_2 (154, 155). For unsupported $\text{H}_3\text{PMo}_{12}\text{O}_{40} \cdot 13\text{H}_2\text{O}$, T_1 is 20 s; but T_1 drastically decreases as a result of dispersion on the support: 2.5 s (loading amount as Mo, 35 wt%) to 430 ms (loading amount as Mo, 2 wt%).

Raman spectroscopy shows that the structure of $\text{PMo}_{12}\text{O}_{40}$ is preserved at high coverages on SiO_2 (156). When the loading decreases, the $\nu(\text{Mo}=\text{O})$ frequency decreases, which is probably due to weakening of the anion–anion interaction. On heating to temperatures >573 K, 23 wt% $\text{H}_3\text{PMo}_{12}\text{O}_{40}/\text{SiO}_2$ produced an unidentified species and/or MoO_3 (157). Upon exposure to water vapor, the unknown species was reconverted to the Keggin anion. When MoO_3 was supported on SiO_2 and treated with H_2O , $\text{H}_4\text{SiMo}_{12}\text{O}_{40}$ formed on the SiO_2 surface (158). Soled *et al.* (159) prepared a unique Cs acidic salt of $\text{H}_3\text{PW}_{12}\text{O}_{40}$, which is present in a ring ~ 10 μm thick located about half-way into an SiO_2 extrudate ~ 1.5 mm in diameter.

IV. Acid-Catalyzed Reactions in the Liquid Phase

Heteropolyacids are more active catalysts for various reactions in solution than conventional inorganic and organic acids, and they are used as industrial catalysts for several liquid-phase reactions (6, 12). Important characteristics accounting for the high catalytic activities are the acid strength, softness of the heteropolyanion, catalyst concentration, and nature of the solvent (6, 7, 9, 116, 160, 161).

Figure 23 shows a correlation between the catalytic activity and the Hammett acidity function (H_0) of Keggin-type heteropolyacids in CH_3CN . The catalytic activity increases with the acid strength (63).

Softness of the polyanion is also important in bringing about unique activity. It has been suggested that reaction intermediates like oxonium ions or carbenium ions are stabilized on the surfaces of heteropolyanions (see below), probably by virtue of the softness (162). Izumi *et al.* (124) observed that $\text{H}_4\text{SiW}_{12}\text{O}_{40}$ was more active for the reaction of dibutyl ether with acetic anhydride than $\text{H}_3\text{PW}_{12}\text{O}_{40}$, although $\text{H}_4\text{SiW}_{12}\text{O}_{40}$ is a weaker acid than $\text{H}_3\text{PW}_{12}\text{O}_{40}$. This difference was explained by the stabilization of the cationic intermediate

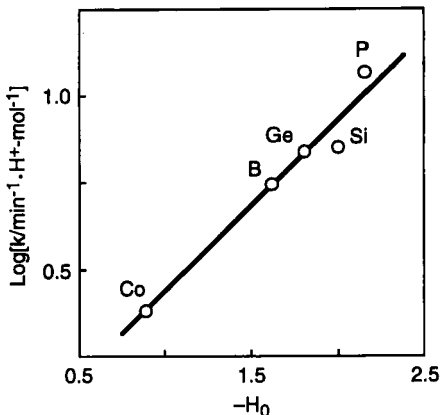


FIG. 23. Rate constants (per mole of protons) for decomposition of isobutyl propionate as a function of H_0 values of $H_nXW_{12}O_{40}$ (acetonitrile solutions). (From Ref. 63.)

through the formation of the intermediate-polyanion complex due to the softness of the polyanion, which is in the order $\text{SiW}_{12}\text{O}_{40}^{4-} > \text{PW}_{12}\text{O}_{40}^{3-}$ (9). The effect of the softness becomes significant for reactions in aqueous solutions, in which the influence of the difference in the acid strength is slight, since most heteropolyacids are completely dissociated.

The concentration of the heteropolyacid is sometimes critical. Excellent performance was demonstrated for the hydration of butenes when heteropolyacids were used in a highly concentrated solution (163). As shown in Fig. 24, the rate increases remarkably with an increase in the concentration of

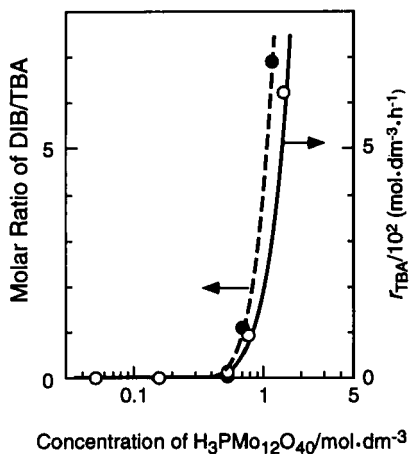


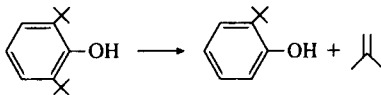
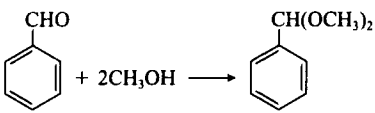
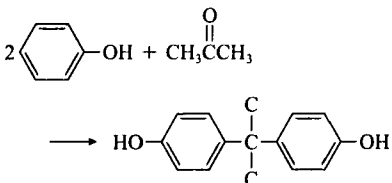
FIG. 24. Dependences of the initial rate of TBA formation and ratio of DIP/TBA on $\text{H}_3\text{PMo}_{12}\text{O}_{40}$ concentration in the hydration of butenes. TBA, *tert*-butyl alcohol; DIB, diisobutylene. 357 K, isobutylene/1-butene = 1/1 (molar). (From Ref. 163.)

TABLE XIV
 Acid-Catalyzed Reactions in the Liquid Phase

Reaction	Catalyst	Remarks ^a	Ref.
$\begin{array}{c} \text{C} \\ \diagup \\ \text{C}=\text{C} \\ \diagdown \\ \text{C} \end{array} + \text{H}_2\text{O} \longrightarrow \begin{array}{c} \text{C} \\ \\ \text{C}-\text{C}-\text{C} \\ \\ \text{OH} \end{array}$	H ₃ PW ₁₂ O ₄₀	T = 313–353 K	162, 166
$\text{C}=\text{C}-\text{C}-\text{C} + \text{H}_2\text{O} \longrightarrow \begin{array}{c} \text{C}-\text{C}-\text{C}-\text{C} \\ \\ \text{OH} \end{array}$	H ₃ PW ₁₂ O ₄₀	T = 473 K, 200 atm	12
$\text{Ph}-\text{CH}=\text{CH}_2 + 2\text{HCHO} \longrightarrow \text{Ph}-\begin{array}{c} \diagup \\ \text{O} \\ \diagdown \end{array}$	H ₃ PW ₁₂ O ₄₀	T = 328 K H ₃ PW ₁₂ O ₄₀ : H ₂ SO ₄ = 300 : 1 (ratio of activity)	162
$\begin{array}{c} \text{R}_2\text{R}_1\text{C}-\text{CH}_2 \\ \\ \text{O} \end{array} + \text{R}_3\text{OH} \longrightarrow \begin{array}{c} \text{R}_2\text{R}_1-\text{C}-\text{CH}_2 \\ \quad \\ \text{R}_3\text{O} \quad \text{OH} \end{array} + \begin{array}{c} \text{R}_2\text{R}_1-\text{C}-\text{CH}_2 \\ \quad \\ \text{HO} \quad \text{OR}_3 \end{array}$	H ₃ PW ₁₂ O ₄₀	T = 318 K H ₃ PW ₁₂ O ₄₀ : H ₂ SO ₄ = 30 : 1	124
$\begin{array}{c} \diagup \\ \text{O} \\ \diagdown \end{array} + \text{AcOH} \longrightarrow \text{AcO}-(\text{CH}_2)_4-\text{OAc}$	H ₃ PW ₁₂ O ₄₀	T = 368 K H ₃ PW ₁₂ O ₄₀ : BF ₃ · Et ₂ O = 50 : 1	124
$\begin{array}{c} \diagup \\ \text{O} \\ \diagdown \end{array} \longrightarrow \text{HO}-(\text{CH}_2)_4-\text{O}-\text{H} \\ \text{(PTMG)}$	H ₃ PW ₁₂ O ₄₀ · nH ₂ O	T = 333 K MW ≈ 3000 (n = 0 ~ 6)	164
Cyclotrimerization of propionaldehyde	H ₃ PW ₁₂ O ₄₀	T = 298 K, Y = 85%	176
$\begin{array}{c} \diagup \\ \diagdown \end{array} + \text{CH}_3\text{OH} \longrightarrow \begin{array}{c} \diagup \\ \diagdown \end{array}$	H ₆ P ₂ W ₁₈ O ₆₂	T = 315 K, S ≈ 100%	179
$\begin{array}{c} \text{O} \\ \\ \text{C} \\ / \quad \backslash \\ \text{C} \quad \text{C} \\ \backslash \quad / \\ \text{O} \end{array} + 2\text{ROH} \longrightarrow \begin{array}{c} \text{O} \\ \\ \text{COR} \\ \\ \text{C} \\ / \quad \backslash \\ \text{C} \quad \text{C} \\ \backslash \quad / \\ \text{O} \end{array}$	H ₃ PW ₁₂ O ₄₀	T = 363–393 K	161
$\begin{array}{c} \diagup \\ \diagdown \end{array} \text{OCOCH}_3 \longrightarrow \begin{array}{c} \diagup \\ \diagdown \end{array} + \text{CH}_3\text{COOH}$	H ₃ PW ₁₂ O ₄₀	T = 373 K H ₃ PW ₁₂ O ₄₀ : H ₂ SO ₄ = 60 : 1	63
Ph-CH ₂ OH	H ₄ SiM ₁₂ O ₄₀	T = 298 K	180
C ₆ H ₅ OCH ₃ + CH ₃ COCl	H ₄ SiM ₁₂ O ₄₀	Reflux	180

continued

TABLE XIV—Continued

Reaction	Catalyst	Remarks ^a	Ref.
	H ₃ PW ₁₂ O ₄₀	T = 357 K H ₃ PW ₁₂ O ₄₀ : H ₂ SO ₄ = 100 : 1	160
	H ₃ PMo ₁₂ O ₄₀	T = 298 K, Y = 100%	182
	H ₃ PW ₁₂ O ₄₀	T = 333 K, Y = 72% (p,p) ^b	

^a T = temperature, Y = yield, S = selectivity. ^b Asahi Chem. Co., LTD., JP 1990-45439.

H₃PMo₁₂O₄₀. In a certain range of concentration of H₃PW₁₂O₄₀, polymerization of THF proceeds efficiently, whereby the molecular weight of the product is also well controlled (164).

In some cases, the effective acid strengths of heteropolyacids level off due to the leveling effect of reactant molecules (63). For example, the difference in activity between heteropolyacids and H₂SO₄ is not significant for ester exchange and esterification because alcohols are good proton acceptors (63). In organic reactants or solvents, high activities of heteropolyacids are often realized (9).

Typical reactions catalyzed by heteropolyacids are listed in Table XIV.

A. REACTIONS IN AQUEOUS SOLUTION

1. Hydration and Dehydration

Tokuyama Soda commercialized a catalytic process for propylene hydration catalyzed by aqueous solutions of heteropolyacids such as H₃PW₁₂O₄₀ (165). In Table XV, the activities of various acids are compared at a constant proton concentration. H₃PW₁₂O₄₀ is two or three times more active than H₂SO₄ or H₃PO₄. The reason for the high activity is assumed to be the stabilization of intermediate propyl cations by coordination.

Izumi *et al.* (162, 166) observed high activities of heteropolyacids for the hydration of isobutylene in dilute solution, as follows. The activation energy is 4 kcal mol⁻¹ lower for H₃PW₁₂O₄₀ than for HNO₃. The reaction order with

TABLE XV
Effect of Anion on Rate of Propylene Hydration^a
(165)

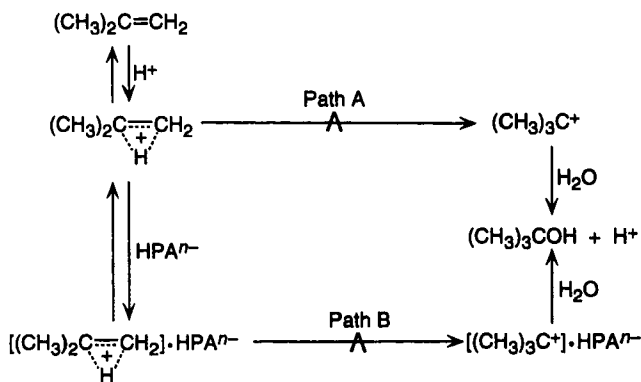
Anion	Concentration of anion (10^{-3} mol dm ⁻³)	Relative specific rate
PMo ₁₂ O ₄₀ ³⁻	1.00	3.4
PW ₁₂ O ₄₀ ³⁻	1.00	1.7
SO ₄ ²⁻	1.50	1.0
PO ₄ ³⁻	1.50	1.0

^a 423 K, 14 atm, [H₃O⁺]; 3.0×10^{-3} mol dm⁻³.

respect to heteropolyacid is about 1.5, whereas that for HNO₃ is 1. The proposed reaction mechanism is shown in Scheme 3. Path A corresponds to specific acid catalysis. Path B involves an intermediate π -complex formed from protonated isobutylene and a heteropolyanion. The overall rate is expressed by the sum of the rates of paths A and B [Eq. (11a)], where k_1 and k_{11} are the rate constants, P_B is the partial pressure of isobutylene, and [heteropolyanion] is the concentration of heteropolyanion, respectively.

$$r = k_1(P_B[H_3O^+]) + k_{11}(P_B[H_3O^+])[heteropolyanion] \quad (11a)$$

The existence of a significant interaction between the heteropolyanion and the carbenium ion is supported by the presence of alkyl-heteropoly complexes. Knoth and Harlow (167) synthesized *O*-alkylated compounds such as [(C₂H₅)₃O]₃PW₁₂O₃₇, where a C₂H₅ cation is bonded to the polyanion. Farneth *et al.* (168) and Lee *et al.* (169) reported the formation of methyl groups and



SCHEME 3

ethyl groups directly attached to the heteropolyanion (methoxy and ethoxy), respectively.

A commercial process for the separation of isobutylene from a mixture of isobutylene and *n*-butenes through direct hydration of isobutylene to give *tert*-butyl alcohol has been established by use of a concentrated solution of heteropolyacids (6, 163, 170). The reaction order in the heteropolyanion varies from 1 to 2 as the concentration of heteropolyanion increases from 0.05 to 10 mol dm⁻³. This increase corresponds to a change from the first to the second term in Eq. (11a). At concentration of the heteropolyanion greater than 0.5 mol dm⁻³, path B in Scheme 3 becomes dominant.

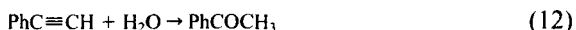
In addition, the solubility of isobutylene increases linearly with the concentration of H₃PW₁₂O₄₀, whereas the solubility is little affected by the concentration of HNO₃ (169). At a 1.5 mol dm⁻³ concentration of heteropolyanion, the solubility of isobutylene is about 2.3 times higher than for mineral acids. Hence the high catalytic activities of heteropolyacids (about 10 times higher than that of HNO₃) are explained by the combination of the three effects of (a) the high solubility, (b) the coordination of isobutylene to the heteropolyanion, and (c) the high acid strength (162, 166). Isobutylene in a mixture of isobutylene and 1-butene is very selectively hydrated in the concentrated solution; diisobutylene formation is negligible, and *sec*-butyl alcohol concentrations are <100 ppm.

An apparently different explanation for the catalysis has been advanced by Kozhevnikov *et al.* (171, 172). The rate constant, *k* (min⁻¹) for H₃PW₁₂O₄₀ and that for H₄SiW₁₂O₄₀ at room temperature show linear relationships with the Hammett acidity function (*H*₀) as shown by Eq. (11b).

$$\log k = -1.04H_0 - 3.46 \quad (11b)$$

The data of H₂SO₄, HCl, HNO₃, and HClO₄ also fit this equation. On this basis, they suggested that the hydration of isobutylene in the presence of heteropolyacids and inorganic acids proceeds via a common mechanism, in which the rate-limiting step is the conversion of the π -complex into a carbenium ion (Scheme 3). The complexation effect as described above is possibly included in the value of *H*₀ according to this explanation.

Heteropolyacids are much more active than H₂SO₄ and HClO₄ for hydration of phenylacetylene [Eq. (12)] (173). Also in this case, the rate of reaction in the presence of heteropolyacids shows an approximately second-order dependence on the catalyst concentration. This observation suggests that this reaction proceeds by a mechanism similar to that of Scheme 3:



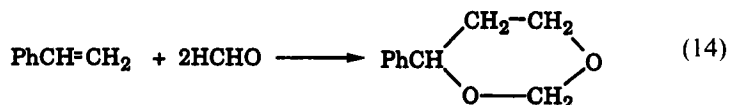
The higher activities of heteropolyacids are also found for the dehydration of 1,4-butanediol to give tetrahydrofuran (THF) (174). The activity order is H₄SiW₁₂O₄₀ > H₃PW₁₂O₄₀ > H₃PMo₁₂O₄₀. Rate data are summarized by

Eq. (13), and the reaction probably proceeds by a mechanism similar to that shown in Scheme 3.

$$r = (k_1 + k_2[\text{SiW}_{12}\text{O}_{40}^{4-}])[1,4\text{-butanediol}][\text{H}^+] \quad (13)$$

2. Prins Reaction

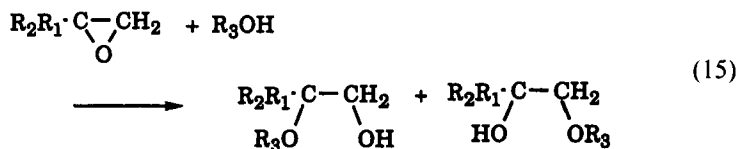
Heteropolyacids catalyze the Prins reaction of alkenes [Eq. (14)] more efficiently than H_2SO_4 and *p*-toluenesulfonic acid (PTS). For example, $\text{H}_3\text{PW}_{12}\text{O}_{40}$ is 10–50 times more active than H_2SO_4 or PTS (162). In this reaction, oxocarbo-cations may be stabilized through complexation with heteropolyanions:



B. REACTIONS IN ORGANIC SOLUTION

1. Ether Cleavage Reactions

$\text{H}_3\text{PW}_{12}\text{O}_{40}$ shows a higher activity for the alcoholysis of epoxides [Eq. (15)] than H_2SO_4 , PTS, or HClO_4 (9, 124, 175). While rapid deactivation is observed with H_2SO_4 , which is probably due to the formation of an alkyl sulfate, $\text{H}_3\text{PW}_{12}\text{O}_{40}$ maintains its high catalytic activity.



Tetrahydrofuran is cleaved with acetic acid to give 1,4-diacetoxy acetate selectively (124) (Table XIV). The activity order is $\text{H}_3\text{PW}_{12}\text{O}_{40} > \text{H}_4\text{SiW}_{12}\text{O}_{40} > \text{H}_3\text{PMo}_{12}\text{O}_{40} \gg \text{BF}_3 \cdot \text{Et}_2\text{O} > \text{PTS}$. The catalytic activities for the reaction of THF with acetic anhydride are in the order $\text{H}_4\text{SiW}_{12}\text{O}_{40} = \text{H}_3\text{PW}_{12}\text{O}_{40} > \text{H}_4\text{GeW}_{12}\text{O}_{40} > \text{H}_4\text{SiMo}_{12}\text{O}_{40} > \text{H}_3\text{PMo}_{12}\text{O}_{40} \gg \text{H}_2\text{SO}_4$ (124). The cleavage of dibutyl ether with acetic acid is also catalyzed by heteropolyacids (124). $\text{H}_4\text{SiW}_{12}\text{O}_{40}$ is the most active among the heteropolyacids, probably due to its higher softness.

2. Polymerization of Tetrahydrofuran

Aoshima *et al.* (164) found that THF can be directly polymerized to give polyoxotetramethyleneglycol (PTMG) is a highly concentration solution of heteropolyacids [Eq. (16)].

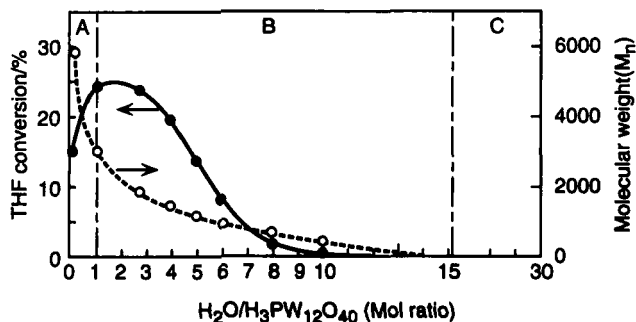
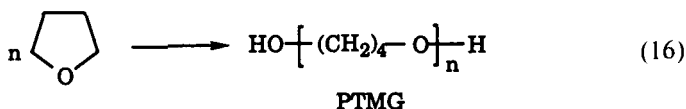


Fig. 25. Influence of the molar ratio of $\text{H}_2\text{O}/\text{H}_3\text{PW}_{12}\text{O}_{40}$ on THF polymerization (333 K). (A) Solid-liquid phase, (B) two-liquid phase, (C) homogeneous liquid phase. (From Ref. 164.)



The water content greatly influences the activity and the molecular weight of PTMG, as shown in Fig. 25. At the ratio of $\text{H}_2\text{O}/\text{PW}_{12}\text{O}_{40}^{3-} = 10$, the reaction mixture consists of two liquid phases; the upper phase is mainly THF and the lower phase is the complex of $\text{H}_3\text{PW}_{12}\text{O}_{40}$ and THF (in the catalyst phase). The THF polymer is formed in the catalyst phase and is transferred to the THF phase. This "phase-transfer polymerization" is illustrated in Fig. 26.

IR spectra of the C—O—C stretching region of the catalyst phase are shown in Fig. 27. The peaks a, b, and c were assigned by Aoshima *et al.* (164) to uncoordinated THF, hydrogen-bonded THF, and protonated THF, respectively. The polymerization activity is associated with the amount of protonated THF.

3. Condensation Reactions

Table XVI is a summary of typical results observed for cyclotrimerization of propionaldehyde to give 2,4,6-triethyl-1,3,5-trioxane (176). In catalysis by $\text{H}_3\text{PMo}_{12}\text{O}_{40}$, the reaction mixture separates into two phases during the course of the batch reaction. The products are present in the upper layer and the catalyst in the lower layer, so that the catalyst solution can be used repeatedly without a catalyst isolation step. Selectivities exceeding 97% and turnovers exceeding 300 moles of product per mole of catalyst have been obtained.

Polymerization of 1,3-trioxane, a cyclic trimer of formaldehyde, is catalyzed by $\text{H}_3\text{PMo}_{12}\text{O}_{40}$ (177). The polymerization is very fast at concentrations of $\text{H}_3\text{PMo}_{12}\text{O}_{40}$ as low as $10^{-6} \text{ mol dm}^{-3}$. To obtain comparable rates using BF_3 catalyst, a BF_3 concentration of $10^{-3} \text{ mol m}^{-3}$ is required.

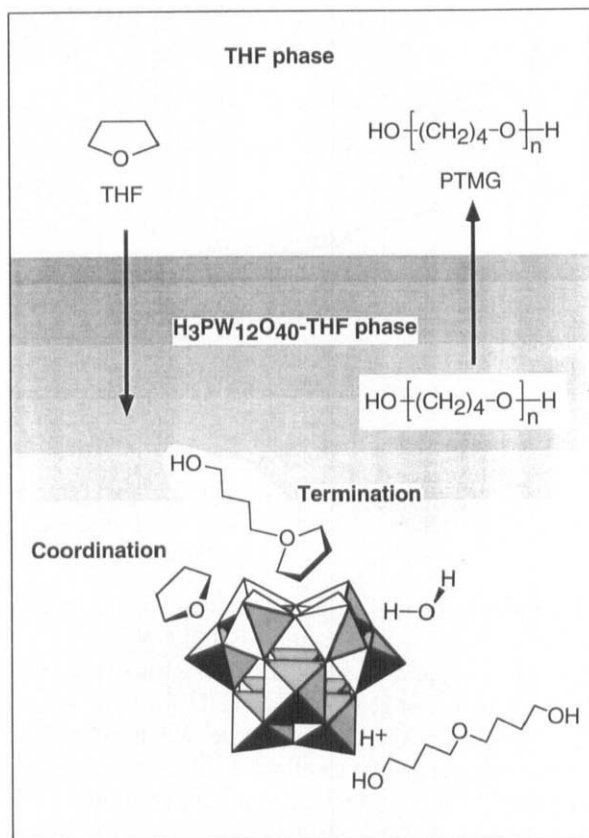


FIG. 26. Reaction model of phase-transfer polymerization. (From Ref. 164.)

Condensation of acetone to give mesitylene is catalyzed by $\text{H}_3\text{PW}_{12}\text{O}_{40}$ at room temperature (178).

4. MTBE Synthesis

Table XVII is a comparison of the catalytic activities for liquid-phase MTBE synthesis from isobutylene and methanol (179). The catalyst structure and composition have a strong effect on the activity. The highest activity per proton was obtained with a Dawson-type heteropolyacid, $\text{H}_6\text{P}_2\text{W}_{18}\text{O}_{62}$, although the acid strength of $\text{H}_6\text{P}_2\text{W}_{18}\text{O}_{62}$ is lower than that of the Keggin-type $\text{H}_3\text{PW}_{12}\text{O}_{40}$ (Section III). Water added to the mixture has little effect on the reaction rate at water concentrations less than 2 wt%, but at 5 wt% the rate is less by a factor of 2.5. At the same time the selectivity is less due to the formation of *tert*-butyl alcohol.

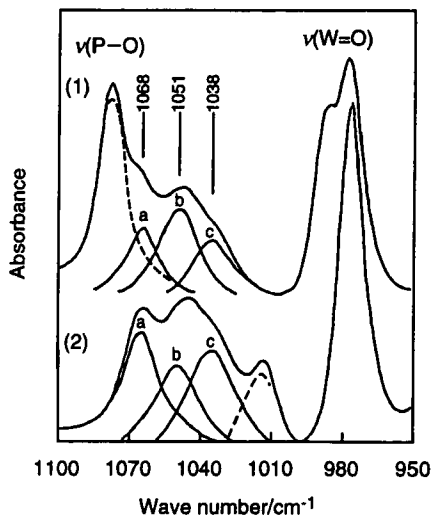


FIG. 27. Infrared spectra of C—O—C stretching vibrations of THF in catalyst phase and their deconvolution results. (1) $\text{H}_4\text{SiW}_{12}\text{O}_{40}/\text{H}_2\text{O}/\text{THF} = 1/7/20$ (molar); (2) $\text{H}_3\text{PW}_{12}\text{O}_{40}/\text{H}_2\text{O}/\text{THF} = 1/7/20$ (molar). (From Ref. 164.)

TABLE XVI
Liquid-Phase Cyclotrimerization of Propionaldehyde^a (176)

Catalyst	Amount (mmol)	Time (h)	Conversion (%)	Selectivity ^b (mol%)	TON ^c
$\text{H}_3\text{PMo}_{12}\text{O}_{40}$	0.4	2	87.1	97.2	350
$\text{H}_3\text{PMo}_{12}\text{O}_{40}$ ^d	0.4	2	84.7	97.5	340
$\text{H}_3\text{PW}_{12}\text{O}_{40}$	0.3	2	86.3	97.2	490
$\text{H}_4\text{SiW}_{12}\text{O}_{40}$	0.3	2	66.2	97.3	370
$\text{SiO}_2\text{-Al}_2\text{O}_3$	—	2	2.8	3.1	—
AlCl_3	7.5	2	91.5	88.6	19
ZnCl_2	7.3	2	87.6	97.5	20
ZnCl_2 ^e	—	72	69.2	92.5	15
<i>p</i> -TsOH	5.3	2	78.5	48.9	13
<i>p</i> -TsOH ^f	—	2	47.3	97.6	15
H_3PO_4 ^g	8.7	4	58.2	97.3	11

^a Reacted at room temperature, 1 g of catalyst to 10 g of propionaldehyde. ^b Selectivity to 2,4,6-triethyl-1,3,5-trioxane. ^c Turnover number (molar ratio of aldehyde reacted to trioxane to catalyst). ^d For twelfth run. ^e Second run. ^f Fifth run. ^g Contained 15 wt% of water.

TABLE XVII
Activity of Heteropolyacid in Synthesis of Methyl tert-Butyl Ether^a (179)

Catalyst	$10^7 \times \text{Activity}$	
	($\text{mol s}^{-1} \text{g}^{-1}$)	($\text{mol s}^{-1} \text{mol}^{-1} \text{H}^+$)
H ₃ PW ₁₂ O ₄₀	2.0	2.0×10^3
H ₄ SiW ₁₂ O ₄₀	3.3	2.0×10^3
H ₃ PMo ₁₂ O ₄₀	2.3	1.5×10^3
H ₄ PMo ₁₁ VO ₄₀	1.8	0.86×10^3
H ₅ PW ₁₀ V ₂ O ₄₀	3.3	1.9×10^3
H ₇ PW ₈ V ₄ O ₄₀	2.0	0.72×10^3
H ₈ CeMo ₁₂ O ₄₀	2.3	0.6×10^3
H ₆ P ₂ W ₁₈ O ₆₂	5.5	4.4×10^3
H ₆ P ₂ Mo ₁₈ O ₆₂	3.1	1.6×10^3
HZSM-5	0.76	0.55×10^3
H ₂ SO ₄	9.0	0.45×10^3

^a Reaction conditions: 315 K, 12 ml CH₃OH, 1 g cat., $P = 100$ kPa.

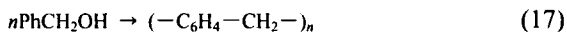
5. Esterification and Ester Decomposition

The addition of carboxylic acids to olefins proceeds in solution in the presence of 10^{-4} – 10^{-2} mol dm⁻³ of H₃PW₁₂O₄₀ at 293–413 K with a selectivity of 100% (7). H₂SO₄ is a less active catalyst than H₃PW₁₂O₄₀ by a factor of 30–90. Esterification of *p*-nitrobenzoic acid with ethanol has been carried out by using H₂SO₄ catalyst in an industrial process (160). In the presence of H₃PW₁₂O₄₀, this reaction takes place with a yield >99% (160). At the end of the reaction, the reaction solution separates into two phases. The upper layer contains ethyl-*p*-nitrobenzoate, toluene, and ethanol, and the lower layer consists of a solution of the heteropolyacid in ethanol. Consequently, the catalyst can be readily separated and reused.

The activities of heteropolyacids for the decomposition of isobutyl propionate were found to be 60–100 times higher than those H₂SO₄ and *p*-toluenesulfonic acid (63). The activity increases with increasing acid strength of heteropolyacids.

6. Alkylation and Dealkylation

Nomiya *et al.* (180) demonstrated that alkylation and acylation [Eqs. (17) and (18)] proceed in the presence of H₄SiMo₁₂O₄₀:



In an acetic acid solution of $\text{H}_3\text{PW}_{12}\text{O}_{40}$, dealkylation of 2,6-di-*tert*-butylphenol to give 2-*tert*-butylphenol takes place at 357 K. The catalytic activity of $\text{H}_3\text{PW}_{12}\text{O}_{40}$ is more than 100 times greater than that of H_2SO_4 (160).

7. Others

In an acetone solution, decomposition of isopropylbenzene hydroperoxide to give phenol and acetone is catalyzed by $\text{H}_3\text{PMo}_{12}\text{O}_{40}$ (181). The heteropolyacid is 3 times more active than H_2SO_4 . Synthesis of 1,1-diacetate from aldehyde and acetic anhydride has been attempted by using $\text{H}_4\text{SiW}_{12}\text{O}_{40}$ and the zeolite HZSM-5 (182). Both catalysts gave more than 98% yield of the diacetate from benzaldehyde. However, the reaction rate was far higher for $\text{H}_4\text{SiW}_{12}\text{O}_{40}$ than for HZSM-5.

V. Heterogeneous Acid-Catalyzed Reactions

A. GENERAL CHARACTERISTICS

Among heteropolyacids, polytungstic acids are the most widely used catalysts owing to their high acid strengths, thermal stabilities, and low reducibilities. As summarized in Section III, the acidic properties (acid strength, acid amount, type of acid, etc.) are controlled by (i) the structure and composition of the heteropolyanion, (ii) the formation of salts (or the counteranions), (iii) the tertiary structure, and (iv) supporting onto carriers such as SiO_2 and active carbon. Factors (ii)–(iv) are specific to the solid state. The acid strength can be controlled mainly by (i), and the number of acid sites is greatly influenced by (ii) and (iii).

In this section, these influences will be described. Besides the acidic properties, the absorption properties of solid heteropolyacids for polar molecules are often critical in determining the catalytic function in "pseudoliquid phase" behavior. This is a new concept in heterogeneous catalysis by inorganic materials and is described separately in Section VI. With this behavior, reactions catalyzed by solid heteropoly compounds can be classified into three types: surface type, bulk type I, and bulk type II (Sections VII and IX). Softness of the heteropolyanion is important for high catalytic activity, although the concept has not yet been sufficiently clarified.

The influence of the heteroatom on the acid strength is shown, for example, in Fig. 28. Here the rates of alkylation of 1,3,5-trimethylbenzene and the decomposition of cyclohexyl acetate catalyzed by the acid forms of several 12-tungstates are plotted against the negative charge of polyanion for solid heteropolyacids (63, 183). The catalytic activities correlate well with the acid strength in solution (Fig. 14). This correlation indicates that the acid strength of

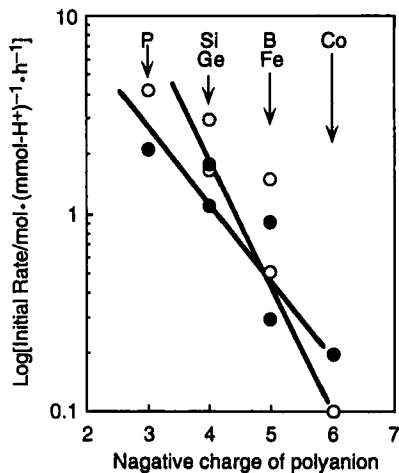


FIG. 28. Catalytic activities (per surface proton) as a function of the negative charge of polyanion, $XW_{12}O_{40}^{n-}$. (○) Alkylation of 1,3,5-trimethylbenzene with cyclohexene; (●) decomposition of cyclohexyl acetate. (From Ref. 183.)

the acid form in the solid state reflects that in solution and decreases with increasing negative charge of the polyanion (Section III).

A correlation between the acid amount of the surface and the catalytic activity for the Cs salts of $H_3PW_{12}O_{40}$ is shown in Fig. 29 (128). The number of surface

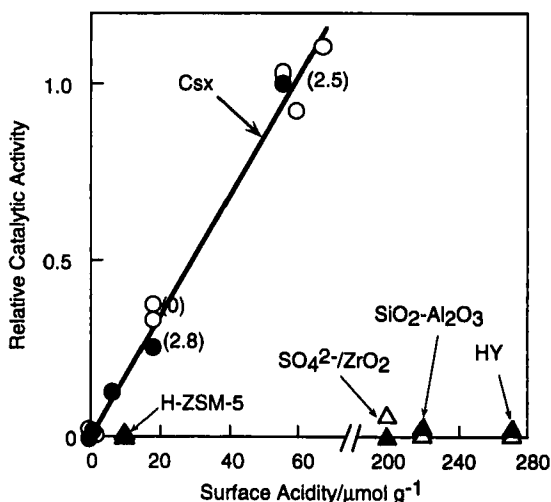


FIG. 29. Surface acidity and catalytic activities for alkylation of 1,3,5-trimethylbenzene with cyclohexene (closed symbols) and decomposition of cyclohexyl acetate (open symbols). (From Ref. 128.)

acid sites was estimated by multiplying the formal concentration of protons on the surface by the specific surface area [e.g., $(0.5) \times (\text{number of polyanion on the surface}) \times (\text{number of protons per polyanion})$] (6, 47). The catalytic activities correlate linearly with the number of surface acid sites. These results are reasonable because the acid strengths of acidic Cs salts are similar to that of the acid form (127). The high catalytic activity of $\text{Cs}_{2.5}\text{H}_{0.5}\text{PW}_{12}\text{O}_{40}$ (Cs2.5) that was reported previously (46a, 48, 127) is thus inferred to be due to the high surface acidity (high surface area and presence of protons).

As described in Section II, the pore size of the acidic Cs salts can be controlled by the Cs content. $\text{Cs}_{2.2}\text{H}_{0.8}\text{PW}_{12}\text{O}_{40}$ (Cs2.2) has pores having an effective size of 6.2–7.5 Å, and the pore size of Cs2.5 is larger than 8.5 Å. Figure 30 shows the catalytic activities of Cs2.1 (the pore size is less than 5.9 Å) and Cs2.2 for each reaction relative to the activity of Cs2.5 (48). Cs2.5 catalyzed all the reactions with considerable activities (the reaction rates are shown in parentheses in Fig. 30). On the other hand, although Cs2.2 was found to be as active as Cs2.5 for dehydration of 2-hexanol (molecular size, 5.0 Å) and decomposition of isopropyl acetate (molecular size, 5.0 Å), it was much less active for the decomposition of cyclohexyl acetate (molecular size, 6.0 Å) and alkylation of 1,3,5-trimethylbenzene (molecular size, 7.5 Å). Therefore, Cs2.2 is

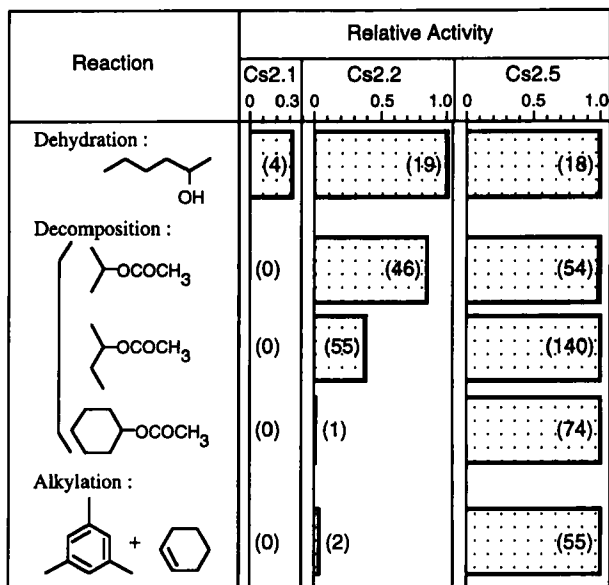


FIG. 30. Relative activities of $\text{Cs}_x\text{H}_{3-x}\text{PW}_{12}\text{O}_{40}$ ($x = 2.1, 2.2, \text{ and } 2.5$) for various kinds of reactions in liquid–solid reaction systems. Catalytic activity was estimated from the initial rate of the reaction. The activity of Cs2.5 for each reaction is taken to be unity. The figures in parentheses are reaction rates in units of $\text{mmol g}^{-1} \text{h}^{-1}$. (From Ref. 48.)

active only for smaller molecules; the reactions are influenced by reactant or transition-state shape selectivity. As for Cs2.1, it is active for the dehydration of 2-hexanol but inactive for other reactions, notwithstanding its high surface area ($55 \text{ m}^2 \text{ g}^{-1}$). To our knowledge, this is the first example of shape-selective catalysis by a solid superacid (47, 48).

A remarkable effect of the counteranion is demonstrated in Fig. 31, where the rates of several reactions are plotted against the extent of neutralization by Na or Cs, that is, x , in $\text{M}_x\text{H}_{3-x}\text{PW}_{12}\text{O}_{40}$ ($\text{M} = \text{Na}$ or Cs) (46, 128). In the case of Na salts, the rates decrease more or less monotonically as the Na content increases. On the other hand, peculiar changes in activity are observed for the Cs salts; activity maxima occur at $x = 0$ and $x = 2.5$. The activity of Cs2.5 relative to that of $\text{H}_3\text{PW}_{12}\text{O}_{40}$ changes depending on the reaction. As will be described in more detail in Section VI, the activity pattern is principally governed by the extent of the contribution of the bulk type I catalysis.

As was described in Section III, the acid strength usually decreases when the catalyst is supported on SiO_2 . Figure 32 shows the influence of the loading of

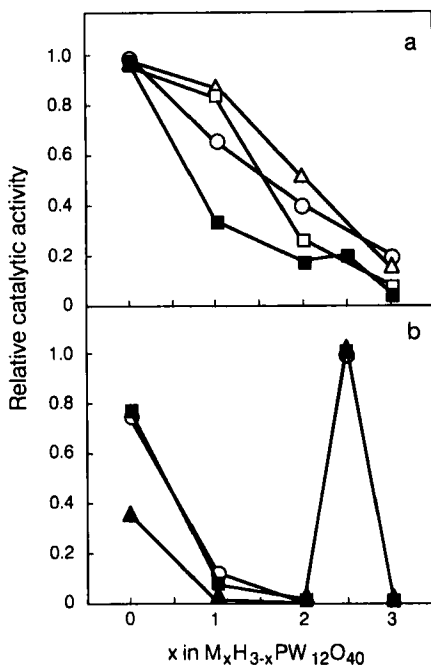


FIG. 31. Catalytic activities of acidic Na or Cs salts of $\text{H}_3\text{PW}_{12}\text{O}_{40}$ as a function of Na or Cs content. (a) $\text{M} = \text{Na}$: (○) dehydration of 2-propanol, (△) decomposition of formic acid, (□) conversion of methanol, (■) conversion of dimethyl ether. (b) $\text{M} = \text{Cs}$: (○) dehydration of 2-propanol, (■) conversion of dimethyl ether, (▲) alkylation of 1,3,5-trimethylbenzene with cyclohexene. (From Refs. 46 and 128.)

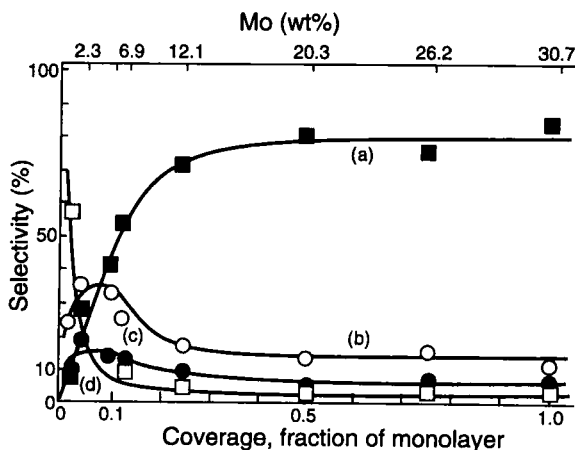


FIG. 32. Dependence of selectivities in methanol oxidation on surface coverage and weight % of Mo for $\text{H}_4\text{SiMo}_{12}\text{O}_{40}$. (a) $(\text{CH}_3)_2\text{O}$, (b) HCHO , (c) $(\text{CH}_3\text{O})_2\text{CH}_2$, (d) HCO_2CH_3 . (From Ref. 184.)

$\text{H}_4\text{SiMo}_{12}\text{O}_{40}$ on the support for catalytic oxidation of methanol (184). At coverages larger than 0.25 monolayer, the selectivities remain constant; dimethyl ether is the main product (about 80%), showing the acidic character of the catalyst. Below 0.25 monolayer, the acidic character is lowered, and dimethyl ether rapidly disappears.

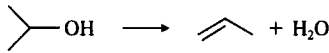
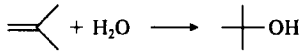
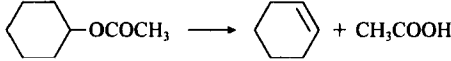
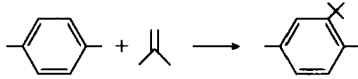
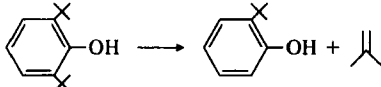
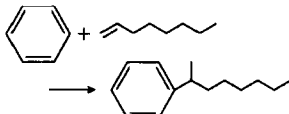
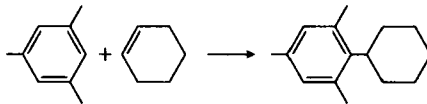
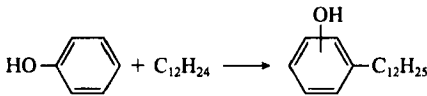
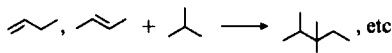
Typical examples of reactions catalyzed by heteropoly compounds in the solid state are summarized in Table XVIII.

B. DEHYDRATION AND HYDRATION

In catalytic dehydration of alcohols, pseudoliquid phase behavior (bulk type I reaction) of heteropolyacids has been demonstrated (Section VI). The high catalytic activity is associated with this behavior and the strong acidity. Unique pressure dependences of the catalytic activity and selectivity are found for $\text{H}_3\text{PW}_{12}\text{O}_{40}$ due to the pseudoliquid phase (Fig. 40).

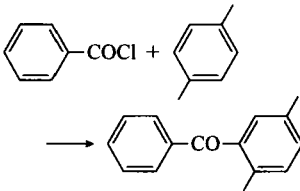
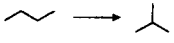
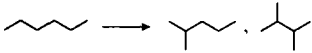
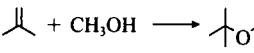
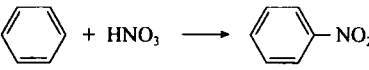
$\text{H}_3\text{PW}_{12}\text{O}_{40}$ was found to be much more active for the dehydration of 2-propanol than $\text{SiO}_2\text{-Al}_2\text{O}_3$ (by a factor of about 30 per weight and about 2000 per surface area) at 398 K (185). The activities of heteropolyacids decrease in the sequence PW_{12} ($\text{H}_3\text{PW}_{12}\text{O}_{40}$) > SiW_{12} > PW_{10}V_2 > PMo_{12} > $\text{PMo}_{10}\text{V}_2$ = SiMo_{12} , which is close to the acid-strength series in solution. Niiyama *et al.* (42) found that the catalytic activities of the water-soluble salts correlate with the electronegativity of the metal cations. Dissociation of coordinated water [type (1) in Section III] has been proposed to account for the acidity.

TABLE XVIII
 Heterogeneous Acid-Catalyzed Reactions

Reaction	Catalyst	Remarks ^a	Ref.
	H ₃ PW ₁₂ O ₄₀	T = 398 K H ₃ PW ₁₂ O ₄₀ : SiO ₂ - Al ₂ O ₃ = 30 : 1 (ratio of activity/g)	185
	H ₄ SiW ₁₂ O ₄₀ / Amberlyst 15	T = 343 K, S = 98.6% (11% conv.)	186
CH ₃ OH(CH ₃ OCH ₃) → C ₁ -C ₆ Hydrocarbons	H ₃ PW ₁₂ O ₄₀ Cs _{2.5} H _{0.5} PW ₁₂ O ₄₀	T = 573 K T = 563 K, S = 74% (C ₂ -C ₄ olefins)	189 195
CH ₃ COOH + C ₂ H ₅ OH → CH ₃ COOC ₂ H ₅ + H ₂ O	H ₃ PW ₁₂ O ₄₀ /SiO ₂	T = 423 K S = 91% (90% conv.)	151
	Cs _{2.5} H _{0.5} PW ₁₂ O ₄₀	T = 373 K Cs _{2.5} : SO ₄ ²⁻ / ZrO ₂ = 43 : 1 (activity/g)	198 199
	H ₃ PW ₁₂ O ₄₀	T = 298 K Y = 75%	203
	H ₃ PW ₁₂ O ₄₀	T = 403 K	205
	H ₃ PW ₁₂ O ₄₀ /SiO ₂	T = 308 K, sensitive to pretreatment	207
	Cs _{2.5} H _{0.5} PW ₁₂ O ₄₀	T = 343 K Cs _{2.5} : H ₂ SO ₄ = 3000 : 1 (activity/H ⁺)	199
	H ₃ PW ₁₂ O ₄₀	T = 373 K H ₃ PW ₁₂ O ₄₀ : H ₂ SO ₄ = 17 : 1 (activity/H ⁺)	249
	H ₃ PW ₁₂ O ₄₀	T = 298 K	209

continued

TABLE XVIII—Continued

Reaction	Catalyst	Remarks ^a	Ref.
	H ₃ PW ₁₂ O ₄₀ /SiO ₂ Cs _{2.5} H _{0.5} PW ₁₂ O ₄₀	T = 411 K	207 214
	Cs _{2.5} H _{0.5} PW ₁₂ O ₄₀	T = 423 ~ 573 K	216 217
	H ₃ PW ₁₂ O ₄₀ /SiO ₂	T = 348 K	215
	H ₄ SiW ₁₂ O ₄₀ /SiO ₂	T = 263 K S = 94.7% (30% conv.)	218 220
CH ₃ NH ₂ → HCN	H ₆ P ₂ W ₁₈ O ₆₂	T = 323 K	
CH ₃ NH ₂ → HCN	H ₃ PW ₁₂ O ₄₀	T = 773 K	226
NH ₃ + CH ₃ OH → (CH ₃) _n NH _m	(NH ₄) ₃ PW ₁₂ O ₄₀	T = 750 K	227
	Cs _{1.5} H _{1.5} PW ₁₂ O ₄₀	T = 413 K S = 97% (94% conv.)	^b

^a T = Temperature, Y = yield, S = selectivity. ^b Sumitomo Chem. Co., LTD., JP 1991-300150.

The Cs salts of H₃PW₁₂O₄₀ show a unique activity pattern for dehydration of 2-propanol (Fig. 32) (46a). Although the change in the catalytic activity resembles that of the surface acidity (Fig. 21), the activity of H₃PW₁₂O₄₀ for this reaction is relatively high. The high activity is explained by the pseudo-liquid phase behavior of H₃PW₁₂O₄₀ and its affinity for the polar molecule, 2-propanol.

H₃PW₁₂O₄₀, H₄SiW₁₂O₄₀, and the supported heteropolyacids catalyze the hydration of isobutylene (186). The supports are listed as follows in the order of activity: Amberlyst 15 [porous sulfonated poly(styrene-divinylbenzene)] ≈ activated carbon > SiO₂ > TiO₂. The maximum activity of H₄SiW₁₂O₄₀/Amberlyst 15 was obtained at about 30 wt% H₄SiW₁₂O₄₀. It was found that polypyrrole and polyacetylene-supported H₃PMo₁₂O₄₀ are much more active than the unsupported parent acid (187). The activity per unit mass of heteropolyacid of the supported catalyst is about 10 times higher for the production of ethylene and ether than that of the unsupported catalyst.

The dehydration of ethanol catalyzed by a membrane comprising H₃PW₁₂O₄₀ and polysulfone was reported (188). The polysulfone is more permeable for

ethylene than for diethyl ether. Thus the selectivity for ethylene in the membrane reactor was higher than that in a fixed-bed reactor containing the same catalyst.

C. CONVERSION OF METHANOL INTO HYDROCARBONS

Ono *et al.* (189) reported that heteropolyacids such as $H_3PW_{12}O_{40}$ and $H_4SiW_{12}O_{40}$ catalyze the conversion of methanol into hydrocarbons, although the activities are less than that of HZSM-5. In contrast to HZSM-5, the main products observed with heteropolyacids are aliphatic C_1 - C_6 hydrocarbons, the selectivities for aromatic hydrocarbons being small (Table XIX).

Counteractions influence the rate and selectivity of this reaction. The activity order, as for cations, was found to be $Ag > Cu, H > Fe > Al > Pd > La > Zn$ (190). The distributions of product hydrocarbons were found to be similar to those observed for $H_3PW_{12}O_{40}$ (Table XIX), suggesting similar reaction mechanisms. Ag and Cu salts of $H_3PW_{12}O_{40}$ are much more active than the acid form catalyst. Protons generated by the reaction of Ag^+ with H_2 are presumed to give the more active catalyst (191).

Hayashi and Moffat (192) reported that the Al salt and the NH_4 salt were effective catalysts for the conversion of methanol to hydrocarbons. They claimed that the NH_4 salts show high catalytic activity and selectivity for the formation of saturated hydrocarbons rather than olefins. The salts of organic

TABLE XIX
Product Distribution in Conversion of Methanol into Hydrocarbons (189)

	Catalyst					
	HTP ^a	CuTP	AgTP	HTS ^a	CuTS	AgTS
Product distribution (%) ^b						
MeOH	1.3	1.2	0	3.9	4.7	0
MeOMe	38.6	37.3	2.0	57.5	35.5	20.1
Hydrocarbons	60.1	61.5	98.0	38.6	50.8	79.9
Hydrocarbons distribution (%) ^b						
CH ₄	3.7	5.2	9.0	1.6	7.3	3.2
C ₂ H ₄	11.3	9.5	9.0	10.3	11.2	10.3
C ₂ H ₆	0.9	0.8	5.2	0.5	0.5	1.2
C ₃ H ₆	8.3	8.5	3.8	8.3	8.7	8.3
C ₃ H ₈	16.1	13.4	34.0	9.8	14.5	21.9
C ₄	39.3	39.2	26.1	41.8	35.1	36.4
C ₅	12.5	13.7	7.2	15.8	15.1	13.3
C ₆	7.9	9.7	5.7	11.9	7.6	5.4

^a TP and TS indicate dodecatungstophosphate and dodecatungstosilicate, respectively. ^b Calculated on a carbon-number basis.

bases are effective for the formation of olefins (193, 194). In the case of an acidic Cs salt, $\text{Cs}_{2.5}\text{H}_{0.5}\text{PW}_{12}\text{O}_{40}$, the selectivity for $\text{C}_2\text{-C}_4$ olefins increased continuously as the Cs content increased, e.g., being 43% for $\text{H}_3\text{PW}_{12}\text{O}_{40}$ and 64% for $\text{S}_{2.5}\text{H}_{0.5}\text{PW}_{12}\text{O}_{40}$ (195).

Pseudoliquid phase behavior is important in this reaction. The kinetics observed with $\text{H}_3\text{PW}_{12}\text{O}_{40}$ is quite different from that observed with HZSM-5. No induction period in the rate of hydrocarbon formation was observed in the former, in contrast to the latter, suggesting that the methanol conversion catalyzed by $\text{H}_3\text{PW}_{12}\text{O}_{40}$ is not autocatalytic (196). The results were explained by pseudoliquid phase behavior of $\text{H}_3\text{PW}_{12}\text{O}_{40}$ (Section VI). The selectivity to lower olefins is improved by control of the pseudoliquid phase behavior. The olefin/paraffin ratio in the product hydrocarbon depends inversely on the ability of the heteropoly compounds to absorb reactant dimethyl ether. The ratio is greatly increased as the contribution to catalysis of the bulk phase of the catalyst (pseudoliquid phase) decreases (Section VI) (195, 197). It was confirmed that the acid strength is not significant in influencing the selectivity of this reaction.

D. ESTERIFICATION AND ESTER DECOMPOSITION

Okuhara *et al.* (198, 199) found that $\text{Cs}_{2.5}\text{H}_{0.5}\text{PW}_{12}\text{O}_{40}$ (Cs2.5) is much more active for the decomposition of cyclohexyl acetate in liquid–solid mixture than Nafion-H (sulfonated fluorocarbon resin), HY zeolite, HZSM-5, $\text{SiO}_2\text{-Al}_2\text{O}_3$, and $\text{SO}_4^{2-}/\text{ZrO}_2$. Figure 33 demonstrates the superiority of Cs2.5 for this reaction as well as the alkylation of 1,3,5-trimethylbenzene. The activity of Cs2.5 is more than 200 times as high as that of $\text{SiO}_2\text{-Al}_2\text{O}_3$. The difference is much greater than that observed for gas–solid mixtures (46a, 195). Cs2.5 works as an insoluble catalyst in esterification of acetic acid with ethanol (200). The

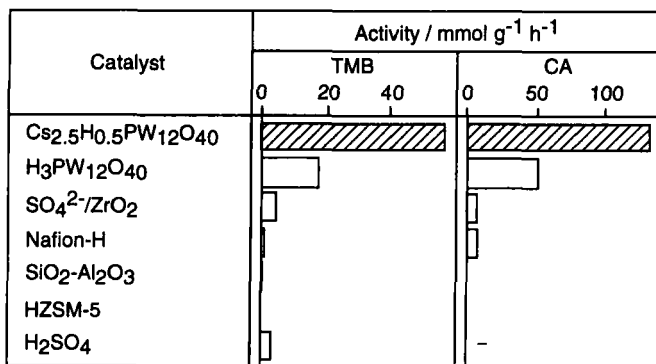


FIG. 33. Catalytic activities of various acid catalysts for liquid-phase reactions. TMB: Alkylation of 1,3,5-trimethylbenzene with cyclohexene; CA: Decomposition of cyclohexyl acetate. (From Ref. 47.)

order of catalytic activities for the esterification at 333 K (acetic acid/ethanol/catalyst = 100/100/1 by weight) is as follows: Amberlyst 15 (1.6×10^{-3}) > Cs2.5 (0.52×10^{-3}) > HZSM-5 (0.03×10^{-3}), where the figures in parentheses are rate constants in units of $\text{min}^{-1} \text{g}^{-1}$. In the hydrolysis of ethyl acetate (ethyl acetate/water/catalyst = 1080/28/0.1 by weight), the activities are in the order Amberlyst 15 > Cs2.5 > HZSM-5.

Izumi *et al.* (201) found that activated carbon firmly entraps $\text{H}_3\text{PW}_{12}\text{O}_{40}$ and the acid is resistant to extraction with hot water or hot methanol. The entrapped $\text{H}_3\text{PW}_{12}\text{O}_{40}$ showed a catalytic activity for the esterification of acetic acid with ethanol comparable to that of Nafion-H. With $\text{H}_3\text{PW}_{12}\text{O}_{40}$ supported on carbon, a selectivity to ethyl acetate of 99.5% at 95% conversion was obtained. Heteropolyacids supported on SiO_2 or carbon are more active than $\text{SiO}_2\text{-Al}_2\text{O}_3$ (202), but Al_2O_3 is not suitable as a support, because Al_2O_3 readily decomposes heteropolyacids due to the high basicity of the surface.

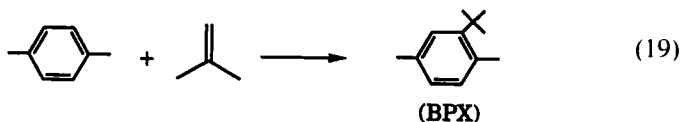
Cs2.5 in water is hardly separable by filtration because of its very fine particle size. Cs2.5/ SiO_2 prepared by the hydrolysis of ethyl orthosilicate in the presence of colloidal Cs2.5 is efficient for the hydrolysis of ethyl acetate, although it is less active than Amberlyst 15 (200).

The catalytic activity of $\text{H}_3\text{PW}_{12}\text{O}_{40}$ for esterification of phthalic anhydride with 2-ethylhexanol is higher than those of conventional soluble acids such as *p*-toluenesulfonic acid (202).

E. ALKYLATION AND DEALKYLATION

Conventional soluble catalysts such as H_2SO_4 and AlCl_3 have been used in industry for alkylation reactions, but these are characterized by operational problems of corrosion, catalyst removal, waste formation, etc. Insoluble solid catalysts are desirable for these reactions.

$\text{H}_3\text{PW}_{12}\text{O}_{40}$ catalyzes the monoalkylation of *p*-xylene with isobutylene (203) [Eq. (19)]. The product *tert*-butyl-*p*-xylene (BPX) is an important precursor for liquid crystalline polyesters and polyamides having low melting points and good solubilities. The introduction of the *tert*-butyl group in the position ortho to the methyl group of *p*-xylene takes place very slowly, with H_2SO_4 or AlCl_3 as the catalysts (whereas alkylation at the meta or para position of *o*- or *m*-xylene occurs rapidly):



The results of Table XX demonstrate that $\text{H}_3\text{PW}_{12}\text{O}_{40}$ is an excellent catalyst for this reaction. The selectivities are in the order $\text{H}_3\text{PW}_{12}\text{O}_{40}$ (75%) >

TABLE XX
*Selectivity for Alkylation of *p*-Xylene with Isobutylene by Various Acid Catalysts (203)*

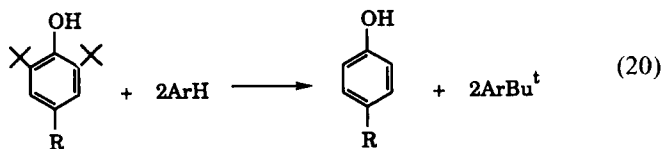
Catalyst	Selectivity ^a (%)				Conversion (%)	Mass balance (%)
	BPX ^b	Oligomers ^c	OPX ^d	PXM ^e		
H ₃ PW ₁₂ O ₄₀	74.6	11.5	6.3	7.6	90	96
H ₄ SiW ₁₂ O ₄₀	26.6	70.2	0.4	2.8	91	108
H ₅ BW ₁₂ O ₄₀	6.1	93.9	0	0	97	119
Cs _{2.5} H _{0.5} PW ₁₂ O ₄₀	50.5	48.0	0.8	0.7	89	110
SO ₄ ²⁻ /ZrO ₂	50.9	26.0	3.4	19.7	86	86
Amberlyst-15	4.2	95.8	0	0	92	109
SiO ₂ -Al ₂ O ₃	1.3	98.7	0	0	75	101
H ₂ SO ₄	7.2	92.8	0	0	86	68
CF ₃ COOH	0	100	0	0	10	81

^a Mol%. ^b *t*-Butyl-*p*-xylene. ^c Sum of dimer, trimer, and tetramer of isobutylene. ^d Octyl-*p*-xylene. ^e Di-*p*-xylylmethane. The reaction was performed at 303 K for 30 min. *p*-Xylene, 0.28 mol; isobutylene, 0.37 mmol min⁻¹; catalyst, 0.45 g.

H₄SiW₁₂O₄₀ (26.6%) > H₅BW₁₂O₄₀ (6.1%) (203). The results indicate that the acid strength is essential for the selectivity; that is, strong-acid sites are effective for the alkylation to BPX, but weak-acid sites preferentially catalyze the oligomerization of isobutylene. Although SO₄²⁻/ZrO₂ is a stronger acid than H₃PW₁₂O₄₀, it is less selective. SO₄²⁻/ZrO₂ also has a large number of weak-acid sites which are probably active for the oligomerization.

Alkylation of *p*-cresol by isobutylene is an important reaction in the synthesis of phenolic antioxidants. The activity of H₃PW₁₂O₄₀ for this reaction is greater by four orders of magnitude than that of H₂SO₄ (160). Alkylation of *p*-(*tert*-butyl)phenol (TBP) with cyclohexene, 1-hexene, styrene, or benzyl chloride proceeds in the presence of H₃PW₁₂O₄₀ at 3373–423 K (204).

Alkylation with styrene gives 2,6-dialkyl TPB with a selectivity of 90% at 100% conversion. When the alkylation of TBP is completed, an excess of *o*-xylene is introduced into the reaction system, and 2,6-dialkylphenol is obtained through the trans alkylation without the need for separation of 2,6-dialkyl-4-*tert*-butylphenol (160) [Eq. (20)].



Dealkylation of 2,6-di-*tert*-butylphenol takes place at 403–423 K in the presence of solid H₃PW₁₂O₄₀. H₃PW₁₂O₄₀ is two orders of magnitude more active than aluminum sulfate for this reaction (205).

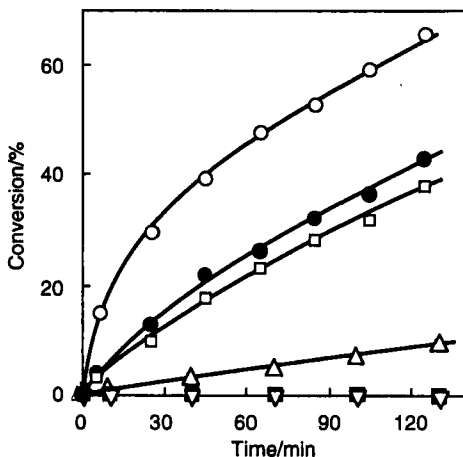
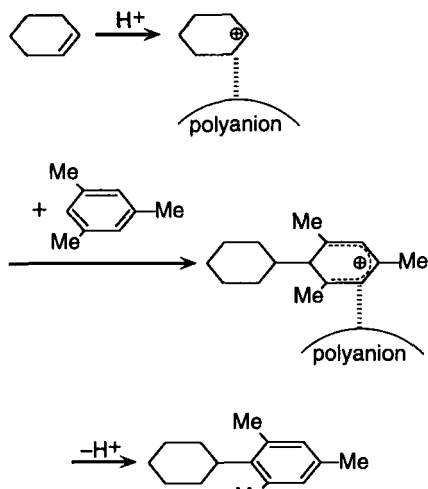


FIG. 34. Time course of alkylation of 1,3,5-trimethylbenzene with cyclohexene at 343 K. (○) Cs_{2.5}H_{0.5}PW₁₂O₄₀(Cs_{2.5}), (●) second run for Cs_{2.5}, (□) third run for Cs_{2.5}, (△) SO₄²⁻/ZrO₂, (▼) Nafion-H, (■) HY zeolite. (From Ref. 199.)

Figure 34 shows the time course of alkylation of 1,3,5-trimethylbenzene with cyclohexene (199). In the presence of Cs_{2.5}, the reaction rate reached a steady value after approximately 1.5 h. When Cs_{2.5} was filtered and reused (in the second and third runs), the rates were nearly equal to the steady-state value of the first run, indicating that there was little catalyst deactivation and that the reaction did not take place in solution. The primary reason for the high activity of Cs_{2.5} is both its strength of acid sites and acid strength (Section III). The specific activities of heteropoly catalysts (rates per acid group) are much greater than the activities of SiO₂-Al₂O₃, SO₄²⁻/ZrO₂, or zeolites. This result cannot be explained simply on the basis of the acidic properties. There are additional effects such acid-base bifunctional acceleration by the cooperation of proton (acid) and polyanion (base) groups (127). A proposed reaction model is illustrated in Scheme 4.

Supported heteropolyacids are also used for alkylation reactions. Alkylation of benzene with 1-dodecene was examined with H₄SiW₁₂O₄₀/SiO₂ as the catalyst (206). SiO₂ is a better support for the catalyst in this reaction than Al₂O₃ or SiO₂-Al₂O₃; H₃PW₁₂O₄₀/SiO₂ catalyzes the reaction at room temperature (207). The pretreatment temperature of the catalyst has a significant effect on the activity. As shown in Fig. 35, the maximum conversion of 1-octene was obtained when the catalyst was treated at 423 K. Pretreatment at a lower temperature such as 373 K gives a reduced acid strength, probably because of the remaining water of crystallization. H₃PW₁₂O₄₀/MCM-41 exhibits a higher activity than H₂SO₄ in liquid phase alkylation of TBP with isobutylene or



styrene (208). Supported heteropolyacids are also active catalysts for alkylation of benzene with ethylene at 473 K in the presence of vapor-phase reactants (151). Recently, Soled *et al.* (159) reported that $C_{2.5}H_{0.5}PW_{12}O_{40}$ supported on SiO_2 extrudate is effective for this reaction.

The alkylation of isobutane with *n*-butenes to give C_8 alkylate [Eq. (21)] is a widely used and increasingly important process in petroleum refining. The

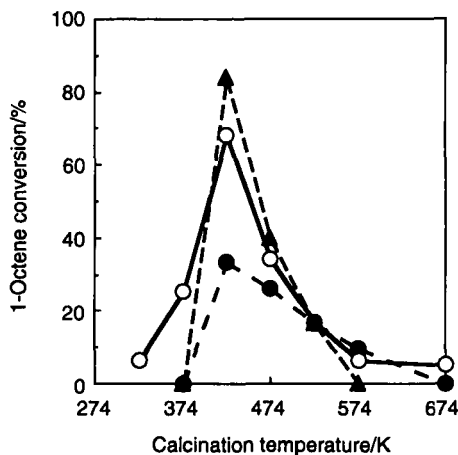
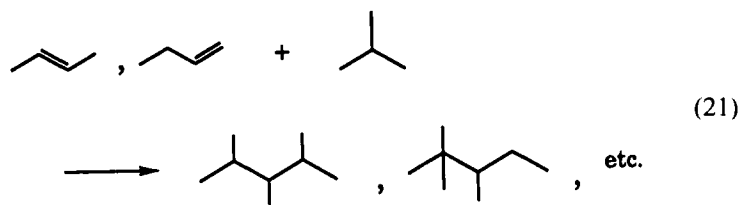


FIG. 35. Alkylation of benzene with 1-octene with $H_3PW_{12}O_{40}$ (303 K). (O) Supported on silica A (15 wt%); (●) supported on silica B (15 wt%), (▲) unsupported. (From Ref. 207.)

commercial catalysts are HF or H₂SO₄; HF has the disadvantages of being highly toxic and corrosive, and H₂SO₄ processes produce large amounts of spent acid. Both liquid acids constitute environmental hazards because of potential spills.



Therefore, new solid catalysts to replace these liquid acids are desirable. Okuhara *et al.* (209) reported that Cs_{2.5}H_{0.5}PW₁₂O₄₀ catalyzes this alkylation reaction at room temperature and that it is much more active than SO₄²⁻/ZrO₂. Yield and selectivity data are summarized in Table XXI. The catalytic activities are in the following order: Cs2.5 > H₃PW₁₂O₄₀ > SO₄²⁻/ZrO₂. The selectivity to C₈ alkylates in the total products was 73.3% for Cs2.5. A patent from Idemitsu Co. (210) also describes the high activity of Cs2.5 for this reaction. Another patent from Mobil gives data for H₃PW₁₂O₄₀/MCM-41 (211).

The alkylation of toluene with methanol is catalyzed by the NH₄ salt of H₃PW₁₂O₄₀ (212).

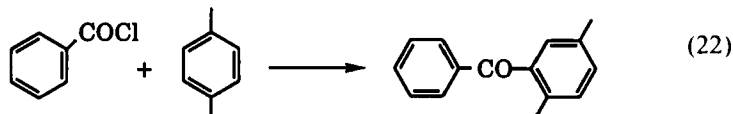
TABLE XXI
Yields and Selectivities of Products in Alkylation of Isobutane with 1-Butene Catalyzed by Solid Acids at Room Temperature (209)

	Cs _{2.5} H _{0.5} PW ₁₂ O ₄₀	H ₃ PW ₁₂ O ₄₀	SO ₄ ²⁻ /ZrO ₂
Total yield (wt%) ^a	79.4	25.1	23.0
Selectivity (wt%) ^b			
224-TMP [RON: 100]	0.3	0.6	1.6
223-TMP [RON: 110]	24.1	18.4	28.0
234-TMP [RON: 103]	23.6	15.2	13.9
233-TMP [RON: 106]	14.5	13.9	10.9
23-DMH	10.8	8.1	7.2
(C ₈ alkylates)	(73.3)	(56.2)	(61.6)
C ₅ -C ₇ ^c	1.5	0.8	0.9
Dimers ^d	13.9	8.5	9.2
C ₉ -C ₁₂ ^e	11.3	34.0	26.6

^a Yield (wt%) is defined by 100 × [the weight of products divided by the weight of 1-butene charged]. ^b 224-TMP = 2,2,4-trimethylpentane, 23-DMH = 2,3-dimethylhexane, etc. Figures in parentheses are research octane number (RON). ^c Hydrocarbons containing 5-7 carbon atoms. ^d Octenes. ^e Hydrocarbons containing 9-12 carbon atoms. Catalyst, 1.0 g; 1-butene, 0.94 g; isobutane, 9.4 g. All data were collected at 7 h.

F. ACYLATION

Industrial acylation of alkylaromatics is generally carried out with acid chlorides as reactants or stoichiometric amounts of AlCl_3 (catalyst). Solid acid catalysts would be desirable. Izumi *et al.* (207) found that SiO_2 -supported $\text{H}_3\text{PW}_{12}\text{O}_{40}$ and $\text{H}_4\text{SiW}_{12}\text{O}_{40}$ are good insoluble catalysts for acylation, with anhydrides or chlorides as acylating agents [Eq. (22)].



It was confirmed that the reaction did not proceed in the liquid phase. A rapid decline in catalytic activity was observed. The deactivation is probably caused by strong adsorption of the product benzophenone on the catalyst; the acylation was retarded when the reaction was started in the presence of benzophenone. The reaction also proceeded with $\text{H}_3\text{PMo}_{12}\text{O}_{40}/\text{SiO}_2$ as the catalyst, but the $\text{H}_3\text{PMo}_{12}\text{O}_{40}$ decomposed during the reaction. It was presumed that the catalytically active species was not the heteropolyacid on the support, but was probably Mo chloride instead (213).

$\text{Cs}_{2.5}\text{H}_{0.5}\text{PW}_{12}\text{O}_{40}$ (Cs2.5) catalyzes the acylation of aromatic compounds with benzyl chloride, benzoyl chloride, benzoic anhydride, benzoic acid, or acetic acid (214). As shown in Table XXII, $\text{H}_3\text{PW}_{12}\text{O}_{40}$ is usually less active than

TABLE XXII
Friedel-Crafts Acylation Catalyzed by $\text{Cs}_{2.5}\text{H}_{0.5}\text{PW}_{12}\text{O}_{40}$ (214)

Substrates		Product yield ^b (%)	
Acylating agent	Aromatic compound	$\text{Cs}_{2.5}\text{H}_{0.5}\text{PW}_{12}\text{O}_{40}$	$\text{H}_3\text{PW}_{12}\text{O}_{40}$
(PhCO) ₂ O	<i>p</i> -xylene	57	3
(PhCO) ₂ O	anisole	85	69 ^c
(PhCO) ₂ O	chlorobenzene	0	0
PhCO ₂ H	<i>p</i> -xylene	11 ^d	8 ^c
PhCO ₂ H	anisole	3	4 ^f
Ac ₂ O	anisole	89	50 ^f
AcOH	anisole	16	15 ^f
<i>n</i> -C ₇ H ₁₅ COCl	mesitylene	80	44 ^f

^aYield is based on acylating agent. ^bAcylating agent/aromatic compound/catalyst = 5/100/0.1 mmol; reflux 2 h. ^cCatalyst was dissolved. ^dAcylating agent/aromatic compound/catalyst = 5/100/0.05 mmol. The water liberated was continuously removed by means of Dean-Stark equipment. ^eAcylating agent/aromatic compound/catalyst = 5/100/0.10 mmol. ^fCatalyst was partly dissolved.

Cs_{2.5} for the acylation. Anisole and *p*-xylene are acylated with benzoic anhydride and acetic anhydride in the presence of Cs_{2.5} without the dissolution of this catalyst. Carboxylic acids are much less reactive as acylating agents than the corresponding anhydrides because of the liberation of water. But when the water is removed, the acylation proceeds smoothly (214). Although the reaction of benzene with acetic acid is attractive in prospect, there is no report of heteropoly compounds as catalysts for this reaction.

G. SKELETAL ISOMERIZATION OF ALKANES

The skeletal isomerization of straight-chain paraffins is important for the enhancement of the octane numbers of light petroleum fractions. The isomerization of *n*-butane to isobutane has attracted much attention because isobutane is a feedstock for alkylation with olefins and MTBE synthesis. It is widely believed that the low-temperature transformation of *n*-alkanes can be catalyzed only by superacidic sites, and this reaction has often been used to test for the presence of these sites.

Nowinska *et al.* (215) reported the isomerization of *n*-hexane catalyzed by (NH₄)₃PW₁₂O₄₀ and by H₃PW₁₂O₄₀/SiO₂. H₃PW₁₂O₄₀/SiO₂ has an appreciable activity at 423 K, but the activity of H₃PW₁₂O₄₀ is low, and SiO₂-Al₂O₃ is inactive at this temperature. Cs_{2.5} catalyzes the isomerization of *n*-butane at 573 K, and the rates of isobutane formation and the selectivity were much higher than those of SO₄²⁻/ZrO₂, as shown in Table XXIII (216, 217). The initial activity of SO₄²⁻/ZrO₂ is very high, but the conversion decreases considerably during the initial stage of reaction. In contrast, the deactivation is relatively small for Cs_{2.5}. Figure 36 shows the effects of reaction temperature for catalysis by Cs_{2.5}. Deactivation was observed at 473–573 K, but not at 423 K. At temperatures less than 473 K, SO₄²⁻/ZrO₂ is more active than Cs_{2.5}. The

TABLE XXIII
Activity and Selectivity for Skeletal Isomerization of *n*-Butane^a (217)

Catalyst	10 ⁸ × Rate ^b	Selectivity ^c (mol%)					
		C ₁	C ₂ + C ₂ ⁻	C ₃ + C ₃ ⁻	Isobutane	C ₄ ⁻	C ₅ (+)
Cs _{2.5} H _{0.5} PW ₁₂ O ₄₀	2.0	1.1	2.0	8.5	83.1	0.8	4.5
H ₃ PW ₁₂ O ₄₀	0.4	1.1	2.4	11.7	80.9	0	3.9
SO ₄ ²⁻ /ZrO ₂	0.4	3.1	9.1	23.0	60.8	0	4.0
H-ZSM-5	2.9	0.7	2.3	74.5	14.1	0.4	8.0
H-Y ^d	0.03	15.8	33.3	18.1	11.1	18.1	2.9

^a 573 K, butane 5%. ^b Formation of isobutane, mol g⁻¹ s⁻¹. ^c C₁, CH₄; C₂ + C₂⁻, C₂H₄ + C₂H₆; C₃ + C₃⁻, C₃H₆ + C₃H₈; C₄⁻, C₄H₈; C₅(+), hydrocarbons containing more than 5 carbons. ^d 673 K.

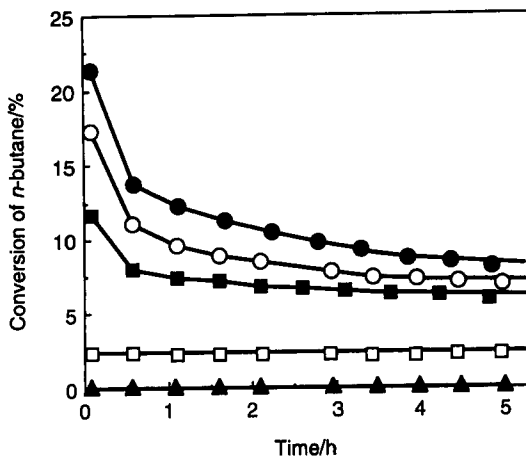


FIG. 36. Time course of *n*-butane isomerization catalyzed by $\text{Cs}_{2.5}\text{H}_{0.5}\text{PW}_{12}\text{O}_{40}$ at various temperatures: (●) 573 K, (○) 523 K, (■) 473 K, (□) 423 K, (▲) 373 K. (From Ref. 217.)

skeletal isomerization of alkanes catalyzed by metal-promoted heteropoly compounds is described in Section XI.

H. MTBE SYNTHESIS

Methyl *tert*-butyl ether (MTBE) is a good, widely used octane improver of gasoline. Igarashi *et al.* (218) reported that $\text{H}_3\text{PW}_{12}\text{O}_{40}$, $\text{H}_3\text{PMo}_{12}\text{O}_{40}$, etc. and their SiO_2 -supported analogs have catalytic activities superior to those of mixed oxides, fluorinated oxides, and mounted mineral acids for the MTBE synthesis from isobutylene and methanol in gas–solid reactors. Among the heteropoly catalysts, 20 wt% $\text{H}_4\text{SiMo}_{12}\text{O}_{40}/\text{SiO}_2$ was most effective; the selectivity was 95% at 30% conversion of isobutylene at 363 K. Ono and Baba (219) used $\text{Ag}_3\text{PW}_{12}\text{O}_{40}$ supported on carbon as a catalyst for MTBE synthesis. The treatment of the Ag salt with H_2 greatly enhanced the activity, whereas no effect was observed for the acid form and Al salt.

Effects of acid strength and structure of heteropolyanion on catalytic activity have been examined (220). The activity order is $\text{H}_6\text{P}_2\text{W}_{18}\text{O}_{62} \gg \text{H}_3\text{PW}_{12}\text{O}_{40} > \text{H}_4\text{SiW}_{12}\text{O}_{40} \approx \text{H}_4\text{GeW}_{12}\text{O}_{40} > \text{H}_5\text{BW}_{12}\text{O}_{40} > \text{H}_6\text{CoW}_{12}\text{O}_{40}$, whereby the selectivity for MTBE exceeded 95%. The results are much better than those observed with $\text{SO}_4^{2-}/\text{ZrO}_2$, $\text{SiO}_2\text{-Al}_2\text{O}_3$, and HZSM-5 (220). It is probable that the pseudoliquid phase behavior of $\text{H}_6\text{P}_2\text{W}_{18}\text{O}_{62}$ is responsible for its high performance. By supporting $\text{H}_6\text{P}_2\text{W}_{18}\text{O}_{62}$ or $\text{H}_3\text{PW}_{12}\text{O}_{40}$ on SiO_2 , the yield of MTBE increased greatly and became comparable to that of the resin Amberlyst 15, which is representative of today's industrial catalysts for MTBE synthesis.

The reaction of *tert*-butyl alcohol and methanol to form MTBE is also catalyzed by heteropoly compounds (221–223). A relationship was found between the amount of pyridine sorbed in or on heteropoly compounds and *tert*-butyl alcohol conversion (221). The dependence of the rate on methanol partial pressure resembles that for the absorption of methanol in the bulk, suggesting pseudoliquid phase behavior (223).

I. OTHER REACTIONS

A wide variety of acid-catalyzed reactions besides those described above have been investigated with heteropoly compounds as catalysts. Al_2O_3 -supported $\text{H}_3\text{PW}_{12}\text{O}_{40}$ (probably decomposed) catalyzed propylene–ethylene codimerization at 573 K to form pentenes with a selectivity of 56% (butenes 17%, hexenes 27%) (224). Propylene oligomerization proceeded on various kinds of salts of $\text{H}_3\text{PW}_{12}\text{O}_{40}$ (225). The activities of the salts decrease in the order $\text{Al} \gg \text{Co} > \text{Ni}$, $\text{NH}_4 > \text{H}$, $\text{Cu} > \text{Fe}$, $\text{Ce} > \text{K}$. The Al salt gave trimers with 90% conversion at 503 K. The selectivities to trimer are about 40% for Al, Ce, Co, and Cu, while that of the acid form is 25%.

Dehydrogenation of monomethylamine to give hydrogen cyanide is catalyzed by $\text{H}_3\text{PW}_{12}\text{O}_{40}$ at 773 K (226). Al_2O_3 and $\text{SiO}_2\text{-Al}_2\text{O}_3$ have no activity for the reaction under the same conditions. $(\text{NH}_4)_3\text{PW}_{12}\text{O}_{40}$ is active for synthesis of methylamines from ammonia and methanol (227). The formation of trimethylamine is suppressed with this catalyst, which is explained by the strong adsorption of trimethylamine. Cracking of paraffins (228, 229), isomerization of olefins (230, 231), transformation of alkylbenzene (232), etc. have also been reported.

VI. Pseudoliquid Phase

In ordinary heterogeneous catalysis of gas–solid and liquid–solid reactions, the reactions take place on the two-dimensional surfaces of solid catalysts (both on the outer surface and on the surfaces of pore walls). In contrast, the reactions of polar molecules in the presence of heteropoly catalysts often proceed not only on the surface but also in the bulk phase. We call this “pseudoliquid phase” behavior. The pseudoliquid phase is a unique reaction medium consisting of the three-dimensional solid bulk, as was first proposed in 1979 (17, 233, 234).

Because of the flexible and hydrophilic nature of the secondary structures of the acid forms and group A salts (Section II), polar molecules like alcohols and amines are readily absorbed into the solid bulk by substituting for water molecules and/or by expanding the distance between polyanions. The number of absorbed molecules is $10\text{--}10^2$ times greater than the amount of monolayer

TABLE XXIV
Types of Acid Catalysis by Salts of Heteropolyacids

Salts ^a	Polar molecules (e.g., dehydration of ethanol)	Nonpolar molecules (e.g., isomerization of butenes)
A salts (e.g., Na)	Pseudoliquid (bulk type I)	Surface type
B salts (e.g., Cs)	Surface type	Surface type

^a Besides the above types, there is bulk type II (Section IX).

adsorption estimated from N₂ adsorption. Heteropoly compounds absorbing significant amounts of polar compounds behave in a sense like concentrated solutions. As classified in Table XXIV, the pseudoliquid behavior is found for acid catalysis of reactions of polar molecules by group A salts at relatively low temperatures. Another bulk-type catalysis (type II) is described in Section IX.

A. ABSORPTION OF POLAR MOLECULES

When pyridine vapor at 298 K is brought in contact with solid H₃PW₁₂O₄₀ or H₃PMo₁₂O₄₀ after dehydration at 403 K, several molecules of pyridine per polyanion (in the entire bulk) are sorbed (5, 125). After evacuation at 298 K, the number of pyridine molecules per polyanion becomes about 6 (twice the number of protons). Single-crystal X-ray and IR analyses revealed that H₃PW₁₂O₄₀ · 6C₅H₅N consists of [(C₅H₅NH)₃ · PW₁₂O₄₀] (39). Considering the surface area of H₃PW₁₂O₄₀ (5 m² g⁻¹) and the cross section of a pyridine molecule (31 Å²), the uptake of 6 pyridine molecules per polyanion corresponds to about 80 times that corresponding to a surface monolayer (235). Some heteropoly compounds swell by absorbing a great number of polar molecules. Deliquescence is observed upon excess absorption. Large uptakes of alcohols into H₃PW₁₂O₄₀ have also been reported (125, 235–238).

In Table XXV, the rates and amounts of absorption of various molecules are summarized (235). Polar molecules such as alcohol, ether, and amine are readily absorbed. In contrast, nonpolar molecules like hydrocarbons are sorbed only on the surface. The initial rates of absorption of molecules are plotted against the molecular size in Fig. 37. The initial rates of alcohol sorption greatly decrease as the molecular size increases from 20 Å² (methanol) to 35 Å² (1-butanol). The rates are higher for amines than for alcohols, regardless of the molecular size. This difference is due to the greater basicity of amines. Thus, it may be stated that the rate is primarily determined by the basicity (or polarity) and secondarily by the molecular size (235).

Diffusion coefficients of molecules in the lattice of H₃PW₁₂O₄₀ are *ca.* 10³ times less than those of molecules in the micropores of zeolites (235). Niiyama *et al.* reported that the effective diffusion coefficient is in the order of

TABLE XXV
Rate and Amount of Absorption of Molecule into $H_3PW_{12}O_{40}$ (235)

Molecule	(pK _a)	Size ^a	μ^b	P ^c	Rate ^d	Absorption amounts ^e	
						S ^f	I ^g
CH ₃ OH	(-2.0)	20	1.71	30 (20)	5.2	6.0	3.1 (26)
C ₂ H ₅ OH	(-3.0)	25	1.73	30 (43)	5.5	14.1	6.1 (64)
<i>n</i> -C ₃ H ₇ OH	(-3.0)	30	1.73	20 (80)	3.8	14.0	6.2 (78)
<i>i</i> -C ₃ H ₇ OH	(-3.2)	31	1.67	30 (57)	3.1	12.1	6.1 (76)
<i>n</i> -C ₄ H ₉ OH	(-3.8)	35	1.81	4 (50)	2.0	5.4	2.8 (41)
(CH ₃) ₂ O	(-3.8)	30	1.30	760 (15)	1.6	4.0	2.6 (33)
(C ₂ H ₅) ₂ O	(-3.6)	37	1.17	350 (59)	6.2	6.3	5.8 (89)
(<i>n</i> -C ₃ H ₇) ₂ O	(-4.3)	45	1.20	30 (52)	1.1	4.9	4.6 (86)
1,4-Dioxane	(-2.9)	33	1.40	30 (76)	2.2	8.3	4.8 (66)
<i>n</i> -C ₃ H ₇ NH ₂	(10.7)	32	1.34	30 (9)	3.1	12.0	7.0 (89)
<i>i</i> -C ₃ H ₇ NH ₂	(10.6)	33	—	30 (5)	4.1	9.5	6.9 (86)
<i>n</i> -C ₄ H ₉ NH ₂	(10.8)	35	1.32	30 (28)	6.0	15.2	8.6 (125)
C ₅ H ₅ N	(5.2)	31	2.32	15 (62)	4.0	8.5	6.0 (78)
C ₆ H ₆	—	34	0	65 (43)	—	0.50	0.10 (1.4)
C ₂ H ₄	—	16	0	60 (0.13)	—	0.04	0.03 (0.2)
NO ^h	—	13	—	0.8 (0.1)	—	2.8	—

^aCross section (\AA^2). ^bDipole moment, Debye. ^cIntroduced at 301 K, Torr. The figures in parentheses are the relative pressure (%). ^dThe initial absorption rate; number of molecules ($\text{anion} \cdot 10 \text{ min}^{-1}$). ^eNumber of molecule \cdot anion⁻¹. ^fSaturated amount. ^gIrreversible amount. The figures in parentheses are the numbers of surface layers (see text). ^hFeed gas: 0.1% NO + 5% O₂ + 5% H₂O + 89.9% He at 423 K (Yang, R. T., and Chen, N., *Ind. Eng. Chem. Res.* **33**, 825 (1994)).

10^{-11} – $10^{-13} \text{ m s}^{-1}$, much less than those in the gas phase but close to those in the liquid phase (239).

The amounts of absorbed molecules in $H_3PW_{12}O_{40}$ tend to be integral multiples of the number of protons (3, 6, 9, etc.), suggesting that these molecules form stable secondary structures throughout the bulk. Transitions between the different absorption states take place as a result of pressure changes (235). These transitions are closely related to the catalytic behavior for the dehydration of alcohol, as described below.

B. EVIDENCE FOR THE PSEUDOLIQUID PHASE

There is circumstantial evidence in our early studies indicating the pseudo-liquid behavior: (1) rapid absorption of a large quantity of polar compounds as described above; (2) expansion of the solid volume of the materials upon absorption; and (3) quite high catalytic activity of $H_3PW_{12}O_{40}$, $H_3PMO_{12}O_{40}$, etc., despite their low surface areas (234). Firm evidence that catalytic reactions

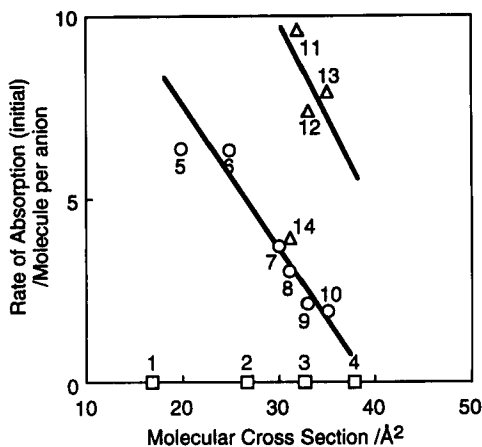


FIG. 37. Initial rates of absorption of various compounds by $H_3PW_{12}O_{40}$ related to cross section of molecules. (1) Ethylene, (2) dichloroethane, (3) benzene, (4) toluene, (5) methanol, (6) ethanol, (7) 1-propanol, (8) 2-propanol, (9) 1,4-dioxan, (10) 1-butanol, (11) 1-propanamine, (12) 2-propanamine, (13) 1-butanamine, (14) pyridine. (From Ref. 235.)

take place in the pseudoliquid phase has been obtained by a transient response analysis using isotopically labeled reactants (236, 240). Figure 38 illustrates a typical result observed for the dehydration of 2-propanol catalyzed by $H_3PW_{12}O_{40}$. The feed gas was instantaneously changed from 2-propanol- d_0 to 2-propanol- d_8 after a steady state of the reaction had been attained. 2-Propanol- d_0 at the outlet was slowly replaced by 2-propanol- d_8 (solid lines, and open and solid circles in Fig. 38), whereas the change was rapid in the absence of the

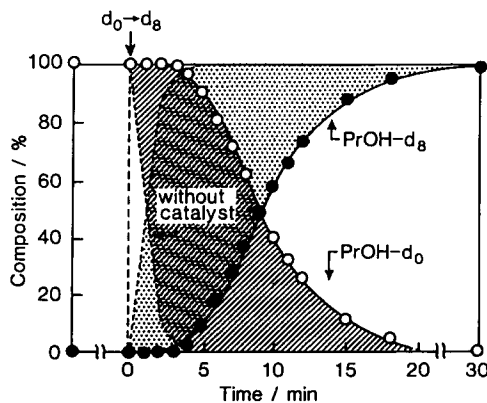


FIG. 38. Transient response in the gas-phase composition resulting from a change of feed from 2-propanol- d_0 to $-d_8$ in the dehydration catalyzed by $H_3PW_{12}O_{40}$ at 353 K (2-propanol, 3.4%; flow rate, $100\text{ cm}^3\text{ min}^{-1}$; 50 mg of $H_3PW_{12}O_{40}$). (From Ref. 236.)

catalyst (broken lines). The amount of 2-propanol- d_0 held by the catalyst under the reaction conditions corresponds to the shaded area, and the amount of 2-propanol- d_8 newly absorbed equals the dotted area. The agreement between these two areas led to the estimate of about 7 molecules per polyanion. This value corresponds to about 100 surface layers, which shows that 2-propanol was mostly in the bulk during the reaction. Furthermore, the rates of absorption and desorption were estimated from these data to be 50 times the reaction rate. It is noteworthy that the concentration of 2-propanol in the bulk ($6 \times 10^{-3} \text{ mol cm}^{-3}$) under the reaction conditions is comparable to that of liquid ($10^{-2} \text{ mol cm}^{-3}$). These results justify the term "pseudoliquid phase."

It was confirmed by the same methods that dehydration of ethanol also proceeds in the pseudoliquid phase of $\text{H}_3\text{PW}_{12}\text{O}_{40}$ (240).

Saito and Niiyama (241) investigated the transient behavior of ethanol dehydration catalyzed by $\text{Ba}_{1.5}\text{PW}_{12}\text{O}_{40}$. When the ethanol feed was stopped after a steady state had been attained, ethylene continued to form for a prolonged period, whereas ether formation decreased rapidly. This transient behavior, as well as the kinetics under stationary conditions, was well simulated with a model based on the assumption that the ethylene and ether are formed by unimolecular and bimolecular reactions in the bulk, respectively.

C. UNUSUAL KINETICS IN PSEUDOLIQUID PHASE

There is evidence that at least two different pseudoliquid phases may be present, even during catalytic reactions, and these may change reversibly with changes in the reactant partial pressures, as shown for dehydration of 2-propanol in Fig. 39 (242). A small change in reactant partial pressure led to an abrupt

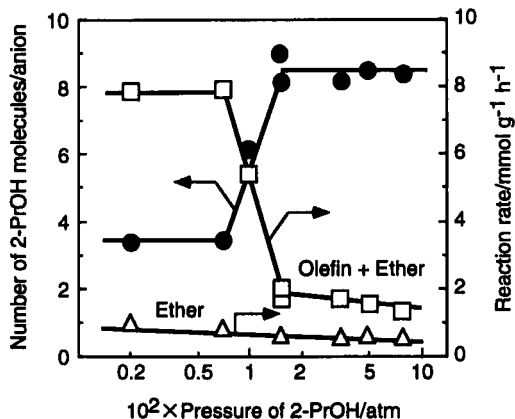


FIG. 39. Pressure dependence of the catalytic reaction rate and the amount of absorbed propanol in the dehydration of 2-propanol catalyzed by $\text{H}_3\text{PW}_{12}\text{O}_{40}$ at 353 K. (From Ref. 242.)

change from a high- to a low-activity state. The transition partial pressure tends to be higher as the reaction temperature increases. The amount of 2-propanol absorbed, which was determined by the transient response method, changed along with the reaction rate. At 353 K, the numbers of molecules absorbed per anion were 3 and 8 for the high- and low-activity states, respectively. At 373 K, these two states varied reversibly and rapidly upon the change in the pressure of 2-propanol; but at a lower temperature, the transition was slower upon the change of the partial pressure.

The unusual pressure dependences of the rate and selectivity associated with the pseudoliquid that were observed for ethanol dehydration catalyzed by $\text{H}_3\text{PW}_{12}\text{O}_{40}$ are shown in Fig. 40 (169, 243). The rates of ether and ethylene

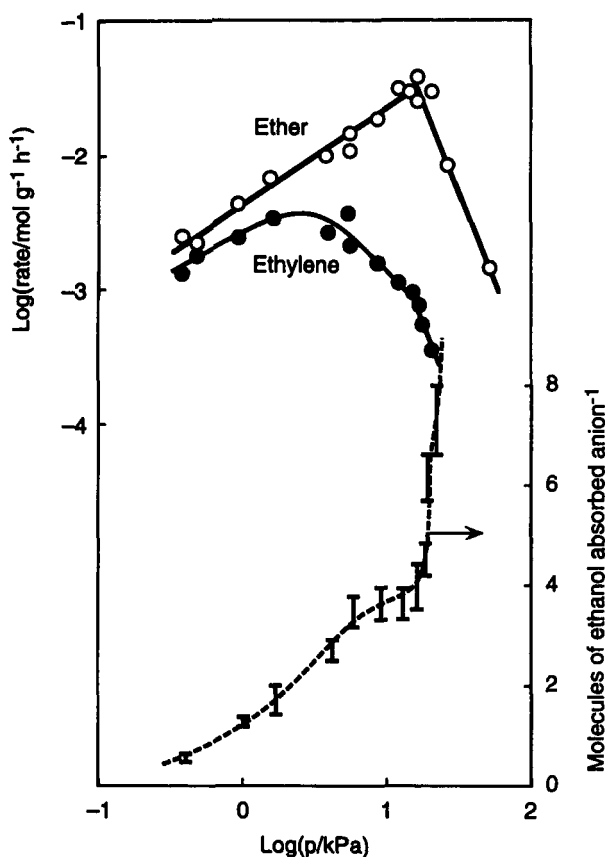
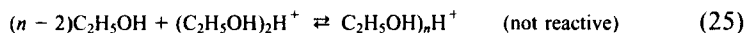
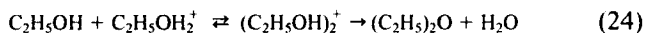
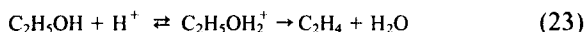


FIG. 40. Rates of formation of diethyl ether and ethylene from ethanol catalyzed by $\text{H}_3\text{PW}_{12}\text{O}_{40}$ as well as the amount of absorbed ethanol under the working conditions as a function of the partial pressure of ethanol at 403 K. (From Refs. 119, 243.)

formation increased at first with increasing ethanol partial pressure, but decreased markedly at higher ethanol partial pressures. The maximum rate was observed at a higher pressure for the ether formation than for the ethylene formation. The amounts of ethanol absorbed corresponded to 4–80 times the monolayer value (20–400 times the number of the surface polyanions), demonstrating that ethanol was absorbed in the bulk.

These results are contrasted to the pressure dependences observed for ordinary solid acids; on Al_2O_3 and $\text{SiO}_2\text{-Al}_2\text{O}_3$ the formation of ethylene is usually zero-order in ethanol and the formation of ether is zero- to first-order in ethanol (244). Furthermore, it is emphasized that the activity of $\text{H}_3\text{PW}_{12}\text{O}_{40}$ is 10^2 times greater than that of $\text{SiO}_2\text{-Al}_2\text{O}_3$.

Since ethylene is formed from one molecule of ethanol and ether from two molecules, it is understandable that ethylene is preferentially formed when the ratio of ethanol to protons in the pseudoliquid phase is low and ether is favored as this ratio increases. Equations (23)–(25) represent a possible mechanism that explains the essential trend in Fig. 40.



Simulation of the pressure dependence—assuming that the reactions of the first steps of Eqs. (23) and (24), and of Eq. (25) are in equilibrium—reproduced essential trends of the rates and the amounts of absorption.

D. SPECTROSCOPIC ANALYSIS OF PSEUDOLIQUID PHASE

Pseudoliquid phase behavior facilitates the spectroscopic investigation of the catalysts as the phenomena occur nearly uniformly in the bulk.

The IR spectrum of adsorbed diethyl ether and its changes during the thermal desorption are shown in Fig. 41 (78). A distinct peak at 1527 cm^{-1} is characteristic of protonated dimer species $\{\nu(\text{O}-\text{H})\}$ mode of $[(\text{C}_2\text{H}_5)_2\text{O}\cdots\text{H}\cdots\text{O}(\text{C}_2\text{H}_5)_2]$ (245). Moffat *et al.* also detected this peak by IR-photoacoustic spectroscopy (PAS) (238). It is reasonable that this band was not observed for diethyl ether adsorbed on Al_2O_3 or SiO_2 due to the absence of strong protonic acids on the surfaces of these solids, or for $\text{D}_3\text{PW}_{12}\text{O}_{40} \cdot 6(\text{C}_2\text{H}_5)_2\text{O}$ due to the formation of $[(\text{C}_2\text{H}_5)_2\text{O}\cdots\text{D}\cdots\text{O}(\text{C}_2\text{H}_5)_2]$ instead of $[(\text{C}_2\text{H}_5)_2\text{O}\cdots\text{H}\cdots\text{O}(\text{C}_2\text{H}_5)_2]$. A protonated monomer, $[(\text{C}_2\text{H}_5)_2\text{OH}]_3\text{PW}_{12}\text{O}_{40}$ (ether/proton = 1), remained after evacuation at 328 K, and the dimer (indicated by the band at 1527 cm^{-1}) disappeared. Further evacuation at 423 K gave four peaks (2954 , 2924 , 2897 , and 2870 cm^{-1}) due to an ethoxide bonded to the polyanion.

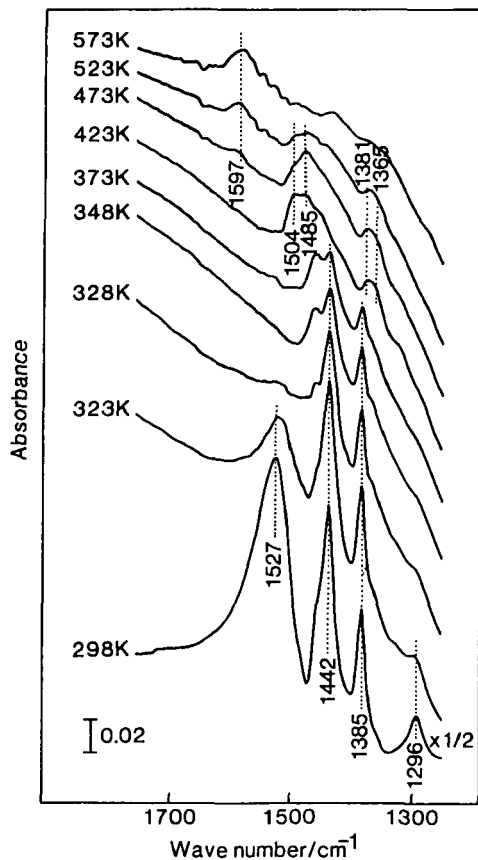


FIG. 41. Changes in the IR spectra of diethyl ether absorbed in $\text{H}_3\text{PW}_{12}\text{O}_{40}$ during stepwise heating in vacuum. (From Ref. 78.)

NMR spectroscopy also provides useful information. As shown in Fig. 42, $\text{H}_3\text{PW}_{12}\text{O}_{40} \cdot 6\text{C}_2\text{H}_5\text{OH}$ gives three ^1H NMR resonances at 9.5, 4.2, and 1.6 ppm, which are assigned to OH, CH_2 , and CH_3 , respectively (169, 246). This is probably the first observation of a well-resolved solid-state ^1H NMR spectrum for protonated organic compounds in this catalyst system. The relative intensities ($\text{OH}/\text{CH}_2/\text{CH}_3 \approx 1.45 : 1.83 : 3.0$), as well as the stoichiometry of ethanol to proton (2 : 1), are consistent with the protonated dimer, $(\text{C}_2\text{H}_5\text{OH})_2\text{H}^+$. The high resolution is explained by the high mobility of the protonated ethanol and the homogeneity of the bulk phase. The chemical shift of the hydroxyl proton of $\text{H}_3\text{PW}_{12}\text{O}_{40} \cdot 6\text{C}_2\text{H}_5\text{OH}$ (9.4 ppm) is close to those reported for protonated ethanol in superacids: 8.3 in $\text{HF}-\text{BF}_3$, 9.3 in $\text{FSO}_3\text{F}-\text{SbF}_5-\text{SO}_2$, and 9.9 ppm in HSO_3F (247) (as compared with a value of 1.0 ppm for a dilute ethanol

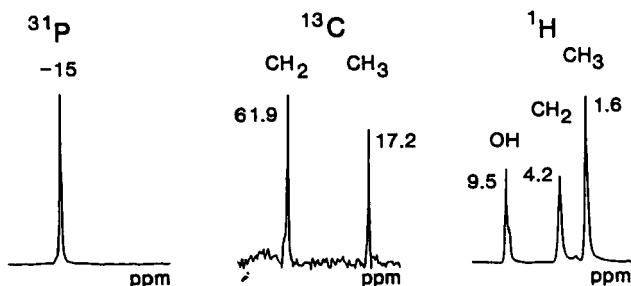


FIG. 42. ^{31}P , ^{13}C , and ^1H MAS NMR spectra of $[(\text{C}_2\text{H}_5\text{OH})_2\text{H}]_3\text{PW}_{12}\text{O}_{40}$. Reprinted with permission from Ref. 169. Copyright 1992 American Chemical Society.

solution). Hence, the pseudoliquid phase of $\text{H}_3\text{PW}_{12}\text{O}_{40}$ may be regarded as a superacidic medium.

The chemical shifts of ^{13}C (61.9 and 17.2 ppm for CH_2 and CH_3 , respectively) are different from those of pure ethanol (57.0 and 17.6 ppm, respectively). Changes in the ^{13}C NMR spectra upon heat treatment are shown in Fig. 43. Peaks at 65.0 and 16.8 ppm detected at 333 K indicate $\text{H}_3\text{PW}_{12}\text{O}_{40} \cdot 3\text{C}_2\text{H}_5\text{OH}$ (169). Further heating gave a new set of peaks at 82.1 (CH_2) and about 14.3 ppm (CH_3). The peak at 82.1 ppm is assigned to an ethoxide. The shift from 65.0 to 82.1 ppm is of similar magnitude to the transformation observed for transformation of adsorbed methanol to methoxide on $\text{K}_{3-x}\text{H}_x\text{PMo}_{12}\text{O}_{40}$ (from 51 to 75 ppm) reported by Farneth *et al.* (168). These shifts are significant but smaller than that observed for alkyl cation formation. For example, *sec*-propyl and *tert*-butyl cations in a superacid solution show a downfield shift of about 260 ppm. Hence, the species at 82 ppm is more like ethoxide than ethyl cation (247, 248).

Main reaction paths of the thermal desorption of ethanol are proposed in Scheme 5. The species observed directly by NMR spectroscopy are surrounded by broken lines. At temperatures less than 323 K, the dehydration did not proceed, and only reversible desorption took place. The protonated ethanol dimer is transformed into protonated ether at temperatures exceeding 323 K. Diethyl ether is formed only in the gas phase by replacement with ethanol. Protonated ethanol monomer probably gives ethylene via the ethoxide at temperatures exceeding 333 K (169).

E. SURFACE AND BULK TYPE I REACTIONS

As shown in Fig. 44a, the catalytic activity of $\text{Na}_x\text{H}_{3-x}\text{PW}_{12}\text{O}_{40}$ for dehydration of 2-propanol, conversion of methanol, and decomposition of formic acid decreased monotonically with the Na content in the salts. The activities for these

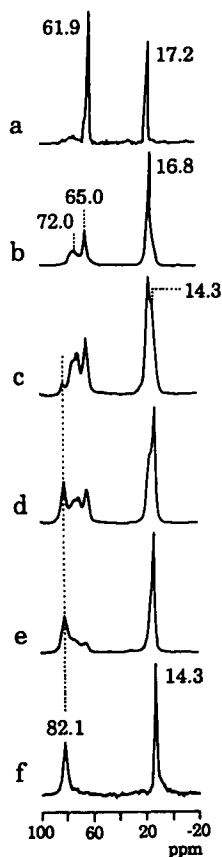
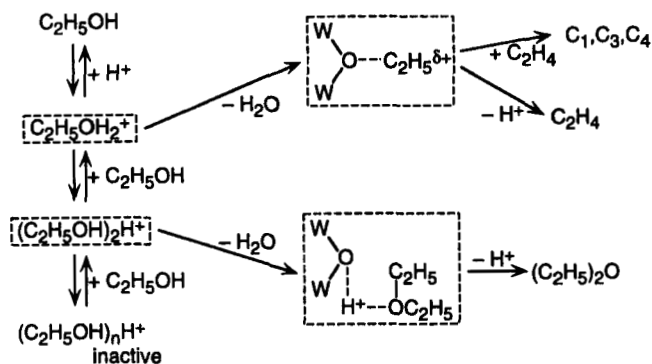


FIG. 43. Transformation of protonated ethanol dimer in $\text{H}_3\text{PW}_{12}\text{O}_{40}$ by heat treatment. Solid-state ^{13}C CP/MAS NMR spectra were obtained by using high purity ^{13}C ethanol: (a) Dimer, (b) 333 K, (c) 343 K, (d) 363 K, (e) 373 K, (f) 423 K. Reprinted with permission from Ref. 169. Copyright 1992 American Chemical Society.

reactions correlate well with the bulk acidities measured by the thermal desorption of pyridine (46b). All the reactants are polar molecules, so that the reactions proceed in the bulk.

On the other hand, the activity pattern for butene isomerization is quite different (Fig. 44b). Butene is nonpolar and not absorbed, and it reacts only on the catalyst surface. The irregular variations probably reflect the surface acidity which changed depending on the Na content and pretreatment.

Niiyama *et al.* (223) found that the reaction rate characterizing MTBE synthesis from methanol and *tert*-butyl alcohol catalyzed by $\text{H}_3\text{PW}_{12}\text{O}_{40}$ increases in proportion to the amount of methanol absorbed in the bulk of $\text{H}_3\text{PW}_{12}\text{O}_{40}$.



SCHEME 5.

The influence of bulk-type behavior also exists in supported heteropoly catalysts. Changes in the activity as a function of the loading of heteropolyacids depend on the reaction type (151). At low loadings, the rates of both the bulk and the surface reactions increase as the loading increases because the

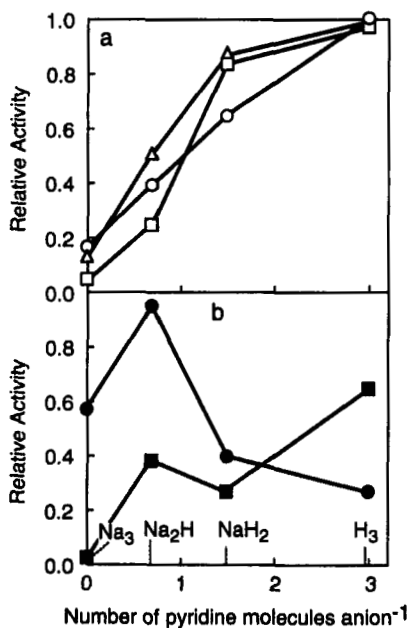


Fig. 44. Relationships between catalytic activity and bulk acidity. (a): (○) Dehydration of 2-propanol, (△) decomposition of formic acid, (□) conversion of methanol. (b): (■) Isomerization of *cis*-2-butene after treatment at 423 K, (●) isomerization of *cis*-2-butene after treatment at 573 K. (From Ref. 46b.)

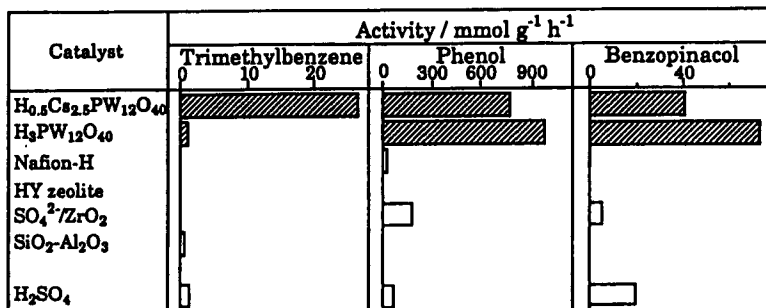


FIG. 45. Catalytic activities of solid acids for reaction of liquids: Alkylation of 1,3,5-trimethylbenzene with cyclohexene (373 K); alkylation of phenol with 1-dodecene; rearrangement of benzopinacol. (From Ref. 249.)

dispersion of the heteropolyacid becomes high. At high loadings, the dispersion becomes low, so that there is little increase in the rate of the surface reaction at increasingly high loadings.

Pseudoliquid phase behavior is also evidenced by the liquid–solid reactions of polar compounds (249). An example is shown in Fig. 45. Heteropoly compounds are much more active than H₂SO₄ and other solid acids. The rate of alkylation of 1,3,5-trimethylbenzene increases in proportion to the surface acidity. Thus Cs_{2.5}H_{0.5}PW₁₂O₄₀ is much more active than H₃PW₁₂O₄₀. On the other hand, H₃PW₁₂O₄₀ is more active for the alkylation of phenol and the rearrangement of benzopinacol than Cs_{2.5}H_{0.5}PW₁₂O₄₀. Since the latter two reactants are polar, the pseudoliquid phase is formed for H₃PW₁₂O₄₀ in the latter reactions. The activity of H₃PW₁₂O₄₀ relative to that of Cs_{2.5}H_{0.5}PW₁₂O₄₀ decreases for these reactions in the order alkylation of trimethylbenzene > alkylation of phenol > pinacol rearrangement. The results indicate that the pseudoliquid phase is most important for the first reaction in this series and least important for the last. When the rearrangement of pinacol in 1,2-dichloroethane was examined in detail at 323 K, the amount of pinacol held by the catalysts was about 20 times the amount corresponding to a surface monolayer for H₃PW₁₂O₄₀, whereas this ratio was less than 1 for the other catalysts.

Niiyama *et al.* (250) attempted to separate isobutylene from a mixture of isobutylene and 1-butene by using a H₃PW₁₂O₄₀-porous glass hybrid membrane, in which H₃PW₁₂O₄₀ was loaded into the pores of the glass. A mixture of butenes and water vapor was brought in contact with one side of the membrane. Since the hydration of isobutylene takes place preferentially, *tert*-butyl alcohol formed on one side of the membrane is absorbed in the H₃PW₁₂O₄₀ and diffused through the bulk to the opposite side. After the *tert*-butyl alcohol reached the surface of H₃PW₁₂O₄₀ at the opposite side, it decomposed to give isobutylene and water.

F. CONTROL OF ABSORPTION PROPERTIES AND CATALYTIC REACTIONS

Absorption is influenced significantly by the cations in the salts (235). Typical examples for absorption of ethanol are shown in Fig. 46. It is clear that the absorption of $\text{H}_3\text{PW}_{12}\text{O}_{40}$ is greatly suppressed when H^+ is replaced by Cs^+ , while the absorptivity varies little when H^+ is replaced by Na^+ . In contrast, there is little difference between the Na and Cs salts when they are characterized by the acid amounts measured by pyridine adsorption.

The pressure dependences as well as the amounts of ethanol held by $\text{Cs}_x\text{H}_{3-x}\text{PW}_{12}\text{O}_{40}$ (CsX) during the catalytic dehydration of ethanol were measured experimentally (240). The pressure dependences for Cs2 and Cs1 resemble those of the low- to intermediate-pressure region observed for ethanol in $\text{H}_3\text{PW}_{12}\text{O}_{40}$, suggesting that the pseudoliquid phase was also present in the acidic Cs salts. Slightly higher pressures are required for the latter to give the same trend because of the lower absorption capability of the Cs salts.

The selectivity is affected strongly by the presence of the pseudoliquid phase. An example is given in Fig. 47. The olefin-to-paraffin ratio in the product of the conversion of dimethyl ether increased markedly as the absorptivity of the heteropoly compounds decreased (195, 197). The ratio observed for catalysis by $\text{Na}_x\text{H}_{3-x}\text{PW}_{12}\text{O}_{40}$ was similar to those observed for catalysis by $\text{H}_3\text{PW}_{12}\text{O}_{40}$. The acidity governs the reaction rate but plays a minor role in determining the selectivity. The change in the olefin/paraffin ratio can be explained by the formation of the pseudoliquid phase as follows. When olefins are produced in the bulk phase, they have a relatively high probability of undergoing hydrogen-

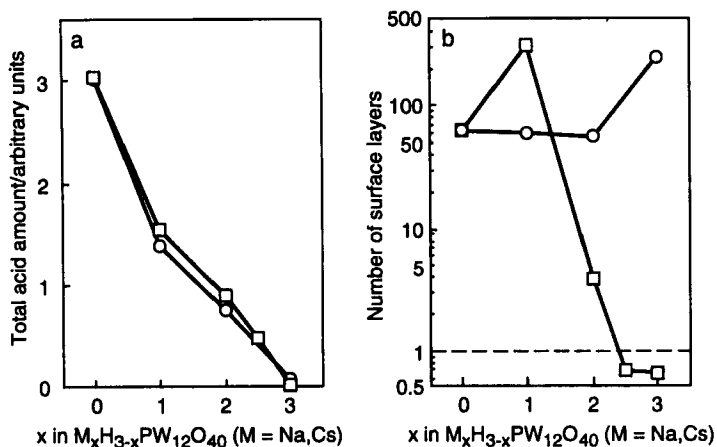


FIG. 46. Total amount (a) and absorption capacities (b) of Na and Cs salts of $\text{H}_3\text{PW}_{12}\text{O}_{40}$: (○) Na, (□) Cs. The acid amounts were measured by pyridine adsorption (adsorption). (From Ref. 235.)

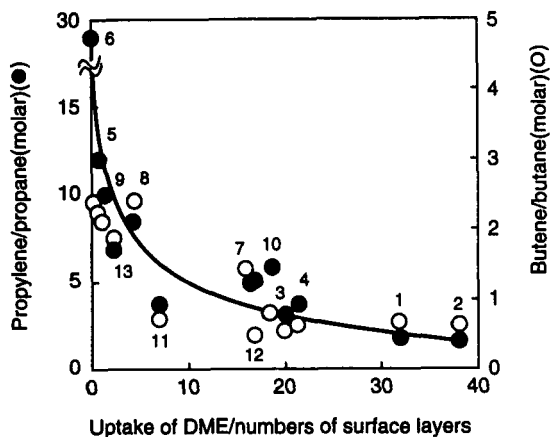


FIG. 47. Olefin-to-paraffin ratio in the product hydrocarbons from dimethyl ether conversion as a function of absorptivity of the heteropoly compounds, expressed in term of the absorption of dimethyl ether in surface layer units: (1) PW_{12} ($H_3PW_{12}O_{40}$), (2) NaH_2PW_{12} , (3) Na_2HPW_{12} , (4) CsH_2PW_{12} , (5) $Cs_{2.5}H_{0.5}PW_{12}$, (6) $Cs_{2.85}H_{0.15}PW_{12}$, (7) $(NH_4)_2PW_{12}$, (8) $(NH_4)_2HPW_{12}$, (9) $(NH_4)_{2.5}H_{0.5}PW_{12}$, (10) 1,4-diazine, (11) 1,3-diazine, (12) 1,4-bis(aminomethyl)benzene, (13) triazine. (From Ref. 197.)

transfer reaction to form paraffins and coke before they desorb. On the other hand, when the reaction occurs near or on the surface, the olefins formed may desorb rapidly into the gas phase without undergoing significant hydrogen-transfer reactions. Similar selectivity patterns associated with the pseudoliquid phase were observed in the dehydration of ethanol to give ethylene and diethyl ether.

VII. Redox Properties

A. REDOX CHEMISTRY IN SOLUTION

A general feature of heteropolymolybdates and heteropolytungstates is their high reducibility. Electrochemical investigations of Keggin-type heteropolyanions in aqueous or nonaqueous solutions have revealed sequences of reversible one- or two-electron ($1e^-$ or $2e^-$) reduction steps [Fig. 48 (3)] which yield deeply colored mixed-valence species ("heteropoly blues"). Electronic spectra of the reduced heteropolyanions show intensified $d-d$ bands in this visible region and intervalence charge-transfer (IVCT) bands in the near-IR region.

Depending on the solvent, the acidity of the solution, and the charge of the polyanion, the reductions involve either single-electron or multi-electron steps, often accompanied by protonation. In protic solvents, the Keggin anions exhibit

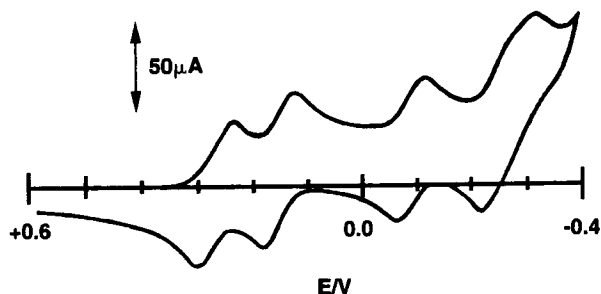


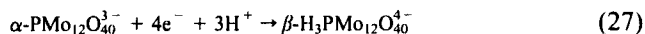
FIG. 48. Cyclic voltammogram of $\alpha\text{-PMo}_{12}\text{O}_{40}^{3-}$ in 0.1 M HCl (50% $\text{H}_2\text{O}/\text{EtOH}$). (From Ref. 3.)

electrochemical reductions by two electrons. The reduction potentials depend on pH as a result of protonation [e.g., Eq. (26)] (251):



Acidification of nonaqueous solutions of an unprotonated $1e^-$ -reduced species causes disproportionation to a $2e^-$ -reduced anion and an oxidized anion (251). At higher pH values, polarograms show a series of $1e^-$ reductions (252).

Reduction of Keggin anions beyond $2e^-$ reduction leads to modest changes in electronic and molecular structure, although the reductions remain reversible. For example, in the case of molybdates, a $4e^-$ -reduced β -Keggin structure is stabilized, with the bridging oxygen atoms being partially protonated [Eq. (27)] (3, 253, 254):



Electronic and NMR spectra of these complexes, together with X-ray structural determinations, indicate that the valence is completely averaged over at least six Mo atoms (251, 253, 254).

ESR and ^{17}O NMR spectra of $1e^-$ -reduced $\text{SiW}_{12}\text{O}_{40}^{5-}$ demonstrate that the unpaired electron is weakly trapped on a W atom at low temperatures but undergoes rapid hopping (intramolecular electron transfer) at room temperature (Section II). Anions generated by $2e^-$ (and $4e^-$) reduction are ESR-silent, but ^{17}O and ^{183}W NMR spectra show that the additional electrons are fully delocalized (on the NMR timescale) at room temperature and generate "ring currents" analogous to those produced by the π -electrons of benzene. In contrast, in the case of $1e^-$ -reduced $\text{PMoW}_{11}\text{O}_{40}^{3-}$, the electron is localized on a more reducible Mo atom at room temperature (251).

The reduction potentials of heteropolyanions containing Mo and V are high, and they are easily reduced. Oxidizing ability decreases in general in the order $\text{V} > \text{Mo} > \text{W}$ -containing heteropolyanions (Fig. 49) (8, 91). As for heteroatoms, the reduction potential (or oxidizing ability) decreases linearly with a

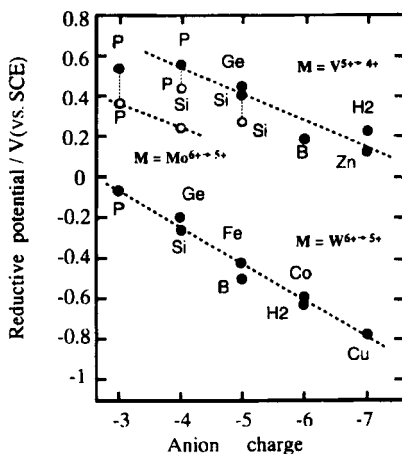
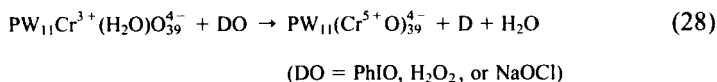


FIG. 49. Dependence of reduction potentials on anion charge: (●) $XW_{11}O_{40}^{n-}$; (○) $XMo_{11}O_{40}^{n-}$; SCE = saturated calomel electrode. (From Ref. 91.)

decrease in their valence or an increase in the negative charge of the heteropolyanion (Fig. 49) (91). For polyanions with mixed-addenda atoms, the reduction potentials have been reported to be $PMo_{10}V_2O_{40}^{5-} > PMo_{11}VO_{40}^{4-} > PMo_{12}O_{40}^{3-}$; and $PMo_6W_6O_{40}^{3-} > PMo_{12}O_{40}^{3-}$ (2).

$XW_{11}MnO_{39}$ ($X = Si, Ge$) forms an oxygen adduct in nonpolar solvents. This was claimed to be the first example of an inorganic oxygen carrier (255). Recently, it was reported that $XW_{11}CrO_{39}$ reacted with $PhIO$, H_2O_2 , or $NaOCl$ to form $XW_{11}(CrO)O_{39}$ [Eq. (28)]:



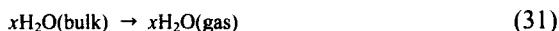
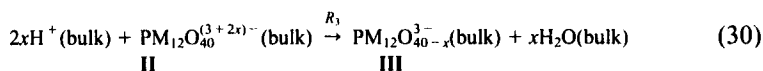
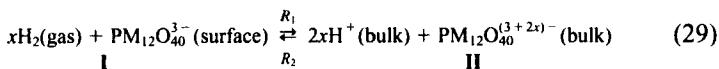
The oxo species further reacted with olefins to form the corresponding epoxides, ketones, and alcohols (256).

In the reoxidation of heteropolyanions, reduced forms of polyoxomolybdates and polyoxovanadates are stable and hardly reoxidized by molecular oxygen, whereas polyoxotungstates undergo facile reoxidation (257).

B. REDUCTION-OXIDATION IN THE SOLID STATE

1. Reduction Mechanism and Oxidizing Ability

Misono *et al.* (17, 258–262) have shown that the reduction of $H_3PM_{12}O_{40}$ ($M = Mo, W$) and its alkali-metal salts by H_2 consists of the following three steps. [A similar mechanism has also been proposed by Eguchi *et al.* (101).]



[R_1 and R_2 are the rates of the forward and reverse reactions of Eq. (29), respectively, and R_3 is the rate of Eq. (30).]

The first step is $\text{H}_2 \rightarrow 2\text{H}^+ + 2\text{e}^-$. Here, the number of electrons introduced per anion may be variable. In the second step, the protons formed in the first step react with the oxygen of the polyanion to form water. Accordingly, in TPR experiments with H_2 , the H_2 uptake takes place but no H_2O is observed at low temperatures ($\text{I} \rightarrow \text{II}$), while H_2O appears in the gas phase at higher temperatures ($\text{II} \rightarrow \text{III}$) (259, 261). Further reduction produces several irreversibly reduced species.

IR spectra indicate that reactive oxygen in the reduction of $\text{H}_3\text{PMo}_{12}\text{O}_{40}$ is the bridging oxygen in the Keggin anion (101, 261, 263). According to a quantum-chemical calculation by the X α method, the LUMO is a mixture of $4d$ orbitals of Mo (50%) and $2p$ orbitals of the bridging oxygen atoms (O_b 21% and O_c 27%), while the HOMO mostly (94%) consists of $2p$ orbitals of bridging oxygen. The LUMO is antibonding with respect to Mo– O_b and Mo– O_c bonds. This result indicates that the interaction with a reductant preferentially takes place at the bridging oxygen atom and loosens the Mo– O_b and Mo– O_c bonds (264). IR spectra change only slightly upon the reduction to **II**, since the Keggin structure is maintained. The spectra change greatly upon the reduction to **III**. [Some authors reported that even the first reduction step ($\text{I} \rightarrow \text{II}$) significantly changed the IR spectrum (265). At present this discrepancy is still controversial.] $\text{H}_3\text{PMo}_{12}\text{O}_{40}$ reduced by H_2 at a lower temperature shows a very weak ESR signal of Mo^{5+} . It is probable that as long as the Keggin structure is maintained ($\text{I} \rightarrow \text{II}$), most of the Mo^{5+} ions are not detectable due to the rapid hopping of electrons. A heat treatment converts **II** into **III**, and the Mo^{5+} signal grows significantly, indicating the localization of electrons. Early reports of ESR spectra of reduced $\text{H}_3\text{PMo}_{12}\text{O}_{40}$ probably should be attributed to these species.

The rates of these reactions (R_1 – R_3) have been determined by the quantitative analysis of the reduction of $\text{H}_3\text{PM}_{12}\text{O}_{40}$ ($M = \text{Mo}, \text{W}$) by a mixture of H_2 and D_2 . With $\text{H}_3\text{PW}_{12}\text{O}_{40}$, the isotopic equilibration of H_2 and D_2 in the gas phase, as well as the isotopic exchange between the entire solid and the gas phase, is very rapid, so that, to our surprise, the content of H in the gas phase increased rapidly (Fig. 50). The detailed kinetics analysis shows that the reactions of Eqs. (29) and (30) are very rapid and that of Eq. (31) is the slow step, the equilibrium strongly favoring the reactions on the left-hand side of Eq. (29) (Fig. 51, left).

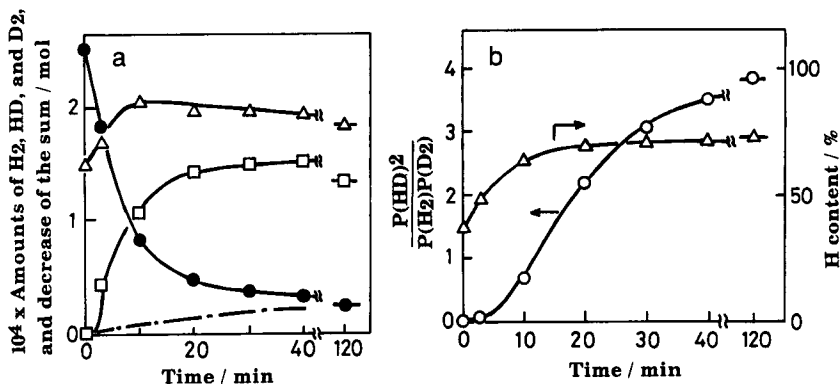


FIG. 50. Isotopic exchange of H₂-D₂ at 573 K: Δ , \square , \bullet , and $-\cdot-$ in Fig. 50a show the amounts of H₂, HD, and D₂, and decrease of the sum, respectively. Sample: H₃PW₁₂O₄₀ · 19H₂O (1.1 g). (From Ref. 260.)

The result obtained for H₃PMo₁₂O₄₀ was essentially the same, except that the equilibrium of Eq. (29) favors the right-hand side (Fig. 51, right) (262).

The reduction rates of H₃PM₁₂O₄₀ (M = Mo, W) by H₂ depend only slightly on the specific surface areas, as shown, for example, in Fig. 52 (260). This dependence is quantitatively explained on the basis of the assumption that R_3 is

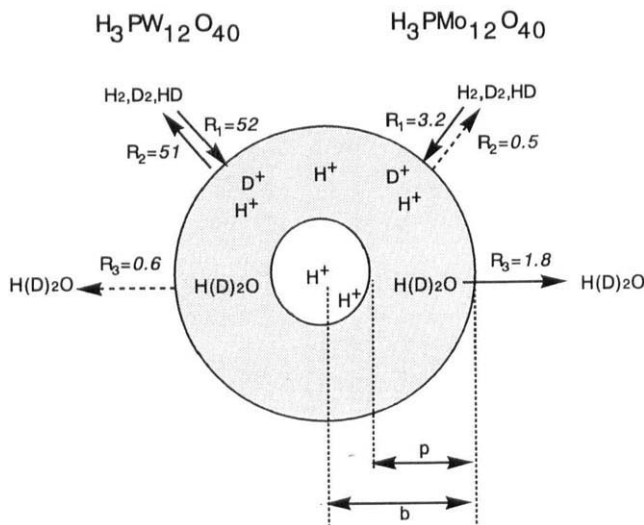


FIG. 51. Models of H₂-D₂ reactions for H₃PMo₁₂O₄₀ (right) and H₃PW₁₂O₄₀ (left). Values are given in units of 10⁻⁶ mol min⁻¹ g⁻¹. Outer circle indicates the surface of H₃PMo₁₂O₄₀ and H₃PW₁₂O₄₀; p and b , respectively, indicate bulk phase and hypothetical portion in which the isotopic concentration is uniform. (From Ref. 262.)

proportional to the number of polyanions in the bulk (p), in which protons as well as electrons migrate rapidly in the bulk (Fig. 52).

Thus, it can be concluded that the rates of reduction of $\text{H}_3\text{PM}_{12}\text{O}_{40}$ by H_2 reflect the oxidizing ability of the catalyst bulk (bulk type II behavior) (260). The reduction is slower for $\text{H}_3\text{PW}_{12}\text{O}_{40}$ than for $\text{H}_3\text{PMo}_{12}\text{O}_{40}$ not because the dissociation of H_2 is slower, but because the reactions of either Eq. (30) or Eq. (31) are slower (Fig. 51).

In contrast, the rates of reduction of $\text{H}_3\text{PMo}_{12}\text{O}_{40}$ and its alkali salts by CO under dry conditions are proportional to the specific surface areas, as is observed for ordinary heterogeneous catalysis (Fig. 52). In this case, because of the slow diffusion of oxide ion, the reduction mainly proceeds only near the surface (266). The slow diffusion of oxide ion is deduced from the following result, as well as the observation of a much slower isotopic exchange for $^{16}\text{O}_2\text{-}^{18}\text{O}_2\text{-H}_3\text{PMo}_{12}\text{O}_{40}$ than for $\text{H}_2\text{-}^{18}\text{O-H}_3\text{PMo}_{12}\text{O}_{40}$ (267). When the reduction by CO (on the surface) is stopped halfway by evacuation, then resumed after a delay, the rate becomes several times greater than the rate just before the interruption in contrast to the small change observed for the reduction by H_2 (bulk type II) in a similar experiment (266). The rate of reoxidation by O_2 is similar to the rate of reduction by CO (both are surface-type reactions). In the case of reduction by CO , the oxide ions diffuse very slowly, so the surface is reduced to a much greater extent than the bulk: During the interruption, the

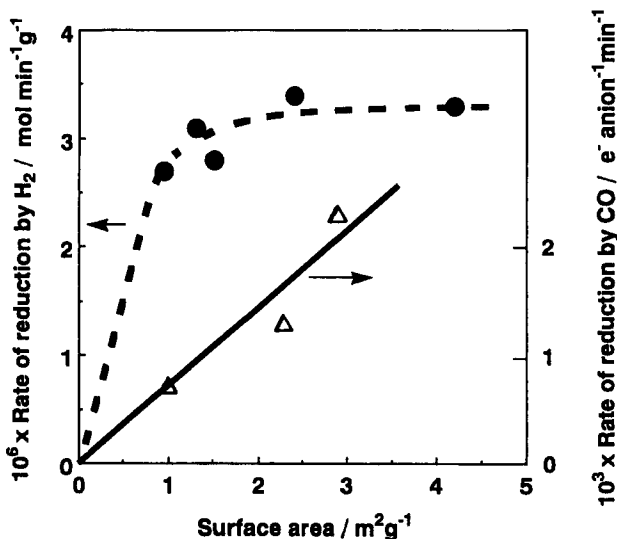


FIG. 52. Dependence of rates of reduction of $\text{H}_3\text{PW}_{12}\text{O}_{40}$ by H_2 and of $\text{Na}_2\text{HPMo}_{12}\text{O}_{40}$ by CO on the specific surface area. (●) Reduction of $\text{H}_3\text{PW}_{12}\text{O}_{40}$. The broken line shows the calculated data (see text). $\text{H}_3\text{PW}_{12}\text{O}_{40} \cdot 19\text{H}_2\text{O}$, 1.0 g; reaction temperature, 573 K. (Δ) Reduction of $\text{Na}_2\text{HPMo}_{12}\text{O}_{40}$. Reaction temperature, 623 K. (From Refs. 260, 266.)

overreduced surface is reoxidized by the oxide ions that diffuse from the bulk; therefore, the reduction rate greatly increases after the interruption.

Hence, to a first approximation, the rate of reduction of these heteropoly compounds by CO expresses the oxidizing ability of the surface, whereas, as described above, the rate of reduction by H_2 reflects the oxidizing ability of the catalyst bulk. If the former rate is divided by the surface area and the latter normalized to the catalyst mass, both oxidizing abilities decrease monotonically with the extent of neutralization with alkali (Figs. 53a and 53c). Although it is not shown in Fig. 53, $Cs_{2.5}H_{0.5}PMo_{12}O_{40}$, a class B salt that has a high surface area, is reduced exceptionally rapidly.

The contrast between the two types is also found for organic reactions. The reduction of $H_3PMo_{12}O_{40}$ by dehydrogenation of isobutyric acid or cyclohexene belongs to the bulk type II classification, and the reduction by oxygenation of methacrolein or acetaldehyde is a surface reaction. For example, when $H_3PMo_{12}O_{40}$ is reduced by repeated pulses of isobutyric acid and methacrolein

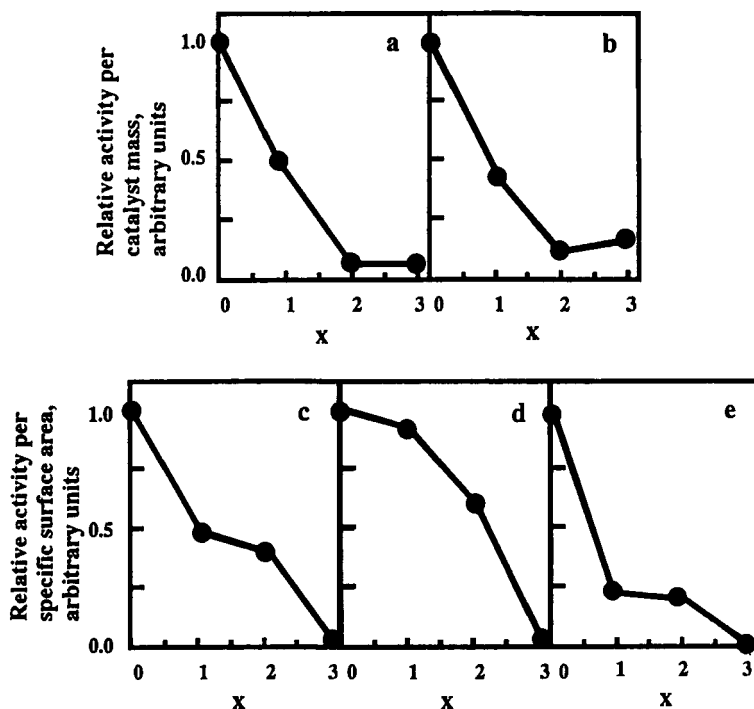
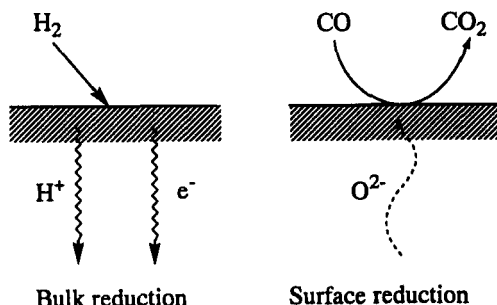


FIG. 53. Stoichiometric reduction of $H_{3-x}Cs_xPMo_{12}O_{40}$ by (a) H_2 , (b) isobutyric acid, (c) CO, and (d) methacrolein, and reoxidation by O_2 [Degree of reoxidation after 10 min at 623 K. Sample was pre-reduced by $1e^-$ at 623 K (from Refs. 258, 266)], (e) at 623 K.



SCHEME 6

and the conversions are plotted against the average extent of reduction of the bulk solid, the conversion of isobutyric acid to methacrolein decreases only gradually, whereas the conversion of methacrolein to methacrylic acid diminishes sharply (268). This contrast is explained as follows. In the oxidative dehydrogenation, protons and electrons formed on the surface rapidly diffuse into the inner bulk, so that whole bulk solid is reduced nearly uniformly. On the other hand, in the case of methacrolein, the surface oxygen removed by the reaction is only slowly replenished by oxide ion diffusion, so that the reduction takes place mainly near the surface (Scheme 6).

2. Reoxidation

As for the reoxidation of reduced heteropoly compounds in the solid state, few reliable studies have been reported. It was reported that the reoxidizability increases with an increase in standard electrode potentials of countercations (108). In the case of reoxidation by O_2 of $1e^-$ -reduced $Cs_xH_{3-x}PMo_{12}O_{40}$, the rates divided by the surface area show a monotonic variation (Fig. 53e) as in Figs. 53c and d, indicating a surface reaction. A similar variation was observed for the Na and K salts. The presence of water vapor sometimes accelerates the migration of oxide ion, probably in the form of OH^- or H_2O , and makes surface-type reactions more like bulk type II reactions (266).

As for the rate and reversibility of redox cycles, the following have been observed. [I, II, III refer to Eqs. (29)–(31) (258b).]

- I (fully oxidized heteropolyanion) \leftrightarrow II: very rapid and reversible;
- I \leftrightarrow III: rapid near the surface, but slow in the bulk and reversible;
- I \leftrightarrow III' (excess reduction species): slow and mostly irreversible.

There are two reversible redox cycles, I \leftrightarrow II and I \leftrightarrow III. Upon reoxidation, water is evolved in I \rightarrow II, but not in III \rightarrow I. In the case of $H_3PMo_{12}O_{40}$, the redox cycle is nearly reversible when the average extent of reduction is less than $3e^-$ /anion at 573 K. The second redox cycle (I \leftrightarrow III) tends to dominate at high temperatures and for extensive reductions.

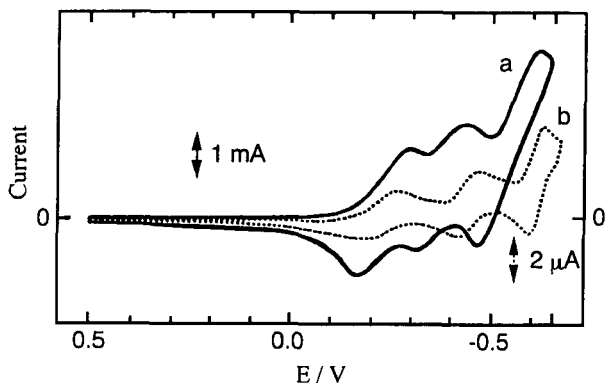
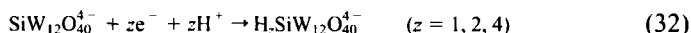


FIG. 54. Cyclic voltammogram of $\text{H}_4\text{SiW}_{12}\text{O}_{40}$ recorded at conventional size glassy carbon disk electrode. (a) Single-crystal sample; (b) 4 mM $\text{H}_4\text{SiW}_{12}\text{O}_{40}$ in 0.5 M H_2SO_4 . (From Ref. 269.)

Recently, Kulesza *et al.* (269) reported cyclic voltammetry with a single crystal of $\text{H}_4\text{SiW}_{12}\text{O}_{40} \cdot 31\text{H}_2\text{O}$. In the potential range of -0.1 to -0.65 V, three reversible redox transitions similar to that in solution (Fig. 54b) (269) are observed with the ratios of numbers of electrons being 1 : 1 : 2 (Fig. 54a). The reduction probably corresponds to Eq. (32):



The cyclic voltammogram of Fig. 54a is not fully symmetrical. The distortion probably originates from the catalytic discharge of protons and evolution of hydrogen in the solid phase. These results suggest the possibility that by using cyclic voltammetry with a single crystal, the reduction potential of solid heteropoly compounds can be measured and that the effects of constituent elements described below can be made clearer.

C. EFFECTS OF CONSTITUENT ELEMENTS ON REDOX PROPERTIES IN THE SOLID STATE

Methods for estimating the oxidizing ability of heteropoly compounds in the solid state involve measurements of the reduction rate at a constant temperature as described above, temperature-programmed reduction (17, 258, 259, 270–273), and ESR and XP spectra indicating changes by reduction (107, 108, 274, 275). As described previously (254), the orders of oxidizing ability obtained experimentally differ significantly, depending on the method adopted and the kind of the reductant as well as the inhomogeneity, nonstoichiometry, and decomposition of the samples. Inconsistencies in the literature may also be explained by lack of recognition of the occurrence of both surface and bulk reactions.

Various parameters such as the heat of oxide formation, ionic potential, electronegativity, and the extent of cation exchange have been proposed to control the redox properties. However, a full understanding is lacking. Nonetheless, the following trends are evident:

1. When Mo–W mixed-addenda heteropolyacids are reduced by H_2 , the rate of reduction decreases in the order $PMo_6W_6O_{40}^{3-} > PMo_{12}O_{40}^{3-} > PMo_{10}V_2O_{40}^{5-} > PW_{12}O_{40}^{3-}$, in parallel with the reduction potentials in solution (except for $PMo_{10}V_2O_{40}^{5-}$) (276).

2. For a given polyanion, the effects of metals are divided into two groups:

- (a) Transition metals play roles in the redox processes; e.g., they activate reducing agents and molecular oxygen and possibly provide reservoirs of electrons (108, 272, 273, 276, 278).
- (b) Alkali and alkaline-earth metals are not reduced. Oxidizing abilities measured by the rate of reduction decrease upon the formation of alkali salts (Fig. 53) (258, 272, 273, 277). The reason for the decrease of the oxidizing ability with alkali content is not fully understood, although suggestions have been made concerning the electronegativity of the cation and the role of protons in the reduction process.

The mixed-addenda atoms affect the redox properties; mixed-addenda heteropoly compounds are used as industrial oxidation catalysts. For example, the rate of reduction by H_2 is slower and less reversible for solid $PMo_{12-x}V_xO_{40}^{(3+x)-}$ than for solid $PMo_{12}O_{40}^{3-}$, although the former are stronger oxidants than the latter in solution (279, 280). The effects of substituting V for Mo on the catalytic activity are controversial (279, 281–284). Differences in redox processes between solutions and solids, the thermal or chemical stability of the heteropoly compounds, and the effects of countercations in solids have been suggested to account for the discrepancies.

It has been demonstrated that V^{5+} in $H_{3+x}PM_{12-x}V_xO_{40}$ ($M = Mo, W$) is eliminated from the polyanion framework upon thermal treatment or during catalytic oxidation, and the VO^{2+} salt of $H_3PM_{12}O_{40}$ is formed (284). It has been reported (103) that $H_3PMo_{12}O_{40}$ is re-formed from thermally decomposed $H_3PMo_{12}O_{40}$ under the conditions of methacrolein oxidation.

VIII. Liquid-Phase Oxidation Reactions

A. OXIDATION WITH DIOXYGEN

Typical examples of liquid-phase oxidation with molecular oxygen catalyzed by heteropoly compounds are listed in Table XXVI. Introduction of V^{5+} or

other transition-metal ions such as CO^{2+} or Mn^{2+} as addenda atoms usually enhances the catalytic activity, reflecting changes in the reduction potential. Recently, paraffin oxidation in the liquid phase, which does not proceed with the V^{5+} - and mono- Co^{2+} -substituted heteropolyanions, has become possible, catalyzed by heteropolyanions having tri-transition-metal (Fe_2Ni or Fe_3) sites. The use of heteropoly compounds in combination with transition metals as in Wacker-type reactions is described in Section XI.

$\text{PV}_2\text{Mo}_{10}\text{O}_{40}^{5-}$ has usually been used in the acid form. $\text{H}_5\text{PV}_2\text{Mo}_{10}\text{O}_{40}$ catalyzes aerobic oxidative cleavage of cycloalkanes, 1-phenylalkanes, and ketones. For example, the oxidation of 2,4-dimethyl cyclopentanone and 2-methylcyclohexanone gives 5-oxo-3-methylhexanoic acid and 6-oxoheptanoic acid, respectively, in yields higher than 90% (285, 286). Bromination of arenes with HBr (287), oxidative dehydrogenation of cyclohexadiene (288, 289) and α -terpinene (290), oxidation of 2,4-dimethylphenol (291) and sulfides (292) are other examples.

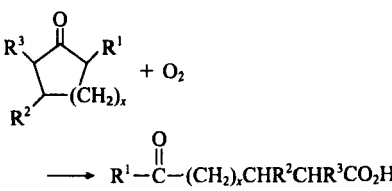
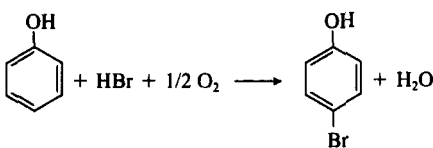
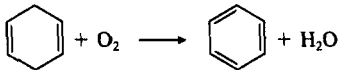
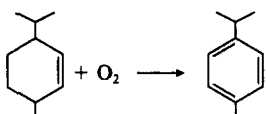
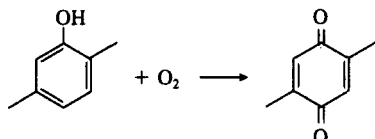
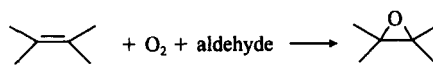
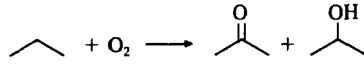
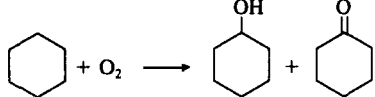
The mechanism of aerobic oxidative dehydrogenation of α -terpinene to give *p*-cymene catalyzed by $\text{PV}_2\text{Mo}_{10}\text{O}_{40}^{5-}$ has been investigated (290). On the basis of kinetics along with the use of UV-visible, ESR, ^{31}P -NMR, and IR spectroscopies, a reaction scheme was proposed, as shown in Fig. 55. In this scheme, a stable α -terpinene \cdot - $\text{H}_6\text{PV}^{5+}\text{V}^{4+}\text{Mo}_{10}\text{O}_{40}$ complex (b) is formed via an electron transfer complex (a), which is a reduced heteropolyanion attached to an oxidized cation radical of α -terpinene. A doubly protonated reduced heteropolyanion and *p*-cymene are generated via the intermediate. On the basis of the kinetics (zero-order reaction in α -terpinene, second-order reaction in $\text{PV}_2\text{Mo}_{10}\text{O}_{40}^{5-}$, and first-order reaction in O_2) and the IR and NMR data, the rate-limiting step is proposed to be the reoxidation of the catalyst. In the reoxidation step, two reduced $\text{PV}_2^{4+}\text{Mo}_{10}\text{O}_{40}^{7-}$ heteropolyanions are reoxidized in a $4e^-$ redox reaction via a μ -peroxo intermediate (c).

Co^{2+} -Substitution at the addenda atoms gives catalysts for the epoxidation of olefins in the presence of aldehyde (293). $\text{PW}_{11}\text{-Co}$ is the most active among the mono-transition-metal-substituted poly-anions; the order of activity is $\text{PW}_{11}\text{-Co} \gg \text{-Mn} \geq \text{-Fe} \geq \text{-Cu} > \text{-Ni}$. Here, $\text{PW}_{11}(\text{M}^{n+})\text{O}_{39}^{(7-n)-}$ ($\text{M} = \text{Co}^{2+}, \text{Cu}^{2+}, \text{Fe}^{3+}, \text{Ni}^{2+}, \text{Mn}^{2+}$) is denoted by $\text{PW}_{11}\text{-M}$. The same order was observed for the oxidation of isobutyraldehyde, suggesting that the oxidation of aldehyde to give peracid is an important step in the reaction. It has been reported that substitution of V^{5+} for Mo^{6+} in $\text{PMo}_{12}\text{O}_{40}^{3-}$ gives a good catalyst for epoxidation and the Baeyer-Villiger reaction (294).

Styrene and 1-decene are selectively epoxidized, as shown in Table XXVII (293). The rates observed for $\text{PW}_{11}\text{-Co}$ are greater than those observed for $\text{Ni}(\text{dmp})_2$ and $\text{Fe}(\text{dmp})_3$, and the selectivities are comparable or higher for the former (295). It is also remarkable that $\text{PW}_{11}\text{-Co}$ polyanion exhibits a steric effect comparable to that of a moderately hindered TTMPP ligand in the

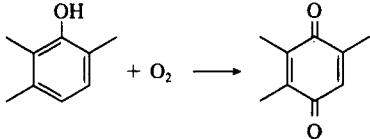
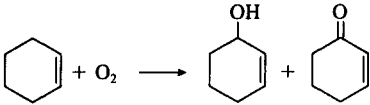
TABLE XXVI

Liquid-Phase Oxidation Reactions with Molecular Oxygen Catalyzed by Heteropoly Compounds

Reaction	Catalyst	Temp. (K)	Ref.
$\text{PhCOCH}_2\text{Ph} + \text{O}_2 \longrightarrow \text{PhCOOH} + \text{PhCHO}$	$\text{H}_5\text{PMo}_{10}\text{V}_2\text{O}_{40}$	333	285
	$\text{H}_5\text{PMo}_{10}\text{V}_2\text{O}_{40}$	633	285, 286
$\text{R}_2\text{S} \longrightarrow \text{R}_2\text{SO} \text{ or } \text{R}_2\text{SO}_2$	$\text{H}_6\text{PMo}_9\text{V}_3\text{O}_{40}$	363	287
	$\text{H}_5\text{PMo}_{10}\text{V}_2\text{O}_{40}$	293	289
	$\text{H}_5\text{PMo}_{10}\text{V}_2\text{O}_{40}$	343	288, 289
	$\text{H}_5\text{PMo}_{10}\text{V}_2\text{O}_{40}$	298	290
	$\text{H}_5\text{PMo}_{10}\text{V}_2\text{O}_{40}$	333	291
	$\text{PW}_{11}\text{CoO}_{39}^{5-}$ $\text{PMo}_6\text{V}_6\text{O}_{40}^{9-}$	303	293, 294
	$\text{H}_7\text{PW}_9\text{Fe}_2\text{NiO}_{37}$	423	297
	$(\text{TBA})_4\text{H}_6\text{PW}_9\text{Fe}_2\text{NiO}_{37}$ TBA, $(n\text{-C}_4\text{H}_9)_4\text{N}$	355	299
$\text{H}_2\text{C}=\text{CH}_2 + \text{O}_2 \longrightarrow \text{CH}_3\text{CHO}$	$\text{PdCl}_2 +$ $\text{Na}_x\text{H}_{3+x-y}\text{PMo}_{12-x}\text{V}_y\text{O}_{40}$ ($x = 2-3$)	393	See Section IX

continued

TABLE XXVI—Continued

Reaction	Catalyst	Temp. (K)	Ref.
 $+ \text{O}_2 \longrightarrow$	$\text{Na}_7\text{PMo}_8\text{V}_4\text{O}_{40}$	293	^a
 $+ \text{O}_2 \longrightarrow$	$\text{SiW}_{11}\text{CoO}_{39}^{6-}$	343	^b
$\text{SO}_2 + 1/2 \text{O}_2 + \text{H}_2\text{O} \longrightarrow \text{H}_2\text{SO}_4$	$\text{H}_8\text{PMo}_7\text{V}_5\text{O}_{40}$	298	^c

^aJ. E. Lyons *et al.*, *Stud. Surf. Sci. Catal.* **67**, 99 (1991). ^bR. Neumann *et al.*, *Dioxygen Activation and Homogeneous Catalysis Oxidation* L. I. Simanded, Ed. Elsevier, Amsterdam, 121 (1991). ^cB. S. Jumakaeva *et al.*, *J. Mol. Catal.* **35**, 303 (1986).

epoxidation of (*R*)-(+)-limonene, 4-vinyl-1-cyclohexene, and 1-methyl-1,4-cyclohexadiene (296).

Activation of paraffins by heteropolyanions has been attempted by using tri-transition-metal-substituted heteropolyanions. Propane, ethane, and methane are oxidized to the corresponding alcohols and ketones in the presence of tri-transition-metal-ion (Fe_2Ni)-substituted $\text{PW}_{12}\text{O}_{40}^{3-}$, although the composition and structure of the catalyst are still to be examined (297). Recently, Mizuno *et al.* (298) characterized its structure, and confirmed that it catalyzed the oxygenation of adamantane, ethylbenzene, and cyclohexane with molecular oxygen alone (299). For example, adamantane was catalytically oxidized mainly to 1-adamantanol with small amounts of 2-adamantanol and 2-adamantanone. The total number of turnovers was 25, calculated on the basis of the bulk polyanion, or 3750, calculated per surface polyanion. This number of turnovers is the highest for the dioxygen oxidation of adamantane on μ -oxo di- or tri-iron and Ru complexes with or without any reductants (300, 301). $\text{Fe}=\text{O}$, $\text{Fe}-\text{OH}$, or $\text{Fe}-\text{OOH}$ species are assumed to play an important role in the reaction.

B. OXIDATION WITH OXIDANTS OTHER THAN O_2

Hydrogen peroxide and alkyl hydroperoxides are important oxidants in organic synthesis, but they usually need to be activated by catalysts such as tungsten, molybdenum, and titanium oxides. Heteropoly compounds are good catalysts for oxygenation of olefins or paraffins and oxidative cleavage of *vic*-diols.

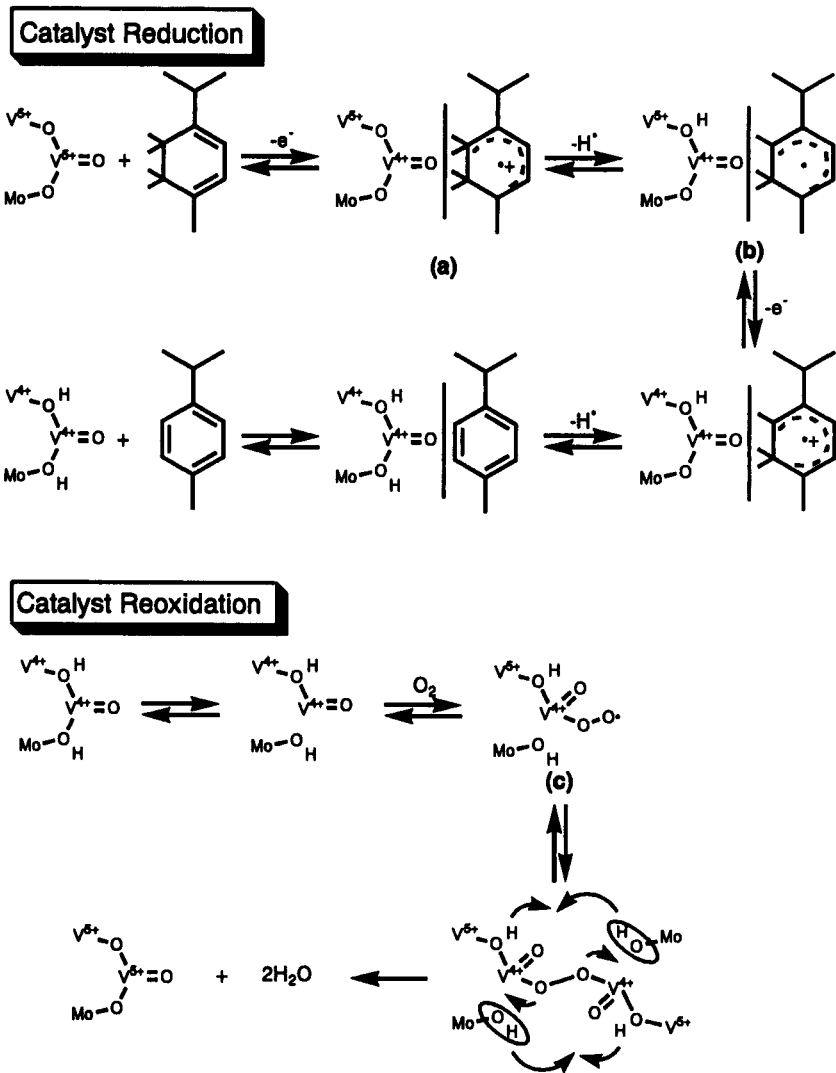


FIG. 55. Mechanistic scheme for oxidative dehydrogenation of α -terpinene catalyzed by $\text{H}_5\text{PMo}_{10}\text{V}_2\text{O}_{40}$. (From Ref. 290.)

1. Hydrogen Peroxide

Typical examples are collected in Table XXVIII. Mixed addenda heteropolyanions show unique catalytic properties. For example, in the oxidation of cyclopentene to glutaraldehyde with hydrogen peroxide, the catalytic activity of

TABLE XXVII
 Epoxidation of Olefins Catalyzed by $PW_{11}-Co$ at 303 K^a (from Ref. 293)

Alkene	Conversion ^b (%)	Selectivity ^c (%)
Cyclohexene ^d	78	90
Styrene ^e	100	91
1-Decene ^f	73	80

^a Olefin, 250 μ mol; isobutyraldehyde, 1000 μ mol; solvent, 1,2-dichloroethane; 1 h. ^b Based on the starting olefin. ^c Based on the converted olefin. ^d $PW_{11}-Co$, 1.2 μ mol; 1.3 h. ^e $PW_{11}-Co$, 4.5 μ mol; 1 h. ^f $PW_{11}-Co$, 1.2 μ mol; 4 h.

$H_3PW_6Mo_6O_{40}$ was observed to be the highest among $H_3PW_{12-x}Mo_xO_{40}$ species, as shown in Fig. 56 (302–304). A theoretical explanation of this activity pattern or synergistic effect has been attempted by accounting for excess electronic energy of nonbonding levels (305). However, there is a possibility that the active peroxo catalysts are formed by the degradation of the Keggin structure (304).

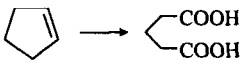
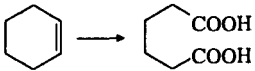
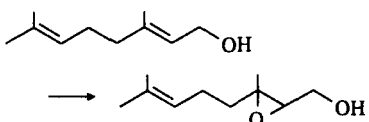
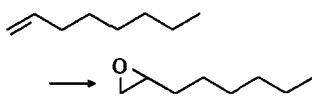
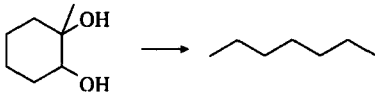
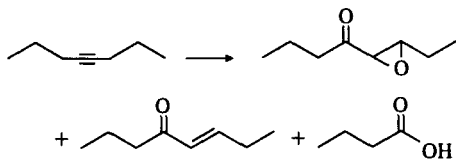

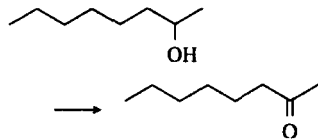
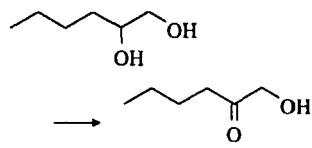
Phase-transfer catalysis has been developed by the combination of Keggin-type heteropolyanions and quaternary countercations such as tetrahexylammonium or cetylpyridinium ion. The oxidations of alcohols (306), allyl alcohols (307), olefins (308), alkynes (309), β -unsaturated acids (310), vic-diols (311), phenol (312), and amines (313) are the examples.

Ishii *et al.* (306, 307, 310, 311, 313) and Venturello *et al.* (308) have developed various oxidation reactions using organoammonium salts of $PM_{12}O_{40}^{3-}$ ($M = Mo, W$) for phase-transfer catalysts. A reaction mechanism of the epoxidation of olefin is proposed in Scheme 7. In epoxidation of long-chain olefins, epoxides are produced in the organic phase by peroxo species which are only slightly soluble in the organic phase. Since the salts dissolve only slightly in the organic phase, they do not catalyze undesirable ring opening of epoxides. At a conversion of olefin of 82–98%, the selectivity to epoxide is more than 98%. A simple molybdenum compound, H_2MoO_4 , shows no catalytic activity under these reaction conditions. It is probable that neither metal oxides nor peroxomolybdates are soluble in the organic phase (288).

Recently, it was claimed that the active catalysts are not the starting Keggin-type heteropolyanions, but rather $PO_4[WO(O_2)_2]_4^{3-}$ and/or $[W_2O_3(O_2)_4(H_2O)_2]^{2-}$, which are peroxo compounds formed in aqueous solution (308, 314–316). $PO_4[WO(O_2)_2]_4^{3-}$ was two orders of magnitude more active than $[W_2O_3(O_2)_4(H_2O)_2]^{2-}$ for olefin epoxidation. It is suggested that the catalytic cycle is mainly $PO_4[WO(O_2)_2]_4^{3-} \leftrightarrow [P_qW_rO_s(O_2)_r]^-$ [r is 4 or 3 (316)], although the composition of the species formed by the reaction depends on the ratio $[H_2O_2]/[H_3PW_{12}O_{40}]$ (316, 317).

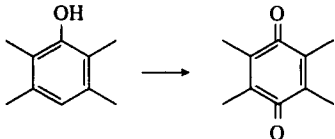
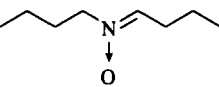
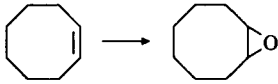
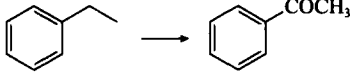
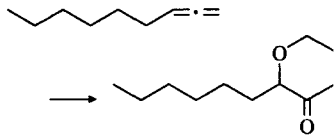
TABLE XXVIII

Liquid-Phase Oxidation Reactions with Hydrogen Peroxide Catalyzed by Heteropoly Compounds

Reaction	Catalyst	Temp. (K)	Ref.
	$H_9PMo_6V_6O_{40}$	303	302-304
	$(CP)_3PW_{12}O_{40}$	reflux	306, 308
	$(CP)_3PW_{12}O_{40}$	298	307a
	$H^+ / WO_4^{4-} / PO_4^{3-} / QX$ $(CP)_3PW_{12}O_{40}$ CP = cetylpyridinium	333 343	308
	$(CP)_3PW_{12}O_{40}$	reflux	308b
	$(CP)_3PW_{12}O_{40}$	r.t.	309a
	$(CP)_3PW_{12}O_{40}$	333-338	310
	$(CP)_3PW_{12}O_{40}$	353	311
	$(CP)_3PW_{12}O_{40}$	r.t.	311

continued

TABLE XXVIII—Continued

Reaction	Catalyst	Temp. (K)	Ref.
	$\text{H}_3\text{PMo}_{12}\text{O}_{40}$	303	312
$(\text{C}_4\text{H}_9)_2\text{HN} \rightarrow$ 	$(\text{CP})_3\text{PW}_{12}\text{O}_{40}$	r.t.	313
	$[\text{WZnMn}_2(\text{ZnW}_9\text{O}_{34})_2]^{12-}$	271	319
	$\text{H}_3\text{PMo}_{12}\text{O}_{40}$	reflux	^a
	$(\text{CP})_3\text{PW}_{12}\text{O}_{40}$	353	^b

^aD. Attanasio *et al.*, *J. Mol. Catal.* **57**, L1 (1989). ^bS. Sakaguchi *et al.*, *J. Org. Chem.* **59**, 5681 (1994).

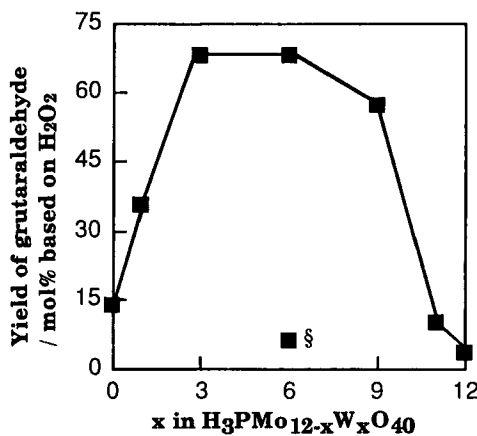
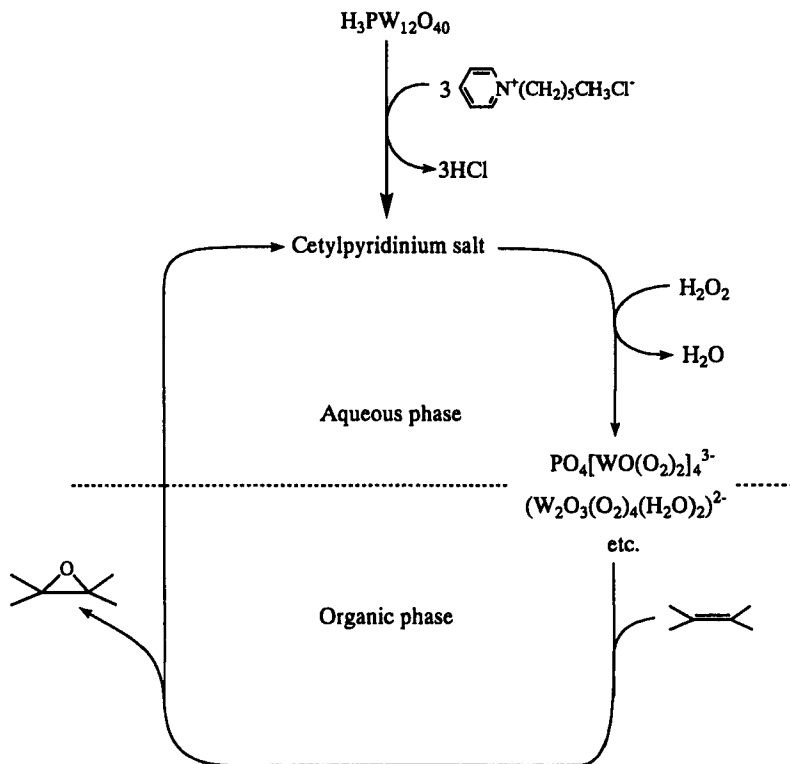


FIG. 56. Effects of addenda atoms on the catalytic oxidation of cyclopentene by H_2O_2 at 303 K. (§) $\text{H}_3\text{PMo}_{12}\text{O}_{40} + \text{H}_3\text{PW}_{12}\text{O}_{40}$. Reaction time, 3 h. (From Ref. 304.)



SCHEME 7

Cetylpyridinium salts of $\text{H}_3\text{PM}_{12}\text{O}_{40}$ ($M = \text{W}, \text{Mo}$) also catalyze the oxidation of secondary alcohols or alkynes to give the corresponding ketones, but they are not active for primary alcohols (308b, 309b). Schwegler (308c) reported that lacunary heteropoly-11-tungstates are better catalysts than tetrahexylammonium 12-tungstophosphate for the oxidation of cyclohexene in biphasic systems.

As described above, catalytic oxidation with hydrogen peroxide is usually limited to polyoxometalates containing only metals in the d^0 state. Recently, however, a tetrairon-substituted heteropolyanion, $\text{Fe}_4(\text{PW}_9\text{O}_{34})_2^{10-}$, and dimanganese-substituted heteropolyanion, $[\text{WZnMn}_2(\text{ZnW}_9\text{O}_{34})_2]^{12-}$ (sandwich-type compound with a WZnMn_2 ring between two $\text{B}-\text{ZnW}_9\text{O}_{34}$ units), have been reported to catalyze selectively the epoxidation of olefins (318). Table XXIX summarizes the oxidation of various reactants with hydrogen peroxide and $[\text{WZnMn}_2(\text{ZnW}_9\text{O}_{34})_2]^{12-}$. At 275 K, the selectivities were more than 99% in all cases. High yields of more substituted olefins indicate that the reactivity of

TABLE XXIX
Oxidation of Various Reactants with 30% H₂O₂ Catalyzed by
[WZnMn₂(ZnW₉O₃₄)₂]¹²⁻ at 275 K^a (from Ref. 318)

Substrate	Products	Turnovers
Cyclohexene	Cyclohexene oxide	1450
	Cyclohexen-2-ol	0
	Cyclohexen-2-one	5
1-Octene	1-Octene oxide	25
2-Methyl-1-heptene	2-Methyl-1-heptene oxide	190
<i>trans</i> -2-Octene	<i>trans</i> -2-Octene oxide	340
	<i>trans</i> -2-Octen-4-one	0
Cyclohexanol	Cyclohexanone	510

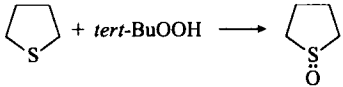
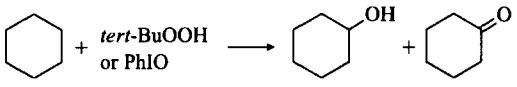
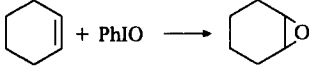
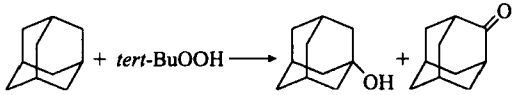
^a Catalyst, 0.2 μmol; reactant, 1 mmol; H₂O₂, 2 mmol; 5 μmol, methyltricaprylammonium chloride.

the reactant is a function of the nucleophilicity of the carbon-carbon double bond.

2. *tert*-Butyl Hydroperoxide and Others

Mixed addenda or transition-metal-ion-substituted heteropolyanions containing Co, Mn, and Ru are catalysts for oxidation reactions with *tert*-butyl hydroperoxide and other oxidants. Typical examples are listed in Table XXX.

TABLE XXX
Liquid-Phase Oxidation Reactions with *tert*-Butylhydroperoxide or Other Oxidants Catalyzed by
Heteropoly Compounds

Reaction	Catalyst	Temp. (K)	Ref.
	H ₅ PMo ₁₀ V ₂ O ₄₀	298	320, 321
	PW ₁₁ CoO ₃₉ ⁵⁻	298	320, 321
	PW ₁₁ MO ₃₉ ⁵⁻ PW ₁₇ MO ₆₁ ¹³⁻ (M = Co, Mn)	297	321 ^a
	[Ni ₃ (PW ₉ O ₃₄) ₂] ¹²⁻	388	320

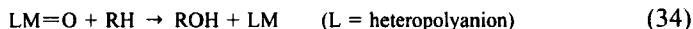
^a D. Mansury *et al.*, *J. Amer. Chem. Soc.* **113**, 7222 (1991).

Strongly acidic $H_3PM_{12}O_{40}$ ($M = Mo, W$) species catalyze oxidation of thioether into sulfoxide and sulfone with 98–99% and 1–3% selectivities, respectively. The V^{5+} substitution increases the selectivity to sulfone up to >99% (319).

Cobalt- or manganese-substituted $PW_{12}O_{40}^{3-}$ and $SiW_{11}O_{39}Ru(OH_2)^{5-}$ catalyze the oxidation of paraffins such as cyclohexane and adamantane (320, 321) as well as the epoxidation of cyclohexene with *tert*-butyl hydroperoxide, iodosylbenzene potassium persulfate, and sodium periodate (321, 322). The reactivity depends on the transition metals. In the case of epoxidation of cyclohexene with iodosylbenzene, the order of catalytic activity of $PW_{11}(M)O_{39}^{5-}$ is $M = Co > Mn > Cu > Fe, Cr$.

A Ni-containing sandwich complex, $Ni_3(\alpha-PW_9O_{39})_2$, is a better catalyst than $PW_{11}(M)O_{39}^{5-}$ ($M = Co, Mn$) for the formation of *N*-alkylacetamide from adamantane and isobutane with *tert*-butylhydroperoxide as the oxidant (323).

As for the mechanism of oxygenation of paraffins with oxygen donors (DO) such as iodosylbenzene and potassium persulfate, Eqs. (33) and (34) have been proposed, whereby oxygenation of metal centers by oxygen donor is followed by oxo transfer from the transition metal to CH bonds of paraffins:



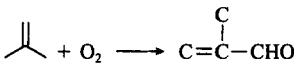
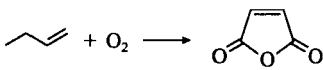
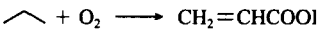
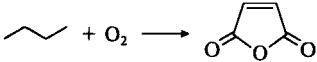
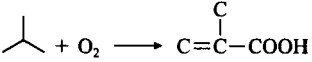
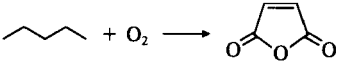
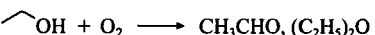
IX. Oxidation Catalyzed by Solid Heteropoly Compounds

Solid heteropoly compounds are suitable oxidation catalysts for various reactions such as dehydrogenation of O- and N-containing compounds (aldehydes, carboxylic acids, ketones, nitriles, and alcohols) as well as oxidation of aldehydes. Heteropoly catalysts are inferior to Mo–Bi oxide-based catalysts for the allylic oxidation of olefins, but they are much better than these for oxidation of methacrolein (5). Mo–V mixed-oxide catalysts used commercially for the oxidation of acrolein are not good catalysts for methacrolein oxidation. The presence of an α -methyl group in methacrolein makes the oxidation difficult (12). The oxidation of lower paraffins such as propane, butanes, and pentanes has been attempted (324). Typical oxidation reactions are listed in Table XXXI and described in more detail in the following sections.

Keggin-type heteropoly compounds having Mo and V as addenda atoms are usually used for such oxidations. The catalysts reported in patents often contain several elements other than Mo, V, and P. An excess amount of P is added to stabilize the structure, and the presence of additional transition elements like Cu improves redox reversibility. Supported heteropoly catalysts are also important for industrial applications and have been characterized (69, 325, 326).

To understand oxidation catalysis by solid heteropoly compounds, the contrast between surface and bulk type II catalysis, and acid–redox bifunctionality

TABLE XXXI
Heterogeneous Oxidation Reactions Catalyzed by Heteropoly Compounds

Reaction	Catalyst	Temp. (K)	Ref.
$\text{CH}_2=\text{C}(\text{CH}_3)\text{CHO} + \text{O}_2 \longrightarrow \text{CH}_2=\text{C}(\text{CH}_3)\text{COOH}$	$\text{CsH}_3\text{PMo}_{11}\text{VO}_{40}$	533	12
$\text{CH}_3\text{CHO} + \text{O}_2 \longrightarrow \text{CH}_3\text{COOH}$	$\text{Cs}_x\text{H}_{3-x}\text{PMo}_{12}\text{O}_{40}$	573	333
$\text{CH}_3\text{CH}(\text{CH}_3)\text{COOH} + \text{O}_2 \longrightarrow \text{CH}_2=\text{C}(\text{CH}_3)\text{COOH}$	$\text{H}_5\text{PMo}_{10}\text{V}_2\text{O}_{40}$	573	342 ^d
$= + \text{O}_2 \longrightarrow \text{CH}_3\text{COOH}$	Pd + $\text{H}_4\text{SiW}_{12}\text{O}_{40}/\text{SiO}_2$	423	^b
	$\text{PbFeBiPMo}_{12}\text{O}_x$	673	^c
	$\text{Cs}_{2.5}\text{H}_{0.5}\text{PMo}_{12}\text{O}_{40}$ + VO^{2+}	563	^d
$\text{CH}_4 + \text{N}_2\text{O} \longrightarrow \text{HCHO}, \text{CH}_3\text{OH}$	$\text{H}_3\text{PMo}_{12}\text{O}_{40}/\text{SiO}_2$	843	^e
$\text{C}_2\text{H}_6 + \text{N}_2\text{O}(\text{O}_2) \longrightarrow \text{C}_2\text{H}_4, \text{CH}_3\text{CHO}$	$\text{H}_3\text{PMo}_{12}\text{O}_{40}/\text{SiO}_2$	540	^f
	$\text{H}_3\text{PMo}_{12}\text{O}_{40}$ (+ As)	613	352, 353
	$\text{BiPMo}_{12}\text{O}_x + \text{VO}^{2+}$	633	324, 350
	$\text{H}_3\text{PMo}_{12}\text{O}_{40}$	623	354–356
	$\text{H}_5\text{PMo}_{10}\text{V}_2\text{O}_{40}$	583	106
$\text{CH}_3\text{OH} + \text{O}_2 \longrightarrow \text{HCHO}, (\text{CH}_3)_2\text{O}$, etc.	$\text{H}_3\text{PMo}_{12}\text{O}_{40}$	473–563	345
	$\text{H}_3\text{PMo}_{12}\text{O}_{40}$ (+ polysulfone)	443	110

^aM. Akimoto *et al.*, *J. Catal.* **89**, 196 (1984). ^bT. Suzuki *et al.*, US Patent, 5405996 (1995).
^cT. Ohara, *Shokubai (Catalyst)* **19**, 157 (1977). ^dM. Ai, *J. Catal.* **85**, 324 (1984). ^eS. S. Hong
et al., *Appl. Catal. A* **109**, 117 (1994). ^fS. Kasztelam *et al.*, *J. Catal.* **116**, 82 (1989).

of heteropoly catalysts must be properly taken into account, along with relationships between the oxidizing properties of catalysts and their catalytic activities (5, 6, 258, 266, 327, 328).

A. CONCEPT OF SURFACE AND BULK TYPE II CATALYSIS AND REDOX (MARS-VAN KLEVELEN) MECHANISM

1. Bulk Type II Catalysis

As described above, heterogeneous catalytic reactions on heteropoly compounds are classified into three different types, surface, bulk type I (pseudo-liquid phase), and bulk type II (Fig. 1). The surface reactions are typical of

ordinary heterogeneous catalysis, and therefore the surface acidity and oxidizing ability are important. Bulk type I reactions proceed within the catalyst.

In the bulk type II reduction, the rapid migration of redox carriers enables the whole catalyst to be reduced (260). The differences between the noncatalytic surface and bulk type II reduction are reflected in *catalytic* oxidations proceeding via redox mechanisms, as described below (258, 260–262, 329). If a catalytic oxidation proceeds by the cyclic reduction and reoxidation of the catalyst (a redox mechanism), the rate of catalytic oxidation and the rates of reduction and reoxidation of the catalyst must coincide if they are measured in the stationary state of catalytic oxidation. Measurements were made for the oxidation of H_2 catalyzed by $H_3PMo_{12}O_{40}$ having different specific surface areas (Fig. 57). While the degree of reduction in the stationary state differs among the catalysts, the rates of reduction of the catalysts by H_2 , the rates of reoxidation, and the rates of catalytic oxidation agree quite well. The agreement indicates that the catalytic oxidation of H_2 proceeds by a redox mechanism. A similar redox mechanism was confirmed for $H_3PW_{12}O_{40}$ and alkali salts of $H_3PMo_{12}O_{40}$.

In addition, the rate of reduction depends only slightly on the surface area (Fig. 52), although the rate of reoxidation is proportional to the surface area. If these rates are compared for a particular degree of reduction at the steady state of the catalytic oxidation, the differences in rates from one catalyst to another

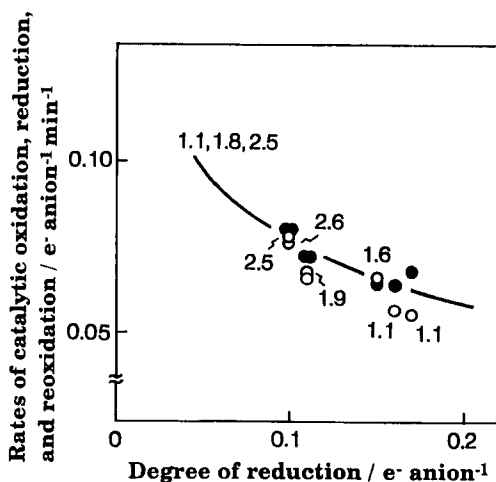


FIG. 57. Rates of catalytic oxidation of H_2 , reduction by H_2 , and reoxidation by O_2 for $H_3PMo_{12}O_{40}$ catalysts having different specific surface areas: Dependence on the degree of reduction of each catalyst at the stationary state. The numbers next to the symbols indicate the surface areas (after reaction) in $m^2 g^{-1}$. (●) Catalytic oxidation; (—) reduction; (○) reoxidation. Reaction temperature, 573 K. (From Ref. 262.)

are small. Consistent with this pattern, the rate of the catalytic reaction is only weakly dependent on the surface area, as shown in Fig. 58.

On the other hand, the rate of catalytic oxidation of CO is proportional to the specific surface area, as shown in Fig. 58. This dependence indicates ordinary heterogeneous catalysis. The linear dependence in Fig. 58 can also be explained on the basis of the redox mechanism, as both the rate of CO conversion and the rate of O₂ conversion are proportional to surface area (Fig. 53).

A weak support effect, as shown in Fig. 59, is another indication of bulk type II behavior (327). With an increase in the loading of the heteropoly compound on the support, the rate of bulk type II catalysis increases to high loading levels, whereas the rate of surface catalysis shows saturation at relatively low loadings because of the decrease in the dispersion of the heteropoly compound on the support (327).

Good correlations are observed between the oxidizing abilities of catalysts and the catalytic activities for oxidation, provided that the bulk and surface catalysis are properly accounted for. Examples are shown in Figs. 60a and b. A linear correlation is observed between the rates of catalytic oxidation of

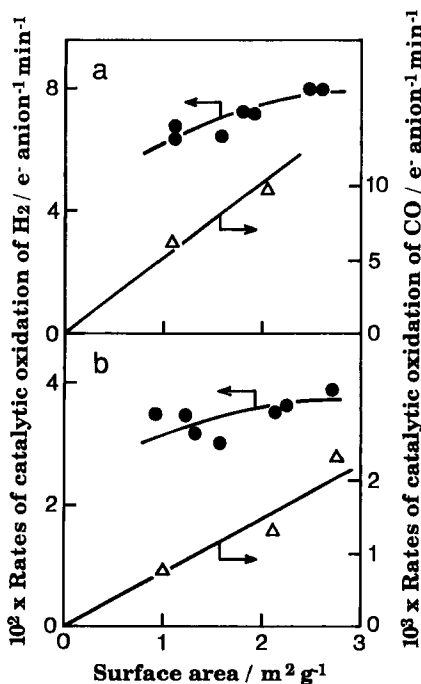


FIG. 58. Rates of catalytic oxidation of H₂ and of CO in the presence of catalysts having different surface areas. (a) H₃PMo₁₂O₄₀ at 573 K, (b) Na₂HPMo₁₂O₄₀ at 623 K. (●) H₂-O₂; (Δ) CO-O₂ (From Ref. 262.)

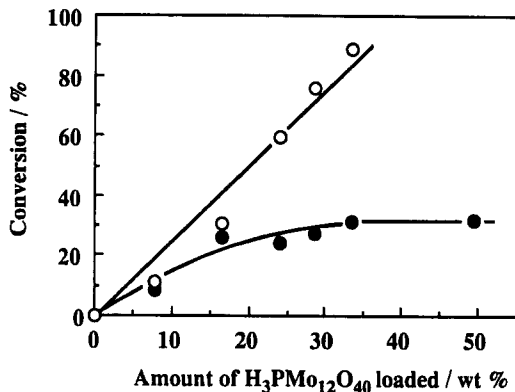


Fig. 59. Catalytic oxidative dehydrogenation of cyclohexene (O, surface catalysis) and oxidation of acetaldehyde (●, bulk-type II); the catalyst was $\text{H}_3\text{PMo}_{12}\text{O}_{40}$ supported on SiO_2 . Masses catalyst: 0.2 g for cyclohexene and 0.1 g for acetaldehyde. (From Ref. 327.)

acetaldehyde (surface reaction) and the rate of reduction of catalysts by CO (indicating surface oxidizing ability). A similarly good relationship for oxidative dehydrogenation of cyclohexene (bulk type II reaction) and the rate of reduction of catalysts by H_2 (bulk oxidizing ability) has also been found. However, the

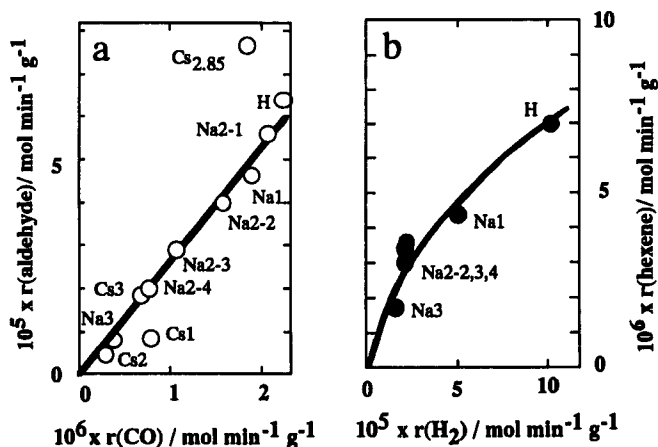


Fig. 60. Correlations between catalytic activity and oxidizing ability for (a) oxidation of acetaldehyde (surface reaction) and (b) oxidative dehydrogenation of cyclohexene (bulk-type II reaction). (From Ref. 327.) $r(\text{aldehyde})$ and $r(\text{hexene})$ show the rates of catalytic oxidation of acetaldehyde and oxidative dehydrogenation of cyclohexene, respectively. (From Ref. 337.) $r(\text{CO})$ is the rate of reduction of catalysts by CO; $r(\text{H}_2)$ is the rate of reduction of catalysts by H_2 . M_x denotes $\text{M}_x\text{H}_{3-x}\text{PMo}_{12}\text{O}_{40}$. Na2-1, 2, 3, and 4 are $\text{Na}_2\text{HPMo}_{12}\text{O}_{40}$ of different lots, of which the surface areas are 2.8, 2.2, 1.7, and 1.2 $\text{m}^2 \text{g}^{-1}$, respectively.

correlation is poor if the rate of the surface reaction is plotted against the bulk oxidizing ability.

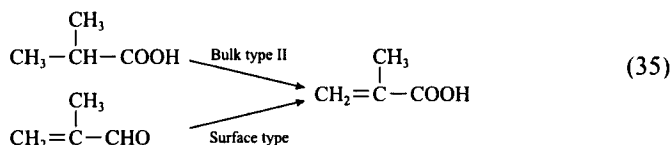
The following are typical reactions that have already been found to be described by either of the two types of catalysis by $\text{H}_3\text{PMo}_{12}\text{O}_{40}$ and its alkali salts:

Surface type: Oxidation of CO, acetaldehyde, and methacrolein.

Bulk type II: Oxidation of H_2 , oxidative dehydrogenation of cyclohexene, isobutyric acid.

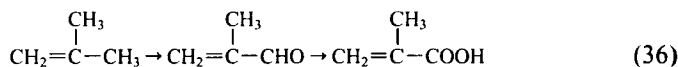
Since the classification is essentially based on rates of catalytic reactions relative to rates of diffusion of redox carriers, there are oxidation reactions that are intermediate between the two limiting cases. We note that neither the molecular size nor the polarity of reactant molecules is the principal characteristic determining the type of catalysis. Although oxide ions migrate rapidly in the bulk, bulk type II catalysis is not observed for oxidation catalyzed by Bi-Mo oxides. In this case the rate-limiting step is a surface reaction.

It is noteworthy that in the two industrial processes to produce methacrylic acid, both involving catalysis by $\text{H}_3\text{PMo}_{12}\text{O}_{40}$ and its alkali salts, one involves bulk type II catalysis and the other, surface type catalysis, as described in the following section.



B. OXIDATION OF ALDEHYDES

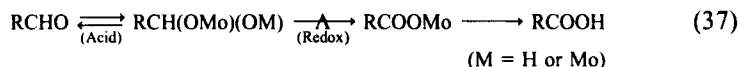
Methacrylic acid has been used for the synthesis of poly(methyl methacrylate). It has been synthesized industrially via a reaction of acetone with hydrogen cyanide (12, 17, 330, 331). However, the process produces ammonium bisulfate and uses the toxic hydrogen cyanide. Recently, an alternative, a two-step oxidation of isobutylene, has been developed. The first step is the oxidation of isobutylene to methacrolein, and the second is the oxidation of methacrolein to methacrylic acid:



1. Mechanism and Roles of Acidity and Oxidizing Ability

In the second step of Eq. (36), methacrolein is oxidized by heteropoly catalysis, of which the active component is essentially $\text{H}_3\text{PMo}_{12}\text{O}_{40}$ or its

equivalent. Therefore, the oxidation mechanism was investigated with $\text{H}_3\text{PMo}_{12}\text{O}_{40}$ and its salts. It was concluded that the reaction proceeds by a redox mechanism according to the reaction scheme shown in Eq. (37):



Equation (37) was derived on basis of the following experimental facts:

- (i) A fair correlation between the rate of catalytic oxidation and the oxidizing ability of the catalyst measured by the reduction with CO was observed (Fig. 61) (17, 332). This result shows that the rate-limiting step is part of the second reaction, that is, the oxidative dehydrogenation of the intermediate. The first reaction requires acidic sites, as nonacidic catalysts were inactive. But the rate-determining step is inferred not to be part of the first reaction because there was no parallel between the acidity and the rate (332).
- (ii) Catalyst oxygen is involved in the reaction, since the reaction continued and the selectivity remained essentially the same for a prolonged period after the supply of oxygen was stopped, with the catalytic reaction proceeding in the stationary state (17).

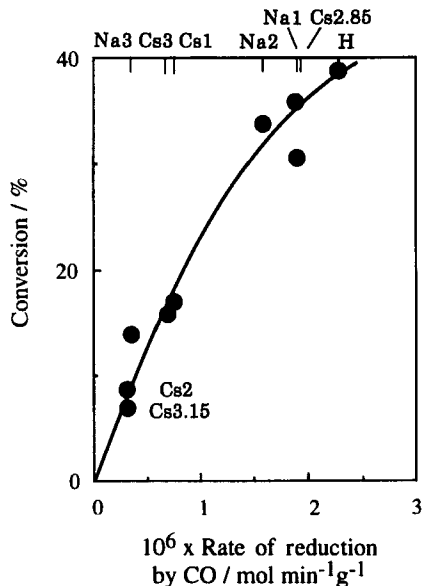
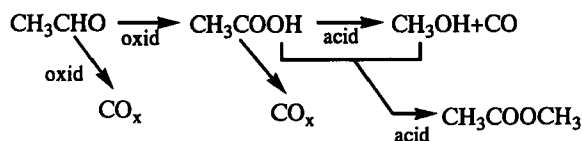


FIG. 61. Correlation between the conversion of methacrolein and the rate of reduction of catalyst by CO. M_x denotes $M_x\text{H}_{3-x}\text{PMo}_{12}\text{O}_{40}$. (From Ref. 332.)



SCHEME 8

(iii) Rapid and direct exchanges of isotopic oxygen between either two of the species, methacrolein, water, and $\text{M}_x\text{H}_{3-x}\text{PMo}_{12}\text{O}_{40}$ ($\text{M} = \text{Na}, \text{Cs}$; $x = 0-3.15$), were confirmed by elaborate pulse-mass spectrometry experiments (17, 332). In addition, the rate of oxygen exchange between methacrolein and the polyanion increased with the number of Brønsted acid sites. This result indicates that the first reaction in Eq. (37) is catalyzed by Brønsted acids.

(iv) The presence of water vapor had a strong influence on the rate and selectivity. This effect was reversible and instantaneous (103).

The roles of acidity and oxidizing ability were investigated in detail for the oxidation of acetaldehyde catalyzed by various salts of $\text{H}_3\text{PMo}_{12}\text{O}_{40}$; the data were interpreted on the basis of the reaction scheme deduced (Scheme 8) (333). The rate of each reaction in the scheme was estimated from the rates of oxidations of acetaldehyde and acetic acid, and compared with the acidities and oxidizing abilities of the catalyst surfaces. The comparisons indicate that the oxidizing ability influences mainly the reactions of $\text{CH}_3\text{CHO} \rightarrow \text{CH}_3\text{COOH}$ and $\text{CH}_3\text{CHO} \rightarrow \text{CO}_x$, and the acidity accelerates $\text{CH}_3\text{COOH} \rightarrow \text{CH}_3\text{OH} + \text{CO}$ and $\text{CH}_3\text{OH} + \text{CH}_3\text{COOH} \rightarrow \text{CH}_3\text{COOCH}_3$.

Ai (334a) investigated the effect of countercation and additives for the oxidation of methacrolein. It was found that the catalytic activity of $\text{Cs}_2\text{HPMo}_{12}\text{O}_{40}$ is enhanced by the addition of oxoanions such as BO_3^{3-} and PO_4^{3-} . The effect was explained on the basis of acidic and basic properties of the heteropoly compounds. Ai *et al.* (334b) also investigated the oxidation of crotonaldehyde to furan catalyzed by $\text{H}_3\text{PMo}_{12}\text{O}_{40}$ and its salts. The rate increased markedly with an increase in the steam concentration but was almost independent of the partial pressures of oxygen and crotonaldehyde. The reaction catalyzed by the Cs salt was faster than that catalyzed by the parent acid. This result was explained as follows. The addition of a basic species such as Cs ion reduces the acidity of the catalyst and the affinity for furan, which is basic. The weaker interaction facilitates the furan desorption, which is assumed to be rate-determining.

2. Catalysts

In industry, heteropoly catalysts of $\text{H}_{3-x}\text{Cs}_x\text{PMo}_{12-y}\text{V}_y\text{O}_{40}$ ($2 < x < 3$; $0 < y < 2$) are used to oxidize methacrolein into methacrylic acid with 60–70%

yields (12, 335). Formation of Cs salts markedly increases the surface area and thermal stability of the catalysts, but the stoichiometric Cs salt is not catalytically active, probably because of the absence of acidity. Thus acidic salts that are nearly stoichiometric are preferred. The acidic salts are often mixtures or solid solutions of the acid form and salts. It is assumed in some cases that the acidic Cs or K salts are the acid form epitaxially formed as thin films on the surface of Cs or K salts (46a, 336, 337).

It has been claimed (335) that preparation of an acid form catalyst by the thermal decomposition of pyridinium salts results in a cubic crystal structure and increases the surface area and pore volume. For example, the surface area of $\text{H}_4\text{PMo}_{11}\text{VO}_{40}$ increases from 1.0 to $5.3 \text{ m}^2 \text{ g}^{-1}$ by the creation of macropores having radii of 10^3 – 10^4 \AA . As a result of macropore formation, higher yields are obtained (Fig. 62). The formation of acetic acid, CO and CO_2 at high conversion is suppressed by treatment of the catalyst with pyridine. The application of this method to acidic Cs salts further improves the activity and selectivity.

C. DEHYDROGENATION OF ISOBUTYRIC ACID

This reaction is another possible route for the production of methacrylic acid, since isobutyric acid can be obtained by an oxo process from propene and CO. Heteropoly compounds and iron phosphates are so far the most efficient catalysts for the reaction. The favorable role of the presence of an α -methyl group is remarkable for oxidative dehydrogenation, as the heteropoly compounds are not good catalysts for the dehydrogenation of propionic acid (338, 339).

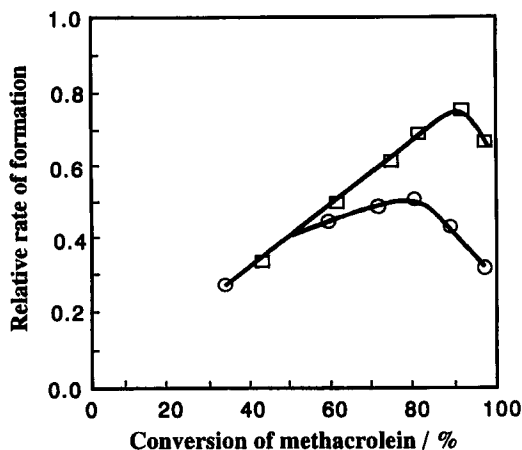
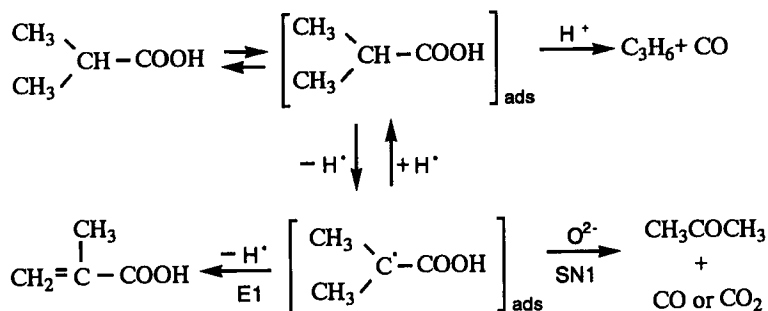


FIG. 62. Oxidation of methacrolein catalyzed by $\text{H}_4\text{PMo}_{11}\text{VO}_{40}$, untreated (○) and treated (□) with pyridine. Catalyst, 10 cm^3 ; reaction temperature, 553 K; SV, 1000 h^{-1} . Reactant composition: methacrolein 2%, oxygen 6%, water 20%. (From Ref. 335.)

The effects of counteranions as well as heteroatoms have been investigated by Akimoto *et al.* (340). The catalytic activity increased in the order $H < Li < Na < Rb < Cs$ at 573 K, and the reverse order was found at 523 K. The authors concluded that the reaction proceeds by a redox cycle involving heteropoly catalysts and that the reduction of the catalyst is rate-determining at 573 K, whereas the reoxidation is rate-determining at 523 K. It was supposed that oxygen atoms bonded to Mo become more reactive as the electronegativity of the counteranion decreases. The authors further suggested that a metal ion having a high oxidation potential, such as Pd or Ag, acts as an electron reservoir and accelerates the reaction. It was reported that Cu^{2+} is also an effective cation (341). Recently, Lee *et al.* (342) have compared the catalytic performance with that of $Cs_xH_{4-x}PMo_{12-y}V_yO_{40}$ ($x, y = 0-4$) and found that $Cs_{2.75}H_{1.25}PMo_{11}VO_{40}$ was effective for the oxidative dehydrogenation of isobutyric acid. For example, the selectivity to methacrylic acid was 78% at 97% conversion and 623 K. Herve *et al.* (284) demonstrated that the elimination of V^{5+} from $H_4PMo_{11}VO_{40}$ took place during the reaction. Notwithstanding the extensive investigations, a consistent explanation is lacking; further investigations are necessary.

The heteropoly catalyst is deactivated during a prolonged reaction period by the loss of Mo to form volatile Mo-containing species via the interaction of isobutyric acid and/or methacrylic acid with the catalyst (343). The deactivation was suppressed by presaturating the feed by flow over a bed of MoO_3 (343).

In the dehydrogenation of isobutyric acid, the by-products in addition to CO and CO_2 are propylene and acetone. Two reaction mechanisms were proposed (340, 341) and the latter is shown in Scheme 9 (340). The formation of methacrylic acid and acetone involves a common intermediate: The E1 elimination of a proton from I yields the methacrylic acid while a nucleophilic S_N1 attack of oxide ion produces CO_2 and acetone (344). On the other hand,



I

SCHEME 9

propylene forms by an acid-catalyzed reaction. Therefore, the acid–basic and redox properties of the catalysts are both important.

A similar competitive action of acidity and oxidizing ability was demonstrated for the reaction of methanol and ethanol (345, 110) and the blending of $\text{H}_3\text{PMo}_{12}\text{O}_{40}$ with polysulfone greatly increased the oxidation performance.

D. OXIDATION OF PARAFFINS

Oxyfunctionalization of lower paraffins such as methane, ethane, propane, and butanes has recently attracted much attention (5, 330, 331, 347–350). Oxidation of *n*-butane to maleic anhydride is an industrial example (346, 351). The oxidation of propane and isobutane with heteropoly catalysts was first reported in 1979 (352). Ai (324a) and Centi *et al.* (324b, 324c) reported that heteropoly compounds catalyze the oxidation of lower paraffins, especially propane, isobutane, and pentane (324).

The oxidation of propane into acrylic acid in the presence of heteropoly catalysts prepared from $\text{H}_3\text{PMo}_{12}\text{O}_{40}$ and antimony pentachloride gave rather low conversion and selectivity [10 and 19%, respectively (2% yield)] (352). Recently, a yield of *ca.* 9% was obtained with $\text{H}_5\text{PV}_2\text{Mo}_{10}\text{O}_{40}$ (353). The addition of Cr ion also enhanced the catalytic performance (354).

Heteropoly catalysts have significant activities for the oxidation of isobutane into methacrolein and methacrylic acid. The yield increased up to 6% by vanadium substitution or salt formation, as follows. With $\text{Cs}_{2.5}\text{Ni}_{0.08}\text{H}_{0.34+x}\text{PV}_x\text{Mo}_{12-x}\text{O}_{40}$, the highest conversion and selectivity were observed at $x \approx 1$ (355). Increases in the reaction temperature to 613 K led to increased yields, up to 9.0%. A similar increase in the yield resulted from the substitution of As for P as a heteroatom or from the addition of various transition metals (106, 356).

When the oxidation of *n*-pentane was carried out in the presence of $\text{H}_{3+x}\text{PV}_x\text{Mo}_{12-x}\text{O}_{40}$ ($x = 0-3$), the only product observed in addition to oxides of carbon was maleic anhydride (357). The activity and selectivity increases when one Mo was replaced by a V atom.

E. HETEROGENEOUS LIQUID-PHASE OXIDATION REACTIONS

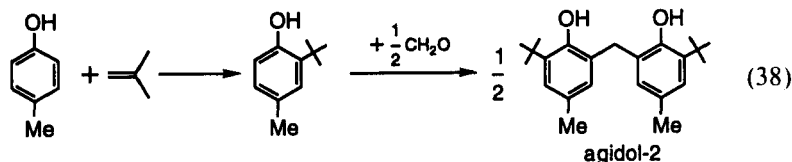
$\text{Na}_5\text{PV}_2\text{Mo}_{10}\text{O}_{40}$ supported on active carbon is active for oxidative dehydrogenation of benzylic alcohols and amines without overoxidation of benzaldehyde and benzylamine in the liquid phase (357). The suppression of the overoxidation may be due to the lower oxidizing ability of $\text{Na}_5\text{PV}_2\text{Mo}_{10}\text{O}_{40}$ relative to its acid form.

Soeda *et al.* (358) used Pd-supported heteropoly compounds for a heterogeneous Wacker-type reaction and found that Pd/Cs_{2.5}H_{0.5}PW₆Mo₆O₄₀ was active for oxidation of cyclohexene to produce cyclohexanone and cyclohex-enone. The active sites are assumed to be Pd²⁺ and Pd⁰ for the two products, respectively. Homogeneous Wacker-type reactions are described in Section XI.

X. Fine Chemicals Synthesis

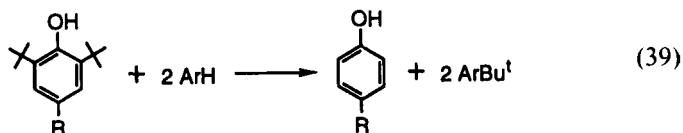
The use of heteropolyacids as catalysts for fine organic synthetic processes is developing. Syntheses of antioxidants, medicinal preparations, vitamins, biologically active substances, etc., have been reported and some are already applied in practice (10, 160).

Alkylation of *p*-cresol with isobutylene to give *tert*-butyl-4-methyl phenol [Eq. (38)] is the first step in the synthesis of agidol-2, an antioxidant for polymeric materials (160).



The activity of H₃PW₁₂O₄₀ is greater by four orders of magnitude than that of sulfuric acid. The use of heteropolyacids instead of H₂SO₄ not only eliminated the formation of waste water containing toxic cresol sulfate, but also reduced the loss of *p*-cresol during neutralization and washing.

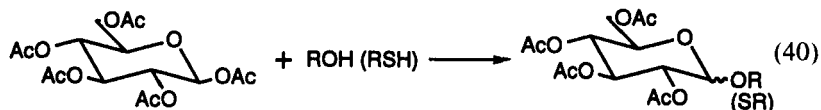
H₃PW₁₂O₄₀ and H₄SiW₁₂O₄₀ are active for transalkylation of 2,6-di-*tert*-butyl 4-R-phenol (R = H, alkyl, aryl, etc.) [Eq. (39)] (359, 360).



These heteropolyacids are superior to Nafion and give 4-R-phenol with 92–98% yields at 373–413 K by use of toluene or *p*-xylene for *tert*-butyl group acceptors. It is claimed that these catalysts can be readily separated from the reaction mixture and reused.

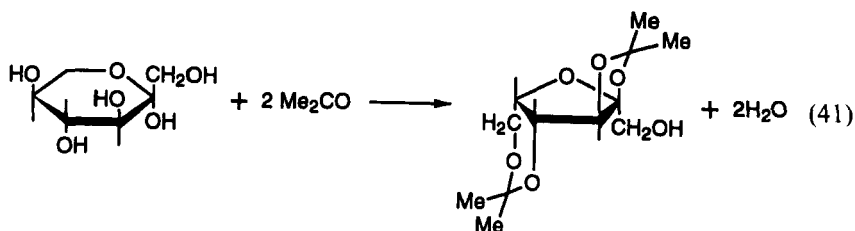
Heteropolyacids are also active for the conversion of sugar derivatives (360). H_{*n*}XM₁₂O₄₀ (X = P, Si, M = W, Mo) are much more active than conventional catalysts such as *p*-toluenesulfonic acid and ZnCl₂ for nucleophilic substitution

of acetylated aldohexose to give the corresponding glycosides [Eq. (40)], which are used as biodegradable surfactants.



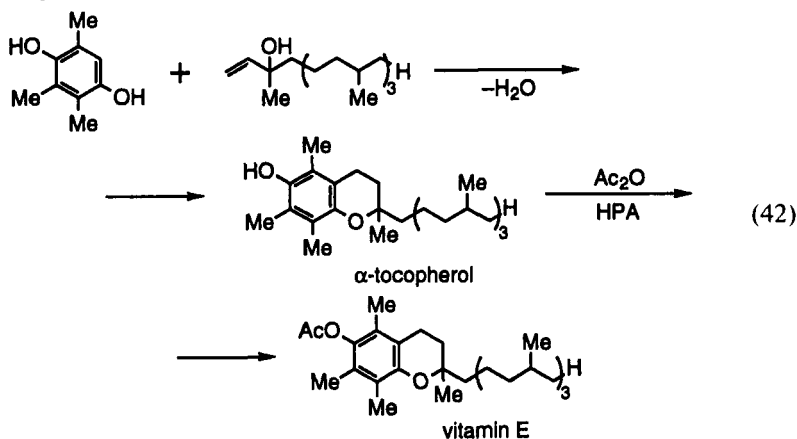
The reaction is performed in a homogeneous liquid phase by use of less than 2 mol% of heteropolyacids with respect to acetylated aldohexose, and 70–90% yields and 60–98% mol% β -anomer selectivity are obtained.

The reaction of L-sorbose with acetone, a step in the synthesis of L-ascorbic acid (vitamin C), takes place in acetone solution [Eq. (41)] (361).



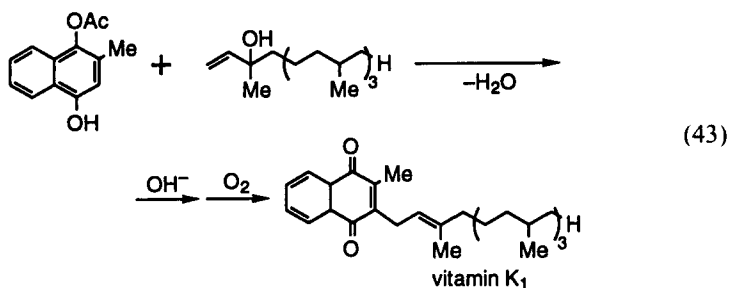
The yield of diacetone-L-sorbose in the presence of 0.1–0.35% of $\text{H}_3\text{PW}_{12}\text{O}_{40}$ or $\text{H}_4\text{SiW}_{12}\text{O}_{40}$ is 85% under reflux.

Heteropolyacids catalyze the condensation reaction in the synthesis of vitamin E (α -tocopherol acetate) as shown in Eq. (42) (362).



With 1% of $\text{H}_3\text{PW}_{12}\text{O}_{40}$ relative to 2,3,5-trimethylhydroquinone, the yield reaches about 92%, and vitamin E in the isolated product is 95%. $\text{H}_3\text{PW}_{12}\text{O}_{40}/\text{SiO}_2$ is less active than bulk $\text{H}_3\text{PW}_{12}\text{O}_{40}$, probably because of the decrease in the acid strength that results from supporting the catalyst. In the case of ZnCl_2 or H_2SO_4 , a large amount of catalyst is required.

$H_3PW_{12}O_{40}$ and $H_4SiW_{12}O_{40}$ are also active for the condensation of isophytol and 1-acetoxy-4-hydroxy-2-methylnaphthalene, which is a key step in the synthesis of vitamin K_1 (2-methyl-3-phytyl-1,4-naphthoquinone) [Eq. (43)]; heteropolyacids are approximately 50 times more active than $ZnCl_2$ (362).



The esterification of steroids is a step in the synthesis of modified hormones. $H_2PW_{12}O_{40}$ and 25% $H_3PW_{12}O_{40}/SiO_2$ (1–9%) in CH_3CN (at 313–353 K) give a quantitative yield (363). The activities of the heteropolyacids are close to that of $HClO_4$ and much greater than that of 5-sulfosalicylic acid.

XI. Hybrid Catalysts

An attractive research target is the design of heteropoly catalysts complexed with organometallics. The use of heteropoly catalysts in combination with noble metals is also promising. Research in these directions has attracted much attention recently.

A. MONO-TRANSITION-METAL-ION-SUBSTITUTED HETEROPOLYANIONS AS INORGANIC SYNZYMES

A recent development concerns the use of polyanions of the type $[XM_{11}O_{39}M'(OH_2)]^{n-}$. In this type, the M' atom easily becomes coordinatively unsaturated by dehydration (255). The resulting dehydrated anion, $[XM_{11}O_{39}M']^{n-}$, can be considered an inorganic metalloporphyrin analog (322, 364, 365). Oxidation catalysis by these polyanions is described in Sections VIII and IX. Here, the catalytic performance and stability are compared with that of metalloporphyrin.

In the majority of the homogeneous oxidations of hydrocarbons by oxometal-based catalysts (including metalloporphyrins), there is appreciable decomposition of catalyst ligands by oxidation, and hence appreciable loss in activity after a few turnovers. A similar degradation of organic ligands, often hydrophobic long-chain carboxylates, is also observed in industrial processes of hydrocarbon

autoxidation. These disadvantages of organic ligands, can be overcome by the use of heteropolyanions.

The rates, selectivities, and stabilities of transition-metal-substituted polyoxometalates in olefin epoxidation are compared with those of metalloporphyrins, Schiff base complexes, and triflate salts, as follows (320b):

Activity: $\text{PW}_{11}\text{Co(II)O}_{39}^{5-} > \text{PW}_{11}\text{Mn(II)O}_{39}^{5-} \geq \text{Fe(III)(TDCPP)Cl} > \text{Fe(III)(TPP)Cl} > \text{M(OTf)}_2$.

Selectivity to epoxide: $\text{PW}_{11}\text{Co(II)O}_{39}^{5-} \approx \text{PW}_{11}\text{Mn(II)O}_{39}^{5-} > \text{M(OTf)}_2 > \text{Fe(III)(TDCPP)Cl} > \text{Fe(III)(TPP)Cl}$.

Stability: $\text{TMSP} > \text{Fe(III)(TDCPP)Cl} > \text{Fe(III)(TPP)Cl} > \text{M(OTf)}_2$

(Abbreviations: TDCPP, tetrakis-2,6-dichlorophenylporphyrin; TPP, tetraphenylporphyrin; OTf, triflate ion).

TMSP is also active for paraffin hydroxylation. Figure 63 is a summary indicating the number of turnovers of a variety of oxo transfer catalysts before catalyst decomposition (320b). When *tert*-butyl hydroperoxide is used as an

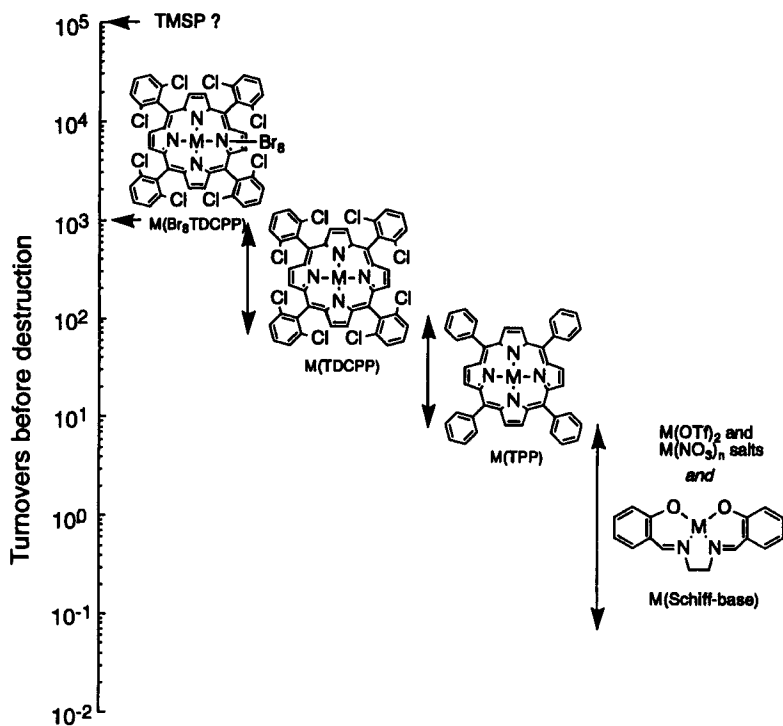


FIG. 63. Stability of transition-metal-substituted polyoxometalate for oxo transfer to hydrocarbons. Values on the ordinate indicate numbers of turnovers for paraffin oxidation. \leftrightarrow shows the ranges of the numbers of turnovers. (From Ref. 320b.)

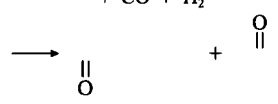
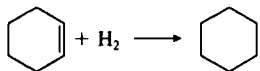
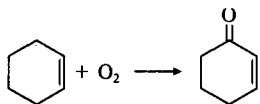
oxygen donor, the turnover of TMSP is higher than those of metalloporphyrins, Schiff base complexes, triflate or nitrate salts, or other soluble transition-metal complexes. Recently, Mansuy *et al.* (366) reported that $P_2W_{17}O_{61}(Mn^{3+} \cdot Br)^{8-}$ was oxidation-resistant and the most active for the epoxidation of cyclooctene with PhIO among $P_2W_{17}O_{61}(M^{n+} \cdot Br)^{(11-n)-}$ (Mn^{3+} , Fe^{3+} , Co^{2+} , Ni^{2+} , Cu^{2+}) catalysts. $P_2W_{17}O_{61}(Mn^{3+} \cdot Br)^{8-}$ also catalyzes the oxygenation of cyclohexane, adamantane, and heptane; the hydroxylation of naphthalene; etc. $P_2W_{17}O_{61}(Mn^{3+} \cdot Br)^{8-}$ shows similar regioselectivities to those of Mn-porphyrin.

B. METAL ION- OR METAL SALT-HETEROPOLYANION COMPLEXES

1. Simple Combinations

Oxidation reactions catalyzed by heteropoly compounds alone are described in Section VIII. Oxidation reactions catalyzed by transition-metal ions in combination with heteropolyanions are shown in Table XXXII (288, 292, 368–375).

TABLE XXXII
Reactions Catalyzed by Combinations of Heteropolyanions with Metal Ions

Reaction	Catalyst	Ref.
$RCH=CH_2 + O_2 \longrightarrow RCHOCH_3$	$PMo_{12-n}V_nO_{40}^{(3+n)-} + PdSO_4$	292, 368
$C_6H_6 + O_2 \longrightarrow (C_6H_5)_2$	$PMo_{12-n}V_nO_{40}^{(3+n)-} + Pd(OCOCH_3)_2$	292
$PhNO_2 + 3CO + CH_3OH$ $\longrightarrow PhNHCO_2CH_3 + 2CO_2$	$H_3PV_2Mo_{10}O_{40} + PdCl_2$	369
CH_3OH (or CH_3OCH_3) + CO $\longrightarrow CH_3CO_2CH_3$	$IrPW_{12}O_{40}$	370
$\equiv-OH + H_2 \longrightarrow \equiv-OH$	$Li_4SiMo_{12}O_{40} + RhCl(PPh_3)_3$	371
+ CO + H ₂	$[(Ph_3P)_2Rh(CO)_4]_4SiW_{12}O_{40}$	372
\longrightarrow 		
	$[(n-C_4H_9)_4N]_5Na_3$ $[(1,5-COD) \cdot IrP_2W_{15}Nb_3O_{62}]$	373
	$[(n-C_4H_9)_4N]_5Na_3$ $[(1,5-COD) \cdot IrP_2W_{15}Nb_3O_{62}]$	374
$CH_4 + O_2 \longrightarrow CH_3OH + CH_3Cl$	Pt salt + $Na_8HPMo_6V_6O_{40}$	375

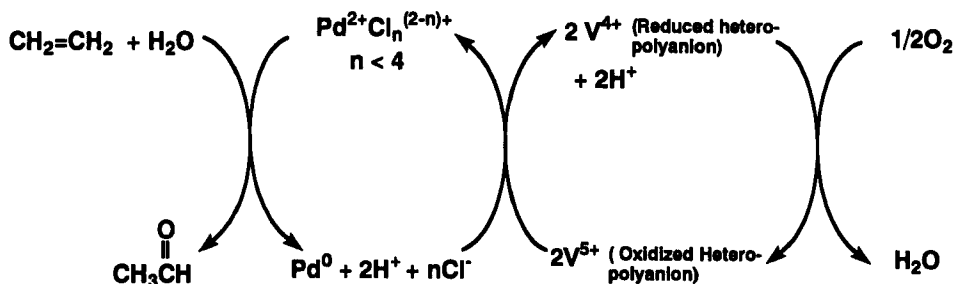


FIG. 64. Redox cycle for the oxidation of ethylene to acetaldehyde. V^{5+} (oxidized heteropolyanion) represents vanadium in the oxidized heteropolyanion. (From Ref. 368.)

The Wacker process is employed industrially for converting ethylene into acetaldehyde. The reaction is usually carried out with a $\text{PdCl}_2\text{-CuCl}_2\text{-HCl}$ catalyst in an aqueous solution at 370–403 K. This process has several drawbacks, such as formation of chlorine-containing by-products and extensive corrosion of the reaction vessel. The development of chloride-free oxidants to replace CuCl_2 for oxidation of Pd^0 has long been desired. Heteropolyanions can be used as reoxidizing reagents for Pd^0 in place of CuCl_2 , as shown in Fig. 64. The idea was first reported by Matveev *et al.* (292) for the oxidation of ethylene with chloride-free PdSO_4 and $\text{H}_{3+x}\text{PV}_x\text{Mo}_{12-x}\text{O}_{40}$ ($x = 1\text{--}4$). 1-Octene is also converted into 2-octanone with a selectivity of 95% at 333–353 K in the presence of PdSO_4 and $\text{H}_9\text{PMo}_6\text{V}_6\text{O}_{40}$ (367). Izumi *et al.* (367) found that the rate-determining step is the reoxidation of Pd^0 to Pd^{2+} for the oxidation of 1-butene and that $\text{PMo}_6\text{W}_6\text{O}_{40}^{3-}$ is an effective heteropolyanion.

Recently, researchers at Catalytica proposed a new technology for ethylene oxidation (368). Typical compositions are aqueous *ca.* 0.1 mM Pd^{2+} , 5–25 mM Cl^- , and *ca.* 0.30 M $\text{Na}_y\text{H}_{(3+x-y)}\text{PV}_x\text{Mo}_{12-x}\text{O}_{40}$ (preferably $x = 2\text{--}3$). The Pd^{2+} and chloride concentrations are only 1/100 those in the ordinary Wacker system. The solutions at pH 0–1 result in high reaction rates and stability of Pd^{2+} , as shown in Fig. 65. The stability of Pd^{2+} is further improved by the presence of chloride ion in a concentration of about 0.01 M. In this system, the phosphomolybdate serves two functions in the Pd^0 reoxidation: (1) It solubilizes high concentrations of V^{5+} in aqueous solution and (2) it accelerates the reoxidation of V^{4+} by dioxygen. Kinetics (the reaction is first-order in Pd^{2+} and in ethylene concentrations and zero-order in V^{5+} concentration) shows that the oxidation of ethylene to produce acetaldehyde is rate-determining.

Izumi *et al.* (369) found that Keggin-type heteropolyanions containing Mo or V show a promoting effect in the reductive carbonylation of nitrobenzene by PdCl_2 to form methyl *N*-phenylcarbamate in the presence of methanol (Eq. 44):



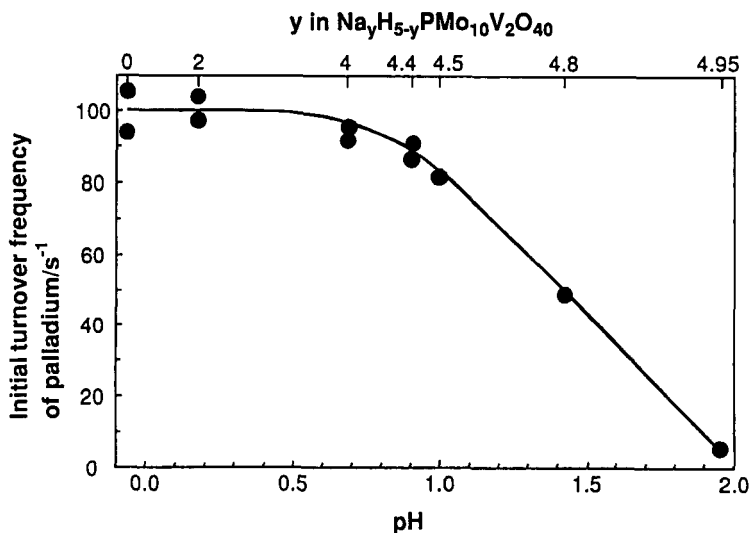


FIG. 65. Dependence of turnover frequency of palladium on pH. Ethylene, 150 psi; $\text{Na}_y\text{H}_{5-y}\text{PMo}_{10}\text{V}_2\text{O}_{40}$, 0.30 M; $\text{Pd}(\text{OAc})_2$, 0.10 mM; reaction temperature, 393 K. (From Ref. 368.)

Figure 66 shows the catalytic activities of $\text{H}_{3+x}\text{PMo}_{12-x}\text{V}_x\text{O}_{40}$ -modified PdCl_2 and the highest reduction potentials of the heteropolyanions. The more reducible heteropolyacids show greater promoting effects, and the highest activity was

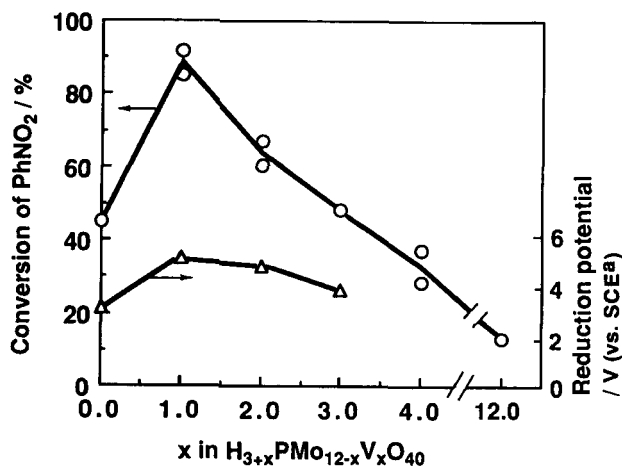


FIG. 66. Catalytic activities of $\text{H}_{3+x}\text{PMo}_{12-x}\text{V}_x\text{O}_{40}$ -modified PdCl_2 and the maximum reduction potential of heteropolyacids: PhNO_2 , 0.01 mol; CO , 41 atm; reaction time, 3 h; reaction temperature, 423 K; 12-vanadophosphoric acid, $\text{Li}_2\text{H}_5\text{PV}_{12}\text{O}_{38}$ · SCE = saturated calomel electrode. (From Ref. 369.)

TABLE XXXIII
Vapor-Phase Carbonylation of Methanol or Dimethyl Ether to Methyl Acetate Catalyzed by Metal-Exchanged $H_3PW_{12}O_{40}$ Supported on SiO_2 (498 K) (from Ref. 370)

Catalyst	Product yield (%)		
	MeOH	DME	MeC(O)OMe
IrPW ₁₂ O ₄₀	8	52	40
RhPW ₁₂ O ₄₀	17	49	34
HPdPW ₁₂ O ₄₀	0	92	8
HMnPW ₁₂ O ₄₀	0	96	4
HCoPW ₁₂ O ₄₀	5	92	3
HNiPW ₁₂ O ₄₀	7	90	3
FePW ₁₂ O ₄₀	7	92	1

obtained for $H_4PMo_{11}VO_{40}$. It is proposed that the rate enhancement is brought about by the coordination of Pd^{2+} on partially reduced heteropolyanion, which is regarded as a macroligand.

Rh- or Ir-exchanged heteropolyacids supported on SiO_2 catalyze vapor-phase carbonylation of methanol or dimethyl ether to give methyl acetate at 498 K and 1 atm (370). As shown in Table XXXIII, with $RhPW_{12}O_{40}/SiO_2$, the yield of methyl acetate is 44%. At this temperature, the yield of methyl acetate dropped rapidly to <1% during 6 h of reaction time accompanied by increases in the yields of dimethyl ether, methanol, and hydrocarbons.

A $RhCl(Ph_3P)_3$ catalyst modified by $Li_4SiW_{12}O_{40}$ shows sterically controlled shape selectivity in homogeneous hydrogenation of olefins (371). The presence of $SiW_{12}O_{40}^{4-}$ retards the reduction of sterically more crowded 1,2- or 1,1-disubstituted ethylene, although the overall catalytic activity for hydrogenation is lower. Probably $SiW_{12}O_{40}^{4-}$ exists in close proximity to the coordination sphere of the Rh complex and hinders the access of bulky olefins.

2. Heteropolyanion-Supported Metals

Heteropolyanion-supported metals are not simple combinations as described above, but instead are complexes of heteropolyanions with organometallic compounds. Siedle *et al.* (372) have shown that $[L_2Rh(CO)(CH_3CN)]_4[SiW_{12}O_{40}]$, or the 16-electron rhodium complex in $[L_3Rh(CO)]_4[SiW_{12}O_{40}]$, catalyzes olefin hydroformylations when suspended in toluene ($L = PPh_3$) as a solid catalyst. However, EXAFS data show that the Rh atom was not bound directly to the polyoxoanion. This result is reasonable because the classical heteropolyanions such as $SiW_{12}O_{40}^{4-}$ [$(SiO_4)^{4-}(W_{12}O_{36})^0$] have low surface charge densities or basicities (in fact, they are ClO_4^- -like) and cannot coordinate with cations such as $(C_5Me_5)Rh^{2+}$ or $CpTi^{3+}$. Therefore, the organometallic cations need to be

supported on (or bound to) reduced heteropolyanions or more negative polyoxoanions such as $\text{SiW}_6\text{M}_3\text{O}_{40}^{7-}$ and $\text{P}_2\text{W}_{15}\text{M}_3\text{O}_{62}^{9-}$ ($\text{M} = \text{V}^{5+}, \text{Nb}^{5+}$). The latter has three full units of negative surface charge that enable tight and covalent bonding of transition metals. Finke *et al.* (376) synthesized highly negative $\text{P}_2\text{W}_{15}\text{Nb}_3\text{O}_{62}^{9-}$ having a high negative surface charge density. They demonstrated that there is direct bonding in the $\text{P}_2\text{W}_{15}\text{Nb}_3\text{O}_{62}^{9-}$ -supported Ir catalyst, $[(n\text{-C}_4\text{H}_9)_4\text{N}]_5\text{Na}_3[(1,5\text{-COD})\text{Ir} \cdot \text{P}_2\text{W}_{15}\text{Nb}_3\text{O}_{62}]$ (377), and that this is active for both hydrogenation (373) and oxygenation (374) of cyclohexene. The turnover frequency was found to be 2.9 h^{-1} at 311 K in CH_2Cl_2 , which is 100-fold greater than that observed with the parent compound, $[(1,5\text{-COD})\text{IrCl}]_2$.

C. METAL-HETEROPOLY BIFUNCTIONAL CATALYSTS

$\text{Pd}_{1.5}\text{PW}_{12}\text{O}_{40}$ supported on SiO_2 catalyzes the skeletal isomerization of C_5 and C_6 paraffins (378–380). The presence of H_2 is necessary to maintain the high activity in the stationary state. This requirement indicates the bifunctional character of the catalysis, with protons being generated by the reduction of Pd^{2+} , as shown in Eq. (45).



This is the same mechanism as that for the generation of H^+ with $\text{Ag}_3\text{PW}_{12}\text{O}_{40}$ (Section III).

However, $\text{Pd}_{1.5}\text{PW}_{12}\text{O}_{40}$ is active for esterification and MTBE synthesis even in the absence of H_2 (378). Therefore, it is concluded that this catalyst is not as simple as $\text{Ag}_3\text{PW}_{12}\text{O}_{40}$. The catalytic activity of $\text{Pd}_x\text{H}_{3-2x}\text{PW}_{12}\text{O}_{40}/\text{SiO}_2$ for hexane isomerization is plotted as a function of x in Fig. 67. The addition of a

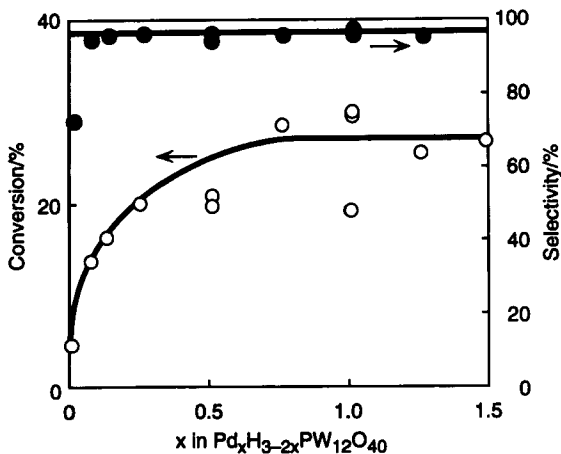


FIG. 67. Effect of Pd content on activities for isomerization of hexane catalyzed by $\text{Pd}_x\text{H}_{3-2x}\text{PW}_{12}\text{O}_{40}$. (From Ref. 378.)

small amount of Pd ($x = 0.05$) greatly enhances the activity, but further increases in x improve the activity only slightly. The combination of Pd and the heteropolyacid is effective for the isomerization of paraffins, as heteropolyacids are very effective components in the bifunctional catalysts.

The combination of Pt or Pd with $\text{Cs}_{2.5}\text{H}_{0.5}\text{PW}_{12}\text{O}_{40}$ (Cs2.5) is also very effective for the isomerization of *n*-butane to isobutane (381). The reaction rate and selectivity for conversion to isobutane are summarized in Table XXXIV (381, 382). The activity in the presence of H_2 changed little with time. Pt- and Pd-Cs2.5 show very high selectivities (94–96%) relative to those of $\text{Pt}/\text{SO}_4^{2-}/\text{ZrO}_2$ (47%) and Pt/HZSM-5 (34%), whereas the activities of Pt- and Pd-Cs2.5 for the formation of isobutane are comparable to those of Pt/HZSM-5 and $\text{Pt}/\text{SO}_4^{2-}/\text{ZrO}_2$. Pt-Cs2.5 catalyzes the reaction even at 473 K and 0.05 atm of H_2 .

The important roles of H_2 and Pt are demonstrated in Fig. 68, in which the conversions for Pt-Cs2.5(A) and Cs2.5 are compared. It is clear that Pt and H_2 enhance the activity and selectivity. In the absence of H_2 , the initial activity of Pt-Cs2.5 is high, but the stationary-state conversion (at 5 h) is very low. H_2 suppresses the deactivation by the hydrogenation of coke or coke precursors, resulting in a high steady-state activity.

The high selectivity to isobutane observed with Pt-Cs2.5 is brought about by the unique roles of protons, which greatly suppress hydrogenolysis (382). When

TABLE XXXIV

Activity and Selectivity for Skeletal Isomerization of *n*-Butane in the Presence of H_2 and Metal-Promoted Catalysts at 573 K (381, 382)

Catalyst ^a	Conversion (%)	$10^8 \times \text{Rate}^b$	Selectivity ^c (mol%)					
			<i>i</i> -C4	C1	C2	C3	C4=	C5
In the presence of 0.5 atm of H_2								
Pt-Cs2.5	25 ^d	7.9	93.9	1.4	2.4	1.8	0	0.5
Pd-Cs2.5	34 ^d	10.9	95.6	0.5	0.5	2.0	0	1.4
Pt- $\text{SO}_4^{2-}/\text{ZrO}_2$	65 ^d	10.4	47.3	6.0	11.6	30.3	0	4.8
Pt-H-ZSM-5	51 ^e	12.0	34.0	18.8	24.9	21.4	0	0.9
In the presence of 0.05 atm of H_2								
Pt-Cs2.5	20.5 ^d	6.2	88.3	0.3	0.5	5.8	0.7	4.4
Pd-Cs2.5	12.9 ^d	3.4	78.4	0.3	0.4	11.3	1.8	7.8
Pt- $\text{SO}_4^{2-}/\text{ZrO}_2$	4.8 ^d	1.2	72.6	1.0	2.3	16.6	0	7.5
Pt-H-ZSM-5	70.4 ^e	8.8	16.4	3.9	6.5	66.8	0	6.4

^a Cs_{2.5} indicates $\text{Cs}_{2.5}\text{H}_{0.5}\text{PW}_{12}\text{O}_{40}$. ^b The rate for isobutane formation: $\text{mol g}^{-1} \text{s}^{-1}$. ^c *i*-C4, C1, C2, C3, C4=, and C5 indicate isobutane, methane, ethane, propane, butenes, and pentanes. ^d $M/F = 41 \text{ g h mol}^{-1}$. ^e $M/F = 18 \text{ g h mol}^{-1}$, where M is the catalyst mass and F is the total flow rate.

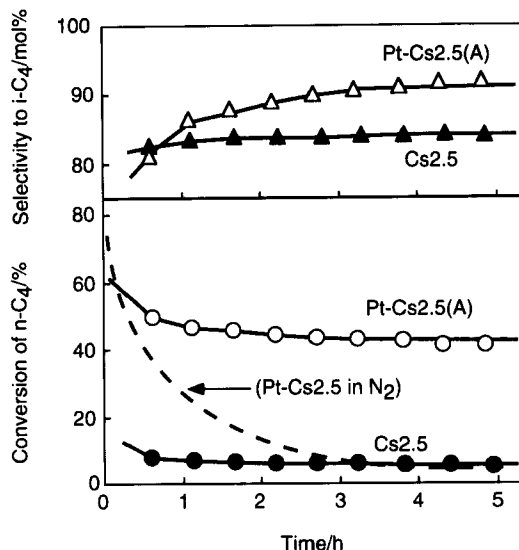
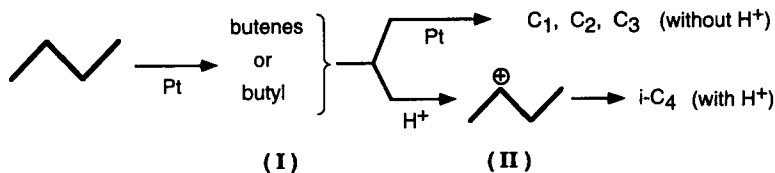


FIG. 68. Time course of *n*-butane isomerization catalyzed by 1% Pt-Cs_{2.5}H_{0.5}PW₁₂O₄₀ (○, △) and Cs_{2.5}H_{0.5}PW₁₂O₄₀ (●, ▲) at 573 K. *n*-Butane: H₂: N₂ = 0.05:0.5:0.45 (*M*). 1% Pt-Cs_{2.5}(A) was prepared from H₂PtCl₆. (From Ref. 382.)

a small amount of H₃PW₁₂O₄₀ was impregnated onto Pt-Cs₃PW₁₂O₄₀ (which exhibited high activity for hydrogenolysis), the isomerization of *n*-butane proceeded very selectively, as the hydrogenolysis activity of Pt-Cs₃PW₁₂O₄₀ was almost suppressed. Scheme 10 is tentatively proposed (382). In the absence of protons, the intermediates (I) react with hydrogen to cause hydrogenolysis, whereas in the presence of protons, the intermediates (I) interact with protons on Pt or at the interface between Pt and Cs_{2.5} to form carbenium ions (II) which are the intermediates for the skeletal isomerization.

D. INTERCALATED POLYANIONS

An isopoly cation, [Al₁₃O₄(OH)₂₄(OH₂)₁₂]⁷⁺, has the Keggin structure and can be intercalated into the layer structure of montmorillonite clay,



SCHEME 10

$[\text{Si}_4(\text{Al}_{5/3}\text{Mg}_{1/2})(\text{OH})_2\text{O}_{10}]^{1/3-} \cdot \text{Na}_{1/3}^+$. By calcination, microporous solid catalysts with pore sizes of about 8 Å have been prepared (383). This catalyst is active for cumene cracking (384), conversion of methanol (385), and alkylation (386); and it can be used as a support for metal catalysts (387, 388). Ru supported on Al_2O_3 intercalating montmorillonite is a catalyst for the production of $\text{C}_6\text{-C}_{12}$ hydrocarbons in CO hydrogenation (388).

Heteropoly anions with Keggin structures are effective reagents for the pillaring of layered double hydroxide (389, 390). $[\text{Zn}_2\text{Al}(\text{OH})_6]\text{NO}_3 \cdot 2\text{H}_2\text{O}$ (abbreviated as Zn_2Al) undergoes facile and complete intercalation by an ion-exchange reaction with $\text{H}_2\text{W}_{12}\text{O}_{40}^{6-}$, $\text{SiW}_{11}\text{O}_{39}^{8-}$, or $\text{SiV}_3\text{W}_9\text{O}_{40}^{7-}$. On the other hand, no reaction is observed for Keggin anions such as $\text{PW}_{12}\text{O}_{40}^{3-}$ and $\text{SiW}_{12}\text{O}_{40}^{4-}$, probably because they have smaller negative charges.

XRD patterns for $\text{Zn}_2\text{Al-SiW}_{11}\text{O}_{39}$ and $\text{Zn}_2\text{Al-SiV}_3\text{W}_9\text{O}_{40}$ include several 001 harmonics corresponding to a basal spacing at 14.5 Å. If the thickness of the double hydroxide layer is taken to be 4.7 Å, the gallery height is 9.8 Å, in accordance with the expected size of the Keggin anions.

IR spectra of $\text{Zn}_2\text{Al-SiV}_3\text{W}_9\text{O}_{40}$ confirm that the Keggin structure of $\text{SiV}_3\text{W}_9\text{O}_{40}^{7-}$ is retained. The surface areas of $\text{Zn}_2\text{Al-SiW}_{11}\text{O}_{39}$ and $\text{Zn}_2\text{Al-SiV}_3\text{W}_9\text{O}_{40}$ were found to be 98 and 113 $\text{m}^2 \text{g}^{-1}$, respectively, whereas that of Zn_2Al was only 26 $\text{m}^2 \text{g}^{-1}$. Besides heteropolyanions, isopolyanions can be intercalated into the layer of various clays. $\text{Zn}_2\text{Al-V}_{10}\text{O}_{28}$ has been synthesized from $[\text{Zn}_2\text{Al}(\text{OH})_6]\text{Cl} \cdot 2\text{H}_2\text{O}$ and $[\text{NH}_4]_6(\text{V}_{10}\text{O}_{28}) \cdot 6\text{H}_2\text{O}$ (391).

It has been pointed out that these pillared intercalates are intrinsically difficult to synthesize in highly crystalline form because the layered hosts are basic, whereas most heteropolyacids are acidic and tend to decompose. Narita *et al.* (392) tried direct synthesis of a heteropolyanion-pillared layered double hydroxide by a coprecipitation reaction of Zn^{2+} and Al^{3+} ions in the presence of a moderately acidic lacunary Keggin anion, $\alpha\text{-SiW}_{11}\text{O}_{39}^{8-}$. XRD of the product showed a basal spacing of 14.6 Å, which corresponds to a gallery height of 9.9 Å. The surface area was found to be 97 $\text{m}^2 \text{g}^{-1}$, which is three times that of the layered double hydroxide.

Drezdron (393) reported a new route to the synthesis of pillared clay intercalates based on the ion-exchange reaction of isopolyanions with a clay that had been intercalated by a large organic anion. By this method, $\text{Mg}_{12}\text{Al}_6(\text{OH})_{36}(\text{Mo}_7\text{O}_{24}) \cdot x\text{H}_2\text{O}$ and $\text{Mg}_{12}\text{Al}_6(\text{OH})_{36}(\text{V}_{10}\text{O}_{28}) \cdot x\text{H}_2\text{O}$ were synthesized; they were claimed to be stable at temperatures up to 773 K. Analogous reaction of Mg_3Al -adipate with the lacunary Keggin species $\text{SiW}_{11}\text{O}_{39}^{8-}$ yielded the corresponding pillared product as a single crystalline phase (basal plane spacing = 14.8 Å), having a surface area of 155 $\text{m}^2 \text{g}^{-1}$ (394).

The intercalated compounds of hydrotalcite $[\text{Mg}_{23.3}\text{Al}_{10}(\text{OH})_{66.6}]$ with $\text{Mo}_7\text{O}_{24}^{6-}$ or $\text{W}_{12}\text{O}_{41}^{10-}$ catalyze the shape-selective epoxidation of olefins; epoxidation of 2-hexene was favored over that of cyclohexene (395).

XII. Photocatalysis and Electrocatalysis

Various polyoxometalates can be reduced electrochemically and reversibly by several electrons at modest potentials (Section VII.A), and these properties are exploited in photocatalysis and electrocatalysis. In both cases, redox properties of heteropolyanions (Fig. 49) and the organic reactants (Table XXXV) are the principal properties that control the catalytic performance. The selection of the electrode is also important in electrocatalysis. Photocatalysis by heteropolyanions has been reported extensively, but there are only a few reports of electrocatalysis by these compounds.

TABLE XXXV
Ranges of Redox Potential of Organic Compounds

	Ranges of electric potential, V (vs. SCE ^a)
Reduction	
Azo compounds	+0.05 ~ -0.1
Aldehydes	-1.5 ~ -2.0
Activated esters	-1.0 ~ -2.0
Activated alkenes	-1.5 ~ -3.5
Diazo compounds	-0.3 ~ -1.0
Sulfones	-1.5 ~ -2.5
Nitro compounds	-0.5 ~ -1.5
Halogenated compounds	-0.3 ~ -3.0
Aromatics	-1.5 ~ -3.0
Hydroxyl amines	-0.5 ~ -1.5
Oxidation	
Azo compounds	+1.5 ~ +2.0
Amides	+1.5 ~ +2.5
Alcohols	+1.5 ~ +2.0
Carboxylates	+2.0 ~ +2.5
Ketones	+1.0 ~ +2.0
Diazo compounds	+1.0 ~ +2.0
Sulfides	+0.5 ~ +1.5
Phenols	+0.5 ~ +1.0
Aromatic amines	+1.0 ~ +2.5
Aromatic hydrocarbons	+1.0 ~ +2.5

^a Saturated calomel electrode. Source: D. K. Kyriacou, *Basics of Electroorganic Synthesis*, John Wiley & Sons, New York (1981).

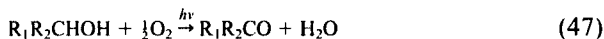
A. PHOTOCATALYSIS

Reports of the photosensitivity of polyoxometalates appeared as early as 1916 (396). Early systematic work on photocatalysis was done by Yamase *et al.* (397–402). For example, methanol is photooxidized to give formaldehyde in the presence of $\text{Mo}_7\text{O}_{24}^{6-}$ according to Eq. (46).



This reaction involves electron transfer from water to $\text{Mo}_7\text{O}_{24}^{6-}$ to form $\text{Mo}_7\text{O}_{23}\text{OH}^{6-}$ and OH radicals.

Papaconstantinou *et al.* (403, 404) applied heteropolyacids to the photooxidation of alcohols and indicated the potential importance of such chemistry [Eq. (47)].



1. Activity of Isopoly and Heteropoly Catalysts

It is known that molecules in photoexcited states are stronger oxidants and reductants than those in the ground states. The potentials of the excited states of polyoxometalates can be estimated by adding the energy of 0,0-transitions to the ground-state reduction potentials (257, 405).

For example, the approximate 0,0-transition energies in acetonitrile for $\text{W}_{10}\text{O}_{32}^{4-}$, $\text{PW}_{12}\text{O}_{40}^{3-}$, $\text{PMo}_{12}\text{O}_{40}^{3-}$, $\text{V}_{10}\text{O}_{28}^{6-}$, and $\text{V}_{13}\text{O}_{34}^{3-}$ are 2.52, 2.75, 2.29, 2.01, and 1.97 V [vs. saturated calomel electrode (SCE)], respectively, and the 0,0-transition energies are roughly one half the ground-state potentials (257). The ground-state redox potentials of these five polyoxoanions are -1.21 , -0.61 , 0.10 , -0.48 , and 0.39 V (vs. SCE), respectively. From these data, the potentials of the excited states of $\text{Q}_4\text{W}_{10}\text{O}_{32}$, $\text{Q}_3\text{PW}_{12}\text{O}_{40}$, $\text{Q}_3\text{PMo}_{12}\text{O}_{40}^{3-}$, $\text{Q}_3\text{H}_3\text{V}_{10}\text{O}_{28}^{6-}$, and $\text{Q}_3\text{V}_{13}\text{O}_{34}$ (Q is tetra-*n*-butylammonium) are estimated to be approximately 1.55, 2.39, 2.43, 1.77, and 2.60 V (vs. SCE), respectively.

However, the emission from the excited states of polyoxometalates is usually so weak that it is difficult to determine the 0,0-transition energies exactly (257).

Polyoxometalates are classified into three groups in terms of reactivity (257, 405):

1. Polyoxometalates such as $\text{Nb}_6\text{O}_{19}^{8-}$ and $\text{Ta}_6\text{O}_{19}^{8-}$, which are hardly photoreduced.
2. Polyoxometalates of Mo and V, the oxidized forms of which are appreciably photoreduced but the reduced forms are too stable to be reoxidized.
3. Polyoxometalates of W, which undergo both photoreduction and facile reoxidation.

Therefore, tungstates are efficient oxidizing photocatalysts under UV irradiation and near-visible light. $\text{PW}_{12}\text{O}_{40}^{3-}$ and protonated $\text{W}_{10}\text{O}_{32}^{4-}$ are reported to promote radical oxidation. On the other hand, unprotonated $\text{W}_{10}\text{O}_{32}^{4-}$ promotes the radical-radical reaction.

2. Reactions Catalyzed by Heteropoly Compounds

Table XXXVI is a list of some catalytic photochemical redox transformation of organic reactants by (Q or H) $_3\text{PW}_{12}\text{O}_{40}$. In the presence of UV light, $\text{Q}_3\text{PW}_{12}\text{O}_{40}$ reacts with paraffins, arenes, alcohols, alkyl halides, ketones, nitriles, thioethers, and water. Under either anaerobic or aerobic conditions, decarboxylation, dehydrogenation, dimerization, polymerization, oxidation, and acylation takes place.

Alcohols such as methanol, 2-propanol, and benzhydrol are cleanly oxidized to the corresponding carbonyl compounds upon photoexcitation with $\text{Na}_3\text{PW}_{12}\text{O}_{40}$ in water or with $(n\text{-Pr}_4\text{N})_3\text{PW}_{12}\text{O}_{40}$ in CH_3CN (406). The quantum yields appear to be governed by the oxidation potential of the alcohol, the availability of α -hydrogens, and the tightness of complexation with the photocatalyst: The reactivity order is primary alcohol > secondary alcohol \gg tertiary alcohol.

Noteworthy features of photoreactions of paraffins are the following (257):

1. The product distributions are affected in some cases by the presence of a hydrogen evolution catalyst such as Pt(0).
2. The secondary reactions of initial products are sometimes significant and informative.
3. Unactivated C—H bonds can be selectively replaced with C—C bonds in some cases.
4. The addition of acids increases the quantum yield.

The heteropolytungstates, which in general have formal redox potentials of ground states that are less negative than -1.0 V vs. $\text{Ag}/\text{AgNO}_3(\text{CH}_3\text{CN})$ [such as $\alpha\text{-PW}_{12}\text{O}_{40}^{3-}$ (-0.63 to -0.67 V) and $\alpha\text{-P}_2\text{W}_{18}\text{O}_{62}^{6-}$ (-0.78 V)], photo-dehydrogenate paraffins in high selectivity to give the most substituted olefins under anaerobic conditions. For example, 2,3-dimethylbutane was dehydrogenated to give 2,3-dimethyl-2-butene with >80% selectivity (407). The major influence on the regioselectivity is the stability of alkyl cations generated from the intermediate radicals.

Photoreactions of *p*-xylene are interesting from the standpoint of C—H activation (408). Figure 69 shows the time course of the anaerobic photoreaction of *p*-xylene with $(\text{TBA})_3\text{PW}_{12}\text{O}_{40}$ in the presence or absence of PtO_2 . In the presence of an equimolar amount of PtO_2 , ca. 4% of the *p*-xylene was selectively converted to 1,2-di-*p*-tolylethane after 30 h of irradiation. No trimers or higher oligomers were detected. It is suggested that the reaction proceeds

TABLE XXXVI

Photocatalytic Transformation of Organic Reactants in the Presence of Heteropoly Compounds

Reaction	Catalyst	Ref.
H ₂ evolution	P ₂ W ₁₈ O ₆₂ ⁶⁻ XM ₁₂ O ₄₀ ⁿ⁻ (X = P, Si; M = Mo, W)	403, 405, 410
2-PrOH $\xrightarrow{\text{O}_2}$ MeCN	P ₂ W ₁₈ O ₆₂ ⁶⁻ PW ₁₂ O ₄₀ ³⁻	404
RR'CHOH \longrightarrow RR'C=O	MW ₁₂ O ₄₀ ⁿ⁻ (M = P, Co, Fe, Si, H ₂)	406
	P ₂ W ₁₈ O ₆₂ ⁶⁻ PW ₁₂ O ₄₀ ³⁻	407
	H ₃ PW ₁₂ O ₄₀ (+ PtO ₂) (TBA) ₃ PW ₁₂ O ₄₀	408
	P ₂ W ₁₈ O ₆₂ ⁽⁶⁺ⁿ⁾⁻ PW ₁₂ O ₄₀ ⁽³⁺ⁿ⁾⁻	409
CH ₄ \longrightarrow CO, CO ₂ , H ₂ O	SiW ₁₂ O ₄₀ ⁴⁻ /TiO ₂	a
	H ₃ PW ₁₂ O ₄₀	b
	H ₃ PW ₁₂ O ₄₀	b
	H ₃ PW ₁₂ O ₄₀ (TBA) ₃ PW ₁₂ O ₄₀	c
CH ₃ OH \longrightarrow HCHO	XW ₁₂ O ₄₀ ⁿ⁻ (X = B, P) PTi ₂ W ₁₀ O ₄₀ ⁷⁻	d
C ₂ H ₅ OH \longrightarrow CH ₃ CHO	PW _{12-x} V _x O ₄₀ ^{(3+x)-}	e
CO ₂ + 4MeOH \longrightarrow CH ₄ + 4HCHO + 2H ₂ O	PTi ₂ W ₁₀ O ₄₀ ⁷⁻	f
	(TBA) ₃ PW ₁₂ O ₄₀	g
	(TBA) ₅ PW ₁₁ CuO ₃₉	h

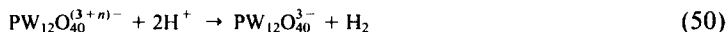
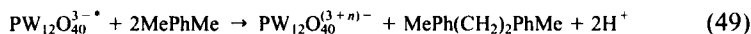
continued

TABLE XXXVI—Continued

Reaction	Catalyst	Ref.
$\text{S} \longrightarrow \text{S-OH}$	(TBA) ₃ PMo ₁₂ O ₄₀	ⁱ
$\text{CCl}_4 + 2\text{-PrOH} \longrightarrow \text{CHCl}_3 + \text{C}_2\text{Cl}_6 + (\text{CH}_3)_2\text{CO}$	H ₃ PW ₁₂ O ₄₀	^h

^a M. Grätz *et al.*, *J. Phys. Chem.* **93**, 4128 (1989). ^b R. F. Renneke *et al.*, *J. Am. Chem. Soc.* **108**, 3528 (1986). ^c R. F. Renneke *et al.*, *Angew. Chem. Int. Ed. Eng.* **27**, 1526 (1988). ^d T. Yamase *et al.*, *J. Chem. Soc. Dalton Trans.*, 1669 (1986). ^e E. S. Ganolina *et al.*, *Russ. J. Inorg. Chem.* **29**, 51 (1984). ^f T. Yamase *et al.*, *Inorg. Chim. Acta* **172**, 131 (1990). ^g R. C. Chambers *et al.*, *J. Am. Chem. Soc.* **112**, 8427 (1990). ^h D. Sattari *et al.*, *J. Chem. Soc. Chem. Commun.* **1990**, 634. ⁱ R. C. Chambers *et al.*, *Inorg. Chem.* **20**, 2776 (1991).

according to Eqs. (48)–(50), and the rate-determining step is associated with Eq. (50).



When the photoreaction was carried out under aerobic conditions, different products, such as *p*-tolualdehyde, *p*-toluic acid, and 4-methylbenzyl alcohol, were obtained in total yields of about 25%. It is probable in this case that benzyl

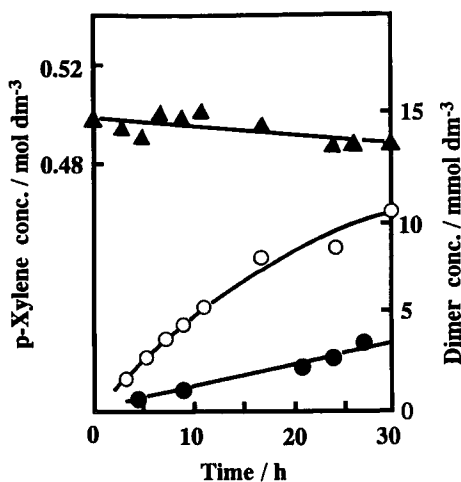
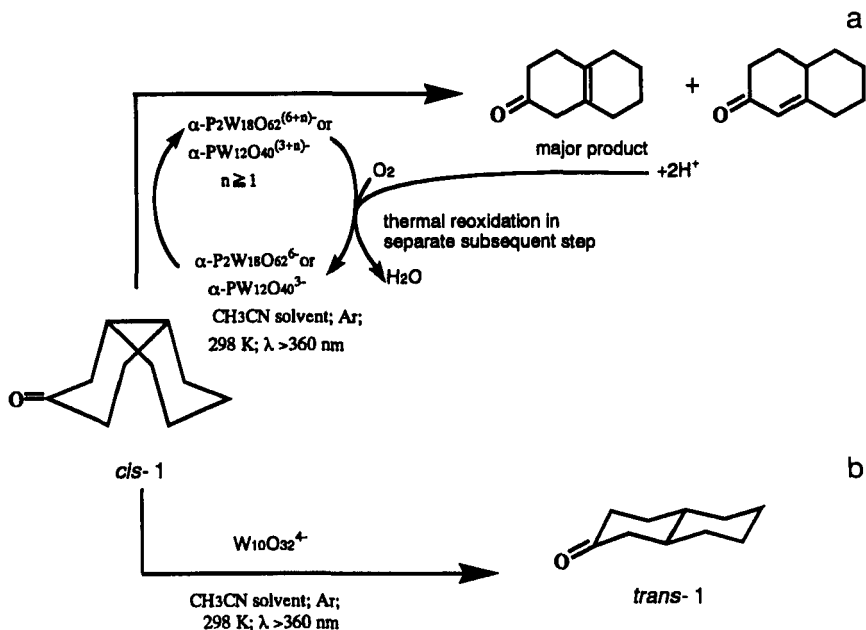


FIG. 69. Anaerobic catalytic photoreaction of *p*-xylene. (▲) *p*-Xylene; (● and ○) (+PtO₂), 1,2-di-*p*-tolylethane. (From Ref. 408.)



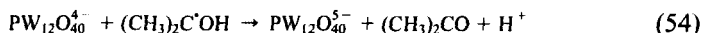
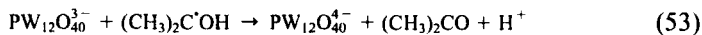
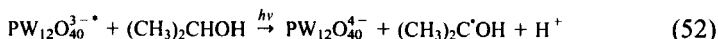
SCHEME 11

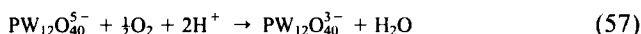
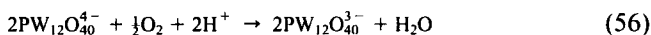
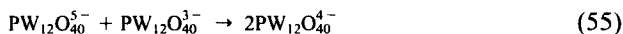
radicals react with dioxygen to form ArCH_2O_2 , giving rise to a classical autooxidation mechanism.

$\alpha\text{-P}_2\text{W}_{18}\text{O}_{62}$ and $\alpha\text{-PW}_{12}\text{O}_{40}$ have selectivities different from that of $\text{W}_{10}\text{O}_{32}^{4-}$ for the transformation of unactivated C—H bonds in ketone (409). The irradiation of the heteropolytungstates selectively transforms *cis*-2-decalone into octalones with the nonthermodynamic isomer, $\Delta^{9,10}$ -2-octalone, in comparable or greater quantity than the conventional thermodynamic isomer, $\Delta^{1,9}$ -2-octalone (Scheme 11a). In contrast, $\text{W}_{10}\text{O}_{32}^{4-}$ transforms *cis*-2-decalone into *trans*-2-decalone (Scheme 11b) (409).

3. Reaction Mechanism

The reaction mechanism shown in Eqs. (51)–(57) was proposed for photooxidation of isopropyl alcohol to acetone under irradiation of $\text{PW}_{12}\text{O}_{40}^{3-}$:

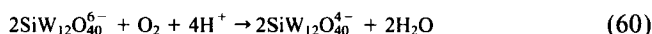
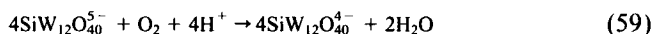
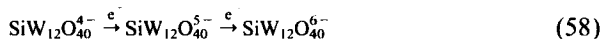




Photoexcitation involves oxygen-to-metal charge transfer in heteropolyanions [(Eq. (51)]. The photoexcited heteropolyanions react with organic species, accompanied by formation of H^\bullet and/or electron transfer, resulting in the reduction of heteropolyanions and the oxidation of organic reactants [Eq. (52)]. The reduced heteropolyanions are reoxidized by dioxygen according to Eqs. (56) and (57). The mechanism is supported by the fact that in the absence of O_2 the system leads to the generation of H_2 by reduction of protons. This process is accelerated by the addition of $\text{Pt}(0)$ as a catalyst for hydrogen evolution (410).

B. ELECTROCATALYSIS

Electrochemical reduction of protons to form H_2 in an acidic aqueous solution can be catalyzed by $\text{SiW}_{12}\text{O}_{40}$ in the presence of glassy carbon, Pt, Si, or TiO_2 as an electrode (411–414). Reduction of O_2 is also catalyzed by $\text{SiW}_{12}\text{O}_{40}$ immobilized in polyaniline on a glassy carbon electrode (415). The following mechanism is proposed:



The idea is supported by the fact that $2e^-$ -reduced $\text{SiW}_{12}\text{O}_{40}^{4-}$ catalyzes the reduction of O_2 (410).

Iron-substituted heteropolytungstates such as $\text{XW}_{11}\text{Fe}^{3+}\text{O}_{39}^{n-}$ (P, As, Si, Ge) are the catalysts for the electroreduction of nitrite to ammonia (Table XXXVII)

TABLE XXXVII

Electrocatalytic Reduction of Nitrite to Ammonia in the Presence of Iron-Substituted Heteropolytungstates, $\text{XW}_{11}\text{Fe}^{3+}\text{O}_{39}^{n-}$ (416, 417)

X^b	Reduction to NH_3^c	Efficiency ^d
Si	21	35
Ge	29	22
P	31	49
As	36	35

^a Supporting electrolyte, 0.1 M $\text{CH}_3\text{COONa}-\text{CH}_3\text{COOH}$; pH 4. Stirred mercury pool kept at -0.9 V. ^b Heteroatom in the catalysts. ^c Percentage of initial NO_2^- converted to NH_4^+ as determined by ion chromatography. ^d Coulombic efficiency for generation of ammonia.

(416, 417). The pH dependence of the rate of formation of a nitrosyl complex shows that nitrous acid is the reactive intermediate in the reaction when the pH is in the range of 2–8. The catalysts are not deactivated during repeat cycles between their oxidized and reduced states. The catalyzed reduction appears to depend on the ability of the multiply reduced heteropolyanions to deliver electrons to the NO group bound to the iron center.

XIII. Conclusions

Heteropoly compounds are already important industrial catalysts, and more applications are anticipated. Much remains to be done. Future desirable goals of research (5, 6) are all related to the advantageous properties of heteropoly compounds listed in Table I: molecular design of catalysts by control of acid and redox properties; understanding of catalytic processes at the molecular level; use of cluster models of mixed oxide catalysts; application of novel polyanions (complexes with organometallics, synzymes, etc.); and photo- and electrocatalysis. Worthy targets of research are suggested to be the following: design of solid acids stronger than $\text{H}_3\text{PW}_{12}\text{O}_{40}$ and acids having moderate but uniform acid strengths; bifunctional acid–base or acid–redox catalysts; exploitation of the unique properties of assembly of heteropoly compounds (e.g., stereo- and shape-selective reactions in pseudoliquid or controlled pores). Worthy noncatalytic applications may include the use of heteropoly compounds as anti-retroviral active substances (418, 419) and as electronic materials, such as photoresists (420, 421), electrochromics (422, 423), and solid electrolytes (424, 425).

REFERENCES

1. Tsigdinos, G. A., *Top. Curr. Chem.* **76**, 1 (1978).
2. Pope, M. T., "Heteropoly and Isopoly Oxometalates." Springer-Verlag, Berlin, 1983.
3. Pope, M. T., and Müller, A., *Angew. Chem. Int. Ed. Engl.* **30**, 34 (1991); "Polyoxometalates: From Platonic Solids to Anti-Retroviral Activity." (M. T. Pope and A. Müller, Eds.). Kluwer, Dordrecht, 1994.
4. Misono, M., in "Proc. Climax 4th Intern. Conf. Chem. Uses of Molybdenum" (H. F. Barry and P. C. H. Mitchell, Eds.), p. 289. 1982.
5. Misono, M., *Catal. Rev.-Sci. Eng.* **29**, 269 (1987); **30**, 339 (1988).
6. Misono, M., in "Proc. 10th Int. Congr. Catal., Budapest, 1992," p. 69. Elsevier, Amsterdam, and Akademiai Kiado, Budapest, 1993.
7. Ono, Y., in "Perspectives in Catalysis" (J. M. Thomas and K. I. Zamarayev, Eds.), p. 341. Blackwell, London, 1992.
8. Kozhevnikov, I. V., and Matveev, K. I., *Appl. Catal.* **5**, 135 (1983).
9. Izumi, Y., Urabe, K., and Onaka, A., "Zeolite, Clay, and Heteropolyacids in Organic Reactions." Kodansha, Tokyo-VCH, Weinheim, 1992.
10. Kozhevnikov, I. V., in "Acid-Base Catalysis II" (H. Hattori, M. Misono, and Y. Ono, Eds.) (Stud. Surf. Sci. Catal., Vol. 90), p. 21. Kodansha, Tokyo-Elsevier, Amsterdam, 1994; *Catal. Rev. Sci. Eng.* **37**, 311 (1995).

11. Killefer, D. H., and Linz, A., "Molybdenum Compounds," p. 87. Interscience, New York, 1952.
12. Misono, M., and Nojiri, N., *Appl. Catal.* **64**, 1 (1990); Nojiri, N., and Misono, M., *ibid.* **93**, 103 (1993).
13. Misono, M., in "Future Opportunities in Catalytic and Engineering Technology" (M. Misono, Y. Moro-oka, S. Kimura, Eds.), p. 13. Elsevier, Amsterdam, 1990.
14. Jeanin, Y., and Fournier, M., *Pure Appl. Chem.* **59**, 1529 (1987).
15. Leigh, G. J., Ed., "Nomenclature of Inorganic Chemistry, Recommendations 1990." Blackwell, Oxford, 1990.
16. IUPAC, "Nomenclature of Inorganic Chemistry (1970 Rules), 2nd Ed." Butterworths, London, 1971.
17. Misono, M., Sakata, K., Yoneda, Y., and Lee, W. Y., in "Proc. 7th Int. Congr. Catal., Tokyo, 1980," p. 1047. Kodansha, Tokyo, Elsevier, Amsterdam, 1981.
18. (a) Jeannin, Y., Herve, G., and Proust, A., *Inorg. Chim. Acta* **189**, 319 (1992); (b) Weakly, T. J. R., *Struct. Bonding* **18**, 131 (1974).
19. Keggins, J. F., *Nature (London)* **131**, 908 (1933); *Proc. R. Soc. London, Ser. A* **144**, 75 (1934).
20. Misono, M., and Hashimoto, M., *Shokubai (Catalyst)* **34**, 152 (1992).
21. Brown, G. M., Noe-Spirlet, M. R., Busing, W. R., and Levy, H. A., *Acta Crystallogr., Ser. B* **33**, 1038 (1977).
22. Spitsyn, V. I., Kazansky, L. P., and Torchenkova, E. A., *Sov. Sci. Rev. B., Chem. Rev.* **3**, 111 (1981).
23. Souchay, P., *Bull. Soc. Chim., France* **18**, 365 (1951).
24. Yamamura, K., and Sasaki, Y., *J. Chem. Soc., Chem. Commun.* **1973**, 648.
25. Matsumoto, K. Y., Kobayashi, A., and Sasaki, Y., *Bull. Chem. Soc. Jpn.* **39**, 3146 (1975).
26. Baker, L. C. W., and Figgis, J. S., *J. Am. Chem. Soc.* **92**, 3794 (1970).
27. Chauveau, F., Doppelt, P., and Lefebvre, J., *J. Chem. Res (S)* **1978**, 130; **1981**, 155.
28. Pettersson, L., Anderson, I., and Ohman, L. O., *Inorg. Chem.* **25**, 4726 (1986).
29. Dawson, B., *Acta Crystallogr.* **6**, 113 (1953).
30. D'Amour, H., *Acta Crystallogr.* **B32**, 729 (1976).
31. Hori, T., Tamada, O., and Himeno, S., *J. Chem. Soc. Dalton Trans.* **1989**, 1491.
32. Chauveau, F., Doppelt, P., and Lefebvre, J., *Inorg. Chem.* **19**, 2803 (1980).
33. Anderson, J. S., *Nature* **140**, 850 (1937).
34. "Crystal Structure of Inorganic Compounds," LB Neue Series, III/7f, Pies/Weiss, p. 200. Springer, Berlin.
35. Spirlet, M. R., and Busing, W. R., *Acta Crystallogr.* **B34**, 907 (1978).
36. Bradley, A. J., and Illingsworth, J. W., *Proc. R. Soc. (London)* **A157**, 113 (1936).
37. Mizuno, N., and Misono, M., *Chem. Lett.* **1987**, 967.
38. Oniani, E. S., Sergienko, V. S., Chuaev, V. F., and Mistryukov, A. E., *Russ. J. Inorg. Chem.* **36**, 1157 (1991).
39. Hashimoto, M., and Misono, M., *Acta Crystallogr.* **C50**, 231 (1994).
40. Attanasio, D., Bonamico, M., Fares, V., Imperatori, P., and Suber, L., *J. Chem. Soc., Dalton Trans.* **1190**, 3221.
41. Prosser-McCartha, C. M., Kadkhodayan, M., Williamson, M. M., Bouchard, D. A., and Hill, C. L., *J. Chem. Soc., Chem. Commun.* **1986**, 1747.
42. Niiyama, H., Saito, Y., and Echigoya, E., in "Proc. 7th Int. Congr. Catal., 1980," p. 1416. Kodansha, Tokyo, Elsevier, Amsterdam, 1981.
43. (a) Gregg, S. J., and Stock, R., *Trans. Faraday Soc.* **53**, 1355 (1957); (b) Gregg, S. J., and Tayyab, M. M., *J. Chem. Soc. Faraday I* **74**, 348 (1978).
44. (a) Taylor, D. B., McMonagle, J. B., and Moffat, J. B., *J. Colloid Interface Sci.* **108**, 2789 (1985); (b) MacMonagle, J. B., and Moffat, J. B., *J. Colloid Interface Sci.* **101**, 479 (1984);

- (c) Moffat, J. B., *J. Mol. Catal.* **52**, 169 (1989); (d) Moffat, J. B., and MacMonagle, J. B., and Taylor, D., *Solid State Ionics* **26**, 101 (1988).
45. Furuta, M., Sakata, K., Misono, M., and Yoneda, Y., *Chem. Lett.* **1979**, 31.
46. (a) Tatematsu, S., Hibi, H., Okuhara, T., and Misono, M., *Chem. Lett.* **1984**, 865; (b) Okuhara, T., Kasai, A., Hayakawa, N., Yoneda, Y., and Misono, M., *J. Catal.* **83**, 121 (1983).
47. Okuhara, T., Nishimura, T., Watanabe, H., Na, K., and Misono, M., in "Acid-Base Catalysis II." p. 419. Kodansha, Tokyo-Elsevier, Amsterdam, 1994.
48. Okuhara, T., Nishimura, T., and Misono, M., *Chem. Lett.* **1995**, 155.
49. Tsigdinos, G. A., *Ind. Eng. Chem. Prod. Res. Dev.* **13**, 267 (1974).
50. Gruttner, B., and Jander, G., in "Handbook of Preparative Inorganic Chemistry," 2nd Ed. (G. Brauer, Ed.), Vol. 2, p. 1716. Academic Press, New York, 1965.
51. Tsigdinos, G. A., in "Heteropoly Compounds. Methodicum Chemicum" (K. Niedenzu and H. Zimmer, Eds.), Vol. 8, Chap. 32. Academic Press, New York, 1976.
52. Fuchs, J., and Flindt, E. P., *Z. Naturforsch Teil B* **34**, 412 (1979).
53. Bailar, J. C., *Inorg. Synth.* **1**, 132 (1939).
54. (a) Hu, H., *J. Biol. Chem.* **43**, 189 (1920); (b) Hall, R. D., *J. Am. Chem. Soc.* **24**, 780 (1907).
55. (a) Souchay, P., "Ions Moireraux Condenses." Masson, Paris, 1969; (b) Izumi, Y., and Otake, M., "Kagaku Sosetsu 34," p. 118. Gakkai Shuppan Senta, 1982.
56. Eguchi, K., Yamazoe, N., and Seiyama, T., *Nippon Kagaku Kaishi* **1981**, 336.
57. Fournier, M., F-Jantou, C., Rabia, C., Herve, G., and Launay, S., *J. Mat. Chem.* **2**, 971 (1992).
58. Rocchiccioli-Deltcheff, C., and Fournier, M., *J. Chem. Soc., Faraday Trans.* **87**, 3913 (1991).
59. Rocchiccioli-Deltcheff, C., *Inorg. Chem.* **22**, 207 (1983).
60. Bondareva, V. M., Sandrushkevich, T. V., Maksimovskaya, R. I., Plyasova, L. M., Ziborov, A. V., Litvak, G. S., and Detusheva, L. G., *Kinet. Catal.* **35**, 114 (1994).
61. (a) Na, K., Okuhara, T., and Misono, M., *J. Chem. Soc. Faraday Trans.* **91**, 375 (1995); (b) Black, J. B., Serwicka, E., Clayden, N. J., Goodenough, J. B., and Scott, J. D., *Polyhedron* **5**, 141 (1986).
62. (a) Rocchiccioli-Deltcheff, C., Thouvent, R., and Franck, R., *Spectrochim. Acta* **32A** 587 (1976); (b) Brown, D. H., *Spectrochim. Acta* **19**, 583 (1963).
63. (a) Hu, C., Hashimoto, M., Okuhara, T., and Misono, M., *J. Catal.* **143**, 437 (1993); (b) Okuhara, T., Hu, C., Hashimoto, M., and Misono, M., *Bull. Chem. Soc. Jpn.* **67**, 1186 (1994).
64. Boesch, F., Brus, B., and Krebs, B., *Acta Crystallogr.* **B30**, 48 (1974).
65. Rocchiccioli, C., Fournier, M., Franck, R., and Thouvenot, R., *Inorg. Chem.* **22**, 207 (1983).
66. Okuhara, T., Hashimoto, T., Hibi, T., and Misono, M., *J. Catal.* **93**, 224 (1985).
67. Rocchiccioli-Deltcheff, C., and Thouvent, R., *J. Chem. Res. (S)* **1977**, 46; (M) **1977**, 546.
68. Rocchiccioli-Deltcheff, C., and Thouvent, R., *Inorg. Chem.* **17**, 1115 (1978).
69. Fournier, M., Thouvenot, R., and Rocchiccioli-Deltcheff, C., *J. Chem. Soc. Faraday* **87**, 349 (1991).
70. Rocchiccioli, C., and Touvenot, R., *Spectrosc. Lett.* **12**(2), 127 (1979).
71. Fukumoto, T., Murata, K., and Ikeda, S., *Anal. Chem.* **56**, 929 (1984).
72. Mioc, U., Colomban, P., and Novak, A., *J. Mol. Struct.* **218**, 123 (1990).
73. Wada, T., *Compt. Rend.* **B263**, 51 (1966).
74. Churaev, V. F., and Spitsyn, V. Y., *Dokl. Akad. Nauk. SSSR* **154**, 908 (1964).
75. Spitsyn, V. I., Chuvaev, V. F., and Bakhchisaritseva, S. A., *Dokl. Akad. Nauk SSSR* **204**, 1403 (1972).
76. Spitsyn, I., Chuvaev, V. F., and Bakhchisaritseva, S. A., *Dokl. Akad. Nauk SSSR* **165**, 1126 (1965).
77. Kanda, Y., Lee, K. Y., Nakata, S., Asaoka, S., and Misono, M., *Chem. Lett.* **1988**, 139.
78. Lee, K. Y., Mizuno, N., Okuhara, T., and Misono, M., *Bull. Chem. Soc. Jpn.* **62**, 1731 (1989).

79. Massart, R., Contant, R., Fruchart, J., Ciabrini, J., and Fournier, M., *Inorg. Chem.* **16**, 2916 (1977).
80. (a) Pope, M. T., O'Donnell, S. E., and Prados, R. A., *J. Chem. Soc., Chem. Commun.* **1975**, 22; (b) Pope, M. T., and Scully, T. F., *Inorg. Chem.* **14**, 953 (1975).
81. (a) Lee, K. Y., Itoh, K., Hashimoto, M., Mizuno, N., and Misono, M., *Stud. Surf. Sci. Catal.* **82**, 583 (1994); (b) Schwegler, M. A., Peters, J. A., and van Bekkum, H., *J. Mol. Catal.* **63**, 343 (1990).
82. Black, J. B., and Clayden, N. J., *J. Chem. Soc., Dalton Trans.* **1984**, 2765.
83. Acerete, R., Hammer, C. F., and Baker, L. C. W., *J. Am. Chem. Soc.* **101**, 267 (1979).
84. Pieprgrass, K., and Pope, M. T., *J. Am. Chem. Soc.* **109**, 1586 (1987).
85. Domaile, P. J., *J. Am. Chem. Soc.* **106**, 1677 (1984).
86. Lefevre, J., Chauveau, F., and Doppelt, P., *J. Am. Chem. Soc.* **103**, 4581 (1981).
87. Filowitz, M., Klemperer, W. G., Messerle, L., and Shum, W., *J. Am. Chem. Soc.* **98**, 2345 (1976).
88. Filowitz, M., Ho, R. K. C., Klemperer, W. G., and Shum, W., *Inorg. Chem.* **18**, 93 (1979).
89. English, A. D., Jesson, J. D., Klemperer, W. G., Mamouneas, T., Messerle, L., Shum, W., and Tramontano, A., *J. Am. Chem. Soc.* **97**, 4785 (1975).
90. Varga, G. M., Papaconstantiou, E., and Pope, M. T., *Inorg. Chem.* **9**, 667 (1970).
91. Altermau, S. L., Pope, M. T., Prados, R. A., and So. H., *Inorg. Chem.* **2**, 417 (1975).
92. So, H., and Pope, M. T., *Inorg. Chem.* **11**, 1441 (1972).
93. Ioannidis, A., and Papapconstatinou, E., *Inorg. Chem.* **24**, 439 (1985).
94. Miyanaga, T., Fujikawa, T., Matsubayashi, N., Fujimoto, T., Yokoi, K., Watanabe, I., and Ikeda, S., *Bull. Chem. Soc. Jpn.* **62**, 1791 (1989).
95. Miyanaga, T., Fujikawa, T., Matsubayashi, N., Fujimoto, T., Yokoi, K., Watanabe, I., and Ikeda, S., *Chem. Lett.* **1988**, 487.
96. Keita, B., and Ndjo, L., *Surf. Sci. Lett.* **254**, L443 (1991).
97. Keana, J. F., Ogan, M. D., Lu, Y., Beer, M., and Varkey, J., *J. Am. Chem. Soc.* **108**, 7957 (1986).
98. Pope, M. T., *Prog. Inorg. Chem.* **39**, 181 (1991).
99. Sanchez, C., Livage, J., Launay, J. P., Fournier, M., and Jeanin, Y., *J. Am. Chem. Soc.* **104**, 3194 (1982).
100. Prados, R. A., and Pope, M. T., *Inorg. Chem.* **15**, 2547 (1976).
101. Eguchi, K., Toyozawa, Y., Yamazoe, N., and Seiyama, T., *J. Catal.* **83**, 32 (1983).
102. Mizuno, N., Katamura, K., Yoneda, Y., and Misono, M., *J. Catal.* **83**, 384 (1983).
103. Konishi, Y., Sakata, K., Misono, M., and Yoneda, Y., *J. Catal.* **77**, 169 (1982).
104. Otake, M., Komiyama, Y., and Otaki, T., *J. Phys. Chem.* **77**, 2896 (1973).
105. Akimoto, M., Ikeda, H., Okabe, A., and Echigoya, E., *J. Catal.* **89**, 196 (1984).
106. Centi, G., Nieto, J. L., and Ipalucci, C., *Appl. Catal.* **46**, 197 (1989).
107. Akimoto, M., Shima, K., and Echigoya, E., *J. Chem. Soc., Faraday Trans. 1* **79**, 2467 (1983).
108. Akimoto, M., Shima, K., Ikeda, H., and Echigoya, E., *J. Catal.* **86**, 173 (1984).
109. Aboukaïs, A., Ghoussoub, D., B-Crusson, E., Rigole, M., and Guelton, M., *Appl. Catal. A* **111**, 109 (1994).
110. Song, I. K., Lee, J. K., and Lee, W. Y., *Appl. Catal. A* **119**, 107 (1994).
111. Black, J. B., Clayden, N. J., Gai, P. L., Scott, J. D., Serwicka, E. M., and Goodenough, J. B., *J. Catal.* **106**, 1 (1987).
112. Serwicka, E. M., Black, J. B., and Goodenough, J. B., *J. Catal.* **106**, 23 (1987).
113. Kazansky, L. P., in "Proc. Climax 3rd Intern. Counf. Chemistry Uses Molybdenum" (H. F. Barry and P. C. H. Mitchell, Eds.), p. 70, 1979.
114. Dorokhova, E. N., and Kazansky, L. P., *Dokl. Akad. Nauk SSSR* **229**, 622 (1976).
115. Viswanathan, B., Omana, M. J., and Varadarajan, T. K., *Catal. Lett.* **3**, 217 (1989).

116. Kozhevnikov, I. V., *Russ. Chem. Rev.* **56**, 811 (1987).
117. Polotebnova, N. A., Kozlenko, A. A., and Furtune, L. A., *Russ. Inorg. J. Chem.* **21**, 1511 (1976).
118. Kozhevnikov, I. V., Kulikov, S. M., and Matveev, K. I., *Izv. Akad. Nauk SSSR, Ser. Khim.* **1980**, 2213.
119. Kulikov, S. M., and Kozhevnikov, I. V., *Izv. Akad. Nauk SSSR, Ser. Khim.* **1981**, 498.
120. Kozhevnikov, I. V., Khankhasaeva, S. Ts., and Kulikov, S. M., *Kinet. Katal.* **29**, 76 (1987).
121. Farcasiu, D., and Li, J. Q., *J. Catal.* **152**, 198 (1995).
122. Kozhevnikov, I. V., and Matveev, K. I., *Usp. Khim.* **51**, 1985 (1982).
123. Baraza, L., and Pope, M. T., *J. Phys. Chem.* **79**, 92 (1975).
124. Izumi, Y., Matsuo, K., and Urabe, K., *J. Mol. Catal.* **18**, 299 (1983).
125. Misono, M., Mizuno, N., Katamura, K., Kasai, A., Konishi, Y., Sakata, K., Okuhara, T., and Yoneda, Y., *Bull. Chem. Soc. Jpn.* **55**, 400 (1982).
126. Otake, M., and Onoda, T., *Shokubai (Catalyst)* **17**, 13 (1975).
127. Okuhara, T., Nishimura, T., Watanabe, H., and Misono, M., *J. Mol. Catal.* **74**, 247 (1992).
128. Misono, M., and Okuhara, T., *CHEMTECH* **23**, 23 (1993).
129. Gillespie, R. J., *Acc. Chem. Res.* **1**, 202 (1968); Olah, G. A., Prakash, G. K. S., and Sommer, J., "Superacids." Wiley, New York, 1985.
130. Hidalgo, C. V., Itoh, H., Hattori, T., Niwa, M., and Murakami, Y., *J. Catal.* **85**, 362 (1984).
131. Jozefowicz, L. C., Karge, H. G., Vasilyeva, E., and Moffat, J., *Microporous Mat.* **1**, 313 (1993).
132. Lefebvre, F., Cai, F. X. L., and Auroux, A., *J. Mater. Chem.* **4**, 125 (1994).
133. Auroux, A., and Vedrine, J. C., *Stud. Surf. Sci. Catal.* **20**, 311 (1985).
134. Kozhevnikov, I. V., Sinnenma, A., Jansen, R. J. J., and Bekkum, H., *J. Chem. Soc., Chem. Commun.* **1994**, 92; *Catal. Lett.* **27**, 187 (1994).
135. Barrows, J. N., Jameson, G. B., and Pope, M. T., *J. Am. Chem. Soc.* **107**, 1771 (1985).
136. Moffat, J. B., *et al.*, *J. Mol. Catal.* **26**, 285 (1984).
137. Kazanskii, L. P., Fedotov, M. A., and Spitsyn, V. I., *Dokl. Akad. Nauk SSSR* **233**, 152 (1977).
138. Baba, T., Watanabe, H., and Ono, Y., *J. Phys. Chem.* **87**, 2406 (1983).
139. Highfield, J. G., and Moffat, J. B., *J. Catal.* **88**, 177 (1984).
140. Saito, Y., Abe, Y., Niiyama, H., and Echigoya, E., *Nippon Kagaku Kaishi* **1986**, 25.
141. Ghosh, A. K., and Moffat, J. B., *J. Catal.* **101**, 238 (1986).
142. Baba, T., and Ono, Y., *J. Phys. Chem.* **87**, 3406 (1983).
143. Baba, T., Nomura, M., Ono, T., and Ohno, Y., *J. Phys. Chem.* **97**, 12,888 (1993).
144. Baba, T., Nomura, M., Ono, Y., and Kansaki, Y., *J. Chem. Soc., Faraday Trans.* **88**, 71 (1992).
145. Baba, T., Nomura, M., Ohno, Y., Hiroyama, Y., and Ono, Y., in "New Aspects of Spillover Effect in Catalysis" (T. Inui, Ed.), p. 81. Elsevier, Amsterdam, 1993.
146. Nowinska, K., Fiedorow, R., and Adamiec, J., *J. Chem. Soc., Faraday Trans.* **87**, 749 (1991).
147. Cheng, W.-C., and Luthra, N. P., *J. Catal.* **109**, 163 (1988).
148. Rao, K. M., Gobetto, R., Lannibello, A., and Zecchina, A., *J. Catal.* **119**, 512 (1989).
149. van Veer, J. A. R., Hendriks, P. A. J. M., Andrea, R. R., Romers, E. J. M., and Wilson, A. E., *J. Phys. Chem.* **94**, 1831 (1990).
150. Kapustin, G. I., Brueva, T. R., Klyachko, A. L., Timofeeva, M. N., Kulikov, S. M., and Kozhevnikov, I. V., *Kinet. Katal.* **31**, 896 (1990).
151. Izumi, Y., Hasebe, R., and Urabe, K., *J. Catal.* **84**, 402 (1983).
152. Mastihkin, V. M., Kulikov, S. M., Nosov, A. V., Kozhevnikov, I. K., Mudrakovsky, I. L., and Timofeeva, M. V., *J. Mol. Catal.* **60**, 65 (1990).
153. Lefebvre, F., *J. Chem. Soc., Chem. Commun.* **1992**, 756.
154. Thouvenot, R., Rocchiccioli-Delcheff, C., and Fournier, M., *J. Chem. Soc., Chem. Commun.* **1991**, 1252.

155. Thouvenot, R., Fournier, M., and Rocchiccioli-Delcheff, C., *J. Chem. Soc., Faraday Trans.* **87**, 2829 (1991).
156. Rocchiccioli-Delcheff, C., Amirouche, M., and Fournier, M., *J. Catal.* **138**, 445 (1992).
157. Payen, E., Kasztehan, S., and Moffat, J. B., *J. Chem. Soc., Faraday Trans.* **88**, 2263 (1992).
158. Ogata, A., Kazusaka, A., Yamazaki, A., and Enyo, M., *Chem. Lett.* **1989**, 15.
159. Soled, S. L., Miseo, S., McVicker, G. B., Baumgartner, J. E., Gates, W. E., Gutierrez, A., and Paes, J., Preprints 209th ACS National Meeting, 1995, Petr. Div., 16.
160. Kozhevnikov, I. V., *Russ. Chem. Rev.* **62**, 473 (1993).
161. Jansen, R. J. J., van Veldhuizen, H. M., Schwegler, M. A., and van Bekkum, H., *Recl. Trav. Chim. Pays-Bas* **113**, 115 (1994).
162. Urabe, K., Fukita, K., and Izumi, Y., *Shokubai (Catalyst)* **22**, 223 (1983).
163. Aoshima, A., Yamamatsu, and Yamaguchi, T., *Nippon Kagaku Kaishi* **1987**, 984.
164. Aoshima, A., Tonomura, S., Yamamatsu, S., *Polym. Adv. Tech.* **2**, 127 (1990).
165. Onoue, Y., Mizutani, Y., Akiyama, S., and Izumi, Y., *CHEMTECH* **1978**, 432.
166. Izumi, Y., Matsuo, K., and Urabe, K., in "Proc. Climax 4th Intern. Conf. on the Chemistry and Use of Mo," p. 302. Climax Molybdenum Co., Ann Arbor (1982).
167. Knoth, W. H., and Harlow, R. L., *Inorg. Chem.* **23**, 4765 (1984).
168. Farneth, W. E., Stanley, R. H., Domaille, P. J., and Farlee, R. D., *J. Am. Chem. Soc.* **109**, 4018 (1987).
169. Lee, K. Y., Arai, T., Nakata, S., Asaoka, S., Okuhara, T., and Misono, M., *J. Am. Chem. Soc.* **114**, 2836 (1992).
170. Aoshima, A., Yamamatsu, S., and Yamaguchi, T., *Nippon Kagaku Kaishi* **1987**, 976.
171. Kozhevnikov, I. V., Khankhasaeva, S. T., and Kulikov, S. M., *Kinet. Katal.* **29**, 66 (1988).
172. Kozhevnikov, I. V., Khankhasaeva, S. T., and Kulikov, S. M., *Kinet. Katal.* **30**, 39 (1987).
173. Matsuo, K., Urabe, K., and Izumi, Y., *Chem. Lett.* **1981**, 1315.
174. Baba, T., and Ono, Y., *J. Mol. Catal.* **37**, 317 (1986).
175. Izumi, Y., and Hayashi, K., *Chem. Lett.* **1980**, 787.
176. Sato, S., Sakurai, C., Furuta, H., Sodesawa, T., and Nozaki, F., *J. Chem. Soc., Chem. Commun.* **1991**, 1327.
177. Bednarek, M., Brzezinska, K., Stasinski, J., Kubisa, P., and Penczek, S., *Makromol. Chem.* **190**, 929 (1989).
178. Khankhasaeva, S. T., Kulikov, S. M., and Kozhevnikov, I. V., *Kinet. Katal.* **1990**, 188.
179. Maksimov, G. M., and Kozhevnikov, I. V., *React. Kinet. Katal. Lett.* **39**, 317 (1987).
180. Nomiyama, K., Ueno, T., and Miwa, M., *Bull. Chem. Soc. Jpn.* **53**, 827 (1980).
181. Kozhevnikov, I. V., and Kulikov, S. M., *Kinet. Katal.* **22**, 747 (1980).
182. Joshi, M. V., and Narasimhan, C. S., *J. Catal.* **120**, 281 (1989).
183. Hu, C., Nishimura, T., Okuhara, T., and Misono, M., *Sekiyu Gakkaishi* **36**, 386 (1993).
184. Tatibouet, J., Che, M., Amirouche, M., Fournier, M., and Rocchiccioli-Delcheff, C., *J. Chem. Soc., Chem. Commun.* **1988**, 1260.
185. Hayakawa, N., Okuhara, T., Misono, M., and Yoneda, Y., *Nippon Kagaku Kaishi* **1982**, 356.
186. Baba, T., and Ono, Y., *Appl. Catal.* **22**, 321 (1986).
187. Pozniczek, J., Kulszewicz-Bajer, I., Zagorska, M., Hasik, M., Bielanski, A., and Pron, A., *Stud. Surf. Sci. Catal.* **75**, 2593 (1993).
188. Song, I. K., Lee, W. Y., and Kim, J. J., *Catal. Lett.* **9**, 339 (1991).
189. Ono, Y., Baba, T., Sakai, J. and Keii, T., *J. Chem. Soc., Chem. Commun.* **1982**, 400.
190. Baba, T., Sakai, J., and Ono, Y., *Bull. Chem. Soc. Jpn.* **55**, 2657 (1982).
191. Ono, Y., Taguchi, M., Gerile, Suzuki, S., and Baba, T., in "Catalysis by Acids and Bases" (B. Imelik *et al.*, Eds.), p. 167. Elsevier, Amsterdam, 1985; Ono, Y., Baba, T., Kanae, K., and Seo, S. G., *Nippon Kagaku Kaishi* **1988**, 985.
192. Hayashi, H., and Moffat, J. B., *J. Catal.* **83**, 192 (1983); **81**, 66 (1983).

193. Kasai, A., Okuhara, T., Misono, M., and Yoneda, Y., *Chem. Lett.* **1981**, 449.
194. Hibi, T., Okuhara, T., Misono, M., and Yoneda, Y., *Chem. Lett.* **1982**, 1275.
195. Hibi, T., Takahashi, K., Okuhara, T., Misono, M., and Yoneda, Y., *Appl. Catal.* **24**, 69 (1986).
196. Baba, T., Sakai, J., Watanabe, H., and Ono, Y., *Bull. Chem. Soc. Jpn.* **55**, 2555 (1982).
197. Okuhara, T., Hibi, T., Takahashi, K., Tatematsu, S., and Misono, M., *J. Chem. Soc., Chem. Commun.* **1984**, 697.
198. Okuhara, T., Nishimura, T., Takahashi, K., and Misono, M., *Chem. Lett.* **1990**, 1201.
199. Nishimura, T., Okuhara, T., and Misono, M., *Appl. Catal.* **73**, L7 (1991).
200. Izumi, Y., Ono, M., Ogawa, M., and Urabe, K., *Chem. Lett.* **1993**, 825.
201. Izumi, Y., and Urabe, K., *Chem. Lett.* **1981**, 663.
202. Schwegler, M. A., Bekkum, H., and Munck, N., *Appl. Catal.* **74**, 191 (1991).
203. Soeda, H., Okuhara, T., and Misono, M., *Chem. Lett.* **1994**, 909.
204. Kozhevnikov, I. V., Tsyganok, A. I., Timofeeva, M. N., Kulikov, S. M., and Sidel'nikov, V. N., *Kinet. Katal.* **35**, 430 (1992).
205. Kulikov, S. M., Kozhevnikov, I. V., Fomina, M. N., and Krysin, A. P., *Kinet. Katal.* **27**, 651 (1986).
206. Sebulsky, R. T., and Henke, A. M., *Ind. Eng. Chem. Process Des. Dev.* **10**, 272 (1971).
207. Izumi, Y., Natsume, N., Tamamine, H., Tamaoki, I., and Urabe, K., *Bull. Chem. Soc. Jpn.* **62**, 2159 (1989).
208. Kozhevnikov, I. V., Sinnema, A., Jansen, R. J., Pamin, K., and Van Bekkum, H., *Catal. Lett.* **30**, 241 (1995).
209. Okuhara, T., Yamashita, M., Na, K., and Misono, M., *Chem. Lett.* **1994**, 1451.
210. Ohgoshi, S., Kanai, J., and Sugimoto, M., EP 561284, 1993.
211. Kresge, C. T., Marler, D. O., Rav, G. S., and Rose, B. H. (Mobil Oil Corp.) US 5324881, 1994.
212. Nishi, H., Nowinska, K., and Moffat, J. B., *J. Catal.* **116**, 480 (1989).
213. Yamaguchi, T., Mitoh, A., and Tanabe, K., *Chem. Lett.* **1982**, 1229.
214. Izumi, Y., Ogawa, M., Nohara, W., and Urabe, K., *Chem. Lett.* **1992**, 1987.
215. Nowinska, K., Fiedorow, R., and Adamiec, J., *J. Chem. Soc., Faraday Trans.* **87**, 749 (1991).
216. Na, K., Okuhara, T., and Misono, M., *Chem. Lett.* **1993**, 1141.
217. Na, K., Okuhara, T., and Misono, M., *J. Chem. Soc., Faraday Trans.* **91**, 367 (1995).
218. Igarashi, A., Matsuda, T., and Ogino, Y., *J. Japan Petrol. Inst.* **22**, 331 (1979).
219. Ono, Y., and Baba, T., in "Proc. 8th Intern. Congr. Catal.," V-405. Verlag Chemie, Berlin, 1984.
220. Shikata, S., Okuhara, T., and Misono, M., *Seikiyu Gakkaishi* **37**, 632 (1994); *J. Mol. Catal.* **100**, 49 (1995).
221. Kim, J., Kim, J., Seo, G., Oark, N., and Niiyama, H., *Appl. Catal.* **37**, 45 (1988).
222. Sugiyama, K., Kato, K., Miura, H., and Matsuda, T., *J. Jpn. Petrol. Inst.* **26**, 243 (1983).
223. Saito, Y., Niiyama, H., and Echigoya, E., *Nippon Kagaku Kaishi* **1984**, 391.
224. Yamamura, T., and Nakatomi, S., *J. Catal.* **37**, 142 (1975).
225. Vaughan, S., O'Connor, C. T., and Fletcher, J. C. Q., *J. Catal.* **147**, 441 (1994).
226. Niiyama, H., Tamai, S., Saito, Y., and Echigoya, E., *Chem. Lett.* **1983**, 1679.
227. Nasikin, M., Nakamura, R., and Niiyama, H., *Chem. Lett.* **1993**, 209.
228. Nayak, V., and Moffat, J. B., *Appl. Catal.* **47**, 97 (1989).
229. Oulmekki, A., and Lefebvre, F., *React. Kinet. Catal. Lett.* **48**, 601 (1992).
230. Matsuda, T., Sato, M., Kanno, M., Miura, H., and Sugiyama, K., *J. Chem. Soc. Faraday Trans. 1* **77**, 3107 (1981).
231. Nayak, V., and Moffat, J. B., *Appl. Catal.* **36**, 127 (1988).
232. Nishi, H., and Moffat, J. B., *J. Mol. Catal.* **51**, 193 (1989).
233. (a) Sakata, K., Furuta, M., Misono, M., and Yoneda, Y., ACS/CSJ Chemical Congr., Honolulu, April, 1979; (b) Misono, M., 1st Japan-France Catal. Seminar, July 1979.

234. Okuhara, T., and Misono, M., in "Dynamic Process on Solid Surface" (K. Tamaru, Ed.), p. 259. Plenum, New York, 1993.
235. Okuhara, T., Tatematsu, S., Lee, K. Y., and Misono, M., *Bull. Chem. Soc. Jpn.* **62**, 717 (1989).
236. Okuhara, T., Hashimoto, T., Misono, M., Yoneda, Y., Niiyama, H., Saito, Y., and Echigoya, E., *Chem. Lett.* **1983**, 573.
237. Highfield, J. G., and Moffat, J. B., *J. Catal.* **95**, 108 (1985).
238. Highfield, J. G., and Moffat, J. B., *J. Catal.* **98**, 245 (1986).
239. Uchida, T., Sugiura, N., Nakamura, R., and Niiyama, H., *J. Chem. Eng. Japan* **24**, 417 (1991).
240. Okuhara, T., Arai, T., Ichiki, T., Lee, K. Y., and Misono, M., *J. Mol. Catal.* **55**, 293 (1989).
241. (a) Saito, Y., and Niiyama, H., *J. Catal.* **106**, 329 (1987); (b) Saito, Y., Cook, P. N., Niiyama, H., and Echigoya, E., *J. Catal.* **95**, 49 (1985).
242. Takahashi, K., Okuhara, T., and Misono, M., *Chem. Lett.* **1985**, 841.
243. Misono, M., Okuhara, T., Ichiki, T., Arai, T., and Kanda, Y., *J. Am. Chem. Soc.* **109**, 5535 (1987).
244. Knözinger, H., *Angew. Chem., Int. Ed. Engl.* **7**, 791 (1968).
245. Klages, F., Gordon, J. E., and Jung, H. A., *Chem. Ber.* **98**, 3748 (1985).
246. Lee, K. Y., Kanda, Y., Mizuno, N., Okuhara, T., Misono, M., Nakata, S., and Asaoka, S., *Chem. Lett.* **1988**, 1175.
247. (a) Olah, G. A., and Namanworth, E., *J. Am. Chem. Soc.* **89**, 3576 (1967); (b) Birchall, T., and Gillespi, R. J., *Can. J. Chem.* **43**, 1045 (1965).
248. Maclean, C., and Mackor, E. L., *J. Chem. Phys.* **34**, 2207 (1961).
249. Nishimura, T., Okuhara, T., and Misono, M., *Chem. Lett.* **1991**, 1695.
250. Niiyama, H., Akiratiwa, S., and Saito, Y., in "Proc. Regional Symposium on Petrochemical Engineering," ST-1, Bangkok, Thailand, 1987.
251. Barrows J. N., and Pope, M. T., *Adv. Chem. Ser.* **226**, 403 (1990).
252. Massart, R., *Ann. Chim.* **3**, 507 (1968).
253. Müller, A., Krickemeyer, E., Penk, M., Witteneben, V., and Döring, J., *Angew. Chem. Int. Ed. Engl.* **29**, 88 (1990).
254. Barrows, J. N., Jameson, G. B., and Pope, M. T., *J. Am. Chem. Soc.* **107**, 1771 (1985).
255. Katsolis P. E., and Pope, M. T., *J. Am. Chem. Soc.* **106**, 2737 (1984).
256. Khenkin A. M., and Hill, C. L., *J. Am. Chem. Soc.* **115**, 8178 (1993).
257. Hill, C. L., and McCartha, C. M. P., in "Photosensitization and Photocatalysis Using Inorganic and Organometallic Compounds" (K. Kalyanasundaram and M. Grätzel, Eds.), p. 307. Kluwer, Dordrecht, The Netherlands, 1993.
258. (a) Komaya, T., and Misono, M., *Chem. Lett.* **1983**, 1177; (b) Misono, M., Mizuno, N., and Komaya, T., in "Proc. 8th Int. Congr. Catal., 1984," Vol. 5, p. 487. Verlag Chemie, Weinheim, 1984.
259. Katamura, K., Nakamura, T., Sakata, K., Misono, M., and Yoneda, Y., *Chem. Lett.* **1981**, 89.
260. Mizuno, N., and Misono, M., *J. Phys. Chem.* **93**, 3334 (1989).
261. Mizuno, N., Katamura, K., Misono, M., and Yoneda, Y., *J. Catal.* **83**, 384 (1983).
262. Mizuno, N., Watanabe, T., and Misono, M., *J. Phys. Chem.* **94**, 890 (1990).
263. Tsunek, H., Niiyama, H., Echigoya, E., *Chem. Lett.* **1978**, 645.
264. Taketa, H., Katsuki, S., Eguchi, K., Seiyama, T., and Yamazoe, N., *J. Phys. Chem.* **90**, 2959 (1986).
265. Akimoto, M., and Echigoya, E., *Chem. Lett.* **1981**, 1759.
266. Mizuno, N., Watanabe, T., and Misono, M., *J. Phys. Chem.* **89**, 80 (1985).
267. Sakata, K., Ph. D. Dissertation, The University of Tokyo, 1981.
268. Komaya, T., Masters Thesis, The University of Tokyo, 1983.
269. Kulesza, P. J., Faulkner, L. R., Chen, J., and Klemperer, W. G., *J. Am. Chem. Soc.* **113**, 379 (1991); Kulesza, P. J., and Faulkner, L. R., *J. Am. Chem. Soc.* **115**, 11879 (1993).

270. Yoshida, S., Niiyama, H., and Echigoya, E., *J. Phys. Chem.* **86**, 3150 (1982); *Nippon Kagaku Kaishi* **1981**, 1703; Yoshida, S., Miyata, Y., Niiyama, H., Echigoya, E., *ibid.* **1982**, 1873.
271. Hodnett, B. K., and Moffat, J. B., *J. Catal.* **91**, 93 (1985).
272. Ai, M., *Appl. Catal.* **4**, 245 (1982).
273. Kim, H. C., Moon, S. H., and Lee, W. Y., *Chem. Lett.* **1991**, 447.
274. Kazanskii, L. P., Fedotov, M. A., Potapova, I. V., and Spitsyn, A. V. I., *Dokl. Akad. Nauk SSSR* **244**, 372 (1979).
275. Massart, R., Fournier, M., and Souchay, P., *C. R. Akad. Sci.* **C267**, 1805 (1968).
276. Misono, M., Igarashi, H., Katamura, K., Okuhara, T., and Mizuno, N., *Stud. Surf. Sci. Catal.* **77**, 105 (1993).
277. Niiyama, H., Tsuneki, H., and Echigoya, E., *Nippon Kagaku Kaishi.* **1979**, 996.
278. Kim, H. C., Moon, S. H., and Lee, K. Y., *Chem. Lett.* **1991**, 447.
279. Matsumoto, H., Lee, K. Y., and Misono, M., 61st National Meeting of The Chemical Society of Japan. Tokyo, 1991.
280. Ziemecki, S. B., in "Proc. 9th Int. Congr. Catal. 1988," Vol. 4, p. 1798.
281. Serwicka, E. M., Bruckman, K., Haber, J., Paukshtis, E. A., and Yurchenko, E. N., *Appl. Catal.* **73**, 153 (1991).
282. Bruckman, K., Haber, J., and Serwicka, E. M., *Faraday Discuss. Chem. Soc.* **87**, 173 (1988).
283. Taouk, T., Ghoussoub, D., Bannani, A., Crusson, E., Rigole, M., Aboukais, A., Decressain, R., Fournier, M., and Guelton, A., *J. Chim. Phys.* **89**, 435 (1992).
284. Cadot, E., Marchal, C., Fournier, M., Teze, A., and Herve, G., in "Polyoxometalates" (M. T. Pope and A. Müller, Eds.), p. 135. Kluwer, Dordrecht, The Netherlands, 1994.
285. Ali, B. E., Bregeault, J.-M., Mercier, J., Martin, J., Martin, C., and Convert, O., *J. Chem. Soc., Chem. Commun.* **1989**, 825.
286. Atlamsani, A., Bregeault, J.-M., and Ziyad, M., *J. Org. Chem.* **58**, 5663 (1993).
287. Gorodetskaya, T. A., Kozhevnikov, I. V., and Matveev, K. I., *Kinet. Katal.* **23**, 992 (1982).
288. Mizuno, N., and Misono, M., *J. Mol. Catal.* **86**, 319 (1994).
289. Neumann, R., and Lisel, M., *J. Org. Chem.* **54**, 4607 (1989).
290. Neumann, R., and Levin, M., *J. Am. Chem. Soc.* **114**, 7278 (1992).
291. Lissel, M., Jansen, H., in de Wal, and R. Neumann, *Tetrahedron Lett.* **33**, 1795 (1992).
292. Matveev, K. I., and Kozhevnikov, I. V., *Kinet. Katal.* **21**, 1189 (1980).
293. Mizuno, N., Hirose, T., Tateishi, M., and Iwamoto, M., *Chem. Lett.* **1993**, 1839; Mizuno, N., Hirose, T., and Iwamoto, M., *Stud. Surf. Sci. Catal.* **82**, 593 (1994).
294. Hamamoto, M., Nakayama, K., Nishiyama, Y., and Ishii, Y., *J. Org. Chem.* **58**, 6421 (1993).
295. Yamada, T., Takai, T., Rhode, O., and Mukaiyama, T., *Bull., Chem. Soc. Jpn.* **64**, 2109 (1991); Takai, T., Hata, E., Yamada, T., and Mukaiyama, T., *ibid.* **64**, 2513 (1991); Mukaiyama, T., Yorozu K., Takai, T. and Yamada, T., *Chem. Lett.* **1993**, 439.
296. Mizuno, N., Tateishi, M., Hirose, T., and Iwamoto, M., *Chem. Lett.* **1993**, 1985.
297. Lyons, J. E., Ellis, P. E., and Durante, V. A., in "Structure-Activity and Selectivity Relationships in Heterogeneous Catalysis" (R. K. Grasselli and A. W. Sleight, Eds.), p. 99. Elsevier, Amsterdam, 1991.
298. Mizuno, N., Tateishi, M., Hirose, T., and Iwamoto, M., *J. Mol. Catal.* **88**, L125 (1994).
299. Mizuno, N., Tateishi, M., Hirose, T., and Iwamoto, M., *Chem. Lett.* **1993**, 2137.
300. (a) Kitajima, N., Fukui, H., and Moro-oka, Y., *J. Chem. Soc., Chem. Commun.* **1988**, 485; Kitajima, N., Itoh, M., Fukui H., and Moro-oka, Y., *ibid.*, **1991**, 102; (b) Murahashi, S., Oda, Y., and Naota, T. *J. Am. Chem. Soc.* **114**, 7913 (1992); (c) Barton, D. H. R., Gastiger, M. J., and Motherwell, W. B. *J. Chem. Soc., Chem. Commun.* **1983**, 731; (d) Onophenko, A., and Shultz, J., *J. Org. Chem.* **38**, 999 (1973); **38**; 3729 (1973).
301. Lau, T.-C., and Mak, C.-K., *J. Chem. Soc., Chem. Commun.* **1993**, 766; Khan, M. M. T., Chatterjee, D., Kumar S. S., Rao, A. P., and Khan, N. H., *J. Mol. Catal.* **75**, L49 (1992).

302. Furukawa, H., Nakamura, T., Inagaki, H., Nishikawa, E., Imai, C., and Misono, M., *Chem. Lett.* **1988**, 877.
303. Mizuno, N., Yokota, S., Miyazaki, I., and Misono, M., *Nippon Kagaku Kaishi* **1991**, 1066.
304. Lee, K. Y., Itoh, K., Hashimoto, M., Mizuno, N., and Misono, M., *Stud. Surf. Sci. Catal.* **82**, 583 (1994).
305. Burdett, J. K., and Nguyen, C. K., *J. Am. Chem. Soc.* **112**, 5366 (1990).
306. Ishii, Y., Yamawaki, K., Yoshida, T., Ura, T., and Ogawa, M., *J. Org. Chem.* **52**, 1868 (1987); Yamawaki, K., Yoshida, T., Nishihara, H., Ishii, Y., and Ogawa, M., *Synth. Commun.* **16**, 53 (1986); Daumas, M., Vo-Quang, Y., and Vo-Quang, L., *Synthesis* **1989**, 64.
307. (a) Motoba, Y., Inoue, H., Akagi, J., Okabayashi, T., Ishii, Y., and Ogawa, M., *Synth. Commun.* **14**, 865 (1984); (b) Ishii, Y., and Ogawa, M., *J. Synth. Org. Chem.* **47**, 889 (1989).
308. (a) Venturello, C., Alneri, E., and Ricci, M., *J. Org. Chem.* **48**, 3831 (1983); Venturello, C., D'Aloiso, R., Bart, J. C. J., and Ricci, M., *J. Mol. Catal.* **32**, 107 (1985); Venturello, C., and D'Aloisi, R., *J. Org. Chem.* **53**, 1553 (1988); (b) Ishii, Y., Yamawaki, K., Ura, T., Yamada, H., Yoshida, T., and Ogawa, M., *J. Org. Chem.* **53**, 3587, 5549 (1988); (c) Schwegler, M., Floor, M., and van Bekkum, H., *Tetrahedron Lett.* **29**, 823 (1988).
309. (a) Ishii, Y., and Sakata, Y., *J. Org. Chem.* **55**, 5545 (1990); (b) Balistreri, F. P., Failla, S., Spina, E., and Tomaselli, G. A., *J. Org. Chem.* **54**, 947 (1989).
310. Oguchi, T., Sakata, Y., Takeuchi, N., Kaneda, K., Ishii, Y., and Ogawa, M., *Chem. Lett.* **1989**, 2053; Sakata, Y., and Ishii, Y., *J. Org. Chem.* **56**, 6233 (1991).
311. Sakata, Y., and Ishii, Y., *J. Org. Chem.* **56**, 6233 (1991).
312. Shimizu, M., Orita, H., Hayakawa, T., Watanabe, Y., and Takehira, K., *Tetrahedron Lett.* **30**, 471 (1989).
313. Sakae, S., Sakata, Y., Nishiyama, Y., and Ishii, Y., *Chem. Lett.* **1992**, 289.
314. Csanyi, L. J., and Jaky, K., *J. Mol. Catal.* **61**, 75 (1991).
315. Aubry, C., Chottard, G., Platzler, N., Bregeault, J.-M., Thouvenot, R., Chauveau, F., Huet, C., and Ledon, H., *Inorg. Chem.* **30**, 4409 (1990).
316. Duncan, D. C., Chambers, R. C., Hecht, E., and Hill, C. L., *J. Am. Chem. Soc.* **117**, 681 (1995).
317. Itoh, K., Hashimoto, M., and Misono, M., Proc. 70th National Meeting of The Catalysis Society of Japan, 4F424 (1992).
318. Neumann, R., and Gara, M., *J. Am. Chem. Soc.* **116**, 5509 (1994).
319. Gall, R. D., Fajaj, M., and Hill, C. L., *Inorg. Chem.* **33**, 5015 (1994).
320. (a) Faraj, M., and Hill, C. L., *J. Chem. Soc., Chem. Commun.* **1987**, 1487; (b) Hill, C. L., in "Activation and Functionalization of Alkanes" (C. L. Hill, Ed.), p. 243. Wiley, New York, 1989.
321. Neumann, R., and A.-Gnim, C., *J. Chem. Soc., Chem. Commun.* **1989**, 1324.
322. Hill, C. L., and Brown, R. B., Jr., *J. Am. Chem. Soc.* **108**, 536 (1986); Neumann, R., and A.-Gnim, C., *J. Am. Chem. Soc.* **112**, 6025 (1990).
323. Faraj, M., Lin, C.-H., and Hill, C. L., *New J. Chem.* **12**, 745 (1988).
324. (a) Ai, M., in "Proc. 8th Intern. Congr. Catal.," Berlin, 1984. Verlag Chemie, Weinheim, 1985, Vol. 5, p. 475; (b) Centi, G., Nieto, J. P., Brückman, C. K., and Servicka, E. M., *Appl. Catal.* **46**, 197 (1989); (c) Centi, G., Lena, V., Trifiro, F., Ghoussoub, D., Aissi, C. F., Guelton, M., and Bonnelle, J. P., *J. Chem. Soc., Faraday Trans.* **86**, 2775 (1990).
325. Tatibouet, J.-M., Che, M., Amirouche, M., Fournier, M., and Rocchiccioli-Deltcheff, C., *J. Chem. Soc., Chem. Commun.* **1988**, 1260.
326. Rocchiccioli-Deltcheff, C., Amirouche, M., Herve, G., Fournier, M., Che, M., and Tatibouet, J.-M., *J. Catal.* **126**, 591 (1990).
327. Mizuno, N., Watanabe, T., Mori, H., and Misono, M., *J. Catal.* **123**, 157 (1990).
328. Misono, M., Mizuno, N., Mori, H., Lee, K. Y., Jiao, J., and Okuhara, T., *Stud. Surf. Sci. Catal.* **67**, 87 (1991).

329. Mizuno, N., and Misono, M., *Chem. Lett.* **1984**, 669.
330. Artz, D., *Catal. Today* **18**, 173 (1993).
331. Sheldon, R. A., "Dioxygen Activation and Homogeneous Catalytic Oxidation," p. 573. Elsevier, Amsterdam, 1991.
332. Mizuno, N., Watanabe, T., and Misono, M., *Bull. Chem. Soc. Jpn.* **64**, 243 (1991).
333. Mori, H., Mizuno, N., and Misono, M., *J. Catal.* **131**, 133 (1990).
334. (a) Ai, M., *J. Catal.* **71**, 88 (1981); Ai, M., in "Proc. Climax 4th Int. Conf. Chemistry and Usage of Molybdenum" (H. F. Barry and P. C. H. Mitchell, Eds.), p. 306. Climax Molybdenum Co., Ann Arbor, 1982; (b) Ai, M., Tsai, T., and Ozaki, A., *Bull. Chem. Soc. Jpn.* **53**, 2647 (1980).
335. Ueshima, M., Tsuneki, H., and Shimizu, N., *Hyoumen* **24**, 582 (1986); Shimizu, N., *Petrotech* **6**, 778 (1983).
336. Black, J. B., Claydon, N. J., Gai, P. L., Scott, J. D., Serwicke, E. M., and Goodenough, J. B., *J. Catal.* **106**, 1 (1987).
337. Tatematsu, S., Masters Thesis, The University of Tokyo, 1984.
338. Otake M., and Onoda, T., *Shokubai (Catalyst)* **18**, 169 (1976).
339. Otake, M., and Onoda, T., in "Proc. 7th Int. Congr. Catal., Tokyo, 1980," p. 780. Kodansha-Elsevier, Tokyo and Amsterdam, 1981.
340. Akimoto, M., Tsuchida, Y., Sato, K., and Echigoya, E., *J. Catal.* **72**, 83 (1981).
341. Aboukais, D., Ghoussoub, A., B.-Crusson, E., Rigole, M., and Guelton, M., *Appl. Catal. A* **111**, 109 (1994).
342. Lee, K. W., Oishi, S., and Misono, M., 67th National Meeting of The Chemical Society of Japan, Tokyo, 2M110, 1994.
343. Watzenberger, O., Emig, G., and Lynch, D. T., *J. Catal.* **124**, 247 (1990).
344. McGarvey, G. B., and Moffat, J. B., *J. Catal.* **132**, 100 (1991).
345. Brückman, K., Tatibouët, J.-M., Che, M., Serwicka, E., and Haber, J., *J. Catal.* **139**, 455 (1993).
346. Centi, G., *Catal. Lett.* **22**, 53 (1993).
347. Krylov, O. V., *Catal. Today* **18**, 209 (1993); Periana, R. A., Taube, D. J., Evitt, E. R., Löffler, D. G., Wentreck, P. R., Voss, G., and Masuda, T., *Nature* **259**, 340 (1993); Hickman, D. A., and Schmidt, L. D., *Nature* **259**, 343 (1993).
348. Hong, S. S., and Moffat, J. B., *Appl. Catal. A* **109**, 117 (1994).
349. Kim, Y.-C., Ueda W., and Moro-oka, Y., *J. Chem. Soc., Chem. Commun.* **1989**, 652.
350. Centi, G., Ed., "Vanadyl Pyrophosphate Catalysts," *Catal. Today* **16** (1993).
351. *The Chemical Engineer*, 13 Sept., 3 (1990).
352. Kringer, H., and Kirch, L. S., European Patent 0010902 (1979).
353. Centi, G., and Trifiro, F., *Catal. Sci. Technol.* **1**, 225 (1991).
354. Brückman, K., and Harber, J., "Proc. 10th Intern. Congr. Catal., Budapest, 1992," p. 742. Elsevier, Budapest, 1993.
355. Mizuno, N., Tateishi T., and Iwamoto, M., *J. Chem. Soc., Chem. Commun.* **1994**, 1411; *Appl. Catal. A* **118**, L1 (1994).
356. JP Patent (Jpn. Kokai Tokkyo Koho); H. Imai, M. Nakatsukasa, and A. Aoshima, 62/132832, H. Imai, T. Yamaguchi, and M. Sugiyama, 63/145249, S. Yamamatsu, and Y. Yamaguchi, 2/42033
357. Neumann, R., and Levin, M., *J. Org. Chem.* **56**, 5707 (1991).
358. Soeda, H., Okuhara, T., and Misono, M., *Nippon Kagaku Kaishi* **1993**, 917.
359. Kozhevnikov, I. V., Kulikov, S. M. M., Timeofeeva, N., Krysin, A. P., and Titova, T. F., *React. Kinet. Catal. Lett.* **45**, 257 (1991).
360. Kinomura, K., Kitazawa, S., Takata, Y., and Sakakibara, T., USP. 4874852; Kinomura, K., and Sakakibara, T., 56th National Meeting of the Chemical Society of Japan, 1988, Abstr. No. IIXB40-41.

361. Kozhevnikov, I. V., Vasilieva, I. B., and Zarutskii, V. V., *React. Kinet. Catal. Lett.* **47**, 83 (1992).
362. Kozhevnikov, I. V., Kulikov, S. M., Chukaeva, N. G., Kirasanov, A. T., Letunova, A. B., and Blinova, V. I., *React. Kinet. Catal. Lett.* **47**, 59 (1992).
363. Timofeeva, M. N., Grosheva, V. S., Demchenko, B. I., and Kozhevnikov, I. V., *React. Kinet. Catal. Lett.* **45**, 215 (1991).
364. Katsoulis, D. E., and Pope, M. T., *J. Chem. Soc. Chem. Commun.* **1986**, 1186.
365. Hill, C. L., and P., McCartha, C. M., *Coord. Chem. Rev.* **143**, 407 (1995).
366. Mansuy, D., Bartoli, J.-F., Battioni, P., Lyon, D. K., and Finke, R. G., *J. Am. Chem. Soc.* **113**, 7222 (1991).
367. Urabe, K., Kimura, F., and Izumi, Y., "Proc. 7th Int. Congr. Catal., Tokyo, 1980," p. 1418. Kodansha, Tokyo, Elsevier, Amsterdam, 1981.
368. Grate, J. H., Hamm, D. R., and Mahajan, A., Preprint distributed at 14th Conference on Catalysis of Organic Reactions, Albuquerque, New Mexico, April 27–29, 1992.
369. Izumi, Y., Satoh, Y., Kondoh, H., and Urabe, K., *J. Mol. Catal.* **72**, 37 (1992).
370. Wegmann, R. W., *J. Chem. Soc., Chem. Commun.* **1994**, 947.
371. Urabe, K., Tanaka, Y., and Izumi, Y., *Chem. Lett.* **1985**, 1595.
372. Siedle, A. R., Markell, C. G., Lyon, P. A., Hodgson, K. O., and Roe, A. L., *Inorg. Chem.* **26**, 219 (1987).
373. Lyon D. K., and Finke, R. G., *Inorg. Chem.* **29**, 1787 (1990).
374. Mizuno, N., Lyon, D. K., and Finke, R. G., *J. Catal.* **128**, 84 (1991).
375. Geletti, Y. V., and Shilov, A. E., *Kinet. Katal.* **24**, 486 (1983).
376. Finke, R. G., Lyon, D. K., Nomiya, K., and Weakley, T. R. J., *Acta Crystallogr.* **C46**, 1592 (1990).
377. Finke, R. G., Lyon, D. K., Nomiya, K., Sur, S., and Mizuno, N., *Inorg. Chem.* **29**, 1784 (1990).
378. (a) Ono, Y., Taguchi, M., Gerile, Suzuki, S., and Baba, T., in "Catalysis by Acids and Bases" (B. Imelik *et al.*, Ed.), p. 167. Elsevier, Amsterdam, 1985; (b) Ono, Y., Baba, T., Kanae, K., and Seo, S. G., *Nippon Kagaku Kaishi* **1988**, 985.
379. Baba, T., and Ono, Y., *Appl. Catal.* **55**, 301 (1989).
380. Suzuki, S., Kogai, K., and Ono, Y., *Chem. Lett.* **1984**, 699.
381. Na, K., Okuhara, T., and Misono, M., *J. Chem. Soc., Chem. Commun.* **1993**, 1422.
382. Na, K., Okuhara, T., and Misono, M., in "Catalytic Science and Technology II" (Y. Izumi, H. Arai and M. Iwamoto, Eds.) p. 245. Kodansha, Tokyo, Elsevier, Amsterdam, 1995.
383. Brindley, G. W., and Semples, R. E., *Clay Miner* **12**, 229 (1977).
384. Shabtai, J., Lazar, R., and Oblad, A. G., in "Proc. 7th Int. Congr. Catal., Tokyo, 1980" (T. Seiyama and K. Tanabe, Eds.), p. 828. Kodansha, Tokyo, Elsevier, Amsterdam, 1981.
385. Kikuchi, E., Nakano, M., Fukuda, I., and Morita, Y., *J. Jpn. Petrol. Inst.* **27**, 153 (1984).
386. Urabe, K., Sakurai, H., and Izumi, Y., *J. Chem. Soc., Chem. Commun.* **1986**, 1074.
387. Bartley, G. J. J., and Burch, R., *Appl. Catal.* **28**, 209 (1986).
388. Mori, H., Okuhara, T., and Misono, M., *Chem. Lett.* **1987**, 2305.
389. Kwon, T., and Pinnavaia, T. J., *Chem. Mat.* **1**, 381 (1989).
390. Narita, E., Kaviratna, P., and Pinnavaia, T. J., *Chem. Lett.* **1991**, 805.
391. Kwon, T., Tsigdinos, G. A., and Pinnavaia, T. J., *J. Am. Chem. Soc.* **110**, 3653 (1988).
392. Narita, E., Kaviratna, P. D., and Pinnavaia, T. J., *J. Chem. Soc. Chem. Commun.* **1993**, 60.
393. Drezdon, M. A., *Inorg. Chem.* **27**, 4628 (1988).
394. Dimotakis, E. D., and Pinnavaia, T. J., *Inorg. Chem.* **29**, 2393 (1994).
395. Tatsumi, T., Yamamoto, K., Tajima, H., and Tominaga, H., *Chem. Lett.* **1992**, 815.
396. Rindl, M., *S. African J. Sci.* **11**, 362 (1916).
397. Yamase, T., *Chem. Lett.* **1973**, 615.
398. Yamase, T., Hayashi, H., and Ikawa, T., *Chem. Lett.* **1974**, 1055.

399. Yamase, T., and Ikawa, T., *Bull. Chem. Soc. Jpn.* **50**, 746 (1977).
400. Yamase, T., *J. Chem. Soc., Dalton Trans.* **1978**, 283.
401. Yamase, T., *J. Chem. Soc., Dalton Trans.* **1987**, 1982.
402. Yamase T., and Kurozumi, T., *J. Chem. Soc., Dalton Trans.* **1983**, 2205.
403. Papaconstantinou, E., Dimotikali, D., and Politou, A., *Inorg. Chim. Acta* **46**, 155 (1980).
404. Papaconstantinou, E., *J. Chem. Soc., Chem. Commun.* **1982**, 12; *Chem. Soc. Rev.* **18**, 1 (1989).
405. Hill, C. L., *Synlett.* 127 (1995).
406. Fox, M., Cardona, A. R., and Gaillard, E., *J. Am. Chem. Soc.* **109**, 6347 (1987).
407. Renneke, R., Pasquali, F. M., and Hill, C. L., *J. Am. Chem. Soc.* **112**, 6585 (1990).
408. Attanasio, D., and Suber, L., *Inorg. Chem.* **28**, 3779 (1989).
409. C.-Walke, L. A., and Hill, C. L., *J. Am. Chem. Soc.* **114**, 938 (1992).
410. Darwent, J. R., *J. Chem. Soc., Chem. Commun.* **1982**, 798; Akid, R., and Darwent, J. R., *J. Chem. Soc., Dalton Trans.*, **1985**, 395.
411. Rouillier, M. C., Thèse de 3ème cycle, Nancy, France, 1968.
412. Keita, B., and Nadjo, L., *J. Electroanal. Chem.* **191**, 441 (1985).
413. Keita, B., and Nadjo, L., *J. Electroanal. Chem.* **199**, 229 (1986).
414. Mavroy A. J., and Gratzel, M., *J. Electroanal. Chem.* **209**, 391 (1986).
415. Bidan, G., Genies, E. M., and Lapkowski, M., *J. Chem. Soc., Chem. Commun.* **1988**, 533.
416. Toth, J. E., and Anson, F. C., *J. Am. Chem. Soc.* **111**, 2444 (1989).
417. Toth, J. E., Melton, J. D., Cabelli, D. B., Bielski, H. J., and Anson, F. C., *Inorg. Chem.* **29**, 1952 (1990).
418. Fukuma, M., Deto, Y., and Yamase, T., *Antiviral Res.* **16**, 327 (1991).
419. Hill, C. L., Weeks, M. S., and Schinazi, R. F., *J. Med. Chem.* **33**, 2767 (1990).
420. Kudo, T., Ishikawa, A., Okamoto, H., Miyauchi, K., Murai, F., Mochiji, K., and Umezaki, H., *J. Electrochem. Soc.* **134**, 2607 (1987).
421. Yoshimura, T., Ishikawa, A., Okamoto, H., Miyazaki, H. Sawada, A., Tanimoto, T., and Okazaki, S., *Microelectron. Eng.* **14**, 149 (1991).
422. Tell, B., and Wagner, W., *Appl. Phys. Lett.* **33**, 837 (1978).
423. Yamase, T., and Naruke, H., *Coord. Chem. Rev.* **111**, 83 (1991).
424. Nakamura, O., Kodama, T., Ogino, I., and Miyake, Y., *Chem. Lett.* **1979**, 17.
425. Kreuer, K. D., Hampele, M., Dolde, K., and Rabenau, A., *Solid State Ionics* **28-30**, 589 (1988).